



ISBN 978-608-4723-05-9

SS. CYRIL AND METHODIUS UNIVERSITY IN SKOPJE  
FACULTY OF DESIGN AND TECHNOLOGIES OF FURNITURE AND INTERIOR – SKOPJE  
REPUBLIC OF NORTH MACEDONIA



6<sup>th</sup> INTERNATIONAL SCIENTIFIC CONFERENCE

# WOOD TECHNOLOGY & PRODUCT DESIGN PROCEEDINGS

13-15 SEPTEMBER 2023, OHRID



# PROCEEDINGS

**6<sup>th</sup> INTERNATIONAL SCIENTIFIC  
CONFERENCE**

**WOOD TECHNOLOGY  
& PRODUCT DESIGN**

**13– 15 SEPTEMBER, 2023  
UNIVERSITY CONGRESS CENTRE – OHRID  
REPUBLIC OF NORTH MACEDONIA**



WOOD TECHNOLOGY & PRODUCT DESIGN  
Ohrid, North Macedonia, 13–15 September, 2023

### PROCEEDINGS

Vol. VI / Pg. 1- 218  
Skopje, 2023

**UDK 674-045.431(062)**  
**684.4(062)**

**ISBN 978-608-4723-05-9**

#### Published

Ss. Cyril and Methodius University - Skopje  
Faculty of Design and Technologies  
of Furniture and Interior – Skopje

#### Dean

**Gjorgji Gruevski, Ph.D.**

#### Organizers:

Ss. Cyril and Methodius University - Skopje  
Faculty of Design and Technologies  
of Furniture and Interior – Skopje  
INNOVAWOOD -Brussels

### PROGRAMME COMMITTEE

**Neno Trichkov** Ph.D. (Bulgaria), **Mathieu Petrissans**, Ph.D. (France), **Leonidha Peri**, Ph.D. (Albania), **Tanja Palijsa**, Ph.D. (Serbia), **Vladimir Jambrekovi** , Ph.D (Croatia), **Svetlana Tereshchenko**, Ph.D. (Russia), **Holta Cota**, Ph.D. (Albania), **Maja Moro**, Ph.D. (Croatia), **Lidia Gurau**, Ph.D. (Romania), **Salah -Eldien Omer**, Ph.D. (Bosnia and Herzegovina), **Josip Istvani** , Ph.D. (Croatia), **Igor Dzinci** , Ph.D. (Serbia), **Zhivko Gochev**, Ph.D. (Bulgaria), **Alan Antonovi** , Ph.D. (Croatia), **Michal Rogozinski**, Ph.D. (Poland), **Minka Cehi** , Ph.D. (Bosnia and Herzegovina), **Julia Mihajlova**, Ph.D. (Bulgaria), **Goran Mili** , Ph.D. (Serbia), **Nencho Deliiski**, Ph.D. (Bulgaria), **Zdravko Popovi** , Ph.D. (Serbia), **Mihaela Campean**, Ph.D. (Romania), **Peter Niemz**, Ph.D. (Switzerland), **Gradimir Danon**, Ph.D. (Serbia), **Branko Glavonji** , Ph.D. (Serbia), **Olga Popovi Larsen**, Ph.D. (Denmark), **Ottaviano Allegretti**, Ph.D. (Italy), **Milan Shernek**, Ph.D. (Slovenia), **Manja Kitek Kuzman**, Ph.D. (Slovenia), **Suleyman Korkut**, Ph.D. (Turkey), **Nadir Ayrilmis**, Ph.D. (Turkey), **Samet Demirel**, Ph.D. (Turkey), **Branko Rabadjiski**, Ph.D. (North Macedonia), **Konstantin Bahchevandjiev**, Ph.D.(North Macedonia), **Borche Iliev**, Ph.D. (North Macedonia), **Zoran Trposki**, Ph.D. (North Macedonia), **Nacko Simakoski**, Ph.D. (North Macedonia), **Zhivka Meloska**, Ph.D. (North Macedonia), **Vladimir Karanakov**, Ph.D.(North Macedonia), **Vladimir Koljozov**, Ph.D. (North Macedonia), **Mira Stankevick Shumanska**, Ph.D. (North Macedonia), **Gjorgji Gruevski**, Ph.D. (North Macedonia), **Elena Nikoljski Panevski**, Ph.D. (North Macedonia), **Violeta Jakimovska Popovska**, (North Macedonia), **Goran Zlateski**, Ph.D. (North Macedonia).

### ORGANIZING COMMITTEE

**Zoran Trposki**, Ph.D. (North Macedonia), **Nacko Simakoski**, Ph.D.(North Macedonia), **Goran Zlateski**, Ph.D. (North Macedonia), **Dime Gjorgiev**, Dipl.ing. (North Macedonia), **Marija Trpkovska**, (North Macedonia), **Katerina Lembovska** (North Macedonia)

#### Editor-in-chief

**Goran Zlateski**, Ph.D.

#### Publisher address:

Faculty of Design and Technologies of  
Furniture and Interior  
Ul. 16 Makedonska Brigada br. 3, PO box 223, 1000 Skopje  
Republic of North MACEDONIA



## CONTENTS

ADHESION STRENGTH OF COATINGS ON WOOD ( <i>Keynote lecture</i> ) Tanja Palija .....	1
WOOD WASTE IN THE SAWMILL INDUSTRY OF WOOD PROCESSING Ana Marija Stamenkoska, Goran Zlateski .....	12
INVESTIGATION OF THE DEPENDENCE OF THE CUTTING POWER AND SURFACE ROUGHNESS ON THE PROCESSING MODE Damjan Stanojevi .....	19
THE PHOTOVOLTAIC SYSTEM AS A PART OF ENERGY PRODUCTION IN THE WOOD INDUSTRY IN SERBIA Mladen Furtula .....	26
ASSESSING SEAR STRAIN DISTRIBUTION IN WOOD UNDER IMPACT USING DIGITAL IMAGE CORRELATION METHOD Mojtaba Hassan Vand, Jan Tippner .....	33
INFLUENCE OF THERMAL MODIFICATION SCHEDULES ON THE NATURAL WEATHERING OF MAPLE AND ASH Marko Veizovi , Goran Cvjetanin, Nebojša Todorovi , Ranko Popadi , Goran Mili .....	40
PROCEDURE OF OPTIMIZING SOLID OAK WOOD ( <i>Quercus robur</i> L.) BENDING PROCESS IN FURNITURE MANUFACTURE Mislav Mikšik, Stjepan Pervan, Silvana Prekrat, Mladen Brezovi .....	45
PARAMETER DETERMINATION AND PERFORMANCE COMPARISON OF THE RHEOLOGICAL MODELS FOR CREEP IN PARTICLEBOARD Mira Miri -Milosavljevi , Vladislava Mihailovi , Marija Turkovi , Sr an Svrzi .....	54
METROLOGY OF THE GEOMETRIC CHARACTERISTICS OF MORTISE AND TENON JOINTS THROUGH GEOMETRIC PRODUCT SPECIFICATION (GPS) STANDARDS Nikola Mihajlovski, Gjorgji Gruevski .....	66
LOADBEARING STRUCTURES FROM RECLAIMED WOOD-STRATEGIES, DESIGN PARAMETERES AND REFLECTIONS Olga Popovic Larsen, Xan Browne .....	77
THE SOUND SIGNAL PROCESSING AND DEEP LEARNING NETWORK AS A TOOLS FOR DETERMINING THE CIRCULAR SAW BLADE SPEED Sr an Svrzi , Mladen Furtula, Marija Turkovi , Vladislava Mihailovi , Aleksandar Dedi .....	88



SPATIAL FLEXIBILITY IN TRADITIONAL MACEDONIAN ARCHITECTURE FROM THE 19 <sup>TH</sup> CENTURY Branko Temelkovski .....	96
HARDNESS OF PLYWOOD REINFORCED WITH FIBERGLASS PREPREG Violeta Jakimovska Popovska, Borche Iliev .....	106
IN-PLANE COMPRESSIVE STRENGTH OF PLYWOOD REINFORCED WITH COTTON PREPREG Violeta Jakimovska Popovska, Borche Iliev .....	111
BENDING STRENGTH AND MODULUS OF ELASTICITY IN BENDING OF BEECH AND BLACK PINE PLYWOOD Violeta Jakimovska Popovska, Borche Iliev .....	118
DETERMINATION OF THE HEAT ENERGY FOR HYDROTHERMAL TREATMENT OF ASHWOOD ( <i>Fraxinus excelsior</i> ) BY LOG SOAKING Ana Marija Stamenkoska, Goran Zlateski .....	125
IMPACT OF FEED RATE ON ROUGHNESS OF THE CUT SURFACE, DURING CUTTING DRY BEECH WOOD WITH A CIRCULAR SAW Anastasija Temelkova.....	134
ANALYSIS OF THE INFLUENCE OF CONSUMERISM ON THE EPHEMERALITY OF THE INTERIORS OF PUBLIC FACILITIES Edona Arifi Sadiku .....	141
THE INFLUENCE OF PARTICLEBOARD SQUARENESS ON THE EDGE BONDING QUALITY Igor Džini , Tanja Palija .....	157
INFLUENCE OF THE MATERIAL FROM WHICH THE PROFILE IS MADE ON THE FINAL QUALITY OF THE WINDOW Elena Jevtoska, Gjorgi Gruevski .....	163
THE INFLUENCE OF COMPUTER SOFTWARE INTENDED FOR CONSTRUCTIVE PREPARATION ON THE TIME FOR THE PRODUCTION OF THE NECESSARY TECHNICAL DOCUMENTATION IN A MICRO-ENTERPRISE FOR THE PRODUCTION OF CUSTOM-MADE FURNITURE Marija Krstev .....	169
IMPACT OF FEED RATE ON ROUGHNESS OF THE CUT SURFACE, DURING CUTTING DRY SPRUCE WOOD WITH A CIRCULAR SAW Anastasija Temelkova.....	180
DEVELOPMENT OF DISCOLORATION DURING CONVENTIONAL DRYING OF OAK TIMBER Bogdan Bukara, Goran Mili .....	187
THE INFLUENCE OF THE QUALITY OF POPLAR LOGS ON THE YIELD IN THE PRODUCTION OF VENEER PACKAGING Aleksandar Lovri , Vladislav Zdravkovi , Nebojša Todorovi , Stefan Milovanovi .....	193



LIGNOCELLULOSE COMPOSITION, PROXIMATE ANALYSIS AND  
HEAT VALUE OF CERTAIN FOREST AND ENERGY CROP  
BIOMASSES AND THEIR POTENTIAL AS RAW MATERIALS  
FOR THE PRODUCTION OF SOLID BIOFUELS

Božidar Matin, Ana Matin, Ivan Brandi , Alen urovi ,  
Josip Ištvan , Alan Antonovi .....

200

ANALYSIS OF HEAT AND STEAM CONSUMPTION DURING  
ARTIFICIAL CONVECTIVE DRYING OF OAK SAWN TIMBER  
OF DIFFERENT THICKNESS

Goran Zlateski, Ana Marija Stamenkoska, Zoran Trposki, Vladimir Koljozov, Branko Rabadjiski .....

210

## ADHESION STRENGTH OF COATINGS ON WOOD

(Keynote lecture)

**Tanja Palija**

*University of Belgrade, Faculty of Forestry, Serbia*

*e-mail: tanja.palija@sfb.bg.ac.rs*

### ABSTRACT

In wood surface finishing coatings present the basic material that is used to protect the surfaces of the final wood products, while preserving or improving its aesthetic characteristics. The coating market is constantly evolving offering improved coatings formulations in terms of environmental eligibility and/or decorative and protective properties. However, the upgraded characteristics of chosen coatings does not mean much if an adequate adhesion between the coatings and the substrate is not achieved. For this reason, the adhesion strength of coating can be considered a key parameter of the quality of a coated wood surface.

This paper explores the possibilities and limitations of different methods of testing the adhesion strength of the coatings on the wood surface.

Further, the impact of the properties of the coated system components (substrate and coatings), both native and the ones that are result of different surface finishing operations (preparation of the substrate, staining, application and drying of the coatings) on the adhesion strength of coatings on wood, was analyzed.

**Keywords:** adhesion strength, wood, coatings

### 1. INTRODUCTION

The wood coating market is constantly evolving offering improved coatings formulations in terms of environmental eligibility (e.g. bio-based coatings, low-VOC coating and powder coatings etc.) and/or decorative and protective properties of coated surface (e.g. anti-fingerprint effect, antibacterial coating, nano UV coating etc.). However, the quality of bond between coating and the substrate still remains the most valuable characteristic of coated surface, since refined properties of coatings become irrelevant if an adequate adhesion between the coatings and the substrate is not achieved.

Adhesion is often used as a measure of the interaction between the coating and the substrate. The main purpose of the adhesion testing methods is to prove if the bond between the layers of coatings and the substrate is sufficient for the use of wood product. The development of testing methods for adhesion strength of coating enables comprehensive perception of the interaction between coatings and wood-based substrates. But at the same time, the use of different methods can lead to misconceptions when interpreting the results of the adhesion strength of coatings on wood and wood-based panels.

There are numerous factors that affect the adhesion of the coating on the wood surface. These factors should not be studied separately, due to connection between components of wood-coatings system; meaning that the change in one component will affect the other components of the system (in some extent).

It is important to understand that the adhesion of the coating can change over time, so knowing the factors needed to achieve sufficient bonding between coating and the substrate is important, but usually not enough. The failure in adhesion of coating can be related to loss of connection between the substrate and the base coating or between individual layers of the coatings. In general, the adhesion of

the coating system to wood surface is mainly conditioned by the adhesion between the primer coating and the substrate (Pavli , Petri , Žigon, 2021). Generally, the first signs of the failure are seen only under the microscope, which highlights the importance of knowing the mechanism of failure of adhesion in wood-coatings system.

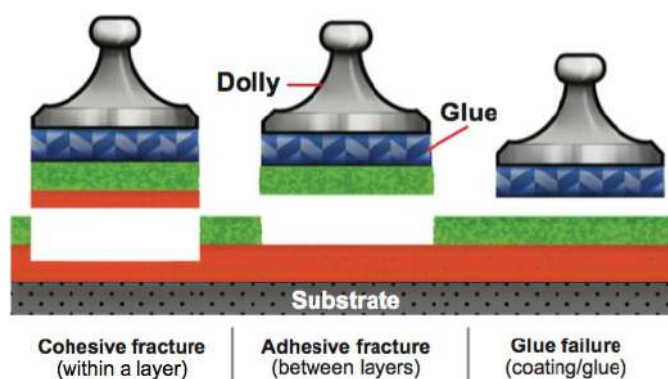
## 2. METHODS FOR TESTING ADHESION STRENGTH OF COATING ON WOOD

The methods for evaluation of adhesions strength of coating are numerous. The most commonly used adhesion strength tests in wood surface finishing are: cross-cut test, pull-off test and scratch test. Each of the named test methods has its advantages and disadvantages, which is why often several standardized methods are needed for the comprehensive assessment of coating adhesion strength on wood and wood-based panels (Palija et al. 2013). Also, alternative adhesion strength test for coatings and other surface lining on wood and wood-based panels are being develop and used in practice.

The cross-cut (cross-hatch) test is based on visual assessment of the damages of coated surface that was cut in the form of a grid. This method is quick and inexpensive, and thus practical for the companies that do not have laboratories, because it is possible to assess the adhesion strength of the coating accurately enough by using only a razor blade. One of the disadvantages of this method is the subjective evaluation of the adhesion strength of coating, based on the observer judgment. A much greater deficiency of this method is the lack of sensitivity for the differences in the adhesion strength for the contemporary coatings used in the wood industry. Namely, most of today's coating formulations will have a rating 0 or 1 (maximum 2) when the coating is applied on wood or wood-based panels (0 is the higher rating – no visible defects; 5 is the lowest rating – the lattice is highly impaired).

The pull-off test, on the other hand, measures the force needed to detach the coating glued to the dolly from the coated substrate in the vertical direction. This method gives a clear difference in the adhesion strength of different coating formulations. There is no standard for expected pull-off strength for each type of coating applied to various substrates (<https://www.defelsko.com/resources/finish-coatings-system-adhesion-and-test-methods>). Based on our researches, as well as data found in literature the expected values of adhesion strength for the most coatings used today in wood industry are from about 1 MPa (for nitrocellulose coatings acc. Ozdemir and Hiziroglu 2007) to about 8 MPa. However, although polyurethane coatings are expected to have higher adhesion values, it is not possible to assume that all polyurethane coating formulations will express the same tension resistance. This method is not recommended for determination of the adhesion of coatings on soft and porous substrates, since failure occurs within the substrate (test result actually shows the strength of the cohesive bonds within the substrate). This means that there are limitations of using this method for wood-based panels (chipboards and fiberboards) as well as for solid wood substrates with lower mechanical properties (thermo treated wood (Palija, Mili , et al. 2018) or wood species of low density (e.g. Paulownia acc. to Jai , Dobi , Palija, 2010). This deficiency can be circumvented to some extent by examining the so-called wet adhesion strength of coatings on “weak substrate”. In comparison to standard pull-off test this method uses water (poured into the groove around the dolly) to loosen the adhesion strength of coating on substrate below the cohesive bonds in wood (so the coating can be detached from the surface of substrate). It should also be noted that EN standard for testing adhesion strength of coating by pull-off test (EN 4624), requires the nature of the fracture to be recorded for each measurement (in percentage of fracture at different layers of substrate-coatings-glue system, Figure 1). This leads to the conclusion that not all test results obtained using this method are comparable, if fracture occurs in different zones of the coated surface. Another disadvantage of this method is the acting direction of the force during testing (perpendicular to the substrate), which is rarely the direction of the load during the use of final product.





**Figure 1:** Preview of different zones of fracture within testing of pull-off strength of coating (<https://www.defelsko.com/resource-pages/positest-at-visual-analysis-and-recording-of-test-results>)

The Table 1 shows the results of the adhesion strength of nitrocellulose, polyurethane and water-based coatings on cherry (Palija, Jai, Jai, 2013) and spruce wood (Palija et al., 2013).

**Table 1:** Comparison between adhesion strength of nitrocellulose (NC), polyurethane (PU) and water-based (WB) coatings measured on spruce and cherry samples by cross-cut and pull-off test (Jai, Palija, 2012; Palija et al., 2013)

Wood species	Type of test	Type of coating		
		NC	PU	WB
spruce	Cross-cut	1.67	1	1
	Pull-off (MPa)	2.43	3.72	4.50
cherry	Cross-cut	1	0.67	1
	Pull-off (MPa)	3.01	6.96	7.91

The results of research presented in the Table 1 (Jai, Palija, 2012; Palija et al., 2013) show a difference of 75.8% in adhesion strength of water-based coating by pull-off test between spruce and cherry wood, although the results of adhesion test of the same samples by cross-cut test were equal. On the other hand, a significant difference in the adhesion strength of the nitrocellulose coating (of almost one unit) measured by the cross-cut test between spruce and cherry wood, gave a difference in adhesion strength of coatings by pull-off test of 23.8%.

Table 2 shows the results of the adhesion strength of different formulations of the top urethane coating on spruce and oak samples, that confirm more precise evaluation of the adhesion strength of the coating on wood substrate when using the pull-off method in relation to the cross-cut method (Jai, Palija, 2012).

**Table 2:** Comparison between adhesion strength of polyurethane, acrylic-isocyanate and alkyd-urethane coating

Wood species	Type of test	Type of coating		
		Polyurethane coating	Acrylic-isocyanate coating	Alkyd-urethane coating
spruce	Cross-cut	1	0.33	0.33
	Pull-off (MPa)	3.35	3.72	3.76
oak	Cross-cut	1	0	0
	Pull-off (MPa)	5.18	5.45	5.49

The scratch (scrape) test evaluates the adhesion strength of the coating by determining the force that leads to the scraping of the coating system by stylus or loop from the substrate. With this test

method, the coated surface is exposed to stress that is expected to arise during use. However, the question is whether the resistance to an external force can guarantee sufficient adhesion between the internal layers of the coatings and wood. This scratch test is usually considered to be indirect method for evaluation of the adhesion of the coatings. The resistance to scratching is related to mechanical properties of the coating system, since the value of the force needed to break through the substrate depends on the hardness of the coating and blade itself.

In the previous research of the mechanical properties of UV acrylic and polyurethane coating on paulownia, force needed to break through the coating system (resistance to scratching) for the samples that was rated with 1 in cross-cut test, was in very wide range (from 4 to 8 N) (Jai , Dobi , Palija, 2010).

Other test methods include the peel test, which is often used in parquet production (since the peeling of adhesion tape simulate the removing of the protective foil from the coated parquet during painting of the walls).

### **3. FACTORS AFFECTING THE ADHESION STRENGTH OF COATING**

Factors that affect the adhesion strength of the coating on wood and wood-based panels are: properties of the liquid coating and properties of the substrate in surface layer. The formulation of the coating mainly determines the bonding mechanism of the coating to the substrate. Although adhesion is mainly based on the combined effect of various mechanisms, specific bonding mechanisms are dominant for certain types of coatings. For example, for the coatings that cure only by physical evaporation of the solvent (e.g. nitrocellulose coatings), the key mechanism of adhesion is mechanical interlocking of coating and surface layer of substrate.

In terms of the properties of coating, viscosity has a key influence on the adhesion. As the viscosity decreases, the coating easily penetrates into the substrate surface leaving a lower thickness of the coating on the surface of the substrate. The influence of the penetration on the adhesion strength of the coating is not linearly dependent, but it is known that the coating penetration is a necessary prerequisite for good adhesion between the coating and the substrate. The penetration of coating into the wood surface layer is also affected by binder type, pigmentation, solid matter content and drying speed appeared (de Meijer, Thurich, Militz, 1998). In previous research (de Meijer, Militz, 2000) acrylic and water-based alkyd coatings had the lowest wet adhesion strength values on white pine and spruce samples, which corresponded to the lowest penetration depth; while alkyd coatings based on organic solvents and "high-solids" alkyd coatings, with the highest penetration depth had the highest wet adhesion values. On the other hand, the higher penetration depth of water-based and polyurethane coating into thermo treated samples of ash and maple wood did not lead to increase of adhesion strength of both types of coatings in comparison to untreated samples (Palija, Mili , et al., 2018). This finding can be related to the test method, since due to the sensitivity of the substrate (thermo treated wood) the adhesion strength of coatings was evaluated by cross-cut method, which is not precise enough, as was shown previously.

The reduction in viscosity can occur during thinning of the coating and/or increase of temperature. The increase of temperature can be caused by the lack of controlled working conditions in the coating booths or by the recirculation of the coating in application machines (spraying machines, roller coaters, curtain coaters, flowcoaters, vacuum coaters). For example, an increase in the temperature of the liquid top coating (from 24.1 to 24.8 °C) caused a decrease in the viscosity (from 18.6 to 17 s, DIN 4 20°C) and a significant reduction in dry film thickness of UV-acrylic top coating applied by roller coater on industrial UV finishing line (Palija, Jai , et al., 2018). In this case, the decrease in the thickness of the dry film thickness of coating caused by the decrease in viscosity was dependent on the position of the samples on the transporter (the distance from the reservoir filled with the coating).

In relation to formulation of coating, higher adhesive strength of solvent-based compared to the water-based polyurethane coating was found on ash and hornbeam samples (Mikle i et al., 2022). Among the properties of dry coating, it was found that coatings with higher tensile strength and hardness, and lower flexibility had higher coating adhesion (Pavli , Petri , Žigon, 2021).

Among the properties of the substrate that can impact the adhesion strength of coating of importance are those in the wood surface layer. Some of these properties are a direct consequence of the wood structure, while the others can be result of the surface preparation of the substrate. The wood anatomical structure and porosity affect the penetration depth of liquid materials. In research on spruce and white pine samples, a higher penetration depth of water-based acrylic coatings into the earlywood resulted in up to 50% higher values of wet adhesion strength (de Meijer, Militz, 2000). In previous research (Palija, Džin i , Vu i evi , 2021) the dry film thickness of the water-based coating was significantly lower on walnut compared to beech samples. This result could be related to the anatomical structure of walnut wood, since the surface roughness of the walnut samples after coating with hydro oils remained unchanged. Filling of surface structural depressions (cut open tracheids) could be the reason for obtaining lower values of dry film thickness of walnut in comparison to beech samples. On the other hand, due to high coefficient of volumetric swelling of beech wood, wetting and lifting of the fibers in the surface layer in contact with water from the coating, reduced the space available for the coating, and thus a higher thickness of the coating film was obtained. In other research, higher penetration of water-based and polyurethane coating in samples of thermally modified maple wood in relation to thermally modified ash wood was related to higher quantity and easier accessibility of vessels in the maple samples (Palija, Mili , et al., 2018).

The penetration pathway of coating into the surface layer of wood is different for hardwoods and softwood. The surface free energy of the wood determines its wettability, which can have impact on the adhesion strength of applied base coating. In the comparison between hardwoods and softwoods, higher values of adhesion strength are expected on hardwood samples. This is confirmed by a comparison of the adhesion strength testing of nitrocellulose, polyurethane and water-based coatings on cherry and spruce samples. (Palija et al., 2013; Palija, Jai , Jai , 2013). The measurement of adhesion strength of different formulations of urethane coatings on spruce and oak wood (Table 2) showed that the wood specie has a decisive impact on the adhesion strength of the coating (Jai , Palija, 2012). The density of the wood has a positive effect on the adhesion strength of the coating (Palija, 2015). Accordingly, a 22% higher adhesion strength of the water-based UV polyurethane/polyacrylic coating was recorded on maple compared to spruce samples (Riedl et al., 2013). In other research, significantly higher values of coating adhesion strength (from 27 to 39%) of different types of urethane coatings were measured on oak in comparison to spruce samples (Jai , Palija, 2012).

Excessive moisture content in wood can result in poor adhesion of the coatings (Kúdela, Liptáková, 2006). This is in agreement with the previous research (Sönmez, Budakçı, Pelit, 2011) where the increase in wood moisture content (from 12 to 15 %) led to lower adhesion strength of the nitrocellulose coating (on white pine, beech and oak samples) and water-based coating (on beech samples); as well as test results (Ozdemir, 2009) where with the increase in wood moisture content (from 7.5 to 14.5%), a significant decrease in the adhesion strength of the cellulose and polyurethane coating was observed (on white pine, spruce, beech and chestnut samples). However, knowing that wood surface finishing is usually one of the last steps in the manufacturing process of wood products, the moisture content of the wood is expected to be low (6-10% for the interior and 10-12(15)% for the exterior). When it comes to water-based coatings, research on samples of beech and white pine showed that wood moisture content (8, 12 and 15%), as well as the wood species, are not statistically significant parameters in the assessment of the adhesion strength of the coating (Sönmez, Budakçı, Pelit, 2011).

Sanding is the most commonly used method for the preparation of the wood before application of the coatings. By sanding the surface roughness is reduced, lowering the contact area between the coating and the substrate, and thus the adhesion strength of the coatings (primarily the ones based on mechanical interlocking principal of adhesion). But this does not mean that surface roughness and adhesion strength are interdependent. The effect of surface roughness on coating adhesion strength has

also been noted for coatings that do not cure purely physically. In research on the ash samples (Vitosyte, Ukvalbergiene, Keturakis, 2012), the highest values of the adhesion strength of the acrylic/polyurethane coating were measured in samples that had the highest surface roughness. In the same research, no clear relation was found between the surface roughness and the adhesion strength of the acrylic/polyurethane coating on birch samples. Increased surface roughness initiated by greater grain raising in low density species, affect wetting properties of wood (Salca et al., 2016). The correlation between surface roughness parameters of wood and adhesion strength of UV-curing polyurethane coating was confirmed on maple wood (de Moura, Hernández, 2005).

On the other hand, lowering the value of roughness beyond the limits of structural roughness of wood leads to filling the pores and smoothing off the surface of the wood, causing blocking of the potential penetration paths for the coating. At the microscopic level, compression and deformation of the cells of the surface layer occur, along with defibrillation of the cell walls (Palija, 2015). As wood dust fills the lumens and reduces the penetration of the coating (de Meijer, Thurich, Militz, 1998), the bonds between the coating and the ash wood became weaker (Vitosyte, Ukvalbergiene, Keturakis, 2012). In the same research, uniformity in the structure of the earlywood and latewood in samples of birch wood may lowered the compression and filling up of surface cells with sanding dust and therefore resulted in higher adhesion strength of coating on samples with lower roughness (that were sanded with higher grits of sanding belts).

On contrary, it was concluded that higher values of adhesion of water-based coatings can be achieved when the wood surface is smoother (Landry, Pierre, 2012). The adhesion of the water-based acrylic coating on spruce samples was improved due to the smaller depth of damage in the surface layer and the greater degree of fibrillation of the cell walls during finer sanding. (Cool, Hernandez, 2011). This phenomena was explained by lowered risk of the formation of mechanically weakened layer that can impair adhesion. On the contrary, there are studies whereas the adhesion strength of water-based coatings on beech samples decreases with the surface roughness decreases (Palija et al., 2014). These disagreement may be related to the differences in structure and properties of the used wood species.

When analyzing the effect of roughness on coating adhesion, it is necessary to take into account the structure of the damage that occurs in the surface layer during wood processing, which depends on the preparation regime parameters. The open lumens of the cut maple wood cells in surface layer provided deeper penetration for the UV-curable polyurethane coating in planed samples compared to sanded ones (de Moura, Hernández, 2005). Nevertheless, regardless of the better wetting and greater penetration depth of the coating into the planed samples, the higher adhesion strength in this research was shown in the sanded samples. The authors assumed that at the boundary layer between the wood and the coating, a composite was formed consisting of polymer particles of the coating and parts of microfibrils that were torn from the wood during the sanding process. This is called a mechanical weak boundary layer between the surfaces of the materials in contact, at the level of particles (the order of size from 0.001 to 1mm acc. to Stehr, Johansson, 2000).

In addition, a chemical weak boundary layer can be formed by various low molecular weight impurities on the boundary surface of the material in contact, at the molecular level (of the order of size from 0.1 to 1nm acc. to Stehr, Johansson, 2000). For example, it is known that extractives can migrate to the surface of wood and impact the adhesion of the coating and decorative properties of coated surface. Also, the impurities can originate from the coating itself. A higher or lower degree of polymer crystallinity in the boundary layer, or a different orientation of chemical groups can lead to the formation of a chemical weak boundary layer (Sandlund, 2004).

Before application of a coating, different decorative treatments of the wood are usual, affecting the adhesion strength of coating. The effect of staining of wood on adhesion strength of coating depends of the type of applied stain and the type of coating. For example, the application of water stain lead to

an increase in roughness in the surface layer on spruce and cherry samples, which favors the adhesion of nitrocellulose coatings and polyurethane coatings; while it had no effect on the adhesion of water-based coatings (Palija et al., 2013; Palija, Jai , Jai , 2013). The type of stain (water or nitro stain) had an effect on the adhesion strength of the nitrocellulose and polyurethane coating on the cherry samples, but not in the case of and water-based coatings (Palija, Jai , Jai , 2013). This confirms that the increase in the contact surface area is important for the adhesion of the coatings for which mechanical anchoring is the basic mechanism of adhesion.

The influence of bleaching on the adhesion strength of the coating system can be observed not only through roughness, but also chemical changes observed through variation in surface tension. In research of (Ozdemir, Hiziroglu, 2007) all of the bleached, stained and preservative treated samples had higher adhesion strength than control samples of spruce, yellow pine, beech, and chestnut.

Application system had an important impact on the adhesion strength of 100% UV coating applied on alder wood samples (Salca et al., 2016). This finding was explained by differences in quality (uniformity and consistency) of coated surfaces when coating was applied by manual spraying and roller coater.

#### 4. FAILURE IN ADHESION

Insufficient adhesion strength of coating is considered one of the most important failure of a coated surface, since the coating loses its protective function, leaving the substrate exposed to the negative environmental factors (Palija, 2020). The absence of adequate bonds between the coating and the substrate can occur during the film formation of the coating (becomes apparent right after curing). One of the common reason of the insufficient bonding between coating and the substrate in contact, are obstacles in wetting of the substrate (Figure 2).



*Figure 2: Problem in the wetting of the water-based base coating by the following epoxy coating (Palija, 2020)*

On the other hand, the adequate adhesion between the coating and the substrate can be partially or completely weakened and even broken during the use of the coated surface. This is especially pronounced when it comes to intensive environmental conditions, e.g. in case of coated surfaces in the exterior. It is known that wood changes its dimensions in relation to moisture, consequently coating system should be flexible enough to overcome the developed stress and maintain its structure and homogeneity. In opposite, failure in coated wood will occur in forms of cracks, flakes, blisters or peeling. Accordingly, it was concluded that elastic modulus must be taken into account for adequate selection of the coating for the use of wood in exterior (Podgorski, de Meijer, Lanvin, 2017).

It is often neglected that not only wood is changes its dimensions in relation to moisture, but the coating film as well. Swelling/shrinkage of coatings can be both higher and lower than swelling/shrinkage of wood, but the difference is that wood swelling will not be the same in all anatomical directions, while dimensional changes of coatings will, due to its isotropic properties (de Meijer, 2002). The dimensional change of the coating in the longitudinal direction will generally be

larger than that of the wood. This means that a positive, contractive stress acts in this direction. In radial or tangential direction, the type of stress depends on whether the dimensional change of the coating is larger or smaller than that of the wood (de Meijer, Nienhuis, 2009).

The cracks are usually caused by the combined effect of an insufficiently elastic coating film on dimensionally unstable substrates. Firstly, the cracks are formed in the base layer of the coating that cannot follow the swelling/shrinkage of the wood. If the top layer of the coating is applied to an insufficiently elastic base layer, the cracks will eventually spread through the subsequent layers of the coating, due to uneven tension between the inner and outer layers of wood-coating system (Dvořák et al., 2023). Line-type cracks in the coating film on a wood substrate usually occur in places where the rate of swelling and shrinkage of the wood is pronounced, for example along the line of the earlywood and latewood, especially in wood species with expressed difference in density between these two zones. A special type of cracks are “breaks” in the coating film that follow the joining line of wood elements in the construction of the product (e.g. finger joints or patches used instead of protruding knots with different orientations of wood fibers, different moisture content, insufficient amount of applied adhesive etc.) (Figure 3a). Irregularly shaped cracks (that do not follow the direction of the wood fibers) most often indicate lack of elasticity of the film of coating (Figure 3b).



**Figure 3:** Cracks: a) along finger joint on the window frame; b) caused by low elasticity of the coating film (Palija, 2020)

The brittleness of the coating can be provoked by external conditions. This usually happens on the coated surfaces in the exterior under the influence of the sun IR radiation, with an increase in the glass transition temperature of the polymer in the coating. Dark coatings show a tendency to crack due to a significantly higher heating temperature, compared to light coatings.

In the first phase, adhesion problems between individual components of the coated surface may remain unnoticed. The presence of bubbles on the coated surface, show the disconnection of certain areas of the coating film. When the moisture is trapped under the coating, water bubble may form under the film of coating (Figure 4a) leading to graduated loss of adhesion (Rowell, Bongers, 2017). In the next phase, an insufficiently strong connection between the components of the substrate/coating system can be manifested by the cracking of the film, which leads to the final stage of loss of adhesion in the form of flaking (Figure 4b) and peeling of the film or chalking (in case of pigment coating). The formation of flakes is triggered by water, trapped in bubbles at the boundary surface between the coating and the substrate, which evaporates leading to bursting of the bubbles into a flakes (large number of small pieces).



**Figure 4:** Failure in adhesion: a) water bubbles; b) flaking of the coating (Palija, 2020)

If the coated wood will be used in an environment with unstable humidity, it is necessary to reduce the swelling and shrinkage of wood and to use a highly elastic coating. "Stiffening" of the wood can be achieved by sealing the end grains, due to the pronounced absorption in the axial direction. It is similar with wood-based panels, where the narrow sides enable potential paths for the moisture transport. When connecting wooden elements, it is necessary to match the orientation of the wood fibers at the joining line. If the construction of the final product requires a joint where the orientation of the fibers of one element is perpendicular to the orientation of the fibers of another element (e.g. the connection of vertical and horizontal element in frames), it is necessary to enable a change in the dimensions of the wood by choosing a system of fitting so that the stress of the joint does not exceed the limit value determined by elasticity of coating (Palija, 2020).

## 5. CONCLUSION

Ensuring an adequate adhesion strength between the coating and the wood substrate is the key aspect of quality of wood surface finishing. To achieve adequate adhesion strength of coating, it is necessary to know the properties of the substrate and the coating material, as well as the conditions of use of the final product. If the parameters of the environment are relatively constant, the achieved adhesion between coating and the substrate, can considered to be stable. However, in intense conditions (e.g. high humidity and/or temperature), and especially in case of fluctuating conditions of use, it is necessary to predict how the components of wood-coatings system will act, to achieve a stable enough bond between the coating and the substrate.

In terms of testing methods, within the established wood finishing process, the inexpensive testing methods based on the subjective assessment of the adhesion strength are usually sufficient. On the other hand, if it is needed to make a choice of a coating that firmly bonds with the substrate, it is necessary to use test methods that will give a precise value of the adhesion strength (especially for products that will be used in conditions of increased humidity). Within these methods, special care should be taken when testing the adhesion strength of the coating on mechanically weak substrates (e.g. thermo treated wood, chipboard and fiberboards, etc.), to prevent the results of the cohesive failure within the substrate to be interpreted as the adhesion strength of the coating.

The preparation of the substrate must be coordinated with the structure of the substrate and the properties of the material that will be applied to it. Preparation of the substrate by sanding gives a clean and fresh surface (in mechanical and chemical sense), which is a prerequisite of adequate adhesion of coating on wood and wood-based panels. Generally, if penetrating materials are being used, it is necessary to enable penetration in the surface layer of wood and wood-based materials (with finer grit sanding). On the other hand, coatings that form a film require for the cut cells in the surface layer of wood to be filled (especially for ring porous wood, where trapped air can lead to later defects).

## REFERENCES

- [1] Cool, J., Hernandez, R. E. (2011): Improving the Sanding Process of Black Spruce Wood for Surface Quality and Water-Based Coating Adhesion. *Forest Products Journal*, 61(5), 372–380.
- [2] de Meijer, M. (2002): Mechanisms of Failure in Exterior Wood Coatings. 3th International Woodcoatings Congress Paint Research Association, paper 40, 1–18.
- [3] de Meijer, M., Militz, H. (2000): Wet adhesion of low-VOC coatings on wood A quantitative analysis. *Progress in Organic Coatings*, 38, 223–240.
- [4] de Meijer, M., Nienhuis, J. (2009): Influence of internal stress and extensibility on the exterior durability of wood coatings. *Progress in Organic Coatings*, 65(4), 498–503.
- [5] de Meijer, M., Thurich, K., Militz, H. (1998): Comparative study on penetration characteristics of modern wood coatings. *Wood Science and Technology*, 32(5), 347–365.
- [6] de Moura, L. F., Hernández, R. E. (2005): Evaluation of varnish coating performance for two surfacing methods on sugar maple wood. *Wood and Fiber Science*, 37(2), 355–366.
- [7] Dvořák, O., Sarvašová Kvietková, M., Šimůnková, K., Machanec, O., Pánek, M., Pastierovi, F., Lin, C. F., Jones, D. (2023): The Influence of the Initial Treatment of Oak Wood on Increasing the Durability of Exterior Transparent Coating Systems. *Polymers*, 15(3251), 1–15.
- [8] Jai, M., Dobi, J., Palijs, T. (2010): The influence of surface finishing of Paulownia Siebold et Zucc. on the mechanical properties of lacquered surface. *Glasnik Sumarskog Fakulteta*, 102, 7–23.
- [9] Jai, M., Palijs, T. (2012): Uticaj vrste drveta i sistema površinske obrade na adheziju premaza. *Zaštita Materijala*, 53(4), 299–303.
- [10] Kúdela, J., Liptáková, E. V. A. (2006): Adhesion of coating materials to wood. *Journal of Adhesion Science and Technology*, 20(8), 875–895.
- [11] Landry, V., Pierre, B. (2012): Surface Preparation of Wood for Application of Waterborne Coatings. *Forest Products Journal*, 62(1), 39–45.
- [12] Mikleš, J., Lonari, A., Veseli, N., Jirouš-Rajkovi, V. (2022): Influence of Wood Surface Preparation on Roughness, Wettability and Coating Adhesion of Unmodified and Thermally Modified Wood. *Drvna Industrija*, 73(3), 261–269.
- [13] Ozdemir, T. (2009): Influence of surface roughness and species on bond strength between the wood and the finish. *Forest Products Journal*, 59(6), 90–94.
- [14] Ozdemir, T., Hiziroglu, S. (2007): Evaluation of surface quality and adhesion strength of treated solid wood. *Journal of Materials Processing Technology*, 186, 311–314.
- [15] Palijs, T. (2015): The impact of polyelectrolyte on interaction between wood and water-borne coatings. University of Belgrade; Faculty of Forestry.
- [16] Palijs, T. (2020): Wood surface finishing. Defects in finishing.
- [17] Palijs, T., Džini, I., Vučević, I. (2021): Decorative properties of wood surface finishing with oils and hydro oils. *International Journal - Wood, Design & Technology*, 10(1), 83–90.
- [18] Palijs, T., Jai, D., Jai, M. (2013): Uticaj bajcovanja drveta trešnje (*Prunus avium* L.) na adheziju premaza. *Zaštita Materijala*, 4, 396–403.
- [19] Palijs, T., Jai, M., Džini, I., Šušur, A., Dobi, J. (2018): Variability of dry film thickness of a coating applied by roller coater on wood in a real industrial process. *Drewno*, 61(201).
- [20] Palijs, T., Jai, M., Šušur, A., Dobi, J. (2014): The impact of wood properties affected by sanding on the gloss of lacquered surfaces. *PTF BPI - Processing Technologies for the Forest and Bio-Based Products Industries*, 608–615.
- [21] Palijs, T., Milić, G., Schabel, T., Djikanović, D. (2018): The impact of temperature increase rate during thermal modification on wood surface-coating interaction. *Living with Modified*



- Wood: COST Action FP1407, Understanding Wood Modification through an Integrated Scientific and Environmental Impact Approach (ModWoodLife) : Book of Abstracts, 72–73.
- [22] Palija, T., Vučković, A., Jevtić, P., Jaić, M. (2013): The Impact of Wood Staining on the Adhesion of Certain Types of Coating. In I. Grbac, S. Pervan, & S. Prekrat (Eds.), 24th International Scientific Conference Wood Is Good User Oriented Material, Technology And Design (pp. 111–119). Faculty of Forestry, Zagreb University.
- [23] Pavlić, M., Petrić, M., Žigon, J. (2021): Interactions of coating and wood flooring surface system properties. *Coatings*, 11(1), 1–13.
- [24] Podgorski, L., de Meijer, M., Lanvin, J. D. (2017): Influence of coating formulation on its mechanical properties and cracking resistance. *Coatings*, 7(10), 1–11.
- [25] Riedl, B., Angel, C., Prigent, J., Blanchet, P., Stafford, L. (2013): Wood Surface Modification by Atmospheric-Pressure Plasma and Effect on Waterborne Coating Adhesion. *Lignocellulose*, 2(1), 292–306.
- [26] Rowell, R., Bongers, F. (2017): Role of moisture in the failure of coatings on wood. *Coatings*, 7(12), 3–11.
- [27] Salca, E.-A., Krystofiak, T., Lis, B., Mazela, B., Proszkyk, S. (2016): Some Coating Properties of Black Alder Wood as a Function of Varnish Type and Application Method. *BioResources*, 11(3), 7580–7594.
- [28] Sandlund, A. B. (2004): A study of wood adhesion and interactions using DMTA. Luleå University of Technology.
- [29] Sönmez, A., Budakçı, M., Pelit, H. (2011): The effect of the moisture content of wood on the layer performance of water-borne varnishes. *Bioresources*, 6(3), 3166–3178.
- [30] Stehr, M., Johansson, I. (2000): Weak boundary layers on wood surfaces. *Journal of Adhesion Science & Technology*, 14(10), 1211–1224.
- [31] Vitosyte, J., Ukvalbergiene, K., Keturakis, G. (2012): The Effects of Surface Roughness on Adhesion Strength of Coated Ash (*Fraxinus excelsior* L.) and Birch (*Betula* L.) Wood. *Materials Science (MEDŽIAGOTYRA)*, 18(4), 347–351.
- [32] <https://www.defelsko.com/resources/finish-coatings-system-adhesion-and-test-methods>
- [33] <https://www.defelsko.com/resource-pages/positest-at-visual-analysis-and-recording-of-test-results>
- [34] EN ISO 4624: Paints and varnishes. Pull-off test for adhesion
- [35] EN ISO 2409: Paints and varnishes. Cross-cut test
- [36] ISO 1518-1: Paints and varnishes — Determination of scratch resistance — Part 1: Constant-loading method

**Authors' Address:**

D.Sc. Tanja Palija, Associate Professor

University of Belgrade, Faculty of Forestry, Kneza Višeslava 1, 11030 Serbia

## WOOD WASTE IN THE SAWMILL INDUSTRY OF WOOD PROCESSING

Ana Marija Stamenkoska, Goran Zlateski

Ss. Cyril and Methodius University in Skopje, North Macedonia,  
Faculty of Design and Technologies of Furniture and Interior-Skopje  
email: stamenkoska@gmail.com; zlateski@fdtme.ukim.edu.mk

### ABSTRACT

Sawmill processing produces a certain amount of waste, as a result of processing sawlogs into sawn lumber. Waste occurs in the form of fine and coarse waste. Fine and coarse waste are generated on the primary milling machine (band saw) and on the circular saws for transversal and longitudinal lumber cutting. In addition to fine and coarse waste, sawdust also occurs as waste, but due to its specificity, it is not quantified.

This paper presents results obtained from several years of research, conducted in five sawmill capacities. The researched capacities were at the territory of the Republic of North Macedonia. The data was gathered under manufacturing conditions.

The wood species covered in the paper are beech (*Fagus sylvatica* L.), pine (*Pinus sylvestris*, *Pinus nigra*), oak (*Quercus sessiliflora*), aspen (*Populus tremula* L.) and fir/spruce (*Abies alba*/*Picea excelsa*). The results indicate that beech has the highest percentage of total waste, and fir/spruce has the lowest percentage of total waste.

**Keywords:** processing, lumber, sawmill, wood waste, fine and coarse waste, relative values

### 1. INTRODUCTION

The industry of sawmill processing produces certain amount of waste, alongside the processed sawn lumber. This waste occurs as coarse and fine waste.

Coarse waste consists of sawlog lids, cut outs and cut offs from transversal and longitudinal trimming of the sawn lumber.

Fine waste appears in the form of sawdust, small chippings of wood and dust that can be found in the air. The air dust occurs from the woodworking machinery and it is not quantified in the total amount of waste.

Coarse and fine waste are often associated with a product with no value, which is not the case. This kind of waste has a strong impact on the complex yield of the sawlogs. In modern technology of sawlogs processing, the wood waste is defined with the expressions "wooden residue" or "by-product" (Brežnjak, 1974).

In classic conception of sawlogs processing, the mean values for the total waste are: for beech  $O = 36,00\%$ , for oak  $O = 42,00\%$ , for softwood species  $O = 28,00\%$ , for hardwood species  $O = 32,00\%$  and for fir/spruce  $O = 29,00\%$  (Brežnjak, 2000).

This paper presents results obtained from several years of research carried out in five sawmill capacities in the Republic of North Macedonia.

The results are defined by relative values.

### 2. AIM OF RESEARCH AND EXPERIMENTAL METHODS

Considering the title of the paper, the aim was to analyze the waste composed as a result of sawlogs processing into lumber. The waste was analyzed as a substantial part of the quantitative yield of the wood material.

The obtained data is expressed with relative values and was processed with classic mathematical formulas, but also with the use of statistical calculations, to confirm the accuracy of the results.

The classification of logs is carried out in accordance with the EN 1316-1:2013 standard. The sawlogs processing and measurement of the sawn lumber is carried out in accordance with the standards M EN 1313-2:2010 and M EN 1312:2010.

### 3. RESEARCH FACILITIES AND MATERIALS

This research was carried out in the following five sawmills in the Republic of North Macedonia:

- 1) "Alpinewood", municipality of Tetovo,
- 2) "Ilinopromet", municipality of Kavadarci,
- 3) "Markisto", municipality of Ohrid,
- 4) "Takovski - MAT", municipality of Berovo and
- 5) "Tri Reki", municipality of Berovo.

In the time period of research in the "Alpinewood" sawmill, in terms of wood species, the research was focused on beech, pine, aspen, oak, walnut and chestnut. In "Ilinopromet" sawmill, the analysis was focused on beech and pine. The research carried out in "Markisto" sawmill was oriented towards beech, fir/spruce and walnut. Beech, pine and oak were analyzed in "Takovski - MAT" sawmill. The fifth object of research was the company "Tri Reki" and the observed species were beech, pine, aspen, oak and fir/spruce.

The amount of annually processed sawlog mass, according to wood species, is shown in table 1.

*Table 1: Annual sawlogs mass in the research facilities*

Wood species	Beech (m <sup>3</sup> /y)	Pine (m <sup>3</sup> /y)	Aspen (m <sup>3</sup> /y)	Oak (m <sup>3</sup> /y)	Fir/Spruce (m <sup>3</sup> /y)	Walnut (m <sup>3</sup> /y)	Chestnut (m <sup>3</sup> /y)
Sawmill							
1) „Alpinewood“	2 400	100	1 500	35	/	35	35
2) „Ilinopromet“	3 450	1 100	/	/	/	/	/
3) „Markisto“	800	/	/	/	100	40	/
4) „Takovski - MAT“	500	1 500	/	500	/	/	/
5) „Tri Reki“	3 000	3 000	400	1 000	1 500	/	/

From the data presented in table 1, it can be concluded that beech logs prevail in all 5 five sawmill capacities. For beech, the quantity of processed logs ranges from 500 to 3 000 m<sup>3</sup>/year. Pine is in the range of 100 to 3 000 m<sup>3</sup>/year, aspen from 400 to 1 500 m<sup>3</sup>/year, oak from 35 to 1000 m<sup>3</sup>/year, fir/spruce from 100 to 1 500 m<sup>3</sup>/year and walnut and chestnut from 35 to 40 m<sup>3</sup>/year.

Figure 1 shows fine waste, and figure 2 shows coarse waste.



*Figure 1: Fine waste*



*Figure 2: Coarse waste*

### 4. RESULTS AND DISCUSSION

According to the research data, the processed sawlogs in the sawmill capacities was from beech, pine, aspen, oak, fir/spruce, walnut and chestnut.

Table 2 shows the results for fine, coarse and total waste, for beech, for each of the five sawmill capacities.

**Table 2: Wood waste for beech sawlogs**

Sawmill	Log length	Log diameter	Quality class	Fine waste	Coarse waste	Total waste
	$l$ (m)	$d$ (cm)	$K$	$1$ (%)	$2$ (%)	(%)
1	2,0 ÷ 4,0	30,0 ÷ 75,0	I/II	11,40	33,90	45,30
2				12,50	33,20	45,70
3				11,70	31,13	42,83
4				11,80	27,20	39,00
5				11,40	30,43	41,83

From the data given in table 1, it can be concluded that the diameter of the logs is in the range of 30,0 to 75,0 cm, the logs length is in the range of 2,0 to 4,0 m. The logs belonged to 1st and 2nd quality class. Fine waste ranges from 11,40 to 12,50 %. Coarse waste is in the range of 27,20 to 33,90 %. The total waste is from 39,00 to 45,70 %.

The statistically processed data is shown with a frequency polygon (Figure 3), on which graphical values for the wood waste in the analyzed sawmills are given for a better overview. The equation is a straight line and has the form  $y = ax + b$ . For fine waste,  $y = 11,97x + 11,47$ , and the correlation coefficient is  $r = 0,978$ . For coarse waste,  $y = 33,84x + 29,13$ , and the correlation coefficient is  $r = 0,927$ . The total waste is expressed by the equation  $y = 45,54x + 40,46$ , and the coefficient is  $r = 0,946$ . The coefficient of determination  $r$  is high in all the three cases, which indicated a very strong correlation between the values.

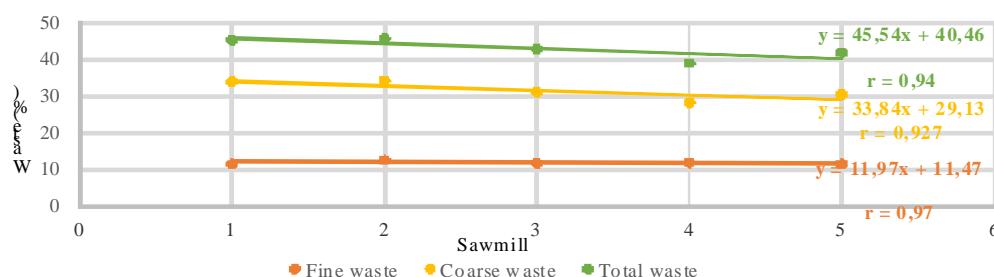
**Figure 3: Wood waste for beech sawlogs - statistics**

Table 3 shows the results for fine, coarse and total waste for pine sawlogs.

**Table 3: Wood waste for pine sawlogs**

Sawmill	Log length	Log diameter	Quality class	Fine waste	Coarse waste	Total waste
	$l$ (m)	$d$ (cm)	$K$	$O_1$ (%)	$O_2$ (%)	(%)
1	3,0 ÷ 6,0	25,0 ÷ 75,0	I/III	11,06	17,60	28,66
2				9,65	20,52	30,17
4				9,34	22,70	32,04
5				10,30	18,83	29,13

From table 3 it can be concluded that the diameter of the logs is from 25,0 to 75,0 cm, the logs length ranges from 3,0 to 6,0 m. Logs were graded within 1st, 2nd and 3rd quality class. Fine waste ranges from 9,34 to 11,06 %. Coarse waste is from 17,60 to 22,70 %. The total waste ranges from 28,66 to 32,04 %.

The statistically processed data is shown on a frequency polygon (Figure 4), on which graphical values for the wood waste in the analyzed sawmills are given for a better overview. The equation is a straight line and has the form  $y = ax + b$ . For small waste, the equation has the form  $y = 10,73x + 9,74$ , and the correlation coefficient is  $r = 0,951$ . For coarse waste, the equation has the form

$y = 19,41x + 20,44$ , and the coefficient is  $r = 0,974$ . The total waste is expressed by the equation  $y = 29,18x + 30,32$ , and the correlation coefficient is  $r = 0,980$ .

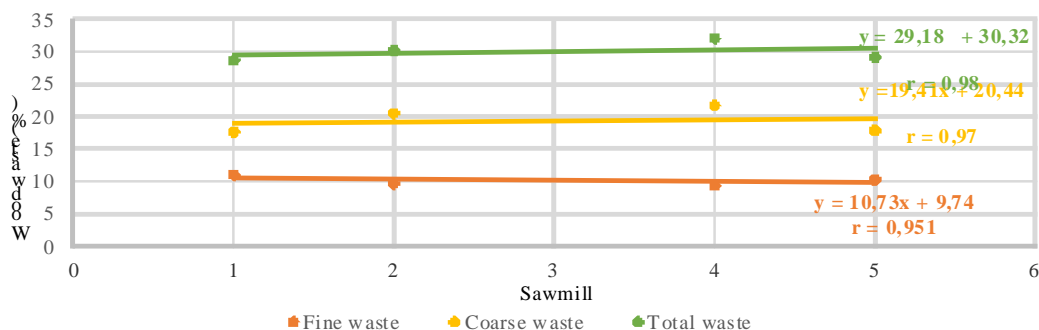


Figure 4: Wood waste for pine sawlogs – statistics

Table 4 shows the results for fine, coarse and total waste for oak sawlogs.

Table 4: Wood waste for oak sawlogs

Sawmill	Log lenght	Log diameter	Quality class	Fine waste	Coarse waste	Total waste
	$l$ (m)	$d$ (cm)	$K$	$O_1$ (%)	$O_2$ (%)	$O$ (%)
1.	3,0 ÷ 4,0	30,0 ÷ 70,0	I/III	10,66	15,76	26,42
4.				11,60	23,40	35,00
5.				10,90	26,30	37,20

From table 4 it can be concluded that the diameter of the logs is from 30,0 to 70,0 cm, the logs length ranges from 3,0 to 4,0 m. Logs belonged to 1st, 2nd and 3rd quality class. Fine waste ranges from 10,66 to 11,60 %. Coarse waste is in the range of 15,76 to 26,30 %. The total waste ranges from 26,42 to 37,20 %.

The statistically processed data is shown on a frequency polygon (Figure 5), on which graphical values for the wood waste in the analyzed sawmills are given for a better overview. The equation is a straight line and has the form  $y = ax + b$ . For fine waste,  $y = 10,78x + 10,81$ , and the correlation coefficient is  $r = 0,997$ . For coarse waste,  $y = 16,03x + 26,8$ , and the coefficient is  $r = 0,776$ . The total waste is expressed by the equation  $y = 26,81x + 38,13$ , and the correlation coefficient is  $r = 0,838$ .

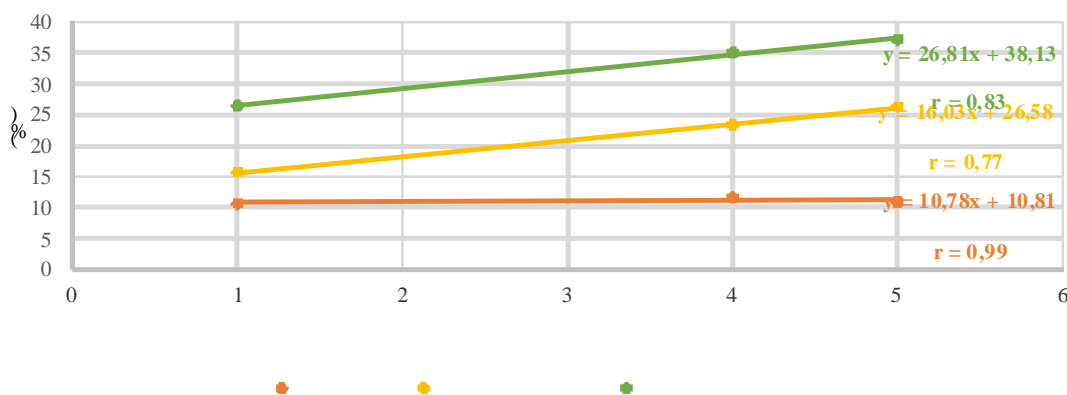


Figure 5: Wood waste for oak sawlogs - statistics

Histograms were used for a better overview of the results of the research conducted on aspen and fir/spruce sawlogs. The histograms show the values for fine, coarse and total waste distributed by different sawmills.

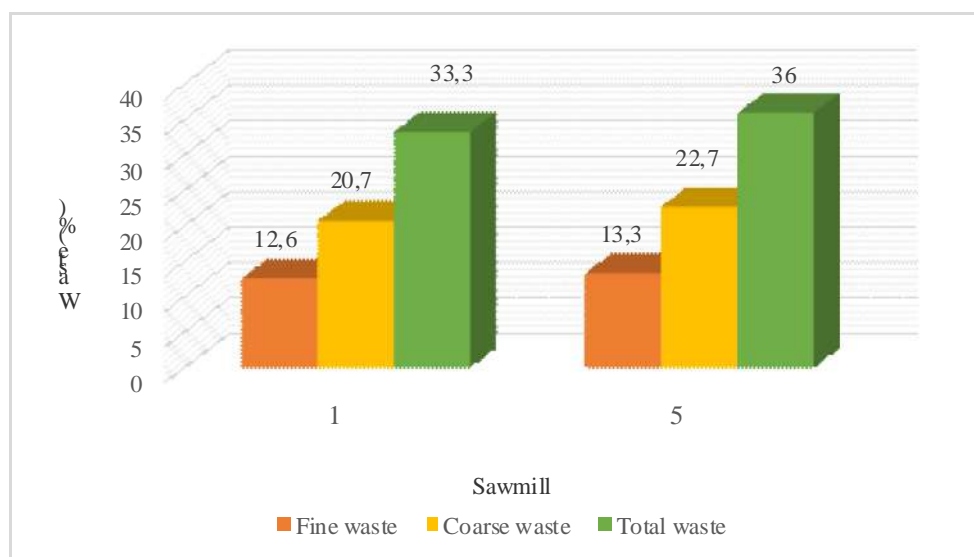
Table 5 shows the values for wood waste for aspen sawlogs.

**Table 5:** Wood waste for aspen sawlogs

Sawmill	Log lenght	Log diameter	Quality class	Fine waste	Coarse waste	Total waste
	<i>l</i> (m)	<i>d</i> (cm)	<i>K</i>	<i>O</i> <sub>1</sub> (%)	<i>O</i> <sub>2</sub> (%)	<i>O</i> (%)
1.	2,0 ÷ 4,0	25,0 ÷ 85,0	I/II	12,60	20,70	33,30
5.				13,30	22,70	36,00

The diameter of aspen logs ranges from 25,0 to 80,0 cm. The logs length of the ranges from 2,0 to 4,0 m. Logs belong to 1st and 2nd quality class.

From the histogram shown in Figure 6, it can be concluded that: fine waste ranges from 12,60 to 13,60 %, coarse waste ranges from 20,70 to 22,70 % and total waste is from 33,30 to 36,00 %.



**Figure 6:** Wood waste for aspen sawlogs - statistics

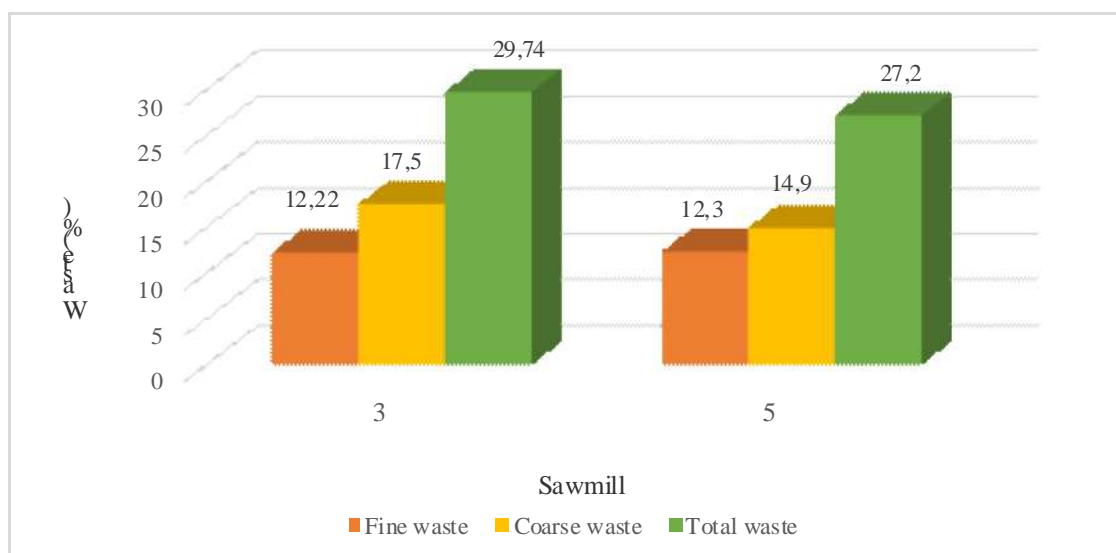
Table 6 shows values for fir/spruce sawlogs.

**Table 6:** Wood waste for fir/spruce sawlogs

Sawlogs	Log lenght	Log diameter	Quality class	Fine waste	Coarse waste	Total waste
	<i>l</i> (m)	<i>d</i> (cm)	<i>K</i>	<i>O</i> <sub>1</sub> (%)	<i>O</i> <sub>2</sub> (%)	<i>O</i> (%)
3	3,0 ÷ 6,0	30,0 ÷ 65,0	I/III	12,22	17,50	29,74
5				12,30	14,90	27,20

The diameter of the fir/spruce logs was in the range 30,0 to 65,0 cm. The log length ranges from 3,0 to 6,0 m. Logs belong to 1st, 2nd and 3rd quality class.

The values for fine, coarse and total waste are shown graphically in Figure 7. Fine waste is in the range of 12,22 to 12,30 %. Coarse waste is in the range of 14,90 to 17,50 %. The total waste is in the range of 27,20 to 29,70 %.



**Figure 7:** Wood waste for fir/spruce – statistics

## 5. CONCLUSIONS

Wood waste is an inevitable phenomenon in the technology of sawlogs processing into sawn lumber. The waste occurs in the form of fine (sawdust) and coarse.

The paper presents the results of experimental research carried out in five sawmills in the territory of the Republic of North Macedonia. The results refer to the amount of fine, coarse and total waste. The waste results are shown with relative values.

Based on what was presented in this paper, the following conclusions can be drawn:

1) Facilities - sawmills in which the research was carried out:

- "Alpinewood" municipality of Tetovo,
- "Ilinopromet", municipality of Kavadarci,
- "Markisto", municipality of Ohrid,
- "Takovski - MAT, municipality of Berovo and
- "Tri Reki", municipality of Berovo.

The values for the analyzed wood species are shown as follows:

2) For beech

- Fine waste:  $O_1 = 11,40 \div 12,50 \%$ ;  $y = 11,97x + 11,47$ ;  $r = 0,978$ .
- Coarse waste:  $O_2 = 27,20 \div 33,90 \%$ ;  $y = 33,84x + 29,13$ ;  $r = 0,927$ .
- Total waste:  $O = 39,00 \div 45,70 \%$ ;  $y = 45,54x + 40,46$ ;  $r = 0,946$ .

3) For pine

- Fine waste:  $O_1 = 9,34 \div 11,06 \%$ ;  $y = 10,73x + 9,74$ ;  $r = 0,951$ .
- Coarse waste:  $O_2 = 17,60 \div 22,70 \%$ ;  $y = 19,41x + 20,44$ ;  $r = 0,974$ .
- Total waste:  $O = 28,66 \div 32,04 \%$ ;  $y = 29,18x + 30,32$ ;  $r = 0,980$ .

4) For oak

- Fine waste:  $O_1 = 10,66 \div 11,60 \%$ ;  $y = 10,78x + 10,81$ ;  $r = 0,997$ .
- Coarse waste:  $O_2 = 15,76 \div 26,30 \%$ ;  $y = 16,03x + 26,58$ ;  $r = 0,776$ .
- Total waste:  $O = 26,42 \div 37,20 \%$ ;  $y = 26,81x + 38,13$ ;  $r = 0,838$ .

5) For aspen

- Fine waste:  $O_1 = 12,60 \div 13,60 \%$
- Coarse waste:  $O_2 = 20,70 \div 22,70 \%$
- Total waste:  $O = 33,30 \div 36,00 \%$

6) For fir/spruce

- Fine waste:  $O_1 = 12,22 \div 12,30 \%$
- Coarse waste:  $O_2 = 14,90 \div 17,50 \%$
- Total waste:  $O = 27,20 \div 29,70 \%$

## REFERENCES

- [1] Brežnjak, M. (1974). Otpadak – ostatak – nusproizvod. *Drvena industrija*, 25 (7 – 8), p. 152 – 155.
- [2] Brežnjak, M. (2000). *Pilanska tehnologija drva, II dio*. Zagreb: Fakultet šumarstva i drvne tehnologije Sveu ilište u Zagrebu, Republika Hrvatska.
- [3] Rabadziski, B., Zlateski, G., Trposki, Z., Koljozov, V. (2016). Analysis of diameters and taper of diameter of beech logs in I/III class of quality. *International Scientific Journal, Wood, Design & Technology*, 4 (1), Faculty of Design and Technologies of furniture and interior, Skopje, Republic of North Macedonia, p. 24 – 31.
- [4] Zlateski, G., Rabadziski, B. (2002). Raspredelba na vlagata podebelina na okrajcena bi ena gragja od smr a. Godišen zbornik na Šumarski fakultet, p. 35 – 40.
- [5] Macedonian standards:
  - EN 1312:2010
  - EN 1313-2:2010
  - EN 1316-1:2013
- [6] Rabadziski, B. (2019). *Pilanska tehnologija na drvoto (zbirka zadaci)*. Skopje: Univerzitet „Sv. Kiril i Metodij“, Fakultet za dizajn i tehnologii na mebel I enterier, Republika Severna Makedonija.
- [7] Rabadziski, B. (2019). *Pilanska tehnologija na drvoto*. Skopje: Univerzitet „Sv. Kiril i Metodij“, Fakultet za dizajn i tehnologii na mebel I enterier, Republika Severna Makedonija.

### **The Authors' Address:**

Ana Marija Stamenkoska, MSc, PhD candidate at the Department of Primary Wood Processing, Faculty of Design and Technologies of Furniture and Interior-Skopje, Ss. Cyril and Methodius University, 16-ta Makedonska brigada 3, 1000, Skopje, Republic of North Macedonia.

Goran Zlateski, PhD, full professor at the Department of Primary Wood Processing, Faculty of Design and Technologies of Furniture and Interior-Skopje, Ss. Cyril and Methodius University, 16-ta Makedonska brigada 3, 1000, Skopje, Republic of North Macedonia.



## INVESTIGATION OF THE DEPENDENCE OF CUTTING POWER AND SURFACE ROUGHNESS ON THE PROCESSING MODE

**Damjan Stanojevi**

*Academy of Technical-Educational Vocational Studies,  
Department of Vranje, Serbia  
e-mail: damjan.stanojevic@akademijanis.edu.rs*

### ABSTRACT

Processing quality is considered one of the significant limiting parameters in maximizing the performance of woodworking machines. Regardless of the type of processing and its perfection, it is not possible to create a detail so that it "ideally" corresponds to the dimensions marked on the corresponding drawing. Newly created surfaces when cutting wood are never perfectly smooth, whether they are flat or curved.

The importance of the quality of the cut surface for practice is extremely high. It is not only about the aesthetic appearance of the surface obtained by cutting, but even more the consequences that a rough or wavy cut has on the value of the product. First of all, a rough or wavy cut results in a greater loss during planing, because a thicker layer must be removed in order to achieve a smooth surface. This means that post-processing creates more waste, and thus costs increase. The cleanliness of the cut depends on many factors. They are on the one hand related to the blade and its work in wood, and on the other hand to the type of blade and the machine that drives it. Knowledge of these factors indicates what should be paid attention to in wood processing when using various blades and machines, in order to achieve the highest possible cleanliness of the cut, less waste and thereby increase the value of the manufactured goods, and at the same time reduce production costs

In practice, the most important thing is to achieve a result, and it is also very important that the entire technological process of wood processing is done with the lowest possible costs. A large part of these costs is the consumption of power for cutting. There are many influencing factors on which power consumption depends. These are: the material being processed, the material from which the tool is made, the geometry of the tool, the speed of the main movement, the feed rate, etc.

In order to conduct a preliminary experimental investigation of the movement of cutting power and roughness of the cut surface as dependent variables depending on the processing mode and the size of bluntness of the tool as independent variables, an experiment was carried out at the Faculty of Forestry in Belgrade. The experiment was supposed to provide answers to questions concerning the choice of processing modes that have a different impact on the quality of the cut surface as well as on the consumption of cutting power.

**Keywords:** Cutting power, cut surface quality, processing mode, circular saw

### 1. INTRODUCTION

In practice, the most important thing is to achieve a result, and it is also very important that the entire technological process of wood processing is done with the lowest possible costs. A large part of these costs is the consumption of power for cutting. There are many influencing factors on which power consumption depends. These are: the material being processed, the material from which the tool is made, the geometry of the tool, the speed of the main movement, the feed rate, etc.

Processing quality is considered one of the significant limiting parameters in maximizing the performance of woodworking machines. Regardless of the type of processing and its perfection, it is not possible to create a detail so that it "ideally" corresponds to the dimensions marked on the corresponding drawing. Newly created surfaces when cutting wood are never perfectly smooth, whether they are flat or curved. Criteria that characterize the quality of the processed surface are surface roughness, waviness, accuracy of processing, tuftedness and fringes.

Better knowledge of the cutting process greatly affects the improvement of the quality of the machined surface, machining accuracy, economy and productivity. The quality of the processed surface, processing accuracy and energy consumption represent a constant challenge in the research of cutting tools with the aim of achieving their optimal ratio. A large number of influencing factors and their interactions are present in every processing process, so it is extremely difficult to theoretically reliably determine the optimal parameters.

For this reason, the application of experiments and the analysis of the results thus obtained are indispensable in the development of new and improvement of existing processing processes and systems. In a large number of experiments, a connection between two or more variables is observed. By forming a suitable mathematical model, the influence of independent factors on dependent variables can be defined, that is, the values of the parameters that figure in the mathematical model can be determined.

The main goal of this research is to show, describe and analyze the correlation between input factors, which achieves the required quality of processing with optimal consumption of cutting power. It is very important to determine the correlation between the selected influencing factors (speed of auxiliary movement, size of protrusion of the circular saw, dullness of the tool) on the one hand and cutting power and quality of the processed surface on the other hand.

Also, one of the goals of the research is that the results of the research contribute to a better understanding of wood cutting with a circular saw through the development of a model for analyzing the quality of the processed surface and cutting power. The goal is also to determine the real possibilities and limitations of obtaining a high quality surface when combining different influencing parameters.

## 2. MATERIAL AND METHODS

To investigate the dependence of cutting power and surface roughness on the processing mode, appropriate boards were selected, then planing was performed on a planer and a thicknesser, and samples of straight fibers, without knots and cracks, measuring 1100 mm × 30 mm × 150 mm were made from these boards. After that, the samples are labeled and each of them has its own label. Uninfected, defect-free, average porosity and density material was selected for testing. The assortments, which were subjected to tests, are marked with codes and are shown in Figure 1.

After that, six tubes measuring 50x50x30 mm were marked and cut on each board, three on each side of the board. Each test tube has a corresponding code (eg test tubes cut from the 4th board are coded D4f1, D4f2, D4f3, D4f4, D4f5 and D4f6). Test tubes for testing physical properties are shown in Figure 2.



**Figure 1:** Raw material for research



**Figure 2:** Test tubes physical properties

Experimental methods used:

- a method of indirect measurement of the power required for cutting using a measuring-acquisition device developed at the Faculty of Forestry in Belgrade,
- quantitative (contact) method for determining the roughness of the cut surface

After determining the physical properties of the boards that were cut in order to examine the effect of the processing mode on the quality of the cut, the cutting power was measured at certain processing modes. Immediately after cutting, the roughness was measured for each processing mode.

Processing modes are determined by the following parameters that represent independent variables:

- ✓ **TW** – (Tool Wearing) – Tool wear – Tool dullness size [ $\mu\text{m}$ ].]

The research was carried out while cutting with a sharp saw (Tool wear rate TW1).

- ✓ **u** – Auxiliary movement speed [m/min].]

The research was carried out at speeds of auxiliary movement  $u_1=4$  m/min,  $u_2=8$  m/min and  $u_3=12$  m/min.

- ✓ **h** – Protrusion of the saw in relation to the workpiece [mm].]

The research was carried out with the dimensions of the protrusion of the saw in relation to the object of work of  $h_1=10$  mm,  $h_2=20$  mm and  $h_3=30$  mm.

The research was carried out at a number of revolutions of  $n=3940$  min<sup>-1</sup>, that is, at a constant speed of the main movement  $V = 61.86$  m/s according to the schedule shown in the table 1.

*Table 1: Schedule of processing modes by work items*

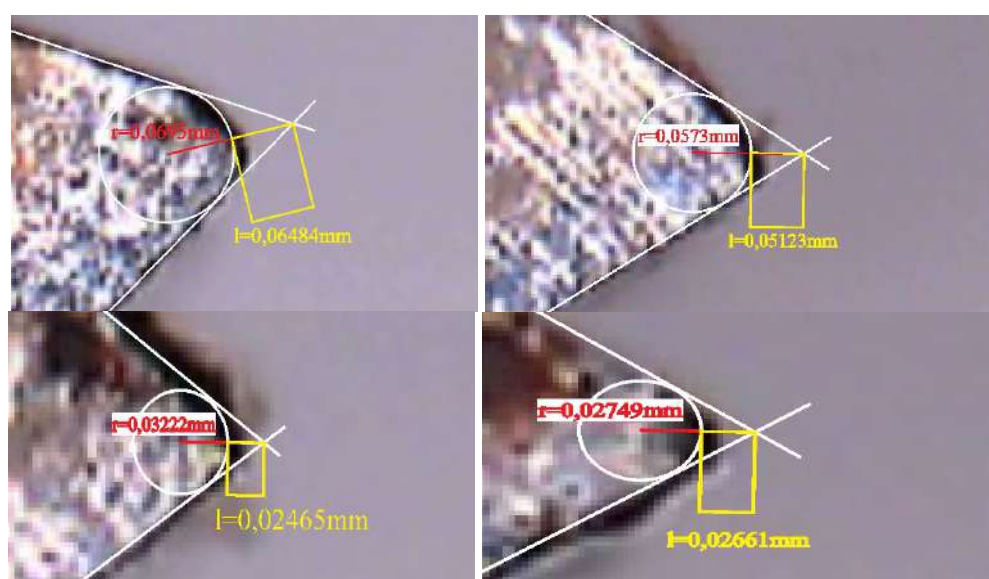
Processing mode	Designation of the subject of work	Description of the work subject
U1H1TW1	D2	Radial - partially twisted fibers
U1H2TW1	D5	Radial - straight fibers
U1H3TW1	D7	Radial - straight fibers
U2H1TW1	D8	Radial - partially twisted fibers
U2H2TW1	D9	Radial - straight fibers
U2H3TW1	D11	Radial - straight fibers
U3H1TW1	D14	Radial-tangential
U3H2TW1	D19	Radial - straight fibers
U3H3TW1	D20	Tangential

Legend: U1=4m/min; U2=8m/min; U3=12m/min; H1=10mm; H2=20mm; H3=30mm;

Tool dullness was measured using a Supereyes digital microscope, in which two parameters were measured on each blade:

- ✓ distance between ideal and real blade,
- ✓ radius of rounding of the blade

Figure 3 shows all four blades with quantified tool wear bluntings TW1.



*Figure 3: Blades with quantified tool wear blunting TW1*

Eight cuts were made for each treatment mode, so that a total of 72 cuts were made. At each cut, the cutting power was measured through the engaged power of the drive electric motor using the SRD1 measurement-acquisition device intended for laboratory and industrial measurements of cutting power on wood processing machines and wood-based boards with a three-phase drive electric motor.

The device collects, analyzes and displays the obtained data. The device uses the Power Expert software package.

Figure 4 shows a screenshot of the recorded data, and Figure 5 shows the device for measuring roughness

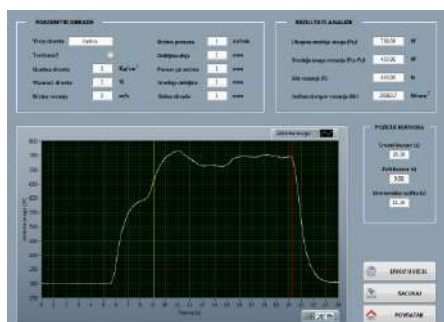


Figure 4: Screen display of recorded data



Figure 5: Mitutoyo roughness meter

### 3. RESULTS

Table 2 gives the bluntness values of four blades that are spaced at equal distance from each other around the circumference of the circular saw.

Table 2: Tool wear values

	Blade 1	Blade 2	Blade 3	Blade 4
l [mm]	0,06484	0,05123	0,02465	0,02661
r [mm]	0,0695	0,0573	0,03222	0,02749

Legend: l - the distance between the ideal and the real blade [mm]  
r - blade radius [mm]

Diagram 1 shows the movement of the average value of cutting power depending on the processing mode. Diagram 2 shows the movement of the standard deviation of the cutting power depending on the processing mode.

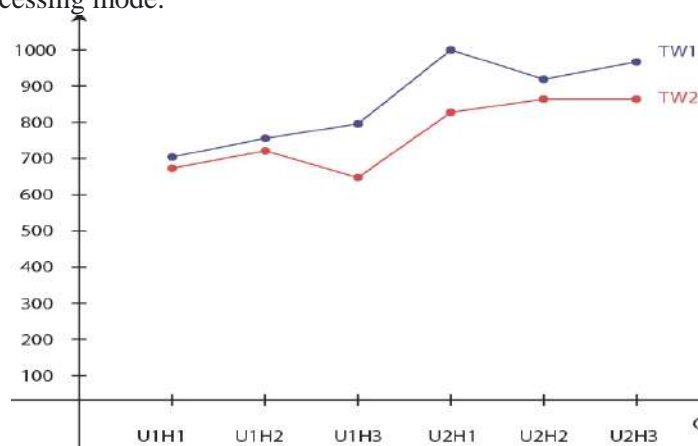
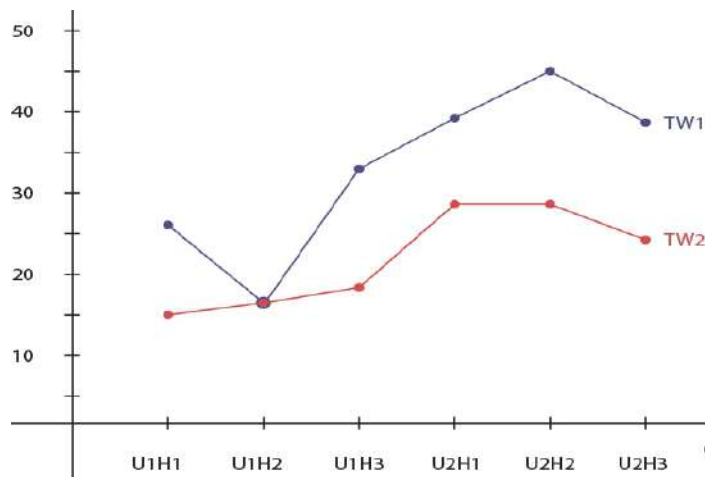
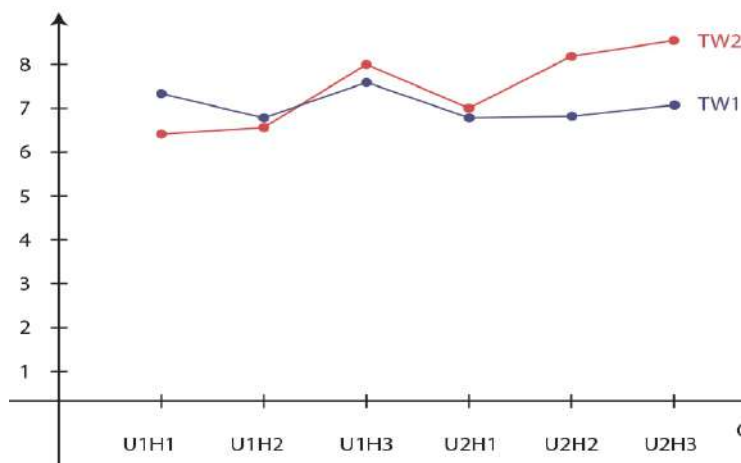


Diagram 1: Diagram of the movement of the average value of cutting power depending on the processing mode

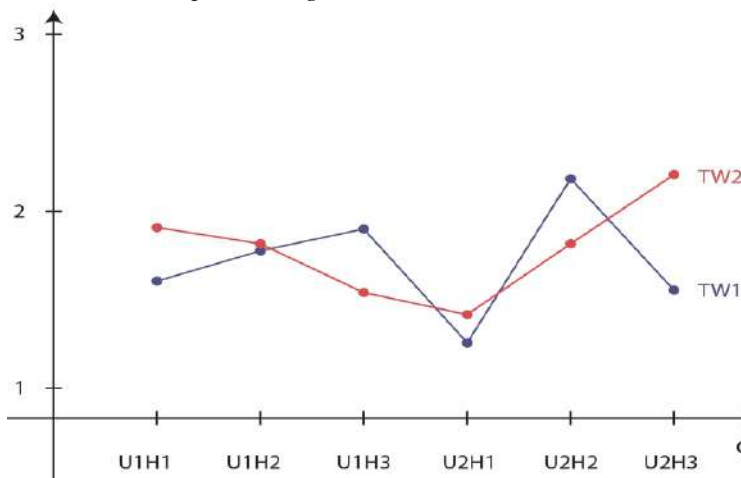


**Diagram 2:** Diagram of the movement of the standard deviation of the cutting power depending on the processing mode

Diagram 3 shows the average value of roughness depending on the processing mode and tool dullness. Diagram 4 shows the standard deviation of roughness depending on the processing mode and tool dullness.

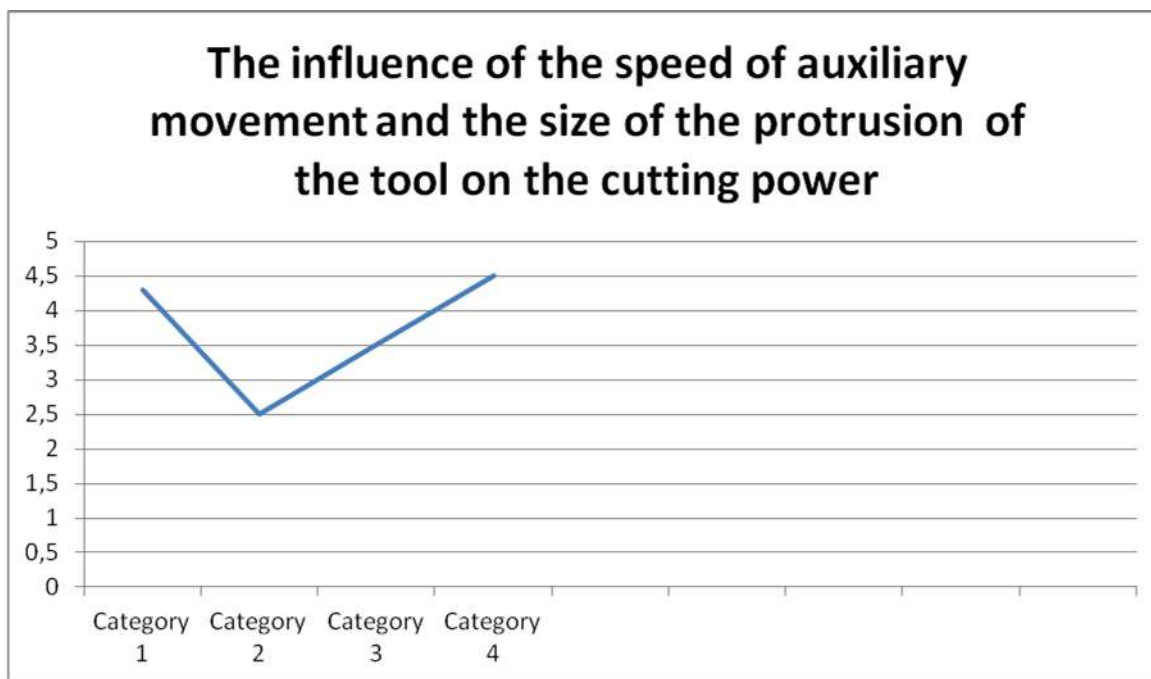


**Diagram 3:** Average value of roughness depending on the processing mode and tool dullness



**Diagram 4:** Standard deviation of roughness depending on the processing mode and bluntness of the tool

Diagram 5 shows the influence of the speed of the auxiliary movement and the size of the protrusion of the tool on the cutting force.



*Diagram 5: The influence of the speed of the auxiliary movement and the size of the protrusion of the tool on the cutting force*

#### 4. CONCLUSIONS

The mean cutting power at the defined processing modes was:

- ✓  $P_1 = 486.77625 \text{ W}$  ( $u_1h_1tw_1$ )
- ✓  $P_2 = 565.4925 \text{ W}$  ( $u_1h_2tw_1$ )
- ✓  $P_3 = 457.205 \text{ W}$  ( $u_1h_3tw_1$ )
- ✓  $P_4 = 863.85125 \text{ W}$  ( $u_2h_1tw_1$ )
- ✓  $P_5 = 833.815 \text{ W}$  ( $u_2h_2tw_1$ )
- ✓  $P_6 = 895.82 \text{ W}$  ( $u_2h_3tw_1$ )
- ✓  $P_7 = 1262.70125 \text{ W}$  ( $u_3h_1tw_1$ )
- ✓  $P_8 = 1197.60125 \text{ W}$  ( $u_3h_2tw_1$ )
- ✓  $P_9 = 1195.8825 \text{ W}$  ( $u_3h_3tw_1$ )
- ✓ At the auxiliary movement speed  $u_1 = 4 \text{ m/min}$ , the cutting power was  $P_1 = 486.77625 \text{ W}$ ,  $P_2 = 565.4925 \text{ W}$  and  $P_3 = 457.205 \text{ W}$ .
- ✓ At the auxiliary movement speed  $u_2 = 8 \text{ m/min}$ , the cutting power was  $P_4 = 863.85125 \text{ W}$ ,  $P_5 = 833.815 \text{ W}$  and  $P_6 = 895.82 \text{ W}$ .
- ✓ At the auxiliary movement speed  $u_3 = 12 \text{ m/min}$ , the cutting power was  $P_7 = 1262.70125 \text{ W}$ ,  $P_8 = 1197.60125 \text{ W}$  and  $P_9 = 1195.8825 \text{ W}$ .
- ✓ With a change in the size of the protrusion of the tool in relation to the workpiece ( $h_1=10\text{mm}$ ,  $h_2=20\text{mm}$ ,  $h_3=30\text{mm}$ ), and at the speed of auxiliary movement  $u_1 = 4 \text{ m/min}$ , the cutting power was  $P_1 = 486.77625 \text{ W}$ ,  $P_2 = 565.4925 \text{ W}$  and  $P_3 = 457.205 \text{ W}$ .
- ✓ With a change in the size of the protrusion of the tool in relation to the workpiece ( $h_1=10\text{mm}$ ,  $h_2=20\text{mm}$ ,  $h_3=30\text{mm}$ ), and at the speed of auxiliary movement  $u_2 = 8 \text{ m/min}$ , the cutting power was  $P_4 = 863.85125 \text{ W}$ ,  $P_5 = 833.815 \text{ W}$  and  $P_6 = 895.82 \text{ W}$ .
- ✓ With a change in the size of the protrusion of the tool in relation to the workpiece ( $h_1=10\text{mm}$ ,  $h_2=20\text{mm}$ ,  $h_3=30\text{mm}$ ), and at the speed of auxiliary movement  $u_3 = 12 \text{ m/min}$ , the cutting power was  $P_7 = 1262.70125 \text{ W}$ ,  $P_8 = 1197.60125 \text{ W}$  and  $P_9 = 1195.8825 \text{ W}$ .

## REFERENCES

- [1] Kováčik, J., Mikleš, M. (2009): Analysis a cutting edge geometry influence on circular saw teeth at the process of crosscutting wood, *Acta universitatis agriculturae et silviculturae mendelianae brunensis sborník mendelovy zemědělské a lesnické univerzity v brněně*, Volume LVII Number 5, 177-182
- [2] Sandak, J., Paľubicki, B., Kowaluk, G.,(2011): Measurement Of The Cutting Tool Edge Recession With Optical Methods, Proceedings of the 20th International Wood Machining Seminar, 7 – 10.06.2011, Skellefteå, Sweden, 97-106
- [3] Kminiak, R., Gašparik, M., Kvietkova, M., (2015): The Dependence of Surface Quality on Tool Wear of Circular Saw Blades during Transversal Sawing of Beech Wood, *BioResources* 10(4), 7123-7135
- [4] Ratnasingam J, Ma TP, Perkins MC., (1999) : Productivity in wood machining processes – a question of simple economics? *Holz Roh- Werkstoff* 57(1): 51–56
- [5] Beljo Lucic, R., Goglia, V., (1998): A contribution to the research of circular saw lateral stability II. Research of some influencing factors on circular saw idling noise levels and noise frequency spectrum, *Drvna Industrija* 49(3): 151-163
- [6] M. T. Alam, N. Kinoshita, C. Tanaka, M. Yoshinobu, (2002): Circular saw lateral stability by optimization of feed speed, *Holz als Roh- und Werkstoff* 60, 207 – 209
- [7] Barčík, Š., Pivolusková, E., Kminiak, R. (2008): Effect of technological parameters and wood properties on cutting power in plane milling of juvenile poplar wood, *Drvna Industrija* 59 (3), (107-112)
- [8] Buřar, B., Buřar, D. G., 2002: The influence of the specific cutting force and cross-sectional geometry of a chip on the cutting force in the process of circular rip-sawing. *Holz als Roh- und Werkstoff* 60:146-151.

## THE PHOTOVOLTAIC SYSTEM AS A PART OF ENERGY PRODUCTION IN THE WOOD INDUSTRY IN SERBIA

Mladen Furtula

University of Belgrade-Faculty of Forestry  
e-mail:mladen.furtula@sfb.bg.ac.rs

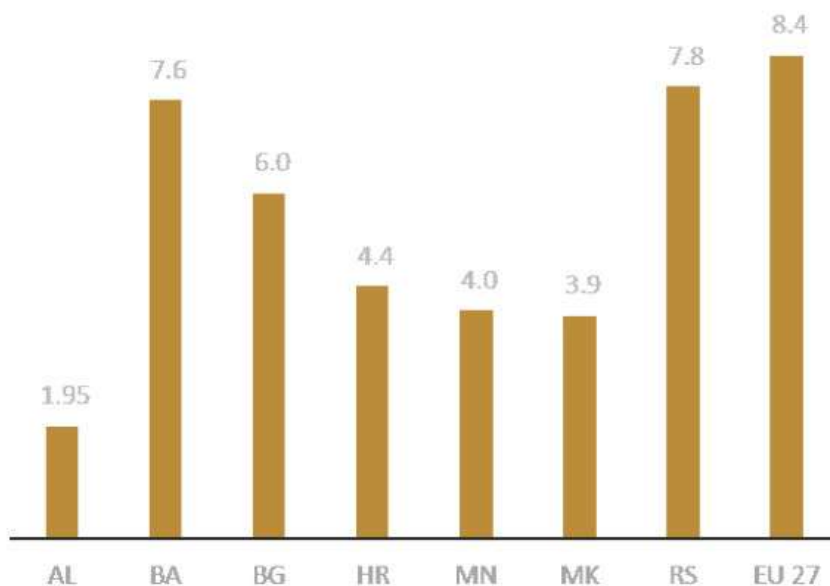
### ABSTRACT

The wood industry is a type of industry that can use its wood residues for energy production and thus be a part of energy producers from renewable sources. Another type of potential green energy production comes from the often large roofs of its buildings that can be covered with solar panels, thus expanding their energy production capacity and thus reduce the need for electricity production from fossil fuels. The paper shows the photovoltaic system's integration into energy production and its impact on the environment. Also, it will be shown how producers can connect to the electric system.

**Keywords:** photovoltaic, energy production, green energy

### 1. INTRODUCTION

In Serbia, every citizen is accountable for emitting 7.8 t CO<sub>2</sub>-eq (Figure 1). This is the highest figure among the nearby countries selected and just a little lower than the average of EU 27 [1].



**Figure 1:** CO<sub>2</sub>-eq emissions per capita for 2019, in million tonnes of CO<sub>2</sub>eq [1]

In 2019, Serbia's energy sector was responsible for the majority of greenhouse gas (GHG) emissions, contributing up to 71%. The power sector was the most significant sub-sector, accounting for 47% of the total GHG emissions (Figure 2). The transport sector followed next, contributing 11%, while industry energy use contributed 5% of the total GHG emissions. Emissions from the power sector and industry energy use decreased by 29% and 47%, respectively, between 1990 and 2019. However, emissions from transport and building increased by 54% and 8%, respectively, during the same time period [2].



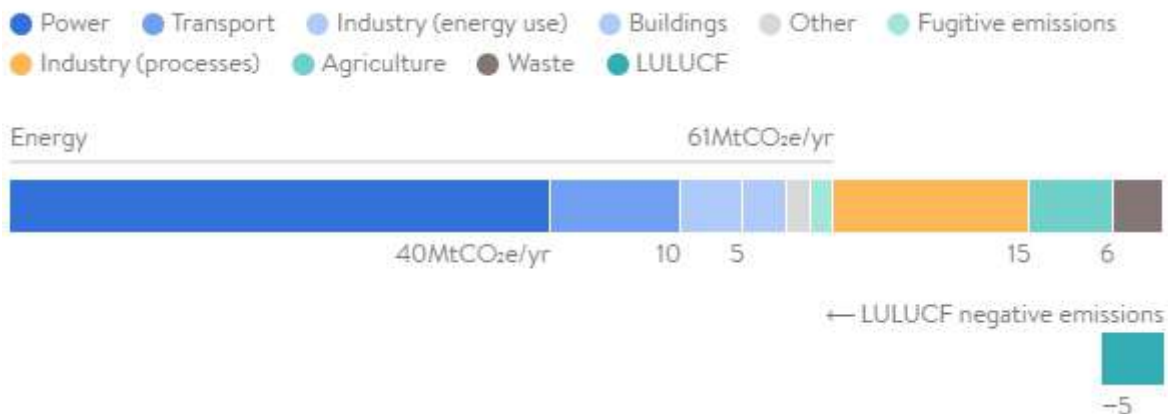


Figure 2: Serbia’s main emitting sectors in 2019 [2]

Out of all the sectors that still emit greenhouse gases, industrial processes make up approximately 17% of the total emissions. The metal industry is responsible for the biggest part of these industrial emissions, followed by cement and lime production, and lastly the chemical industry [2].

In Serbia, the main sources for power generation have stayed roughly level for years, with coal at 67% and hydro at 24% in 2022 [3].

Achieving global climate goals outlined in the Paris Agreement of 2015 require the global energy system to be decarbonized. This involves reducing greenhouse gas emissions from energy sources through various decarbonization methods, due to changes in energy supply, demand, and prices. Renewable energy and energy efficiency measures can potentially achieve as much as 90% of the necessary carbon reductions, according to IRENA’s 2020 report.

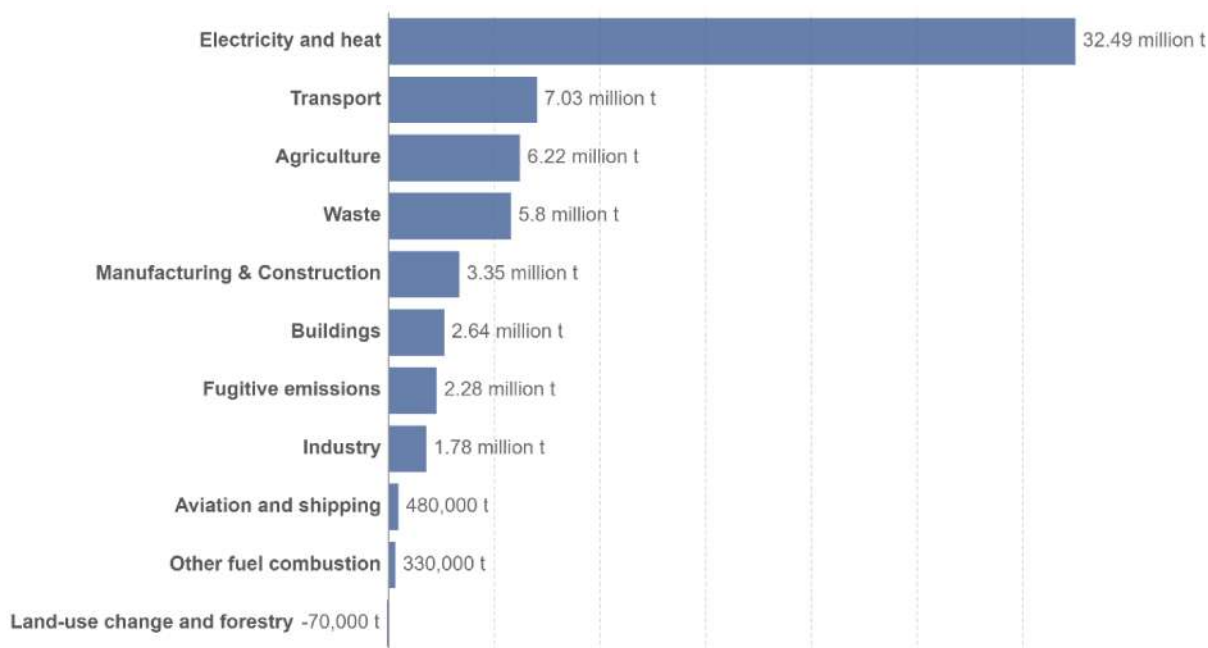


Figure 3: Greenhouse gas emissions by sector, Serbia 2019 [4]

Serbia’s Renewable Energy Sources (RES) share in electricity production is 30.1%, which is 4.5% lower than the EU 27. It’s higher than Bulgaria and North Macedonia, but lower than other countries due to their installed capacity mix [1].



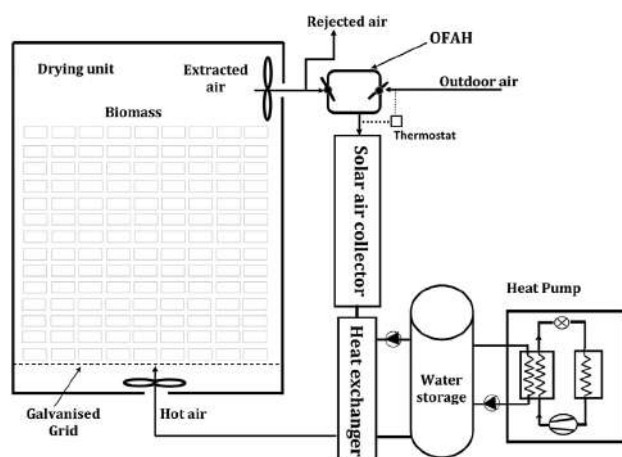
**Figure 4:** RES share in electricity production for 2019, in % [1]

Due to the lack of substantial policies to encourage renewable energy investment, wind, and solar power have only been able to contribute a small percentage to total power generation. As of 2022, wind power accounted for 4.6%, while solar power had a negligible share.

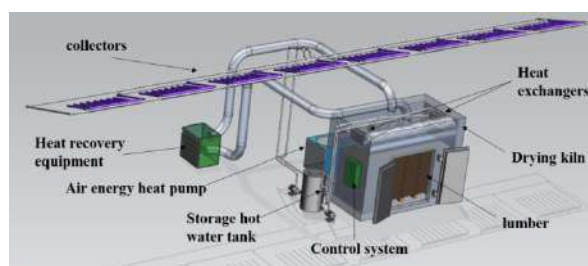
#### Solar energy in wood processing

Solar energy can be used in the wood industry in two ways: as a source of heat or electricity.

Thermal energy from the sun has been used since ancient times. It is primarily used in air drying, but it has long been used in kiln wood drying as well. Solar kilns have been perfected since the seventies of the last century, but lately, they have been increasingly considered as an opportunity to save energy in the technological process that requires the most energy in the production of wood products. Some of the new ideas of using solar energy are shown in Figures 3 and 4.



**Figure 5:** Schematic diagram of the hybrid solar kiln. [5]



**Figure 6:** 3D view of the Air-energy assisted solar dryer [6]

Electricity from solar energy can also be used in all wood industry processes. Thus, in the aforementioned drying process, it can be used to drive heat pumps, but also for fans and automation. By using solar energy to obtain electricity, wood industry companies have the opportunity to reduce their consumption of electricity from non-renewable energy sources to reduce the carbon footprint of their products, reduce energy costs, increase revenue streams, etc.

## 2. LEGISLATIVE MEASURES

Serbia created its first National Renewable Energy Action Plan (NREAP) in 2013 as required by Directive 2009/28/EC, which outlines targets for using renewable energy in transport, electricity, heating, and cooling by 2020. The country ratified the Paris Agreement in 2017 and submitted its Second National Determined Contribution (NDC) in August 2022, aiming to reduce emissions by 13.2% compared to 2010 levels or 33.3% compared to 1990 levels by 2030 (excluding LULUCF). Serbia also signed the Sofia Declaration on the Green Agenda for the Western Balkans in November 2020, pledging to work with the European Union toward a carbon-neutral continent by 2050 [1].

To ensure the success of the Integrated National Energy and Climate Plan, a comprehensive approach that addresses five key areas is necessary. Specifically, the plan should focus on decarbonization through the use of greenhouse gas reduction and renewable energy sources, energy efficiency, energy security, the internal energy market, and research, innovation, and competitiveness. The Rulebook on determining national goals for the plan's implementation outlines these provisions. Qualitative objectives have also been established, which include enhancing energy supply interconnectivity and security, increasing competitiveness of energy markets, promoting optimal development and operation of energy systems and infrastructure, empowering and protecting consumers, promoting energy-efficient and low-emission fuels, boosting national economic competitiveness, and supporting research and innovation in environmental and energy issues [1].

In April 2021, the Republic of Serbia passed a new law concerning the use of renewable energy sources. This law was accompanied by amendments to the existing Law on Energy. The new law aims to encourage the generation of electricity from renewable sources through the implementation of a market premium incentive system. Additionally, a limited feed-in-tariff scheme is available through separate quotas and auction processes, with both forms of incentives obtainable within the auction process. This regulatory framework creates a more favorable environment for investments in various-scale electricity generation from renewable energy sources of various capacities. Small capacity investments are still supported through the feed-in tariff mechanism for projects with installed capacities under 3 MW for solar and wind energy and under 0.5 MW for other renewable power plants. The Law on the use of RES also facilitates the establishment of energy communities and allows individuals to become prosumers, promoting further market penetration of renewable energy sources.

### Internal Energy Market

Currently, there are several ways to organize a solar power plant in Serbia. There is a possibility of on-grid, off-grid, and mixed production. Also, there are 11 companies in Serbia that can trade with electricity. With on-grid production, the prosumer can partially or fully satisfy their electricity needs. The consumer is obliged to be connected to the electricity grid and to transfer to it the excess electricity produced during certain (summer) months and also has the right to be supplied with electricity in months when the solar power plant does not produce enough electricity for its needs. For this reason, the prosumer concludes a contract on full supply, that is, a contract on the purchase of electricity with the supplier in accordance with the Law on Energy ("Official Gazette of the RS", no. 145/2014, 95/2018 - other laws and 40/2021, Law on Energy").

The supplier is obliged to offer the prosumer a full supply contract with net settlement in accordance with the criteria and conditions prescribed by the Regulation on criteria, conditions, and methods of payment of claims and obligations between the buyer - producer, and supplier ("Official Gazette of RS", No. 83/2021 ). Net billing is a way of calculating net electricity, in which the value of excess electricity delivered is calculated and charged within a month based on the contract between the Consumer and the supplier. Elektroprivreda Srbije ("EPS"), in its capacity as a supplier, announced on March 4, 2022, the model of these contracts. The subject of the contract is the amount and price of electricity, the method of calculation and billing, the rights and obligations of both contracting parties, the suspension of supply, etc. It is important to say that neither the Law nor the Regulation regulates the purchase price for excess electricity that prosumer transfers to the grid. It is subject to agreement between the contracting parties, which will depend on several factors that have not been publicly announced.

An alternative is to sell the generated electricity to other electricity traders. A company that trades in electricity purchases renewable energy with guaranteed production balancing from around 40 companies, primarily photovoltaic, and a smaller portion from mini hydro plants. While there is a

chance to export the electricity produced, there are no known instances of this occurring, as far as the author is aware.

### 3. SOLAR POWER PLANTS IN THE WOOD INDUSTRY IN SERBIA

Production halls, warehouses, and kilns in the wood industry usually have spacious roofs that can accommodate a significant number of solar panels, resulting in a high-capacity solar power plant. For optimal performance, the roofs should face towards the south and have a sturdy structure capable of supporting the added weight of the panels.

For the purposes of this paper, two projects of solar power plants in the wood industry in Serbia will be presented. Both projects are in the initial phase and the opinion of the EPS for the capacity of the power plant is awaited.

According to the available documentation in both projects, the capacity is calculated from 1,060 to 1,160 kWh/kWp.

The first example is a sawmill that does not operate at full capacity but has regular electricity consumption. The sawmill has several facilities (Figure 7.), but two facilities are suitable due to their orientation. It is possible to install a maximum of 100 kWp on both facilities, but due to lower consumption, the project is based on only one facility and a total power of about 56 kWp (Figure 8.).



Figure 7: Objects of the sawmill

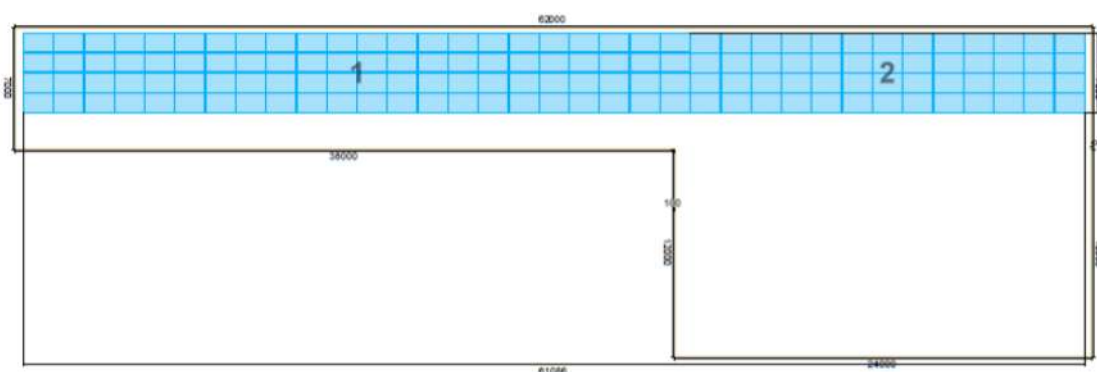


Figure 8: Solar panel position on sawmill roof

According to the project, it is necessary to install 140 panels with a total power of 56.7 kWp, with a 50 kW inverter. The total CO<sub>2</sub>eq reduction after 20 years would be 442 t.

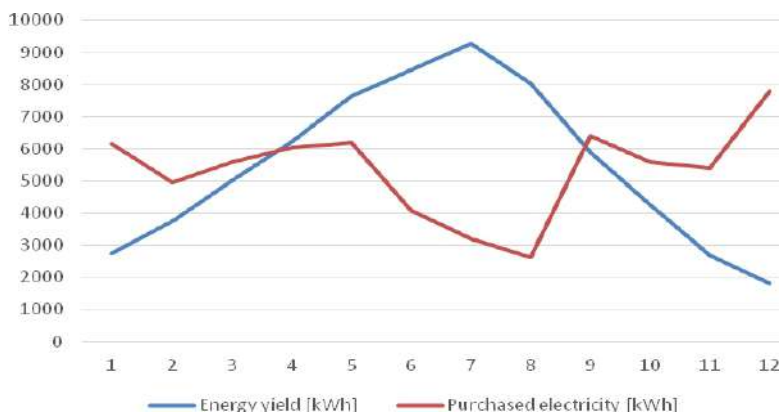


Figure 9: Annual production and purchased electricity for the first case

In the first case, the PV system is adjusted so that it is very little over the current consumption and thereby ensures a complete replacement of electricity from the grid with production from solar panels. The second plant is the final processing of wood and has a high consumption of electricity. Their electricity consumption is over 1 MW of power, with production in three shifts, seven days a week. Therefore, the solar power plant is not able to fully meet the needs for electricity, but only partially, which can be seen in Figure 10.

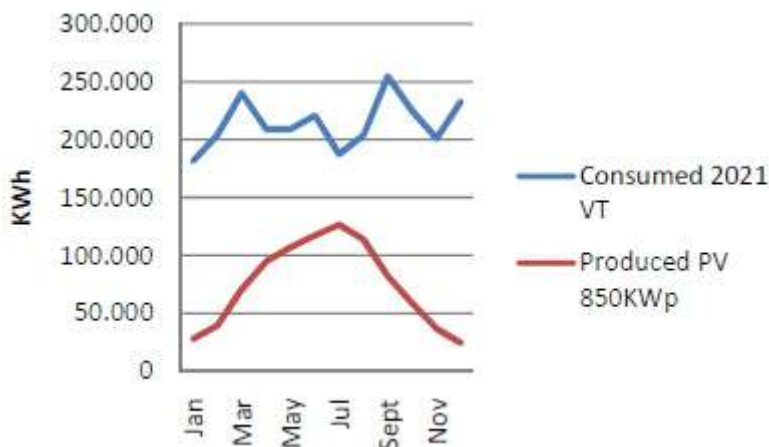


Figure 10: Annual production of PV plant (850 kWp) for the second case

Total annual energy produced from installed PV is expected 900,000 kWh (with CO<sub>2</sub>eq reduction after 20 years of 6,000 t). and consumption is around 3,500,000 kWh.

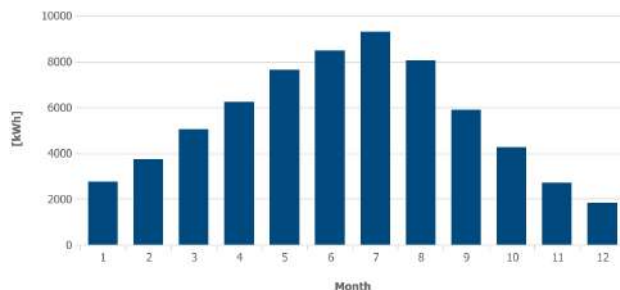


Figure 11: Energy production of the 50kWp solar power plant through the year

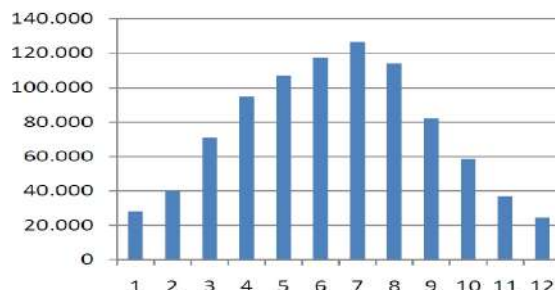


Figure 12: Energy production of the 850kWp solar power plant through the year

Figures 11 and 12 show the expected production of electricity from solar power plants. These amounts depend on weather conditions throughout the year and are not always the same. It should be

noted here that the production of electricity can also be affected by the dust that occurs in the wood industry, so it is necessary to take additional care in cleaning the panels.

Analyzing previous research [7, 8, 9, 10, 11, 12], it is possible to completely replace energy from the grid with its own production by combining PV with cogeneration (CHP) [7].

#### 4. CONCLUSION

In the wood industry, there is an opportunity and a need to construct solar power plants. This is mainly due to the large roof areas of the manufacturing buildings where production takes place. The drying of wood (thermal energy) is the most significant consumer of energy in the wood industry. This energy is obtained from the residues in production, which already belong to renewable energy sources. By incorporating solar power plants with CHP, the wood industry can achieve the target of zero greenhouse gas emissions.

#### Acknowledgements

This research was financed by the Ministry of Education, Sciences and Technological Development of the Republic of Serbia (Project no.: 451-03-9/2023-14/ 200169).

#### REFERENCES

- [1] The Ministry of Mining and Energy of Serbia (2023): The Draft Decree on the Determination of the Integrated National Energy and Climate Plan (INECP) of the Republic of Serbia until 2030, with a vision until 2050.
- [2] Gütschow, J., Günther, A. & Pflüger, M. (2023): The PRIMAP-hist national historical emissions time series v2.3 (1750-2019)
- [3] EMBER (2023): <https://ember-climate.org/countries-and-regions/countries/serbia/>
- [4] Our World in Data based on Climate Analysis Indicators Tool (CAIT) (2023) <https://ourworldindata.org/grapher/ghg-emissions-by-sector?time=latest&country=~SRB>
- [5] Khouya A. (2021): Modelling and analysis of a hybrid solar dryer for woody biomass, *Energy* Volume 216, February 2021, <https://doi.org/10.1016/j.energy.2020.119287>
- [6] Chi X, Tang S, Song X, Rahimi S, Ren Z, Han G, Shi SQ, Cheng W, Avramidis S, Energy and quality analysis of forced convection air-energy assisted solar timber drying, *Energy* (2023), doi: <https://doi.org/10.1016/j.energy.2023.128718>
- [7] Danon G., Furtula M., Luka ev D.(2017): Energy Efficiency in Wood Industry: Example of Wood Pellets Production, Maintenance Forum 2017, Budva, 24-26. June 2017, pp 44-52. IIPP, University of Belgrade, Mechanical Faculty, [www.iipp.rs](http://www.iipp.rs) (2017).
- [8] Johnsson S., Andersson E., Thollander P., Karlsson : (2019): Energy savings and greenhouse gas mitigation potential in the Swedish wood industry, *Energy*, Volume 187, November 2019, <https://doi.org/10.1016/j.energy.2019.115919>
- [9] Danon G., Furtula M., Mandi M. (2012): Possibilities of implementation of CHP (combined heat and power) in the wood industry in Serbia, *Energy*, Volume 48, Issue 1, December 2012, Pages 169–176.
- [10] Popadi R., Furtula M., Mili G. (2019): „Influence of Diameter and Quality of Beech Logs on the Potential Energy of Sawmill Residues“, *BioResources* 14(3), pp. 6331-6340
- [11] Danon G., Furtula . (2018): The role of wood biomass in the decarbonization of the electricity sector in the Republic of Serbia, *Zbornik radova International Conference Energy and Ecology EEI2018*, Beograd 10.-13.10.2018., pp 234-241, Izdava Akademija inženjerskih nauka
- [12] Danon G., Furtula ., andi . (2012): Possibilities of implementation of CHP (combined heat and power) in the wood industry in Serbia, *Energy*, vol. 48, br. 1, pp. 169–176.

**The Authors' Address:** Dr. Mladen Furtula, Ph.D., University of Belgrade, Faculty of Forestry, Kneza Višeslava 1, Belgrade

## ASSESSING SEAR STRAIN DISRIBUTION IN WOOD UNDER IMPACT USING DIGITAL IMAGE CORRELATION METHOD

Mojtaba Hassan Vand, Jan Tippner

Mendel University in Brno, Czech Republic  
Faculty of Forestry and Wood  
e-mail: [xhassanv@mendelu.cz](mailto:xhassanv@mendelu.cz)

### ABSTRACT

The demand for biobased materials across various industries is growing fast and it necessitates a comprehensive study of the high-rate loading effects on wood. While the 3-point impact bending test is commonly employed for evaluating material behavior, but determining the strain distribution of the specimen remains challenging due to the fact that the impact takes place in a short period and it needs specialized equipment and methods. Additionally, wood's heterogeneous nature and orthotropic structure make it difficult to identify the location of the highest shear strain. This research explores the potential of digital image correlation methods to determine the shear strain distribution in a wooden beam subjected to impact. The study determined the maximum shear strain in beech wood (*Fagus sylvatica* L.) and investigated the progressive pattern of shear strain during impact. The results demonstrate that, with appropriate equipment, the digital image correlation method can effectively determine the shear strain distribution during impact loading.

**Keywords:** impact loading, shear strain, digital image correlation method

### 1. INTRODUCTION

Wood's mechanical properties can be considered as an orthotropic material which depends on the three anatomical directions and also on the other natural individual characteristics of it (Glass et al, 2013). There are comprehensive studies about the mechanical properties of wood in the static state, which commonly study the behaviour of the wood by tension, compression and shear tests in the three anatomical directions and the results are mainly based on the determination of the mechanical properties such as Young's moduli, shear moduli and Poisson's ratios (Clauß, Pescatore, Niemz, 2014), however, the number of the studies for the high-rate loading is significantly less than experimental studies for static loading (Poloco er et al, 2018). Three-point bending test is a common testing method for studying the mechanical behavior of materials under impact and high-rate loading (Marur, Simha, Nair, 1994). It should be stated that different parameters, such as type of species (Jacques et al, 2014) and moisture content (Skaar, 2012), can affect the behaviour of the wood under loadings, and the severity of the effect can be significant. The loading rate effect on the behavior of wood has been investigated in laboratories for many years (Johnson, 1986), but, this task has many obstacles to overcome since the deformation of a sample is a global response, but the failure of the specimen is a local phenomenon, and an increase in the loading rate makes the failure more local (Yu and Jones, 1997). Due to the relative complexity of the impact loading and lack of possibility for using connected sensors, non-contact methods are better and advantageous. Digital image correlation method (DIC) is one these non-contacted methods. DIC is a robust optical method for displacement measurement and strain calculation based on image processing (Zhang and Arola, 2004). Due to its unique advantages, it has been used for various biomaterials, especially wood (Haldar et al, 2011). Although DIC has been used to evaluate strain distribution static (low-rate) loading tests, analysing wood samples under impact loading was not studied adequately as static tests (Dave et al, 2018).

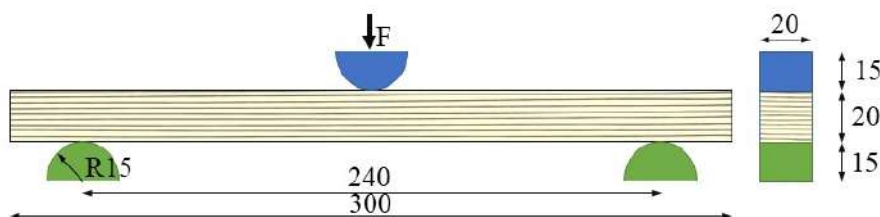
During the bending of a beam, a region parallel to the beam's longitudinal axis would be created in which all of its points have no longitudinal strains (Beer, Johnston, DeWolf, 2002). This hypothetical line is called the neutral axis, located at the centroid of the beam cross-section for homogeneous isotropic materials (Gere and Timoshenko, 1997). For wood, a heterogeneous,

orthotropic material, the neutral axis would be near the centroid of the beam but not on it (Betts, Miller, Gupta, 2010). The location of the neutral axis for wood is not a clear straight line but a jagged line with curves, and the location of this axis varies along the beam (Davis, Gupta, Sinha, 2012). However, these studies were for static bending tests, and there are necessities for measuring the shear strain for beams under impact loading. The effectivity and potential of the DIC for measuring the shear strain of wood under high-rate loading were measured in this research, and the effect of the moisture content on the maximum shear strain was shown.

## 2. TESTS AND MEASUREMENTS

### 2.1 Experiments

Beech lumbers (*Fagus sylvatica L.*) were provided from local sawmill wood supplier in Brno, Czech Republic. A deliberate selection process was employed to use lumbers from various trees, due to the fact that wood of different trees of same species differ from each other. From the purchased raw material, the test samples were prepared for impact testing. These specimens were 20\*20\*300 mm (longitudinal × radial × tangential direction). A thorough visual inspection was conducted to discard samples with knots and defects. The prepared defect-free specimens were categorized into two distinct groups: the first group as the higher moisture content group (H-Group), and the second as the lower moisture content group (L-Group). The L-group specimens were stored in an environment maintained at 20°C and 65% relative humidity, in order to reach a balanced moisture content of 12% of equilibrium moisture content (EMC). Conversely, the H-Group specimens underwent a process involving submerging in water for several days, followed by storing in a sealed chamber with elevated humidity levels, resulting 56% of the EMC. Figure 1 shows a schematic of the dimension of specimens and the impact test boundary conditions.



*Figure 1: A schematic of the test samples*

After preparation of the test samples, the specimens were tested in Josef Ressel Research Centre (Mendel University in Brno, Út chov, Czech Republic). The test was carried out on the drop-weight impact testing machine DPFest 400 (LamorTech s.r.o., Czech Republic). The impact test was in strict adherence to established Czech standards (SN 490115, 1979) and (SN 490117, 1980). The tests were done in a common temperature room (20 °C). The test is high-rated 3-point bending test with same conditions. The weight and the initial height of the hammer were 9.5 kg and 815.7 mm respectively, making it able to provide 72.4 J potential energy for the impact. The accuracy of the location of the hammer was  $10^{-5}$  m. Both ends of the samples were on the fixed supports and the hammer enforces the loading on the centre of the samples. Half of the specimens from each group were tested in the radial direction and the other half in the tangential direction to consider the effect of the growth-rings.

### 2.2 Recording equipment and considerations

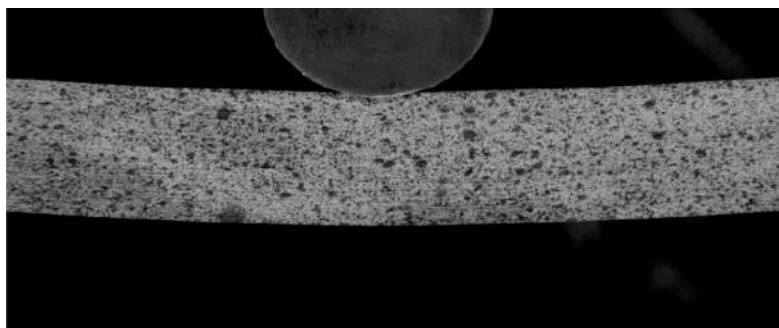
Recognizing the clear influence improvement of the random speckled pattern on the accuracy of the result of DIC (Pan, 2011), a speckled pattern was created on the surface of the samples. Due to extreme high speed of the process of the impact, a set of high-speed (HS) equipment is used. The HS equipment was made of two cameras. For lower resolution (1024×672 Px), a Photron Fastcam SA-X2 1000K-M2 with a cell size of 20 μm equipped with a lens Nikon Micro-Nikkor G and two teleconverters was used. For higher resolution (2048×600 Px), an Olympus i-SPEED 726R camera



with a cell size of 13.5  $\mu\text{m}$  equipped with a lens Nikon Macro-Nikkor was used. The frame rate of both camera was 50000 fps rate. Since the light setting has a clear effect on the quality of the ultimate result, the texture contrast on the captured surface was enhanced by two high-speed MultiLED QT light sources. Acknowledging the critical significance of precise alignment of camera and the specimens, both cameras were positioned horizontally to ensure alignment with the specimens' longitudinal axis, consequently their captured images were parallel to the surface of the specimens, thereby the integrity of the output was secured.

### 3. DIC EVALUATION

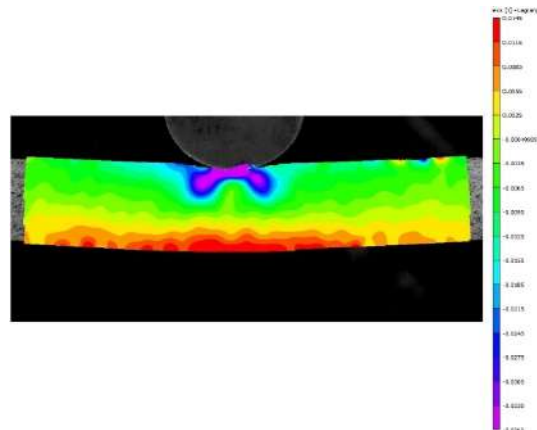
The next step after recording of the impact, was the processing of the images. For this task, a highly effective software called Vic-2D v. 2010 (Correlated Solutions Inc., USA) was used. Although the Vic-2D software can determine the conversion factor by using a simple scale calibration, there was no need for conversion factors since the strain has no unit. Lagrange notation was used for computing of the strain tensors. The lowest possible displacement field of  $3 \times 3$  points and the strain filter size of  $5 \times 5$  points were applied. The standard correlation with the same image was used. Figure 2 illustrates an output image of the camera being used as the input for the Vic-2D software.



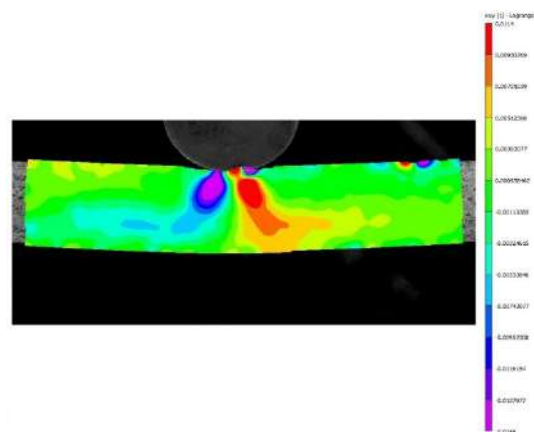
*Figure 2: An illustration of an output image*

Despite of many distinctive advantages of the DIC, it has some certain challenges and limitations for evaluation of the impact bending test. The first limitation is lack of ability for evaluating of the region near the hammer since the movement of the hammer from outside region of the sample causes considerable local compression, causing loss of data points adjacent to the hammer impact point. The second limitation emerges for processing of images after crack initiation. The relative location of the pixels drastically changes after crack and consequently causing error and losing the output's accuracy. However, our main interest is the period leading up to crack initiation, where DIC provides valuable information.

Bending of the beams at any loading rate always creates a neutral axis on the beam. This axis represents a surface wherein all of the points are not under neither tension nor compression and the normal strain is zero. On the other hand, not only the shear strain is present on the neutral axis but also its optimum values are on this axis at two points near the longitudinal center of the beam (Hibbeler, 2013). For isotropic homogenous material the neutral axis can be determined easily since it is on the centroid, however for finding a heterogeneous anisotropic material, determination of the neutral axis is not straightforward. The varying grain patterns and knots located throughout wood due to natural origin of wood, make wood anisotropic and non-homogeneous making the pinpointing of neutral axis a challenging task (Jeong, Zink-Sharp, Hindman, 2010). Knowledge of the true location of the neutral axis would facilitate a better understanding of the mechanical behavior of beams and it is vital for calculation of the maximum shear strains (Beer, Johnston, DeWolf, 2002). In essence, for finding the neutral axis the results of the longitudinal strains should be evaluated and the area with zero strain defines the neutral axis. Figure 3 depicts a longitudinal strain results of the bending wood and the approximate neutral axis can be seen as the zero strain area. By setting the inspecting polyline option on this area. The shear strain on the neutral axis can be derived. Figure 4 shows the shear strain pattern of the wooden beam.



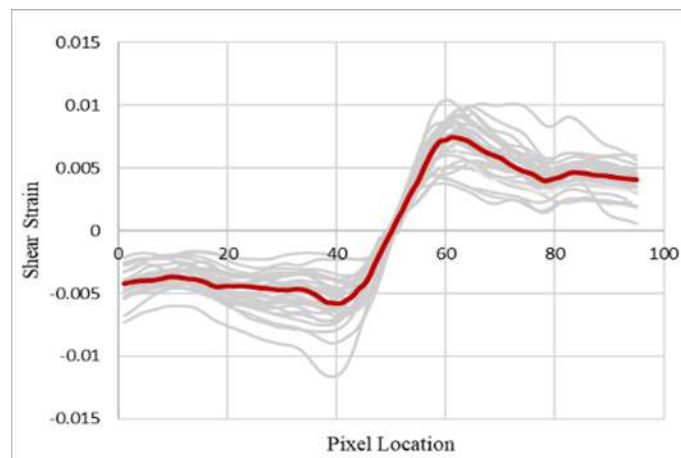
**Figure 3:** The longitudinal strain pattern of one specimen before crack initiation



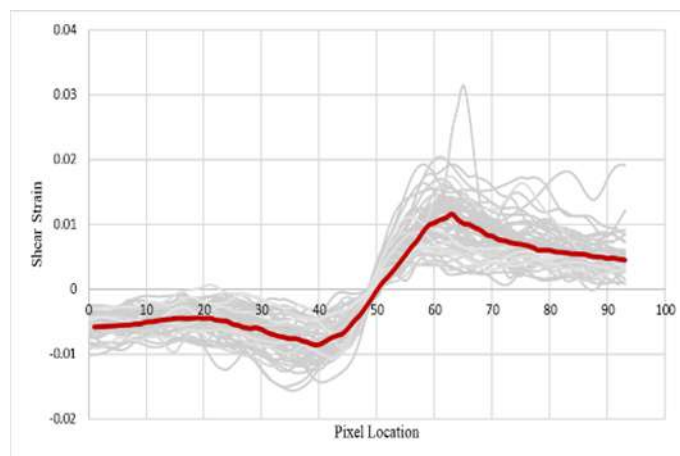
**Figure 4:** The shear strain pattern of one specimen before crack initiation

#### 4. RESULTS AND CONCLUSION

By processing of the test records, the shear strain values on the neutral axis were determined. Figures 5 and 6 depict the shear strain curves for both the L-group and H-group, where the individual test results are the light shadow curves, while the red curve signifies the collective median value of all tests within the respective groups.

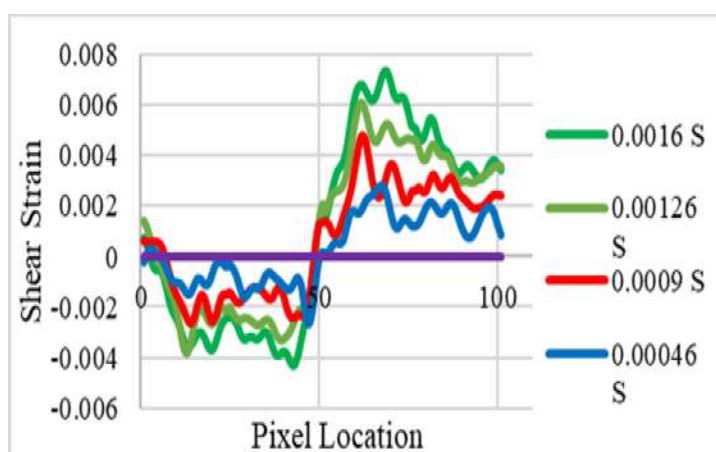


**Figure 5:** The shear stress patterns on the neutral axis of the central region of the L-Group samples



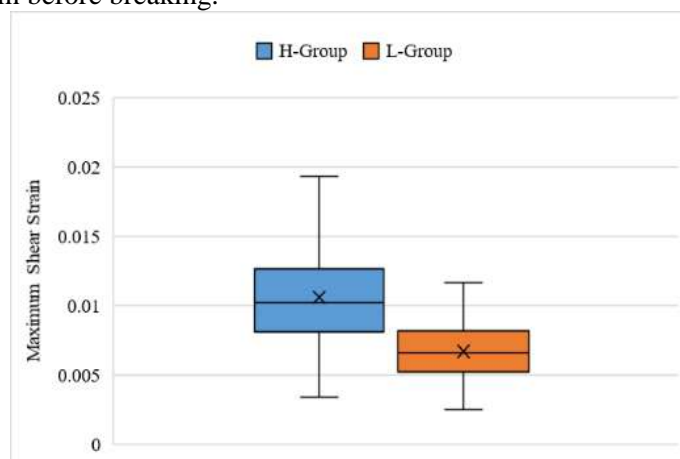
**Figure 6:** The shear stress patterns on the neutral axis of the central region of the H-Group samples

Another ability of the DIC for measuring of the shear strain of the impact is measurement of it in all of the moments of the impact. Figure 7 illustrates the value of the shear strain of the points located on the neutral axis of one specimen. The value of the maximum shear strain increases up to the crack initiation during the time. However, the increase of the shear strain has no clear pattern except the overall increase.



**Figure 7:** The shear stress patterns on the neutral axis of the central region of one of the tests during different moment of the impact

Another important aspect of the result is its distribution. Figure 8 shows the boxplot of the optimum points of the shear strain for both groups. It can be seen that H-group clearly shows higher level of the shear strain before breaking.



**Figure 8:** Boxplot of the shear strain optimum points

It should be mentioned that for measurement of the values in impact tests, the choices for tools and methods are limited and this lack of variety of tools magnifies the importance of DIC in these types of tests. The DIC has a great potential as a non-contact method for measuring the strains for high-rate loading. However, due to high variability of the values for each samples, it is recommended to have a high number of the specimen.

### Acknowledgements

This work was supported by the Ministry of Education Youth and Sports in the Czech Republic [Grant Number #LL1909, ERC CZ]

### REFERENCES

- [1] Beer, F. P., Johnston, E. R., DeWolf, J. T. (2002): "Mechanics of Materials." Singapore: McGraw-Hill.
- [2] Betts, S.C., Miller, T.H. and Gupta, R. (2010): "Location of the Neutral Axis in Wood Beams: A Preliminary Study." *Wood Material Science and Engineering*, 5(3-4), pp. 173-180.
- [3] Clauß, S., Pescatore, C., Niemz, P. (2014): "Anisotropic Elastic Properties of Common Ash (*Fraxinus excelsior* L.)." *Holzforschung*, 68(8), 941-949.
- [4] SN 490115 (1979): "Wood. Detection of Static Bending Strength." Czech Standards Institute, Prague, Czech Republic.
- [5] SN 490117 (1980): "Wood. Impact Strength in Bending." Czech Standards Institute, Prague, Czech Republic.
- [6] Dave, M. J., Pandya, T. S., Stoddard, D., Street, J. (2018): "Dynamic Characterization of Biocomposites Under High Strain Rate Compression Loading with Split Hopkinson Pressure Bar and Digital Image Correlation Technique." *International Wood Products Journal*, 9(3), 115-121.
- [7] Davis, P. M., Rakesh, G., Arijit, S. (2012): "Revisiting the Neutral Axis in Wood Beams." *Holzforschung*, Vol. 66, pp. 497–503.
- [8] Glass, S. V., Cai, Z., Wiedenhoef, A. C., Ross, R. J., Wang, X., Hunt, C. G., Rammer, D. R. (2013): "Wood Handbook—Wood as an Engineering Material." CreateSpace Independent Publishing Platform; Centennial edition.
- [9] Gere, J., Timoshenko, S. *Mechanics of Materials* (4 th edition). PWS Publishing Co, 1997.
- [10] Haldar, S., Gheewala, N., Grande-Allen, K. J., Sutton, M. A., Bruck, H. A. (2011): "Multi-Scale Mechanical Characterization of Palmetto Wood Using Digital Image Correlation to Develop a Template for Biologically-Inspired Polymer Composites." *Experimental Mechanics*, 51(4), 575-589.
- [11] Hibbeler, Russell C. (2013): "Mechanics of Materials." United Kingdom: Pearson Education.
- [12] Jacques, E., Lloyd, A., Braimah, A., Saatcioglu, M., Doudak, G., Abdelalim, G. (2014): "Influence of High Strain-Rates on the Dynamic Flexural Material Properties of Spruce–Pine–Fir Wood Studs." *Canadian Journal of Civil Engineering*, 41(1), 56-64.
- [13] Jeong, G. Y., Zink-Sharp, A., & Hindman, D. P. (2010). Applying digital image correlation to wood strands: influence of loading rate and specimen thickness.
- [14] Johnson, W. (1986): "Historical and Present-Day References Concerning Impact on Wood." *International Journal of Impact Engineering*, 4(3), 161-174.
- [15] Marur, P. R., Simha, K. R. Y., Nair, P. S. (1994): "Dynamic Analysis of Three Point Bend Specimens Under Impact." *International Journal of Fracture*, 68(3), 261-273.
- [16] B. Pan, "Recent Progress in Digital Image Correlation. *Experimental Mechanics*, 51(7), 1223–1235, 2011.
- [17] Poloco er, T., Kasal, B., Stöckel, F., Li, X. (2018): "Dynamic Material Properties of Wood Subjected to Low-Velocity Impact." *Materials and Structures/Materiaux et Constructions*, 51(3). <https://doi.org/10.1617/s11527-018-1186-z>
- [18] Skaar, C. (2012): "Wood-Water Relations." Springer Science & Business Media.
- [19] Yu, J. L., Jones, N. (1997): "Numerical Simulation of Impact Loaded Steel Beams and the Failure Criteria." *International Journal of Solids and Structures*, 34(30), 3977-4004.

- [20] Zhang, D. M., Tan, Y. H., Gao, S. X. (2014): "Evaluation of the Maximum Shear Strain of Clamped Composite Plate Using Digital Image Correlation Method." *Advanced Materials Research*, 945, 427-431.
- [21] Zhang, D. S. & Arola, D. D. (2004): "Applications of Digital Image Correlation to Biological Tissues." *Journal of Biomedical Optics*, 9(4), 691-699.

## INFLUENCE OF THERMAL MODIFICATION SCHEDULES ON THE NATURAL WEATHERING OF MAPLE AND ASH WOOD

Marko Veizovi<sup>1</sup>, Goran Cvjeticanin<sup>1</sup>, Nebojša Todorovi<sup>1</sup>, Ranko Popadi<sup>1</sup>, Goran Mili<sup>1</sup>

<sup>1</sup>University of Belgrade – Faculty of Forestry, Department of Wood Science and Technology, Belgrade, Republic of Serbia

e-mail: marko.veizovic@sfb.bg.ac.rs; goran.cvjeticanin@sfb.bg.ac.rs;

nebojsa.todorovic@sfb.bg.ac.rs; ranko.popadic@sfb.bg.ac.rs; goran.milic@sfb.bg.ac.rs

### ABSTRACT

This study aimed to compare the influence of two thermal modification (TM) schedules — with short (65 h) and long (112 h) heating phases — on the natural weathering of maple (*Acer pseudoplatanus* L.) and ash (*Fraxinus excelsior* L.) wood. Over a duration of almost 21 months (October 2021 – June 2023), the changes in wood colour and moisture content (MC) were monitored. The samples were exposed to all weather conditions facing south, positioned 1 m above ground level under a 45-degree slope with horizontal grain orientation. As the weathering process progressed, a pronounced alteration in the inherent colouration of the control and TM samples (both schedules) was observed in both wood species. At the end of the weathering process, the colour of all samples, whether treated or untreated, had reached a similar appearance. In the initial phase of the experiment (first winter - from October '21 to March '22) MC variations were more pronounced, but the extent of these changes diminished with time. The control samples were found to be the most responsive to weather condition changes, while TM (fast schedule) samples exhibited slightly higher MC variations compared to samples modified under a slow schedule. Throughout the duration of the experiment, MC of the maple control samples was mostly between 15% and 45%, whereas the MC of maple TM samples ranged from 8% to 25%. The ash control samples had a MC ranging from 12% to 27%, while the ash TM samples had MC mainly between 5% and 15%.

**Keywords:** weathering, thermal modification schedule, maple wood, ash wood

### 1. INTRODUCTION

Wood is a versatile and widely used material in various applications, including outdoor structures, furniture, and decorative elements. However, when exposed to outdoor conditions, wood is subjected to a range of abiotic and biotic factors, such as weather conditions and biodegradation, which can adversely affect its physical, biological, chemical, and mechanical properties [Marais et al., 2020]. One prominent advancement in wood treatment technology is thermal modification (TM), an approach that offers chemical-free enhancements in both dimensional stability and durability of wood. Through reduced hygroscopicity, TM wood products have found their niche in outdoor applications, particularly in situations involving demanding weather conditions.

Weathering of wood is a combination of biotic and abiotic degradation mechanisms acting on the wood surface (Hill et al., 2022). The effects of weathering can manifest differently depending on wood species, treatments, exposure setup and exposure duration and location (Kropat et al., 2020).

The goal of this study was to examine the influence of thermal modification schedules on the natural weathering of maple and ash wood.

### 2. MATERIAL AND METHODS

The study was conducted using kiln-dried maple (*Acer pseudoplatanus* L.) and ash (*Fraxinus excelsior* L.) timber that was free of defects. Following the drying process, the boards from both species had dimensions of approximately 28 mm thickness, 120 mm width, and 2.4 m length. Fourteen boards were chosen for each species, and these boards were divided into halves for the purpose of

thermal modification (Mili et al., 2023). The modification was carried out in an industrial chamber using a superheated steam atmosphere achieved through water spraying with high- and low-pressure nozzles. This process was performed on a subset of a larger batch of 20 m<sup>3</sup> of maple/ash timber.

Two different methods of thermal modification were used - slow (TMS) and fast (TMF). The only difference between these treatments (peak temperature 200°C, 3 hours) was the duration of the heating phase: for the TMS process, the heating took 112 hours (heating rate 1.1°C/h); TMF method had a shorter heating phase of 65 hours (2.5°C/h).

After conducting standard laboratory tests on TM samples and allowing for long-time climatization under room conditions, four samples (2xTMS and 2xTMF) were selected for each wood species. Together with two control (unmodified) samples, total of 12 samples were used for the weathering test (6 for ash and 6 for maple). The samples were exposed to all weather conditions facing south, positioned 1 m above ground level under a 45-degree slope with horizontal grain orientation (Fig. 1). The test began on October 19, 2021, and measurements were conducted until July 4, 2023.



*Figure 1: The setup for weathering test*

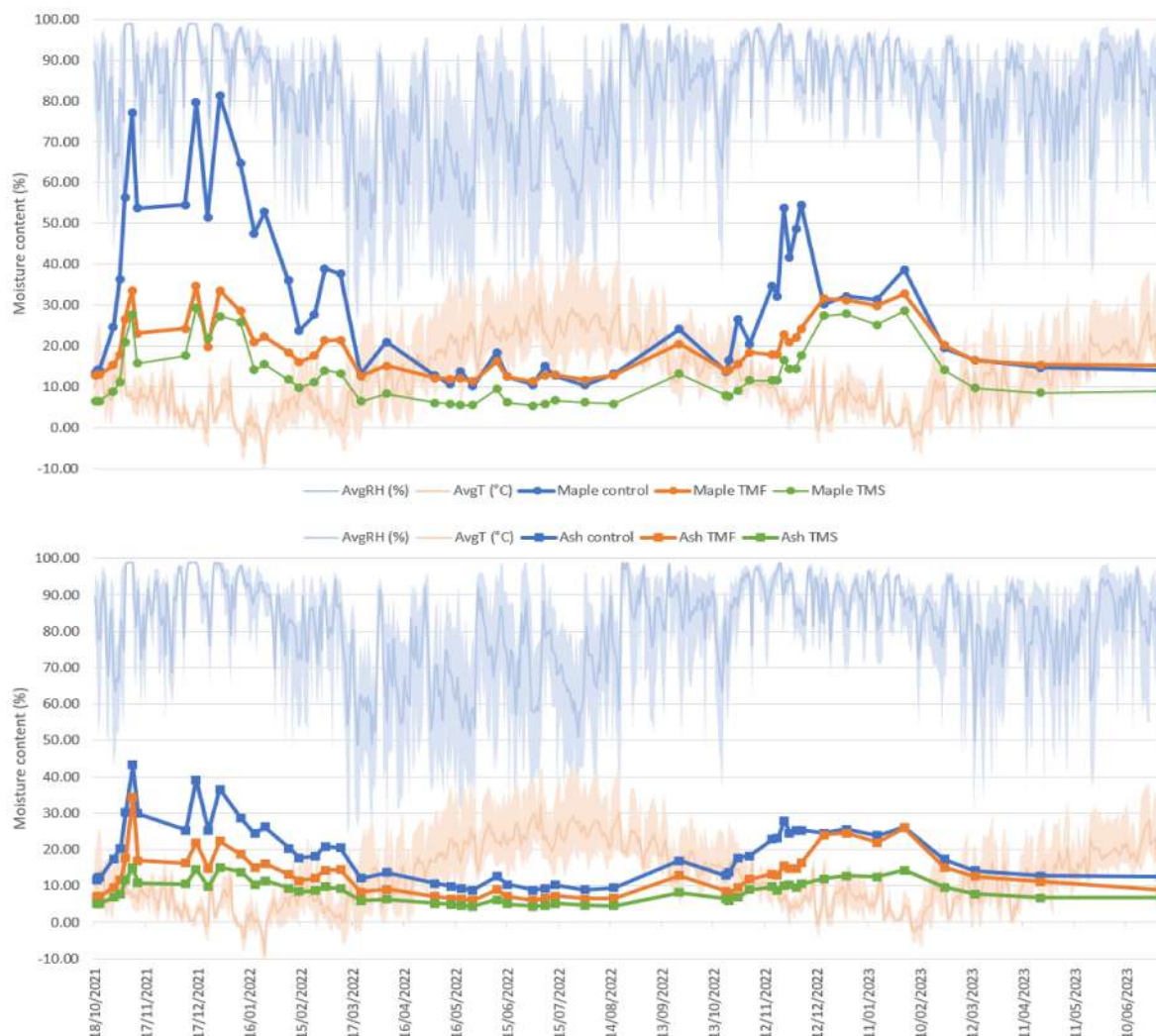
Depending on weather conditions, the color of the samples was assessed 1 or 2 times each month. In total, 30 measurements were conducted for each sample, consistently at a designated measuring point. The colour was measured using Easyco colorimeter, manufactured by Erichsen. The diameter of the lenses was 10 mm, the device was set at the observing angle of 10°, and illumination D65 for daylight. This colorimeter displays colors in CIELAB color space, and the color difference was determined using the corrected value of the colour change (CIEDE2000 – E<sub>00</sub>), which, according to numerous authors (Hauptmann et al., 2012), is closer to the human perception of the difference in wood colour.

During the experiment, the mass of all samples was measured 1 to 3 times per month (in total 50 measurements), and after the completion of the weathering test, the samples were dried to their oven-dry state and then reweighed in order to determine moisture content (MC).

### 3. RESULTS

At the beginning of the weathering test, the initial MC of the control samples varied between 11.5% and 13.4%. For the TMF samples, the MC ranged from 7.0% to 12.8%, while for the TMS samples, the MC was within the range of 5.0% to 6.4%. The outdoor temperature during the experiment varied from -12°C to 43.8°C, while the air relative humidity ranged from 24% to 100% (Fig. 2). The MC of the control samples for maple consistently remained significantly higher than that of the TM samples. Additionally, it can be noticed that climate parameters (temperature - T and relative humidity - RH) had a more significant impact on the MC variation in control samples as compared to the TM samples (Fig. 2, top). Unexpectedly, this was not entirely the case for ash, where the differences in MC between control and TM samples were considerably smaller, accompanied by minor fluctuations. (Fig. 2, bottom).

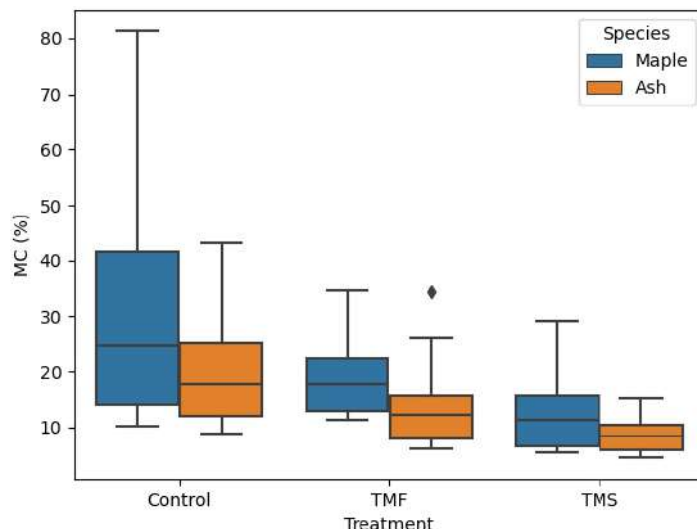
The control samples of maple exhibited higher moisture content and absorbed moisture more rapidly than the ash samples. This is in line with expectations, as high permeability of maple wood enables MC changes even in the inner sections of the wood during the rainy or snowy days. Certain measurements, especially from Nov. '21 to Jan. '22, depict notably higher moisture levels. This is attributed to the fact that the measurements were taken under various weather conditions, including rain and snow. It can be observed from the graphs that there are time intervals when the RH is at 100%, during which the samples were entirely covered with snow.



**Figure 2:** Wood moisture content, temperature and relative humidity of air during the weathering test

During the experiment, MC of maple control samples was mostly between 15% and 45%. On the other hand, maple TM samples mainly had MC ranging from 15% to 25% (TMF) and 8% to 18% (TMS) (Fig. 3). Moisture content of the ash control samples was in range from 12% to 27, TM samples were mainly between 7% to 15% (TMF) and 5% to 12% (TMS) of moisture content (Fig. 3). A clear trend can be observed where TMS samples exhibited the lowest MC, with the maximum MC of 29.2% for maple samples and 15.1% for ash samples. This is in agreement with previous results obtained under indoor conditions (also in a climate chamber), which demonstrated that the slow heating process during TM leads to the lowest equilibrium moisture content (EMC) values for both maple and ash wood (Mili et al., 2023). This further confirms the significant influence of heating duration on the intensity of thermal degradation of wood (Allegretti et al., 2021).





**Figure 3:** Moisture content of maple and ash (unmodified and TM) samples during weathering test

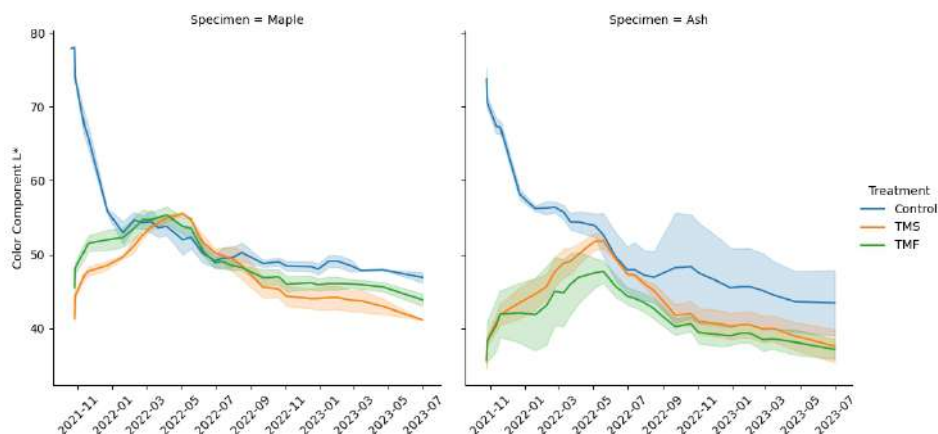
At the beginning of the weathering test unmodified samples exhibited a natural, light color, while TM samples displayed a dark brown hue, with small differences between TMF and TMS (Fig. 4). The primary color difference arises from the lightness component,  $L^*$ . For unmodified samples, the  $L^*$  component at the start of the experiment ranged from 72 to 78, whereas for TMF and TMS samples, it ranged from 34 to 46. The  $a^*$  component (representing the redness) showed approximately 3-5 higher values in TMF and TMS samples compared to control samples, while differences in the  $b^*$  component were minimal. Throughout the weathering process, a pronounced alteration in the inherent colouration of the control and TM samples (both schedules) was observed in both wood species. Visually observed, in the twelfth month of the experiment, there was a relative equalization of the color of all samples, where the predominant color was gray.



**Figure 4:** Heatmap visualization of color change during the weathering test

At the end of the experiment, all samples underwent significant color changes compared to the initial state. The greatest color difference was recorded in the control sample of ash ( $E_{00}=31.4$ ), while the sample of ash TMS underwent the least color change ( $E_{00}=11.5$ ). The color difference between TMF and TMS samples at the end of the experiment was small, with values of  $E_{00}=2.1$  for maple and  $E_{00}=0.2$  for ash.

The most significant changes in control samples occurred within the initial two months, during which the  $L^*$  component decreased significantly to a level between 50 and 60, which is in line with the results reported in Kropat et al. (2020). In the case of the TM samples, the  $L^*$  component initially increased (over the first 2-3 months), and then began to decrease until the end of the experiment, eventually returning to a state approximately resembling the initial condition (Fig. 5). For the unmodified ash samples, a significant variation in the  $L^*$  component can be observed, emerging around the midpoint of the experiment. This phenomenon is a result of localized peeling of the wood's surface layer (caused by surface checks), unveiling an underlying surface that has not yet undergone the graying process.



**Figure 5:** Change of color component  $L^*$  during weathering test

#### 4. CONCLUSIONS

In this study, the effects of diverse thermal modification schedules on the natural weathering of maple and ash wood were investigated. All samples were subjected to natural weathering over a period of almost 21 months. During exposure to various outdoor conditions, the moisture content and color change of wood were measured.

Notably, the moisture content (MC) of control maple samples consistently exceeded that of TM samples, while this distinction was less pronounced for ash wood. This differential MC behavior can be attributed to different permeability of the wood species. Additionally, a distinct trend emerged, with TMS samples exhibiting the lowest MC levels. This pattern aligns with prior indoor results, underscoring heating duration's impact on wood hygroscopicity, both in dry and wet climate conditions.

Moisture content of unmodified maple samples was mostly between 15% and 45%, but TM samples mainly had moisture content ranging from 8% (TMS) to 25% (TMF). Unmodified ash samples had moisture content in range from 12% to 27%, while MC of TM samples saw mainly between 5% (TMS) to 15% (TMF).

Color alterations were evident in all samples during the weathering process. Among the control samples, the most notable change was identified in the  $L^*$  component (decreased for about 41%), whereas in the case of TM samples, the greatest impact on color variation had changes in both components  $a^*$  and  $b^*$  which decreased for about 87% and 81% respectively. Within the initial two months, the  $L^*$  component decreased in control and increased in TM samples, eventually reaching similar values. A gray hue prevailed in all samples after approximately 12 months of weathering.

#### REFERENCES

- [1] Allegretti, O., Cuccui, I., Terziev, N., Sorini, L. (2021) A model to predict the kinetics of mass loss in wood during thermo-vacuum modification. *Holzforschung* 75:474–479.
- [2] Hauptmann, M., Pleschberger, H., Mai, C., Follrich, J., Hansmann, C., Mai, C., & Follrich, J. (2012). The potential of color measurements with the CIEDE2000 equation in wood science. *Eur J Wood Prod*, 70, 415–420.
- [3] Hill, C., Kymäläinen, M. & Rautkari, L. (2022) Review of the use of solid wood as an external cladding material in the built environment. *J Mater Sci* 57, 9031–9076
- [4] Kropat M., Hubbe M., Laleicke F. (2020) Natural, accelerated, and simulated weathering of wood: a review. *BioResources* 15:9998–10062
- [5] Marais, B.N., Brischke, C., Militz, H. (2020) Wood durability in terrestrial and aquatic environments—A review of biotic and abiotic influence factors. *Wood Mater Sci Eng*, 1–24.
- [6] Mili, G., Todorovi, N., Veizovi, M., Popadi, R. (2023) Heating Rate during Thermal Modification in Steam Atmosphere: Influence on the Properties of Maple and Ash Wood. *Forests* 2023, 14, 189.

## PROCEDURE OF OPTIMIZING SOLID OAK WOOD (*Quercus robur* L.) BENDING PROCESS IN FURNITURE MANUFACTURE

Mislav Mikšik, Stjepan Pervan, Silvana Prekrat, Mladen Brezovi

University of Zagreb, Zagreb, Republic of Croatia,  
Faculty of Forestry and Wood Technology,  
e-mail: mmiksik@sumfak.unizg.hr; pervan@sumfak.unizg.hr; sprekrat@sumfak.unizg.hr;  
mbrezovic@sumfak.unizg.hr

### ABSTRACT

Solid wood bending is the type of processing with certain levels of mechanical destruction. Higher material utilization, small investments in technology, high strength and stiffness of bent wood elements, and uniformity of structure in furniture parts are some advantages of wood bending. Sawn elements have their grain slope cut off in certain parts which lowers the strength and load-bearing capacity of the final piece of furniture contrary to continuous grain slope in bent counterparts.

In this research procedure of optimization of solid oak wood bending (*Quercus robur* L.) process in furniture manufacture will be explained. All the challenges encountered while attempting to optimize bending process by using combination of steaming and drying with high frequency (HF) will be described and explained. Utilization comparisons at the beginning of process and after optimizing it, including current state, will be presented.

**Keywords:** oak (*Quercus robur* L.), solid wood, bending, high frequency, steaming

### 1. INTRODUCTION

Solid wood bending is a type of wood processing that has been known for thousands of years. Earlier, it was mostly used for bending bows by using green wood. Later and nowadays, it is mostly used in manufacturing ships and boats, sports equipment, fishing rods, bows, tool equipment and furniture. The most recognizable and significant advantage of wood bending is higher utilization of used materials. Lesser-known advantages are higher strength and stiffness of bent wood parts when compared to same parts which are sawn due to continuous grain slope.

When bent, wood compresses on the concave side and stretches on convex side. After bending convex side becomes longer than concave side which results in accumulation of stresses which results in well-known phenomena spring-back effect that tends to force wood to return to its original shape. Before bending, wood is commonly softened by combination of heat and moisture or with chemicals which causes lower stress development. The reason why wood is softened prior to bending is because wood cannot be stretched significantly even after softening which is why concave side is forced to absorb all the compressive deformation and stresses. This is done by using metal strip on convex side which are preventing elongation on convex side. Sandberg et al. (2013) stated after plasticizing, wood compressibility in the longitudinal direction is increased up to 30 - 40 % which is suitable when bending wood. If the end-force is too small it causes longitudinal tensile failure, on the other hand an excessively large end-force causes premature longitudinal compressive failure. Because of those reasons Stevens and Turner (1970) suggested that controlling the length and longitudinal tensile strain in the vicinity of the convex surface of a wood specimen during a bending process is a very important feature. Báder et al. (2019) stated that compression in longitudinal direction causes changes in wood tissue which result in better bendability. After plasticizing wood is formed and after cooling and drying it keeps its bent shape.

Báder and Németh (2019) and Taylor (2008) suggest that the best flexibility for bending is achieved when the moisture content (MC) of wood is close to its fibre saturation point or around 25-30 %. This statement has been shown to be true but after conducting many experiments and bending tests it was concluded that MC can and should be lower in most of the cases which will be explained later.

Navi and Sandberg (2012) and Taylor (2008) along with many others suggest that around 2 minutes of steaming per millimetre of width is optimal for bending, and it turned out to be correct. Liquid ammonia can also be used for plasticization of wood which results in bent wood without spring-back effect but will not be described here, because this method is not used in manufacturing process. Softening of wood is mostly done by steaming but many companies use combination of steaming and high frequency (HF) process. In that way heating, plasticizing, bending, and drying is done in succession. Although bent pieces are partially dried in HF press, they still need to be air dried or conventional dried afterwards to desired MC while being fixated with metal straps or wood slats (which are mostly used to prevent spring-back effect during drying).

In this paper optimizing of oak wood bending process will be explained. In general oak wood is a desired species for manufacture of furniture which is the reason why it was decided to try and bend it. In literature most data on wood bending that was found was about beech wood. To optimize the process, the data about steaming temperature and duration, initial MC of wood, and press parameters were taken as if beech wood was bent. It was used as a starting point due to lack of knowledge in general about oak wood bending. Later, it was optimized and adapted to oak wood bending by trial-and-error method and by further studying of available literature and data. Niemiec and Brown (1995) noted many other factors that also affect wood bending as radius of bending, wood species, moisture content, thickness, width of wood, steaming time, fibre direction and wood defects. Wood selected for bending should be defect-free with straight fibres, but in practice it was observed that it is not the case since wood parts with knots and interlocked or wavy fibres can also be bent properly depending on the final use.

Wood can also be bent in a cold state, in contrast to the other methods, with the pre-compressed method. First, wood is compressed in a longitudinal direction after plasticizing it with steam. It is fixed to avoid deflection during compression. According to Navi and Sandberg (2012) wood is longitudinally compressed by approximately 20%, then it is allowed to cool to room temperature and finally it is dried to moisture content of 12%. After that wood is processed to desired cross-sectional shape and it can be bent in a cold state.

## **2. BEGINNINGS OF OAK WOOD BENDING PROCESS EXPERIMENT**

All bending experiments conducted were done as part of a project on which faculty was partnered with manufacturing company.

When first started conducting bending experiments, little to no knowledge was possessed about the whole process. The only information possessed was from the machine seller. Steaming chambers, steam boilers, presses, and high frequency (HF) generators were bought in order to conduct test bends and to be implemented in production later. During the period of 2.5 years a lot of field work has been done where the process of bending was monitored, and attempts were made to optimize it. The first challenge was to get the raw materials which had the optimal moisture content (MC) which ranged from 16 – 25 %. It became a problem due to manufacturers usual kiln drying programs which dried all the goods to the MC of 8 – 10 % but in this case had to be stopped halfway through to take out the material for bending. For those reasons material was often overdried and it would be 11 – 15 % MC which was shown to be too low for greater bends with large cross section. Smaller bends for chair legs with smaller cross-section could handle MC as low as 13% but not lower than that. A small experiment was conducted to see if in any way wood with MC ranging from 8 - 10% can be used as bending material because, in that way drying would not have to be stopped midway to take out raw material for bending. Results suggested that no amount of steaming can soften wood enough not to break after it was kiln dried to such a low MC. Perhaps if wood pieces would be immersed in water prior to bending they could be softened later with sufficient amount of steaming but the whole process would show too complicated and time consuming. The best drying method for bending material would be air drying but it requires a lot of material in advance and is time consuming.

When first started, the overpressure in steam boiler was 3.2 bar which amounted to temperature of 145 °C. It was quickly realized that the temperature was too high because it resulted in high number of checks and cracks on bent pieces. When taken out of the steaming chamber wood dimension parts were very hot but not moistened at all. Higher temperature can heat the wood faster, but if it is too high it only makes wood more brittle. High temperature steam also possesses lower amount of

moisture which otherwise helps to soften the wood pieces. Overpressure in steaming the chamber was 0.8 bar. According to Peck (1957) steaming at a high pressure causes wood to become plastic in a shorter time, but wood treated with high-pressure steam does not generally bend as successfully as wood treated at atmospheric or low pressure.

During the project technology sellers in Italy were visited few times to obtain more information about the steaming. It was seen there that they also steam their material at atmospheric pressure which produced good bends. It was also noticed that their steam is slowly circulating and passing through steaming chamber. In that way fresh wet steam enters the whole system at all times and is better at moistening and keeping the desired temperature inside.



*Figure 1: Steaming chambers*



*Figure 2: Mechanical press during bending*

Due above-mentioned reasons, it was decided that the process would try to be imitated as much as possible to see if that way good bent parts could be produced. Steaming chambers used can be seen in figure 1. On top of it a manual valve, which was opened in order to gradually eject the steam. Chamber needs to be under constant pressure because its lid cannot be closed otherwise. It is equipped with sensors that automatically add more steam when pressure gets too low, but pressure is kept at minimum levels in order to get as close as possible to atmospheric pressure. In that way steam is constantly gradually released while at the same time new fresh steam enters the system. Figure 2 shows mechanical press during bending “U” shaped back of semi-armchair.

### **3. HIGH FREQUENCY HEATING PROCESS**

The second problem encountered was HF heating during bending. After steaming, wood is mechanically bent and heated with HF to dry it sufficiently to keep its form. Presses are equipped with a 20 kW, 10 MHz HF generator. This type of generator is intended for bending beech wood and has specifications made for it. For that reason, high power ceramic disc capacitor needs to be used when bending oak wood to store excess electrical energy in order not to overheat the wood too fast when heating. Ceramic capacitor added to the press can be seen in figure 5. Heating was done in cycles of 2 minutes 3 to 7 times depending on the size of cross-section, bending radius, and MC. It has been shown that it is easier to dry and keep the shape of specimens with smaller bending radii (greater curvature) than those with greater bending radii (smaller curvature). The reason for that is when curvature is too small wood still remains in its elastic state and this makes it harder to retain it.

When HF heating bent wood, one needs to be very careful not to overheat it even with capacitors. Some smaller tests were conducted with thermal camera to see how temperature is spread in press and in specimens individually. It was noticed that specimens with higher MC are heating much faster than those with lower MC which is logical due to the way HF heating functions. For those reasons

specimens of individual load were paired in groups with similar MC to avoid large differences in temperature. Figures 3 and 4 show what happens when wood is heated excessively and too fast. Wood for bending still contains a lot of bound water and in some cases small amounts of free water. When heated fast and on high temperatures (above 100°C) water starts to evaporate rapidly and steam expands. Since the whole system is very closed and specimens are trapped in the press as can be seen in figure 2, vapour cannot exit the specimen fast enough and water vapour erupts which destroys wood tissue completely and render parts unusable.



**Figure 3 and 4:** Cracks and gapes in wood tissue due to excessive HF heating

During bending, wood adjusts and starts creaking regularly because of its resistance. As nonstandard procedure as it sounds it is really important to listen to wood during bending and heating. It gives a sound as a warning to adjust parameters such as to lower longitudinal pressure, reduce or turn off HF heating. Specimens will start to crackle, and steam will start bursting rapidly from certain places if the temperature is too high and heating should be turned off immediately in order not to destroy parts. That is why heating is done in cycles of 2 minutes to heat them gradually with pause in between lasting 1 to 5 minutes depending which cycle repetition it is. The last few cycles when wood is already close to 100 °C pauses are longer to allow wood to cool itself a bit in order not to overheat them. Longitudinal pressure should be put to the maximum by the presses when bend starts, but later in the bend when press is almost completely closed that pressure should be lowered a little bit so that specimens can adjust better to the mould.



**Figure 5:** Heating specimens, capacitor can be seen added to the press

After heating, wood is left for additional 10 minutes to rest at a heated temperature. After those 10 minutes cooling fans are turned on which are placed underneath the press. Fans are used to cool down mould and specimens faster to retain their shape. The whole bending cycle which includes loading the press, bending, heating and cooling specimens lasts  $90 \pm 15$  minutes depending on desired shape and cross-section of wood.

#### 4. TYPES OF PRESSES AND METHODS OF BENDING

During bending two types of presses were used. One type is mechanical press which uses mould on top and steel strips with end stops at the bottom that adjust to the shape accordingly. Steel strip also benefits to the convex side and keeps it in place and prevents specimens from elongation. Preventing wood from lengthening is a very important feature (as already mentioned in introduction) which is why additional metal sheet is used on top of iron strips to further reinforce convex side. Oak wood in contact with iron will cause black colouring but it is not important since it will be removed in further processing. This type of press uses hydraulic cylinders to provide longitudinal pressure. Longitudinal pressure at the same time prevents specimens from elongation and slightly compresses them which favours the bendability as it was mentioned by Báder et al. (2019).



*Figure 6: Chair legs in different type of press*



*Figure 7: Chair backs after bending*

This type of press is also connected to the HF generator. Two presses of each type are currently located in the factory. Smaller press is mostly used for bending more demanding curves such as chair backs and aprons for chairs, tables etc. The chair back and aprons are bent completely in this type of press, as all operations are done at one place which includes bending and heating. The chair legs and backs with lower curvature are done on larger press which operates a bit differently and cannot make such demanding curvatures. Larger press is used only to mechanically bend specimens. After that they are transferred into a second type of presses which uses male and female bending form as moulds as shown on figure 6.

That type of press uses high pressure combined with HF heating to dry and keep the specimens in shape. Because curvatures are small, high pressure up to 300 bar is used to press specimens from both sides. The second type of presses are slightly larger and can bend more specimens at once. One of the reasons why the combination of two types of press is used is because it speeds up a process a bit, as certain operations are overlapping. In earlier stages bending specimens were left in first press for 60 minutes but would often get too cold and lose a lot of moisture. For that reason, the time was reduced to 30 minutes and in that way, specimens would still remain warm and moist. After that period bent specimens are moved fast to other press and put under pressure. Heating is also done in cycles of 2 minutes but this time each cycle pressure is also increased.

After heating specimens are left to cool down. The whole operation lasts for 90 minutes including both presses, heating and cooling. After taking out specimens from press, they are left at room temperature to condition themselves a bit before grading them. Grading is done in that way that bent

specimens are compared to final sample which passed through all parts of the processing. Overmeasure of each individual specimen is monitored to check if it can handle all upcoming processes. Steaming and grading the specimens are processes which overlap with bending which is favourable for the whole process because no additional time is spent for those operations.

Figure 7 shows bent chair backs. All the specimens are from one cycle of bending and they all passed the grading. This grading is slightly different because specimens are compared to thin mould samples made of plywood, which provide check of bending radius and shape.



**Figure 8:** Chair legs after further processing



**Figure 9:** Framework after further processing

After the shape is checked, specimens are additionally tightened to fit to the mould with clamps, because there is always slight spring-back effect which tends to return specimens to their original shape. Specimens are fixed with metal straps and wooden sticks and nails from both sides in order to stop them from returning to their original shape. Those straps and sticks should be kept on until the very end of kiln drying. Only when fully dried to desired MC and cooled down, specimens will stop returning to their original shape. Figures 8 and 9 present bent specimens for chair legs and different frameworks after further processing.

## 5. CURRENT STATE OF THE ART OF WOOD OAK BENDING

Spring-back effect is big problem when bending wood, but what was encountered when first started was completely reversed situation. Bent shapes tend to go more inwards as they are cooling and drying. Initial response from bent specimens is spring-back but it is only normal after releasing it from the press. After some time when specimens start drying and cooling down, they tend to bend inwards. The reason for this is that wood is compressed on concave side and it is well known that shrinkage and swelling of densified wood is twice the number of normal values. This phenomenon shows that shrinkage of densified wood is stronger than spring-back effect. This actually favours whole process when bending leg chairs and specimens with small curvature and small cross-section, because forces of shrinkage and spring-back will mostly equalize and keep them in place. The problem arises when chair backs and frameworks are bent with demanding curvatures and large cross-sections. Larger cross-sections and larger curvatures result in more intensely compressed wood on concave side of specimen. More compressed wood means more shrinkage. This problem must be treated the same as spring-back and specimens need to be banded with straps and sticks. If not attended specimens will go far too inward after drying and will be deemed defective. Figures 10 and 11 show collapsed structure of specimens due to small bending radius and possibly far too great longitudinal pressure.

When the experiment was first started, percentage of utilization of the whole process was very low, around 50 %. With a lot of trials and new information gathered from all the possible sources,



utilization improved significantly. Nowadays, if the specimens have optimal MC utilization goes up to 95 % and even more in some cases. When bending chair legs one cycle of bending can have up to 25 specimens. A problem may occur if the whole cycle is faulty because that way most of those 25 will be deemed defective. That is why when bending solid wood, one should always be aware of what is happening in presses and if there are problems should adjust accordingly.



**Figure 10 and 11:** Collapsed structure of specimens in places of small bending radius

One of the missions in further period is to find optimal ration between overmeasure of specimens and the need for overmeasure due to the further processing on CNC machines. So far, overmeasures were maybe too great and were causing a lot of collapses of structure on concave side of thick specimens. Those specimens could still be further processed and prove to be satisfactory due to great overmeasures. But collapses of structure are also causing problems to CNC tools due to great densification. Bending chair legs and small curvature chair backs at the moment is satisfactory and high utilization rates are proof of that. Now, it only remains to develop optimal drying process to speed it up, so far 2 to 3 weeks of drying after bending, depending on MC, has been shown to be adequate. If the drying step is skipped a whole lot of problems can appear. Specimens will not stick properly if they need to be glued, they will tend to spring-back or to move inwards during further processing, and CNC machines will make rough cuts if the tools are not new and sharp. On figure 12 stack of bent chair backs banded with sticks and ready for drying, can be seen.



**Figure 12:** Stack of chair backs banded with wooden sticks



**Figure 13:** Turned chair pieces bent in two planes

According to Sandberg et al. (2013) straight-grained, knot-free wood materials should be used for bending work, especially if the bend is to be of a small radius. Practice has shown somewhat different case. Knots should be avoided on the side under tension mandatory, but smaller knots can be tolerated on concave side especially if they are not in the bending zone. Cracks and all other defects should be avoided at all costs since cracks are only increasing in number and size after steaming and especially after bending and all those specimens will be graded defective. Straight-grain on the other hand has not turned out to be such a big problem. All kinds of grain angles and shapes were bent properly even when it was expected for them to fail.

During the visit to the manufacturer in Italy the attempt was made to bend oak wood in two planes. When bending in two planes, significantly more demanding bend should be made across the radial section and smaller bend should be made across the tangential section. First, specimens were bent in “U” shape, then heated with HF and left to cool. After that only straight parts of specimens were steamed again in special constructed steaming chambers because if whole specimens were steamed, they would straighten out. After a second steaming specimens were placed in press with special mould to bend them in different plane. When cooled, specimens were turned and sanded. Test specimens are shown in figure 13.

The type of process in Italy includes a lot of handwork which is not suitable in manufacture where serial production is done. The problem will be further processing of specimens bent in two planes. It is impossible to tighten specimen bent like that on to worktable of CNC machine. Figure 13 shows mould made of plywood with specimen tightened in it. It turned out to be the only possible option, but it was decided too complex. All the specimens would have to be perfect in order to fit mould that is tight by itself, which is almost impossible. Specimens would have to be always in perfect position when drilling holes in order for them not to go outside the given dimensions. Another idea that occurred was just to bend specimens in one plane with great width, then imitate the second bend by routing on CNC machine.

The idea of bending oak wood in two planes has been abandoned for now. Focus will be directed towards further optimizing and speeding-up the process of all bending types and shapes. Bending on the press with male and female bending form initially should be learned also. This type of press does not have longitudinal pressure and end stops which makes it difficult to bend. Some small chair backs with minimum curvatures were done in that way so far, but more demanding curves are still not an option. Without end stops wood tends to break on convex side. For that reason, it has to be slowly heated with HF and slowly adjusted to shape without breaking. In future that technique will also be learned and implemented into the process.

## 6. CONCLUSIONS

Wood bending techniques have been around for a long time and are still used today. Bending wood can result in innovative shapes with improved mechanical properties. To bend wood at all, if it is not wood in green state, it needs to be plasticized. Plasticization can be done with high temperature and moisture or with chemicals. Most important parameters when bending wood are; initial MC of specimens, steam temperature and pressure, thickness of wood, steaming time, proper HF heating, longitudinal pressure, use of metal straps and end stops on convex side. Without metal straps and end stops more demanding bends of wood with big cross-sections cannot be produced. Only slight curves with smaller dimensions can be done that way. For further studies the focus will be on finding even better drying schedules and even better bending parameters to speed up the whole process. There is a possibility of implementing even more different bending techniques and obtaining more machinery to experiment on.

## REFERENCES

- [1] Báder, M., Németh, R., Konnerth, J. (2019): Micromechanical properties of longitudinally compressed wood, *European Journal of Wood and Wood Products*, 77:341–351
- [2] Báder, M., Németh, R. (2019): Moisture dependent mechanical properties of longitudinally compressed wood, *European Journal of Wood and Wood Products*, 77:1009–1019

- [3] Navi, P., Sandberg, D. (2012): Thermo-hydro-mechanical processing of wood. Presses polytechniques et universitaires romandes, Lausanne, ISBN 978-2-940222-41-1
- [4] Niemiec, S.S., Brown, T.D. (1995): Steam Bending Red Alder. In: Green D, von Segen W, Willits S, editors. Western hardwoods-value-added research and demonstration program. Gen. tech. rep. FPL-GTR-85. Madison (WI): U.S. Department of Agriculture, Forest Service, Forest Products Laboratory
- [5] Peck, E.C. (1957): Bending solid wood to form. U.S. Department of Agriculture, Forest Service, Agriculture Handbook No. 125.
- [6] Sandberg, D., Haller, P., Navi, P., (2013): Thermo-hydro and thermohydro-mechanical wood processing: An opportunity for future environmentally friendly wood products, Wood Material Science & Engineering, 8:1, 64-88
- [7] Stevens, W.C., Turner, N. (1970): Wood bending handbook. Parkersburg: Woodcraft & Supply Corp.
- [8] Taylor, Z., (2008): Wood Bender's Handbook; Sterling Publishing Co., Inc New York.

### **Acknowledgements**

The article was published as part of the project "Development of innovative products from modified Slavonian oak" by Spin Valis d.d. and partner University of Zagreb Faculty of Forestry and Wood Technology. The total value of the project is HRK 55,064,343.84, while the amount co-financed by the EU is HRK 23,941,527.32. The project was co-financed by the European Union from the Operational Program Competitiveness and Cohesion 2014-2020, European Fund for Regional Development.

### **Authors' Address:**

Research assistant **Mislav Mikšik**, mag. ing. techn. lign.; Professor **Stjepan Pervan**, PhD; Professor **Silvana Prekrat**, PhD; Professor **Mladen Brezovi**, PhD.  
University of Zagreb, Faculty of Forestry and Wood Technology, Department of Wood Technology, Zagreb, Republic of Croatia.

## PARAMETER DETERMINATION AND PERFORMANCE COMPARISON OF THE RHEOLOGICAL MODELS FOR CREEP IN PARTICLEBOARD

Mira Miri -Milosavljevi , Vladislava Mihailovi , Marija Jurkovi , Srđan Svrzi

University of Belgrade Faculty of Forestry, Serbia  
e-mail: mira.miric-milosavljevic@sfb.bg.ac.rs; vladislava.mihailovic@sfb.bg.ac.rs;  
marija.djurkovic@sfb.bg.ac.rs; srdjan.svrzic@sfb.bg.ac.rs

### ABSTRACT

A rheological model presents the stress-strain relationship in a material throughout the entire exploitation period. The change of the properties of a stressed and strained material in the time domain could be assessed on the basis of the rheological model. This paper focused on the determination of model parameters and comparison of several rheological models for particleboard coated with melamine foil. The model parameters were defined for four models: the purely mathematical Power-law model (two-parameter), and two viscoelastic models, i.e. the Zener (three-parameter) and Burger (four-parameter) models, as well as a semi-empirical modified Burger (five-parameter) model. The performance of models was compared in two ways: (i) according to the fit to the experimental data and (ii) according to the better total strain prediction. The Power-law and modified Burger models stood out as the best. The modified Burger model achieved better fitting to the experimental data, and the Power-law model was slightly better at making predictions.

**Keywords:** rheological model, viscous creep, particleboard

### 1. INTRODUCTION

Mechanical properties of wood and wood-based materials vary over time because they depend on the conditions of exploitation (temperature, humidity, etc.), but they are also highly dependent on the duration and rate of loading. That is why many studies have dealt with the influence of time-dependent effects on the mechanical properties of wood and wood-based materials during the second half of the 20th century and up until today (e.g. Clouser, 1959; McNatt, 1975; Gerhards, 1977; Laufenberg, 1987; Laufenberg 1988; Holzer, Loferski and Dillard, 1989; Gerhards, 1991; Hunt, 1999; Laufenberg, Palka and McNatt, 1999; Nielsen, 2006; Miri -Milosavljevi , 2012; Miri -Milosavljevi , 2015; Miri -Milosavljevi et al., 2019; Mihailovi et al., 2022).

Duration-of-load effect refers to changes in stress and strain that occur over time under the impact of external load. These changes are very important for all engineering materials, including wood and wood-based materials that are installed into building structures, furniture or interiors. Changes in stress and strain which occur over time can be represented by constitutive equations which are used for a particular rheological model and type of material and have their own specific parameters. In the engineering practice, we commonly use constitutive equations which do not include all types of strain (elastic, viscous, viscoelastic or plastic), but only the strains that prevail. In particleboards, the strain develops from an instantaneous elastic strain into a time-dependent viscous and viscoelastic strain and all the way to a plastic strain. During the period of particleboard exploitation, it is desirable that its properties remain in the domain of viscoelasticity, because this means that there will neither be material fractures nor excessive strains that endanger the stability of the structure.

Two types of changes that occur over time are typical for viscoelastic materials, and those are: a change in strain at constant stress, i.e. viscous creep, and a change in stress at constant strain, i.e. the relaxation of stress. The simplest uniaxial tension or compression tests are commonly used methods for creep testing. However, three-point and four-point bending creep testing is often used, because in

this type of test the deformation is larger and therefore easier to measure than in the case of uniaxial stress. Creep testing can be performed in two ways: data in the given time range is recorded and then extrapolated outside that range, or special methods are used to speed up or slow down the viscoelastic process (by changing the stress level, temperature or humidity), and then the time scale is empirically modified for a longer period of time. Both approaches are semi-empirical and the obtained data may be more or less accurate.

Numerous rheological models have been used to model the particleboard creep phenomenon, ranging from the linear, power, exponential and polynomial models to the viscoelastic model. Pierce and Dinwoodie (1977) and Pierce, Dinwoodie and Paxton (1979) used the viscoelastic three- and four-parameter models to describe properties in different chipboards. They came to the conclusion that one of the parameters of the Burger model is not constant but can vary over time. That study lasted for 26.5 months. Further, based on tests which lasted for 44 months, Pierce, Dinwoodie and Paxton (1985) came to the conclusion that the four-parameter Burger model is a good predictor of viscoelastic properties for the 30% stress level (relative to the maximum stress that leads to fracture) and for a period of 6 months, while it showed much higher strains than the actual ones after that time. Deviations were smaller for the 60% stress level. In order to reduce deviations from the actual strains that occur after a long period of time, these authors proposed to modify the Burgers model so that the viscous component is nonlinear with respect to time in order to gradually reduce the strain rate, and thus a new semi-empirical five-parameter model was obtained. The modified Burger model gives a more accurate overall strain than the Burger model, but does not reveal a clear (elastic, viscous or viscoelastic) strain structure. Dinwoodie et al. (1990) compared the prediction of deflection after 7 to 10 years according to the Burger model and modified Burger model, on the basis of an experiment with particleboard specimens which lasted for 24 weeks. Compared to the actual deflection, the errors of the modified Burger model ranged from +23% to -26%, which is considered acceptable. However, in the case of the Burger model, the errors were in the range from +170% to +430%. These authors also found that an extension of the experiment duration to 39 weeks would reduce the error by half. Mundy et al. (1998) suggested using a 6-month long experiment to determine the model parameters. They found that the model parameters obtained from such an experiment can be used to predict strain with great certainty even after 12 years. Following research by Pierce, Dinwoodie and Paxton (1985), Dinwoodie et al. (1990) and Mundy et al. (1998), BS DD ENV 1156 was issued in 1999, as a standard which refers to the determination of duration of load and creep factors for wood-based panels. According to that standard, a minimum of 26 and a maximum of 52 weeks were proposed for the duration of the experiment. The recommended experiment duration according to BS DD ENV 1156 (1999) is demanding to perform in practice, while it also increases the price of the experiment. For this reason, some authors have tried to reduce the duration of measurements, e.g.: Chen and Lin, 1997 (experiment duration 30 days); Fan et al., 2006 (experiment duration 14 days); Palija et al., 2006 (experiment duration 7 days); Houanou, Tch  houali and Foudjet, 2014 (experiment duration 15 hours and creep prediction in 60 hours).

Albin et al. (1991) state that in practical use about 80% of the final particleboard deflection can be considered to have already been reached after 7 days. It is further stated that because of that, according to DIN 68874 (1985) which refers to shelves and shelf supports of cabinet furniture, the prescribed load in standardized shelf creep testing is a uniformly distributed load lasting 28 days. It should be noted that, in most of the aforementioned studies, the bending creep test setup was a simply supported beam, symmetrically loaded with one or two concentrated loads, and that the actual load, especially for cabinet furniture elements (e.g. shelves) is very often in the form of a uniformly distributed load (DIN 68874, 1985; Tankut, Tankut and Karaman, 2012).

The main idea in this research was to examine the possibilities of bending creep modelling of particleboard under conditions that are similar to the real conditions of use of cabinet furniture shelves. The dimensions of the specimens as well as the type and level of load were selected according to this principle. The bending creep was modelled using four rheological models: a two-parameter (Power-law) model, a three-parameter (Zener or Standard Linear Solid) model, a four-parameter (Burger) model and a five-parameter (modified Burger) model. After the estimation of the parameters, the models were compared in 2 ways: (i) based on the fit to the experimental data, and (ii) according to the better total strain prediction after 28 days. For the purpose of assessing the predictive capability of the

model, the assumption was adopted (Albin et al., 1991) that the measured deflection after 7 days was 80% of the total deflection reached on day 28.

## 2. MATERIALS AND METHODS

### 2.1 Material

For the purpose of the experiment, a three-layer particleboard was used coated with melamine foil, with a nominal thickness of 18 mm, exposed to uncontrolled atmospheric influences of the temperature and humidity at the warehouse. A total of 30 specimens were cut, for different purposes (Table 1). The bending strength and modulus of elasticity were tested in both the parallel (designation  $\parallel$ ) and perpendicular (designation  $\perp$ ) directions of the board.

*Table 1: Number and dimensions of specimens, standard/type of test and physical property to be determined*

Number of specimens	Dimensions (mm)	Standard or test type	Physical property to be determined
6	50 x 50 x 18	EN 323 (1993)	Density
4	50 x 50 x 18	EN 322 (1993)	Moisture
6	350 x 50 x 18	EN 310 (1994)	Bending strength and modulus of elasticity
6 $\perp$	350 x 50 x 18	EN 310 (1994)	Bending strength and modulus of elasticity
8 $\perp$	850 x 350 x 18	Creep testing	Deflection, bending strength and modulus of elasticity

The dimensions of the creep testing specimens were selected to match the dimensions of cabinet furniture shelves. The specimens for creep testing were cut in the direction perpendicular to the fibers, as this is a direction with poorer characteristics. After cutting, all the specimens were conditioned by being kept in chambers with low temperature and humidity variations for 10 days. The air temperature in the room, where the experiment was subsequently conducted, reached within  $27 \pm 5$  °C, whereas the humidity was in the  $71 \pm 4\%$  range.

For creep testing, the specimens were placed on horizontal supports so that the overhangs were symmetrical. Comparators for deflection measurement were placed in the midspan of the specimens. The supports span was 0.8 m, and the specimens were loaded with a uniformly distributed load in the form of sand-filled bags from which air was removed (Figure 1).



*Figure 1: The testing method for bending creep behavior*

Three load levels were selected to correspond to the load range prescribed for classes L25 and L50 according to the standard for testing shelves in cabinet furniture DIN 68874 (1985). The magnitudes of uniformly distributed load and load durations by specimens are shown in Table 2. The deflection was measured after 1, 5, 10, 50, 100, 500, 1440 min from the load applying and then once daily. For the specimens loaded with 14 kg, the load duration was 14 days, and for the ones loaded

with 19.6 kg and 25 kg it was 7 days. Already after 100 minutes, a large deflection, which was beyond the range of the measuring instrument, was measured on specimen 5, and inconsistent results were recorded on specimen 6, which was the reason to exclude those two specimens from further consideration.

**Table 2:** The duration and load levels on the creep testing specimens

Specimen no.	Sand mass (kg)	Total load (sand and self-weight) (N)	Total load per unit area (N/m <sup>2</sup> )	Total load per unit length (N/m)	Stress in the midspan $max\sigma_x = \sigma_0$ (MPa)	Duration of load (days)
1	14	171.63	613	214.53	0.908	14
2	14	171.68	613	214.59	0.908	14
3	25	279.19	997	348.99	1.477	7
4	25	279.24	997	349.05	1.477	7
5*	14	171.14	611	213.92	0.905	14
6*	19.6	226.07	807	282.59	1.196	7
7	19.6	225.92	807	282.41	1.195	7
8	14	171.09	611	213.86	0.905	14

\* Specimens excluded from further consideration.

## 2.2 Methodology

Four rheological models were used to show the relationship between stress and strain, and those were: the Power-law (two-parameter) model, the Zener (three-parameter) model, the Burger (four-parameter) model and the modified Burger (five-parameter) model. Equations (1-4) show the mathematical formulations of strain development over time for all four models.

The Power-law model:

$$\varepsilon(t) = \varepsilon_0 + \alpha t^b. \quad (1)$$

The Zener model:

$$\varepsilon(t) = \frac{\sigma_0}{E_H} + \frac{\sigma_0}{E_K} \left( 1 - e^{-\frac{E_K t}{\eta_K}} \right) = \beta_1 + \beta_2 (1 - e^{-\beta_3 t}). \quad (2)$$

The Burger model:

$$\varepsilon(t) = \frac{\sigma_0}{E_H} + \frac{\sigma_0}{E_K} \left( 1 - e^{-\frac{E_K t}{\eta_K}} \right) + \frac{\sigma_0}{\eta_N} t = \beta_1 + \beta_2 (1 - e^{-\beta_3 t}) + \beta_4 t, \quad (3)$$

The modified Burger model:

$$\varepsilon(t) = \frac{\sigma_0}{E_H} + \frac{\sigma_0}{E_K} \left( 1 - e^{-\frac{E_K t}{\eta_K}} \right) + \frac{\sigma_0}{\eta_N} t^{\beta_5} = \beta_1 + \beta_2 (1 - e^{-\beta_3 t}) + \beta_4 t^{\beta_5}. \quad (4)$$

In the above equations,  $\varepsilon_0$  represents instantaneous deformation (the first recorded data),  $\varepsilon(t)$  deformation at an arbitrary moment of time  $t$ , and  $\sigma_0$  is a constant applied stress (Table 2).

Coefficients  $a$ ,  $b$ ,  $\beta_1$ ,  $\beta_2, \dots, \beta_5$  are parameters of the model. The Power-law model is purely mathematical, and coefficients  $a$  and  $b$  in Equation (1) have no physical meaning. Parameters  $\beta_1$  and  $\beta_2$ , as can be seen from Equations (2) – (4), have physical meaning and represent a deformation: the elastic deformation ( $\beta_1$ ) and the viscoelastic deformation ( $\beta_2$ ). Parameters  $\beta_3$  and  $\beta_4$  also have physical meaning: the reciprocal value of parameter  $\beta_3$  represents retardation time, while the reciprocal value of parameter  $\beta_4$  is the time it takes for viscous deformation to develop. Parameter  $\beta_5$  has values  $0 \leq \beta_5 \leq 1$ , and no physical meaning. Thus, models (2) – (4) allow the estimation of the following material parameters from the experiment: the initial modulus of elasticity  $E_H$ , the viscoelastic modulus  $E_K$ , the dynamic viscosity of the viscoelastic part of the model  $\eta_K$ , and the dynamic viscosity of the viscous part of the model  $\eta_N$ , as well as the aforementioned characteristic times.

Retardation time  $\tau_r$  is an important parameter that has a physical meaning and represents the critical time required for changes in the molecular structure of the material to occur under the action of external load and for a new equilibrium state to be established at the molecule level, i.e. for a second-order phase transition (non-adiabatic) to occur. Different names can be found in the literature for parameter  $\tau_r$ , such as retardation time (Ferry, 1980; Shaw and MacKnight, 2005), creep time (Lakes, 2009) or viscous creep time (Miri -Milosavljević, 2012). The term retardation time will be used here. After reaching the retardation time, further changes, such as a small subsequent increase in strain under the action of external load over time, are not critical, as they do not lead to a change in molecular structure. Retardation time is also the time which can help estimate the minimum required duration of the experiment.

For a simply supported beam (with rectangular cross-section of height  $h$  and beam span  $l$ ), loaded with a uniformly distributed load, the measured deflection  $f(t)$ , was converted into a longitudinal deformation  $\varepsilon(t)$  according to the equation:

$$\varepsilon(t) = (24h/5l^2) \cdot f(t). \quad (5)$$

Based on the experimental data, the parameters of the rheological models in Equations (1) – (4) were estimated using the GRG nonlinear solving method in the Excel's Solver add-in. The performance of the established rheological models was compared in two ways: (i) according to the fit to the experimental data and (ii) according to the better prediction of creep deformation after 28 days.

After fitting data with four nonlinear theoretical models, and visual examination of the fitted curves, goodness-of-fit was assessed based on two quantitative measures: the Sum of Squared Residuals (SSR) and Residual Standard Error (RSE). The estimation of the non-linear regression model parameters in the solving method used is based on the method of least squares, i.e. minimizing SSR. RSE was calculated through SSR and the number of experimental data, but the number of model parameters was also taken into account.

In the second phase, the prediction potential of each of the models was examined. Prediction means that the theoretical model, whose parameters are estimated by fitting to experimental data in a certain time range, is extrapolated into the future. The idea in this paper was to obtain performance assessment for each model, as well as to compare the models regarding prediction in the near future (2-4 times longer than the duration of the experiment). Due to the fact that there were no measurements longer than 14 days to compare the results of the model, following the statements from Albin et al. (1991), the assumption was adopted in this paper that the measured deflection after 7 days was 80% of the deflection that would be reached on day 28. Therefore, based on the measurements, the predicted deflection and the predicted deformation after 28 days were easily calculated, as  $f_{28} = f_7/0.8$ , and  $\varepsilon_{28} = \varepsilon_7/0.8$ . Here,  $f_7$  and  $\varepsilon_7$  are the measured deflection and deformation after 7 days. The model performance was assessed based on the differences between the predicted deflection, i.e. longitudinal deformation,  $f_{28}$  and  $\varepsilon_{28}$ , and the estimated deflection and deformation after 28 days obtained by the four rheological models,  $\hat{f}_{28}$  and  $\hat{\varepsilon}_{28}$ .

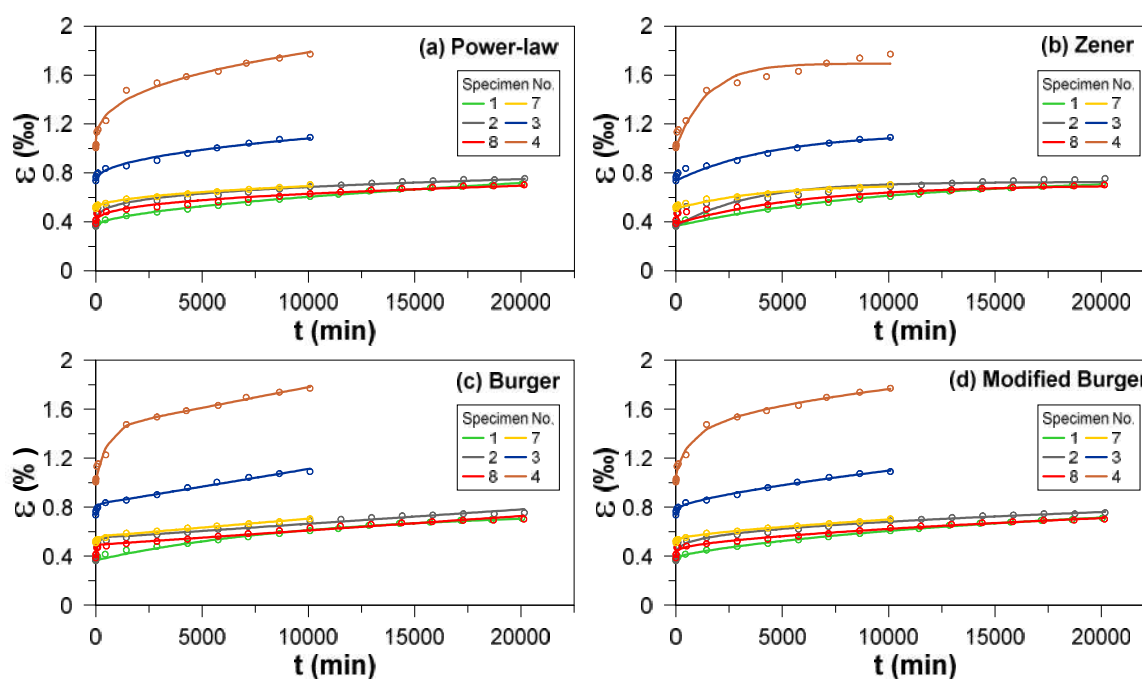


### 3. RESULTS AND DISCUSSION

The basic physical characteristics of particleboard were determined according to the standards specified in Table 1. The measured moisture content and density of the specimens was  $8.51 \pm 0.13\%$  and  $638 \pm 8.28 \text{ kg/m}^3$ , respectively. The mean bending strength was  $12.66 \pm 0.82 \text{ MPa}$ , and the modulus of elasticity  $3139 \pm 66.51 \text{ MPa}$ . The average specimen density for the bending creep experiment was  $635 \pm 4.15 \text{ kg/m}^3$  and the average mass was  $3.46 \pm 0.025 \text{ kg}$ .

#### 3.1 Fitting rheological models to experimental data

Figure 2 shows the development of deformation over time on all specimens: the experimental data (open circles) calculated using Equation (5) and fitted theoretical curves for the four models used. For each specimen, the experimental data and corresponding theoretical curve are displayed in the same color. When observing the experimental data, the differences in the size of the deformation depending on the load level can clearly be seen in the figure. Specimens 1, 2 and 8, which were loaded with 14 kg each, had the lowest deformation, both initially and at a later time of measurement; the initial part is less steep, and the increase in deformation over time is slower than in the two specimens loaded with 25 kg each (specimens 3 and 4). Based on the visual examination of theoretical curves fit to the experimental data in the Figure 2, it seems that the best model was the modified Burger model, followed by the Power-law and Burger models, while apparently the worst one was the Zener model.



**Figure 2:** Experimental data (open circles) for all six specimens and corresponding fitted theoretical models (lines): (a) the Power-law model; (b) the Zener model; (c) the Burger model; (d) the Modified Burger's model

The results of parameter estimates, as well as goodness-of-fit (GoF) measures, Sum of Squared Residuals (SSR) and Residual Standard Error (RSE), for the Power-law, Zener, Burger and modified Burger models, are shown in Table 3, for each specimen. Table 3 also shows the material parameters calculated through model parameters, for the Zener, Burger and modified Burger models (Eqs. 2 – 4).

It can be seen from the table that retardation time for the Zener model for specimens 2, 3, 4, 7 and 8 ranged from 1 to 4.27 days, and for specimen 1 it amounted to as much as 6.94 days. For the Burger's model for specimens 2, 3, 4, 7 and 8, it was from 0.02 to 0.36 days, and for specimen 1 as much as 6.03 days, and for the modified Burger's model it ranged from 0.49 to 65.57 days.

**Table 3:** Fitted model parameters, material parameters and estimated GoF measures SSR and RSE of the Power-law, Zener's, Burger's and modified Burger's models

Model	Model and material parameters and GoF's	Specimen No.					
		1	2	8	7	3	4
Power-law	$a$ ( $10^3$ /day)	0.08081	0.19375	0.12420	0.07693	0.14411	0.39378
	$b$ (-)	0.55934	0.26222	0.34690	0.44930	0.45399	0.35278
	SSR (%) <sup>2</sup>	0.0010679	0.0078971	0.0064494	0.0005535	0.0038207	0.0123774
	RSE (%)	0.0077025	0.0209458	0.0189288	0.0070937	0.0186369	0.0335443
Zener	$S_1$ ( $10^3$ )	0.36585	0.36315	0.38610	0.50895	0.73575	1.00575
	$S_2$ ( $10^3$ )	0.39269	0.36245	0.31609	0.19490	0.38943	0.68897
	$S_3$ (1/day)	0.14406	0.41803	0.23368	0.36575	0.31719	0.99291
	$t_r$ (day)	6.94	2.39	4.27	2.73	3.15	1.00
	$E_H$ (MPa)	2482.09	2501.26	2344.52	2348.69	2007.76	1469.02
	$E_k$ (MPa)	2312.42	2506.07	2863.79	6133.24	3793.22	2144.45
	$K$ (MPa·s)	1.39E+09	5.18E+08	1.06E+09	1.45E+09	1.03E+09	1.87E+08
	SSR (%) <sup>2</sup>	0.0038777	0.0561229	0.0236422	0.0030229	0.0123017	0.0431492
	RSE (%)	0.0151030	0.0574574	0.0372924	0.0173866	0.0350738	0.0656881
	Burger	$S_1$ ( $10^3$ )	0.36585	0.36315	0.38610	0.50895	0.73575
$S_2$ ( $10^3$ )		0.32960	0.18394	0.10594	0.05069	0.08796	0.43637
$S_3$ (1/day)		0.16569	25.13668	41.26481	14.77633	27.33819	2.77308
$S_4$ (1/day)		0.00305	0.01690	0.016970	0.02108	0.04143	0.04868
$t_r$ (day)		6.03	0.04	0.02	0.07	0.03	0.36
$E_H$ (MPa)		2482.09	2501.26	2344.52	2348.69	2007.76	1469.02
$E_k$ (MPa)		2755.08	4938.31	8544.65	23580.35	16793.91	3385.81
$K$ (MPa·s)		1.44E+09	1.70E+07	1.79E+07	1.38E+08	5.31E+07	1.05E+08
$N$ (MPa·s)		2.57E+07	4.64E+06	4.61E+06	4.90E+06	3.08E+06	2.62E+06
SSR (%) <sup>2</sup>		0.0037745	0.0040376	0.0032179	0.0006674	0.0020618	0.0153943
RSE (%)	0.0153592	0.0158854	0.0141816	0.0086114	0.0151356	0.0413580	
Modified Burger	$S_1$ ( $10^3$ )	0.36585	0.36315	0.38610	0.50895	0.73575	1.00575
	$S_2$ ( $10^3$ )	0.38535	0.31717	0.35609	0.49990	0.75808	0.17326
	$S_3$ (1/day)	0.07711	0.01525	0.04305	0.02871	0.04761	2.0237
	$S_4$ (1/day)	0.04890	0.18191	0.10145	0.05828	0.09691	0.27827
	$S_5$ (1/day)	0.25693	0.23342	0.18228	0.27719	0.22201	0.38330
	$t_r$ (day)	12.96	65.57	23.22	34.84	21.00	0.49
	$E_H$ (MPa)	2482.09	2501.26	2344.52	2348.69	2007.76	1469.02
	$E_k$ (MPa)	2356.49	2863.88	2542.12	2391.20	1948.61	8527.29
	$K$ (MPa·s)	2.64E+09	1.62E+10	5.10E+09	7.20E+09	3.54E+09	3.64E+08
	$N$ (MPa·s)	1.60E+06	4.31E+05	7.71E+05	1.77E+06	1.32E+06	4.59E+05
SSR (%) <sup>2</sup>	0.0004276	0.0080683	0.0029651	0.0001746	0.0013333	0.0074514	
RSE (%)	0.0053391	0.0231924	0.0140596	0.0046716	0.0129100	0.0305192	

### 3.2 Comparison of models according to the goodness-of-fit measures

It is difficult to compare the results of GoF measures for all specimens and models, which are shown in Table 3. Therefore, those results were summarized in Table 4 in a way that shows only the ranks of individual models according to SSR and RSE (rank "1" indicates the best model, i.e. the one with the lowest SSR, i.e. RSE error, and so on). These results confirmed the initial conclusions drawn on the basis of the visual inspection of diagrams in Figure 2. The modified Burger's model was the best in all specimens, except specimen 2. The Power-law model was the second best, whereas the Zener's model was the worst.

**Table 4:** Ranking of the rheological models for all specimens according to the goodness-of-fit measures SSR and RSE

Spec. No.	SSR				RSE			
	Power-law	Zener	Burger	Modif. Burger	Power-law	Zener	Burger	Modif. Burger
1	2	4	3	1	2	3	4	1
2	2	4	1	3	2	4	1	3
8	3	4	2	1	3	4	2	1
7	2	4	3	1	2	4	3	1
3	3	4	2	1	3	4	2	1
4	2	4	3	1	2	4	3	1

### 3.3 Comparison of models according to the creep prediction

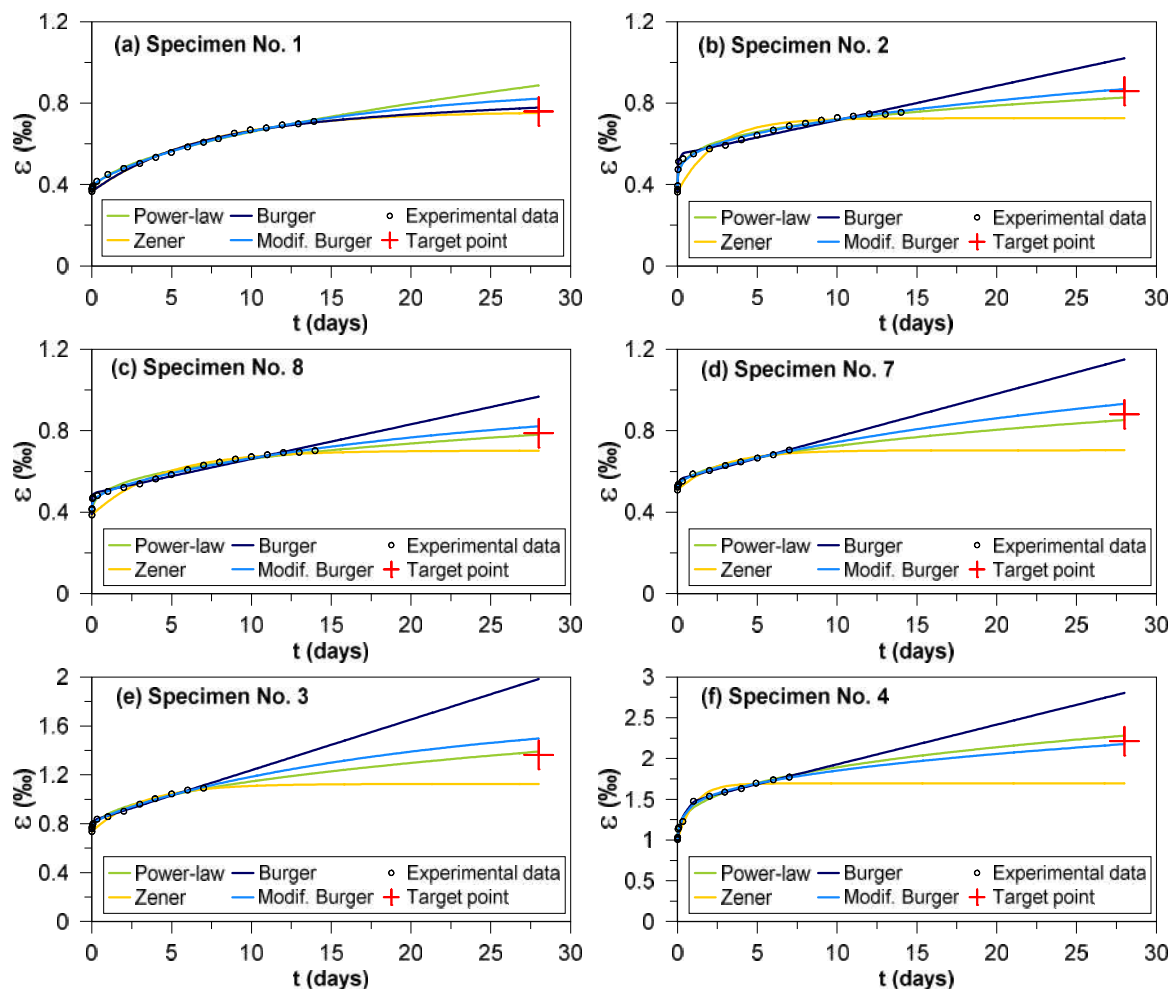
The accuracy of a 28-day prediction of bending creep of the theoretical models was estimated here in relation to the target points – predicted deflection and deformation after 28 days,  $f_{28}$  and  $\varepsilon_{28}$ . The calculation procedure for  $f_{28}$  and  $\varepsilon_{28}$  was explained in the Methodology chapter. Figure 3 shows the experimental data (open circles) and target points  $\varepsilon_{28}$  (red crosses) for each specimen. The theoretical bending creep curves for 28 days (coloured lines) are shown next to them. These theoretical curves represent the prediction of 28-day bending creep based on 14-day creep data, (specimens 1, 2 and 8), or 7-day creep data (specimens 7, 3 and 4).

Figure 3 shows the development of deformation over time, and for practical application it is also important to have data on the predicted deflection. The predicted deflection according to each theoretical model was calculated from the deformation using Eq. (5). Table 5 shows the predicted deflection after 28 days ( $f_{28}$ ) for each specimen (target points), and the deflections calculated according to four theoretical models  $\hat{f}_{28}$ . Relative errors of the model prediction in relation to  $f_{28}$  are also shown in parentheses. For each of the specimens, the results of the best model are bolded.

In general, Table 5 and Figure 3 show that the theoretical curves for the Power-law and modified Burger's models are always between the curves for the Zener's and Burger's models. It is obvious that the predictions of deflection according to these two models are much closer to the target points than the predictions obtained using the Zener's and Burger's models. Only the results for specimen no. 1 deviated from this general conclusion. For other specimens, the Burger's model significantly overestimates the target points (between 19% and 45%) and the Zener's model significantly underestimates the target points (15% to 24%). The Power-law model had the smallest error in three specimens, so it could be said that according to the prediction criterion, it was the best overall of all the investigated models. Admittedly, this model overestimated the target point by almost 17% in specimen 1, but for other specimens, the absolute value of the error did not exceed 4%. The Modified Burger model was the best in two cases, and its error was always lower than 10% in absolute value. This model generally slightly overestimated the target points.

In specimens loaded with a higher load, and the measurements which lasted for 7 days (specimens 3, 4 and 7), the Power-law and modified Burger's models were much better than the Zener's and Burger's models. An explanation for the poor predictions of the Zener's and Burger's models can be

found in the relatively short duration of the experiment, combined with the mathematical formulations of these models. Namely, coefficient  $\beta_2$  in Eq. (2) of the Zener model is a key factor for the magnitude of the predicted deformation, since the sum  $\beta_1 + \beta_2$  ( $\beta_1$  is the initial deformation) represents the asymptote to which the creep curve (2) tends to approach, whose reliability is compromised when the duration of the experiment is short. In the Burger model, the last term in Eq. (3) gave a constant strain rate, and therefore this model overestimated the target points.



**Figure 3:** Prediction of 28-day of bending creep based on 14-day creep data (specimens 1, 2 and 8), or 7-day creep data (specimens 3, 4 and 7). For each specimen circles represent experimental data, the red cross represents the target point, and the coloured lines theoretical creep curves.

For practical application, it is important to compare the predicted and measured deflection with the permissible deflection (DIN 68874, 1985), which is  $\ell/100 = 8 \text{ mm}$  (where  $\ell$  is the shelf span). Table 5 shows that for specimens 3 and 4 the predicted deflection  $\hat{f}_{28}$  and predictions of the theoretical models  $\hat{f}_{28}$  exceed the permissible deflection. Those specimens were loaded with  $997 \text{ N/m}^2$ , which corresponds to class L50 according to standard DIN 68874 (1985). In fact, the deflection measured after 7 days on specimen 3 slightly exceeded the permissible limit (8.08 mm), but for specimen 4 it amounted to as much as 13 mm. This was expected, because at higher load levels, the viscoelasticity range is exited. For specimens loaded with lower levels of stress, neither  $\hat{f}_{28}$  nor  $f_{28}$  exceeded the permissible deflection, except for the Burger model prediction for specimen 7.

All the results indicated that the Power-law and modified Burger's models were the best. The modified Burger's model achieved a better fit to the experimental data, and the Power-law model was slightly better at predicting. If those two models are compared, their characteristics should be taken into account, as well as the usability of the data that can be obtained after determining model parameters. The Power-law model has only two parameters to be estimated, and it has not proved to be

worse than the Modified Burger model, which has as many as five. Therefore, the Power-law model should be given priority if it is necessary to quickly and easily estimate the parameters of the model after a not-so-long measurement. This would be “a parsimonious modelling”. On the other hand, the Power-law model is purely mathematical and not related to the properties of the material. The modified Burger model is not purely physical, but properties of a material can be determined based on it (Eq. 4 and Table 3). This model is certainly not parsimonious, as it has as many as five parameters, but nowadays there are a number of software tools that can easily solve the problem of non-linear regression in complicated models.

**Table 5:** Deflections after 28 days for all specimens: the predicted deflection  $f_{28}$ , and theoretical deflections estimated on the basis of the four models  $\hat{f}_{28}$ . The relative error of each model in respect to  $f_{28}$  is shown in brackets

Spec. no.	Load (sand) mass (kg)	Duration of the experiment (days)	Predicted deflection $f_{28}$ (mm)	Theoretical deflection, $\hat{f}_{28}$ (mm)			
				Power-law	Zener	Burger	Modif. Burger
1	14	14	5.63	6.57 (16.8%)	<b>5.57</b> <b>(-1.03%)</b>	5.76 (2.44%)	6.09 (8.23%)
2	14	14	6.36	6.13 (-3.68%)	5.37 (-15.52%)	7.56 (18.78%)	<b>6.44</b> <b>(1.21%)</b>
8	14	14	5.84	<b>5.78</b> <b>(-0.94%)</b>	5.20 (-10.95%)	7.16 (22.73%)	6.09 (4.28%)
7	19.6	7	6.53	<b>6.32</b> <b>(-3.19%)</b>	5.21 (-20.10%)	8.52 (30.55%)	6.90 (5.79%)
3	25	7	10.10	<b>10.30</b> <b>(1.94%)</b>	8.33 (-17.48%)	14.69 (45.49%)	11.09 (9.80%)
4	25	7	16.40	16.90 (3.05%)	12.55 (-23.45%)	20.78 (26.71%)	<b>16.13</b> <b>(-1.67%)</b>

\* The results of the model with the lowest error compared to  $f_{28}$  are bolded.

#### 4. CONCLUSIONS

This study deals with the modeling of the bending creep of particleboard based on the results of an experiment conducted on specimens loaded with a uniformly distributed load. The parameters of the model were estimated for four models, i.e. the Power-law, Zener, Burger and modified Burger models. After the comparison of performance of these models according to the goodness-of-fit to the experimental data and according to the better prediction of the creep deflection, the following conclusions can be summarized:

1. On specimens exposed to uniformly distributed load, corresponding to the class L50 (DIN 68874, 1985), the deflections exceeding the allowable ones, have already been recorded after 7 days.
2. The Power-law and modified Burger models stood out as the best. The modified Burger model achieved better fitting to the experimental data, and the Power-law model was slightly better at making predictions. The Zener model significantly underestimated, and the Burger model overestimated the target points.
3. The Power-law, as a parsimonious model, could be recommended when there is a need to quickly and easily estimate the parameters of the model after a not-so-long measurement. On the other hand, this model is purely mathematical and is not related to the properties of the material.
4. If it is important to estimate the parameters of the material, and even to estimate future deformations, our results indicated that the modified Burger model should be recommended.

### Acknowledgements

The authors owe great gratitude to the Chipboard Testing Laboratory, Faculty of Forestry, Belgrade University, for the donated testing material and the Furniture Quality Control Institut, Faculty of Forestry, Belgrade University, for the equipment and space provided.

This research was partially funded by the Ministry of Education, Science and Technological Development of the Republic of Serbia, grant number 451-03-47/2023-01/200169.

### REFERENCES

- [1] Albin, R., Dusil, F., Feigl, R., Frochich, H.H., Funke, H., J. (1991): Grundlagen des Möbel- und Innenausbaus. DRW – Verlag, Stuttgart, Germany.
- [2] BS DD ENV 1156 (1999): Wood-based panels —Determination of duration of load and creep factors.
- [3] Chen, T.Y., Lin, J.S. (1997): Creep behaviour loading at room of commercial wood based boards under long-term conditions in Taiwan. Holz als Roh- und Werkstoff 55, 371-376.
- [4] Clouser, W.S. (1959): Creep Of Small Wood Beams Under Constant Bending Load. USDA, Forest service, research paper 2150, Forest product laboratory Madison, Wiskonsin.
- [5] DIN 68874 (1985): Möbel-Einlegeböden und – Bodenträger, Anforderungen und Prüfung im möbel.
- [6] Dinwoodie, J.M., Higgins, J.A., Robson, D.J., Paxton, B.H. (1990): Creep in chipboard Part 7: Testing the efficacy of models on 7-10 years data and evaluating optimum period of prediction. Wood Science and Technology 24: 181-189.
- [7] EN 310 (1994): Wood-based panels. Determination of modulus of elasticity in bending and of bending strength.
- [8] EN 322 (1993): Wood - based panels. Determination of moisture content.
- [9] EN 323 (1993): Wood-based panels. Determination of density.
- [10] Fan, M., Bonfield, P., Dinwoodie, J., Enjily, V. (2006): Effect of Test Piece Size on Rheological Behavior of Wood Composites. Journal of Engineering Mechanics, Vol. 132, No. 8, 815 – 822, DOI: 10.1061/(ASCE)0733-9399(2006)132:8(815).
- [11] Ferry J.D. (1980): Viscoelastic properties of polymers. John Wiley & Sons, New York, USA.
- [12] Gerhards, C.C. (1977): Effect Of Duration And Rate Of Loading on Strength Of Wood And Wood-Based Materials. USDA, Forest service, research paper FPL 287, Forest product laboratory Madison, Wiskonsin.
- [13] Gerhards, C.C. (1991): Bending Creep And Load Duration Of Douglas-Fir 2 By 4S Under Constant Load. Wood and Fiber Science, 23(3): 384 – 409.
- [14] Holzer, S.M., Loferski, J.R., Dillard, D.A. (1989): A Review Of Creep In Wood: Concepts Relevant To Develop Long-Term Behavior Predictions For Wood Structures. Wood and Fiber Science, 21(4): 376-392.
- [15] Houanou, K.A., Tchéhouali, A., Foudjet, A.E. (2014): Effect of the loading duration on the linear viscoelastic parameters of tropical wood: case of *Tectona grandis* L.f (Teak) and *Diospyros mespiliformis* (Ebony) of Benin Republic. SpringerPlus, 3:74.
- [16] <http://www.springerplus.com/content/3/1/74>Hunt, D.G. (1999): A unified approach to creep of wood. Proceedings Royal Society, Vol. 455, 4077 – 4095.
- [17] Lakes R.S. (2009): Viscoelastic materials. Cambridge university press, New York, USA.
- [18] Laufenberg, T.L. (1987): Creep Testing Of Structural Composite Panels: A Literature Review And Proposed Standard. In: Maloney, T.M., ed. Proceedings, 21st International particleboard/composite materials symposium; Pullman, WA. Pullman, WA: Washington State University, 297-313.
- [19] Laufenberg, T.L. (1988): Composite Products Rupture Under Longterm Loads: A Technology Assessment. In: Proceedings, 22d International particleboard/composite materials symposium; Pullman, WA. Pullman, WA: Washington State University, 247-256.
- [20] Laufenberg, T.L., Palka, L.C., McNatt, J.D. (1999): Creep and creep–rupture behavior of wood-based structural panels. Res. Pap. FPL–RP–574. Madison, WI: U.S. Department of Agriculture, Forest Service, Forest Products Laboratory, Madison, USA.

- [21] McNatt, J., D. (1975): Effect of rate of loading and duration of load on properties of particleboards, USDA, Forest service, research paper FPL 270, Forest product laboratory Madison, Wisconsin, USA.
- [22] Mihailovi , V., Miric-Milosavljevi , M., Djurkovi , M., Mladenovi , G., Milosevi , M., and Trajkovi , I. (2022): Loading rate effects on MOE and MOR distributions in testing of small clear beech wood specimens. *BioResources* 17(1): 1818-1835. DOI: 10.15376/biores.17.1.1818-1835.
- [23] Miri -Milosavljevi , M., (2015): Comparative analysis of rheological model of wood. In: *Proceedings of 26th International Conference on Wood Science and Technology*, 165-172, Faculty of forestry, Zagreb, ISBN: 978-953-292-040-6.
- [24] Miric-Milosavljevi , M., Mihailovi , V., Djurkovi M. (2019): Impact of the loading rate on MOR and MOE of the particleboard applying a standard bending test. In: *Proceedings of the 4th International Scientific Conference “Wood Technology & Product Design”, Ohrid, Republic of North Macedonia*, Vol.8, No.1: 33-40.
- [25] Miri -Milosavljevi , M. (2012): Zener model viscoelasticity for orthotropic solid and application in mechanics of wood. (In Serbian.) PhD thesis, Faculty of Forestry, Belgrade. Available at 10.2298/BG20120713MIRICMILOSAVLJEVIC.
- [26] Mundy, J.S., Bonfield, P.W., Dinwoodie, J.M., Paxton, B.H. (1998): Modelling the creep behaviour of chipboard: The rheological approach. *Wood Science and Technology* 32: 261-272
- [27] Nielsen, L.F. (2006): Power-Law creep as related to adapted Burgers creep representations and incremental analysis. BYG•DTU R-137, Danmarks Tekniske Universitet, ISSN 1601-2917, ISBN 87-7877-208-7.
- [28] Palija, T., Skaki , D., Džin i , I., Nestorovi , B. (2009): Creep in particle board coated with melamine sheath and beech veneer. *Prerada drveta*, pp. 41-51.
- [29] Pierce, C.B., Dinwoodie, J.M. (1977): Creep in chipboard Part I: Fitting 3- and 4-element response curves to creep data. *Journal of materials science*, 12: 1955-1960.
- [30] Pierce, C.B., Dinwoodie, J.M., Paxton, B.H. (1979): Creep in chipboard Part II: The Use of Fitted Response Curves for Comparative and Predictive Purposes. *Wood Science and Technology*. 13: 265-282.
- [31] Pierce, C.B., Dinwoodie, J.M., Paxton, B.H. (1985): Creep in chipboard Part V: An improved model for prediction of creep deflection. *Wood Science and Technology*, 19:83-91.
- [32] Shaw, M.T., MacKnight, W.J. (2005): Phenomenological treatment of viscoelasticity. Viscoelastic models. Time temperature correspondence. In: *Introduction to polymer viscoelasticity*. John Wiley & Sons, New York, USA.
- [33] Tankut, A., N., Tankut, N., Karaman, A. (2012): Creep Performance Of Ready To Assemble (Rta) Fasteners In Bookcase Construction. In: *Proceedings of 23th International Conference on Wood Science and Technology*, 95-208, Faculty of forestry, Zagreb, ISBN: 978-953-292-026-0.

#### **The Authors' Addresses:**

Mira Miri - Milosavljevi , Ph.D., Vladislava Mihailovi , Ph.D., Marija urkovi , Ph.D., Srdjan Svrzi , Ph.D.  
Belgrade University, Faculty of Forestry, Kneza Višeslava 1, 11030 Belgrade, SERBIA

## **METROLOGY OF THE GEOMETRIC CHARACTERISTICS OF MORTISE AND TENON JOINTS THROUGH GEOMETRICAL PRODUCT SPECIFICATION (GPS) STANDARDS**

**Nikola Mihajlovski, Gjorgji Gruevski**

*Ss. Cyril and Methodius University in Skopje, North Macedonia,  
Faculty of Design and Technologies of Furniture and Interior-Skopje,  
e-mail: mihajlovski@fdtme.ukim.edu.mk; gruevski@fdtme.ukim.edu.mk*

### **ABSTRACT**

The mutual interaction of the contact surfaces of the mortise and tenon joints is complex. The geometry of the joint affects the tribology of these surfaces. The optimal shape of mortise and tenon joints is also represented by their geometric features.

The Geometrical Product Specification System (GPS) is a set of guidelines, concepts, and symbols that establish the geometry of a part's allowable tolerances to guarantee its functionality.

This review paper presents an investigation of the possibilities for metrology of the geometrical characteristics of mortise and tenon joints and their expression and representation through Geometrical Product Specification (GPS) standards. For this purpose, the metrology of the most commonly used joint in wood chair construction is presented. The following types of tolerances are presented: dimension tolerances (length, width and thickness); form tolerances (straightness and flatness); orientation tolerances (parallelism and perpendicularity) and location tolerances (symmetry).

Metrology and presentation of the geometric characteristics of mortise and tenon joints through GPS standards is a useful method that satisfies functional requirements and quality control during processing. The phases and operations of measuring the geometric characteristics of the joints using manual instruments are presented.

**Keywords:** geometric characteristics, mortise and tenon joints, tolerances, metrology

### **1. INTRODUCTION**

The application of tolerances and fits and the control in the accuracy of the processing of the compositions are necessary necessities of any modern furniture production.

Mortise and tenon joints are the most common compositions in wooden constructions, and the most common application is in chair construction. Numerous studies have been carried out on the systematization and dimensioning of all types of mortise and tenon joints, as well as research on the strength of joints, by many authors (Haviarova et al. 2001, Jivkov and Marinova 2006, Gruevski 2007, Prekrat and Smardzewski 2010, Hajdarevic and Martinovic 2014 and others).

The strength and durability of the construction depend on several factors that are interdependent, making this characteristic complex. Joints in wooden construction represent critical places where defects often occur, so special attention should be paid to tolerances and the type of fit during construction (Eckelman 2003).

The influence of the tolerances and the type of fit in the mortise and tenon joints on the strengths has been investigated by several authors (Potrebic 1970, Skacic and Janicevic 2000, Smardzewski and Papruga 2004, Mackerle 2005, Gawronski 2006). In general, all authors state that the type of fit and the accuracy of the processing of the mortise and tenon joints have an impact on the strength of the joints. They recommend a tight fit with an overlap of 0.1 to 0.2mm. It is characteristic of these studies that all authors take only the tolerance in the thickness of the mortise and tenon without taking into account other dimensions. The first research in which broad information is given about other characteristics of the joint is from (Tkalec 1990), in which the author characterizes the deviations as "errors and inaccuracies during processing".



Interest in the quality of processing in industry initially appeared in the thirties of the last century, and it received a more serious development during the Second World War for the needs of weapons production and the machine industry. With the development of CAD/CAM technology, there is a greater need for quality control and processing accuracy, so in 1996, by the Technical Committee for International Standardization (ISO/TC 213), a series of standards were published for the first time (GPS – Geometrical product specifications) which include all the geometrical characteristics of the products. Geometrical characteristics mean tolerances in dimensions, geometrical tolerances and the quality of the surface of the parts.

This review paper presents an investigation of the possibilities for metrology of the geometric characteristics of mortise and tenon joints and their representation through Geometric Product Specification (GPS) standards. For this purpose, one of the most commonly used joints in chair constructions is taken as an example. The method of measurement is adapted for the use of manual measuring instruments.

## 2. GEOMETRICAL PRODUCT SPECIFICATIONS (GPS) SYSTEM

### 2.1 Meaning, rules and matrix

The system of standards - GPS (Geometrical product specifications), consists of more than a hundred standards that prescribe tolerances, drawings, markings, symbols, measuring equipment, measurement rules, and more. The basic standard that prescribes the rules of the system is ISO 8015:2011. In addition to other rules, the basic rule that characterizes this standard is the "Principle of independence," which emphasizes that each geometric feature should be considered independently of other features. This rule clearly defines the form, orientation and position characteristics of the product as well as the relationships between them. In this system, the standard that prescribes the geometric tolerances of the parts is ISO 1101:2017. Table 1 shows the division of the geometric characteristics of the product according to the mentioned standard. In the GPS system, a matrix with the ISO 14638:2015 standard is prescribed, which includes all the characteristics of the element: dimensions, form, orientation, position, angles, and the quality of the surfaces.

*Table 1: Geometric characteristics of the product according to ISO 1101:2017*

Tolerances	Characteristics	Symbol	Datum needed
Form	Straightness	—	no
	Flatness	▭	no
	Roundness	○	no
	Cylindricity	∅	no
	Profile any line	∩	no
	Profile any surface	∪	no
Orientation	Parallelism	//	yes
	Perpendicularity	⊥	yes
	Angularity	∠	yes
	Profile any line	∩	yes
	Profile any surface	∪	yes
Location	Position	⊕	yes or no
	Concentricity (for centre points)	⊙	yes
	Coaxiality (for axes)	⊙	yes
	Symmetry	≡	yes
	Profile any line	∩	yes
	Profile any surface	∪	yes
Run-out	Circular run-out	↗	yes
	Total run-out	↘	yes

## 2.2 Possibilities for the use of GPS system in the wood industry

So far, there is not much data in the literature about the use of the GPS system in the wood industry. The first to write about this problem was (Riegel 2018). In his paper, he highlights the need for the application of the GPS system in the furniture industry. He believes that the system is particularly applicable in the production of case furniture, where there are many openings for fittings and dowels and exact positioning of the openings is required. The authors (Warmefjord et al. 2019) highlight the possibility of using the GPS system when applying tolerances in the production of ready-to-assemble furniture. Other authors who emphasize the applicability of the GPS system in the production of furniture are (Turbanski et al. 2021, Sydor et al. 2021). All these authors point out that the standard for tolerances in the wood industry DIN 68100:2010 is not correlated with the GPS system.

In the aforementioned literature examining the influence of tolerances and fit on mortise and tenon joints, the authors methodologically measure only the thickness dimensions of the mortise and tenon. By measuring the thickness, data is obtained about the contact between the wider sides of the mortise and tenon, and the type of fit mostly depends on them. These sides have the largest surface area in the whole composition and are the most represented in the tribology of the joint. To this, it should be added that the most orientation of growth rings in a mortise and tenon is tangential direction, and swelling and shrinkage are greatest in these directions (Wood Handbook 2021). Therefore, the thickness dimension must be controlled in order to add tolerance for moisture changes in the wood.

However, measuring only the thickness dimension does not provide an accurate state of the contact surfaces in the joint. The thickness of the tenon may be within the tolerance interval, but it may be slanted at the side (inaccuracy in location) or its thickness will not be the same throughout the length of the tenon (inaccuracy in orientation). Possible occurrences (errors) during the processing of joints are systematized by (Tkalec and Prekrat 2000). The presence of gaps in the mortise and tenon joints is due to the lack of contact on the tribological surfaces in the joint, which results in the filling of those gaps with adhesive. Compositions that have greater tolerances and a loose fit have a thick glue line (Dzindzic and Zivanic 2013), and this leads to a lower strength of the joint (Tankut 2007).

Analyzing the mechanisms of action forces occurring in mortise and tenon joints is a difficult and complex task. In this joint, forces of pressure, tensile and torsion occur through mutual interaction. When the joint is subjected to a torsional force, the surfaces of the narrower sides of the tenon press against the narrower sides of the mortise (Xie et al. 2021). Here, there are two forces of action that, with increased load, lead to the appearance of a gap and relative sliding in the joint. The present gap and its influence on joints have been studied by (Chang et al 1987, Ogawa et al 2016).

## 2.3 Use of the GPS system in the metrology of the mortise and tenon joints

Measuring only joint tolerance dimensions is in accordance with the ISO 8015:2011 Independence rule. When measuring the characteristics of the mortise and tenon joints, the "Envelope principle" or "Rule #1" from the American standard ASME Y14.5-2018 is more adequate. According to this, the measurement of dimensional tolerances is related to the measurement of form tolerances. This rule was later accepted in ISO 8015:2011, but when using it, it must be emphasized to respect the rule of independence. In all cases, the use of tolerances in dimensions and form is not enough because there is a need to provide tolerances for parallelism, perpendicularity and symmetry, that is, tolerances for orientation and location. In this case, a whole chain of tolerances according to ISO 14638:2015 should be used.

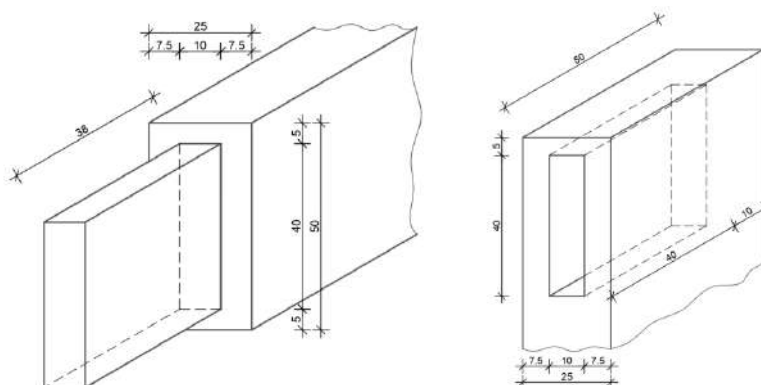
From previous literature analysis and due to the complexity of the requirements for functionality and durability of the mortise and tenon joint, we believe that the determination and control of the tolerances and fits of the joint should be within the matrix of ISO 14638:2015. In this way, all the geometric characteristics of the joint (dimensions, form, orientation and location) will be covered.

### 3. MEASUREMENT OBJECT AND MEASURING INSTRUMENTARY

#### 3.1 Joint type

In order to perform the metrology of mortise and tenon joints, we present an example of one of the most commonly used joints in chair construction, the square edge mortise and tenon joint (Figure 1).

According to the GPS matrix, the geometric characteristics of the presented joint can be measured: straightness, flatness, parallelism, perpendicularity and symmetry.

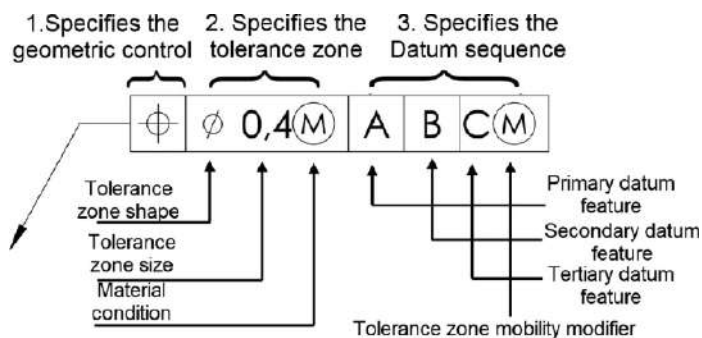


**Figure 1:** Square edge mortise and tenon joint

#### 3.2 Indicating Geometrical Tolerance

According to ISO 1101:2017, geometric tolerances should be marked on the drawings using indicators, that is, a rectangular frame divided into several parts. The frame from left to right should contain the following: a geometric tolerance symbol, a tolerance zone symbol, a value, and a datum reference. The content of the indicator is shown in Figure 2.

The values for the geometric tolerances are usually taken from one of the accuracy classes of the free measurement standard ISO 22081-1:2021 (formerly ISO 2768 – 2:1982).



**Figure 2:** Indicating Geometrical Tolerance according to ISO 1101:2017

#### 3.3 Measuring equipment

According to the International vocabulary of metrology VIM - JCGM 200:2012, when one or more instruments or devices are used in the measurement to obtain a quantitative value, it is called a "measuring system." A term that indicates the measurement system for geometric characteristics is the Geometric Measurement System (GMS). This term includes all the instruments, procedures and tasks that are used in the measurement of the features in the GPS system. The list of measuring equipment is quite large and it is prescribed by standards. The standard to which the manual measuring instruments are prescribed is ISO 14978:2018, the plain limit gauges of linear size are according to ISO 1938-1:2015, and the coordinate machines are according to ISO 10360-2:2009.

For measuring the geometric characteristics of the parts in the wood industry, manual instruments are the most applicable. This group of instruments includes calipers, micrometers, dial gauges, lever type dial indicators, and dial bore gauges. The advantages of these instruments are multiple: they are inexpensive, quick to use, long-lasting, portable and provide sufficient accuracy for measuring wooden parts. A disadvantage of these measuring instruments is their limitation for measuring curved parts. The coordinate measuring machine (CMM) is usable on control by measurement in the wood industry, but there should be an economic justification for it.

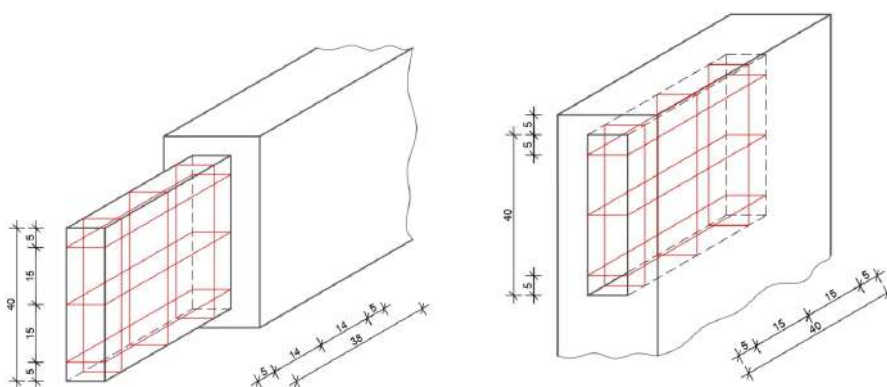
### 3.4. Datum reference

The reference surface is theoretically a plane, line or point, that is, one or more geometric elements that serve as a basis for measuring geometric characteristics. The rules for applying the datums are prescribed according to the ISO 5459:2011 standard. In measurement, there can be a reference system composed of primary, secondary and tertiary planes. A requirement for using a surface of the part as a datum is that it satisfies the tolerances of straightness and flatness.

## 4. METROLOGY OF GEOMETRIC CHARACTERISTICS MORTISE AND TENON

### 4.1 Measurement of dimensional tolerances

This tolerance represents the difference between the smallest and largest measurements that correspond to the tolerance interval. The dimensions are measured in length, width and thickness. The standards that are prescribed for tolerances and dimensions in the GPS system are ISO 286-1:2010 and ISO 286-2:2010. These standards are made for the machine industry, but to some extent they are also applied in the wood industry. In these standards, a tolerance unit is calculated according to the equation:  $i = 0.45 \cdot \sqrt[3]{D} + 0.001 \cdot D$ , which is a generally accepted unit of tolerance in the wood industry. Other standards that prescribe dimensional tolerances and are intended for wood processing are DIN 68100:2010 and GOST 6449:76. Mortise and tenon joints have functional surfaces and are subject to the fit rules of ISO 286-1 and 2. The measurement of the mortise and tenon dimensions (length, width and thickness) is given in Figure 3. The location of the measuring points is determined according to the rules prescribed in the ISO 17450-3:2016 standard.



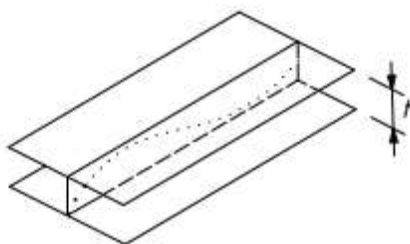
**Figure 3:** Location and measuring points for mortise and tenon dimension measurement

### 4.2 Measurement of form tolerances

#### 4.2.1 Straightness

It represents the basic tolerance characteristics of the parts. A datum is not required to measure this characteristic. First, we measure the straightness of the surfaces and then they can be used as reference surfaces for measuring other characteristics.

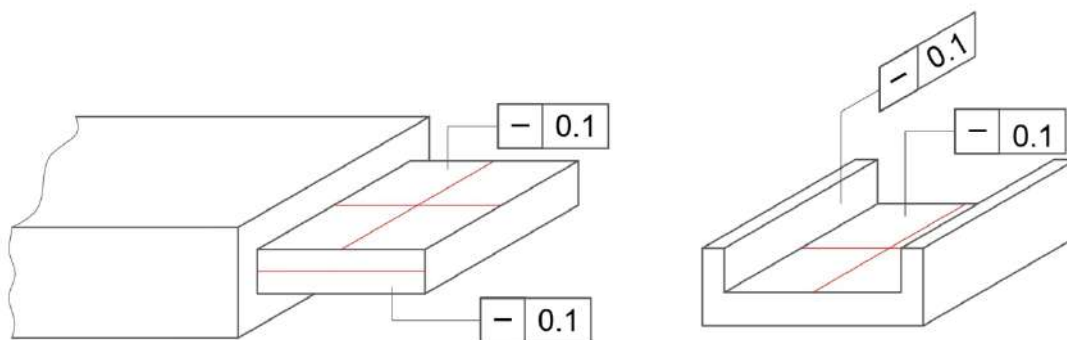
The tolerance zone of straightness describes the deviation of one or more lines on the surface of a part (Figure 4).



**Figure 4:** Tolerance zone of straightness

In mortise and tenon joints, straightness is controlled on all functional surfaces, especially those that serve as datum. The measurement is performed using a dial gauge mounted on a stand.

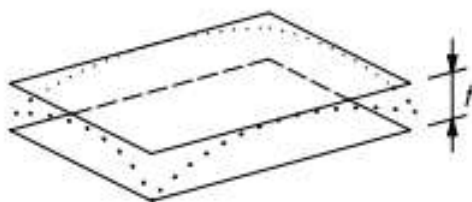
Figure 5 shows the measuring points and flatness indicator of the joint. To enable measurement of the flatness of the wall edges of the mortise, it should have been previously cut along the longitudinal axis.



**Figure 5:** Specifications for the straightness measurement of a mortise and tenon joint

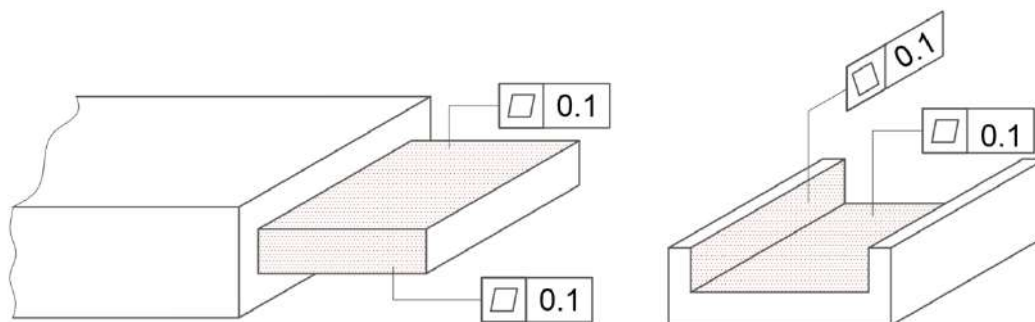
#### 4.2.2 Flatness

Flatness is closely related to straightness, but flatness is measured over the entire plane of the part. This characteristic is fundamental for the surface to be used as a datum. It represents a tolerance in which the tolerance zone lies between two planes and all points of the part's surface must fall between those two planes, as shown in Figure 6. A flatness measurement does not require a reference datum. This measurement is performed with a dial gauge mounted on a stand.



**Figure 6:** Flatness tolerance zone

For mortise and tenon joints, flatness is measured at the faces, edges, shoulders and side wall surfaces. The number and location of the measuring points are determined according to one of the schemes in the ISO 12781-2:2011 standard. The rectangular scheme is most often used for measuring planes. Measuring the flatness of the side walls of the mortise is possible only if it is cut longitudinally. The flatness measurement specifications are given in Figure 7.



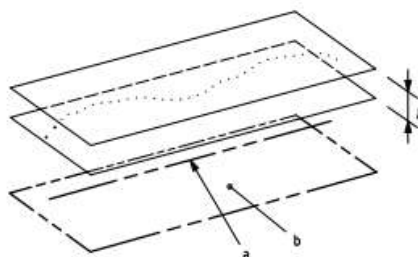
**Figure 7:** Specifications for the flatness measurement of a mortise and tenon joint

### 4.3 Measurement of orientation tolerances

#### 4.3.1 Parallelism

Parallelism tolerance is defined as a plane whose points lie between two parallel planes that are parallel to the reference surface.

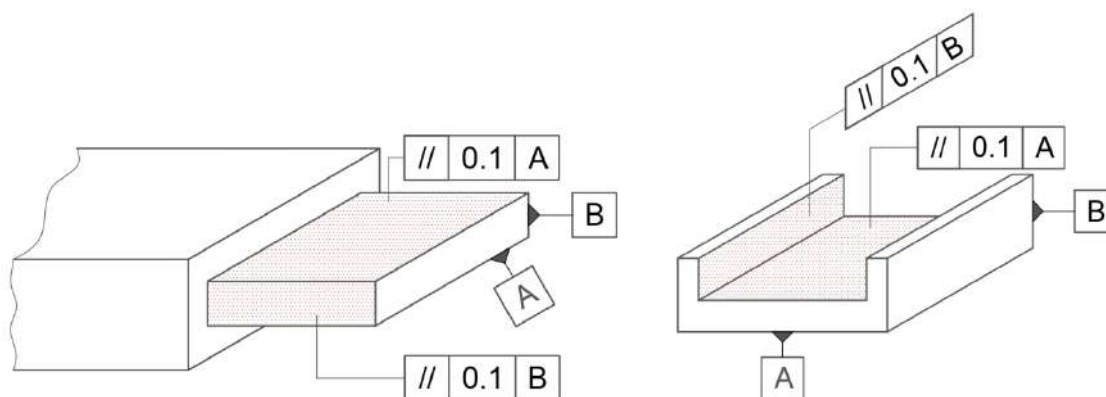
The tolerance zone is located between these two planes and is shown in Figure 8. This measurement is performed using a dial gauge. In the same order, the faces, edges, side walls and shoulders of the mortise and of the tenon are measured. A datum is required to measure this geometric characteristic.



**Figure 8:** Parallelism tolerance zone

Tenon parallelism is measured by initially measuring the straightness and flatness of the surface of the face and edge to serve as a datum. The inspected surface is placed on the base surface of the stand and the measurement is made on the opposite surface. The measurement specifications are shown in Figure 9.

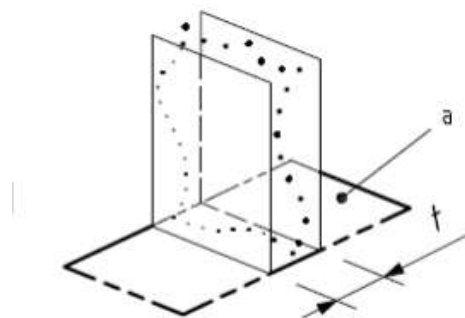
The number and location of the measurement points are according to the same standard as the flatness measurement. To measure the parallelism of the wall sides of the mortise, it should be cut longitudinally beforehand. Then measure the straightness and flatness of the parallel free surface of the part to serve as a datum. The measurement should also be performed on the cut part.



**Figure 9:** Specifications for parallelism measurement in mortise and tenon joint

### 4.3.2 Perpendicularity

Tolerance of perpendicularity is defined as the permissible deviation between two parallel planes oriented at an angle of  $90^\circ$  to the reference plane. The tolerance zone is shown in Figure 10.

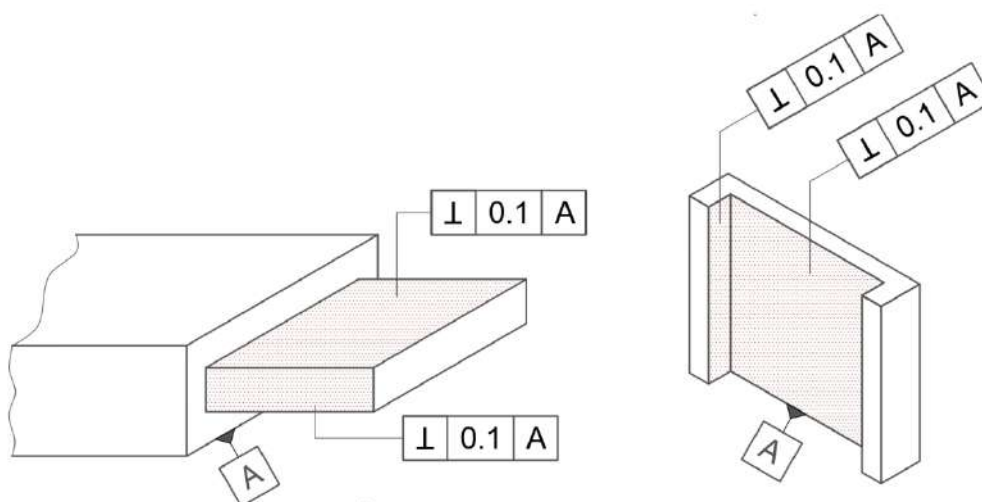


**Figure 10:** Perpendicularity tolerance zone

To measure this tolerance, a datum is required on which straightness and flatness must be measured beforehand.

The measurement of the perpendicularity of a tenon is performed on faces and edges on shoulders as a reference datum. First, we control the flatness of the tenon shoulders. This measurement is performed with a lever type dial gauge mounted on the stand. Then the shoulder surface is placed on the base surface of the indicator stand and the tolerance of the surfaces and the faces and edges of the tenon are measured.

The perpendicularity of the mortise is measured on the side walls. First, we measured the flatness of the free surface where the tenon shoulders touch the mortise part. Then the measured surface will serve as a datum for measuring the side walls' perpendicularity. In order to accurately measure the side walls, the mortise must first be cut longitudinally. The measurement specifications are shown in Figure 11. Measuring can be performed with a dial gauge or lever type dial gauge mounted on a stand with a base surface.



**Figure 11:** Specifications for measuring perpendicularity of mortise and tenon joint

## 4.4 Measurement of location tolerances

### 4.4.1 Symmetry

Symmetry tolerance is very similar to position tolerance. According to the recommendations of (Hanzold 2006), when it comes to measuring a plane in relation to an axis from another plane, it is more appropriate to measure tolerance of symmetry than of position.

Symmetry tolerance is defined as the deviation of two planes in relation to a third one that is a reference. The tolerance zone is represented by the two parallel planes that are at the same distance from the third one in which the longitudinal axis of the element lies (Figure 12). This tolerance is complex to measure because the tolerance zone is limited between two virtual planes. This measurement is performed with a dial gauge mounted on a stand with a base surface.

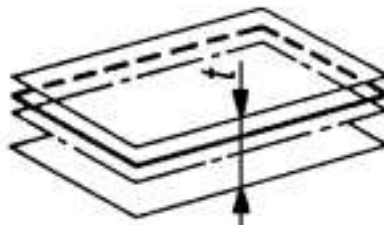


Figure 12: Symmetry tolerance zone

The tolerance of symmetry in the tenon represents the deviation of the faces and edges of the tenon in relation to the longitudinal axis. If the free surfaces of the part are parallel to each other, it means that the imaginary axis of symmetry is in the center. First, we check the flatness and parallelism of all free non-functional surfaces of the part. Then we use these surfaces as datum (Figure 13).

The measurement of the symmetry tolerance of the mortise represents the deviation of the side wall surfaces with respect to the longitudinal axis of the part. For accurate measurement, the mortise must be cut along the longitudinal axis.

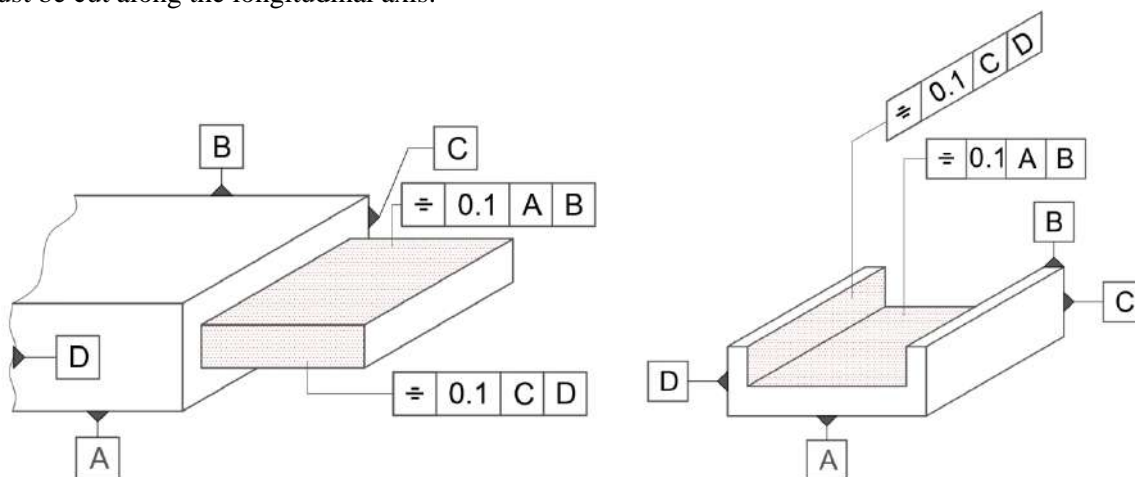


Figure 13: Specifications for measuring symmetry in mortise and tenon joint

## 5. CONCLUSION

From the analysis of the metrology possibilities of the geometric characteristics of the mortise and tenon through the GPS system, the following conclusions can be made:

- Due to the complexity of the requirements for functionality and durability of the mortise and tenon joint, the control of the geometric characteristics of the joint should be within the matrix of ISO 14638:2015.

- The geometric characteristics of form - straightness and flatness are the basic characteristics of the mortise and tenon, on which the measurement of all other characteristics depends.

- The method of measuring the geometric characteristics of the joint with manual measuring instruments is a fast and functional way of measuring.

- The disadvantage of this method of measurement is the limitation of measuring the geometric characteristics of a mortise without cutting it longitudinally.

- By determining the phases and operations of measuring the geometric characteristics, this review paper makes a contribution to the metrology of mortise and tenon joints as a function of quality control in production.



Further research should be directed at a comparative investigation of tolerance standards used in the wood industry, including tolerances added for dimensional changes in wood.

## REFERENCES

- [1] ASME, (2019): ASME Y14.5-2018: Dimensioning and Tolerancing, American Society of Mechanical Engineers, NY.
- [2] Chang WR, Etsion I, Bogy DB (1987): An elastic-plastic model for the contact of rough surfaces. *J Tribol* 109(2):257–263
- [3] DIN 68100:2010-07 - Tolerance system for wood working and wood processing - Concepts, series of tolerances, shrinkage and swelling
- [4] Džin i I, Živani D., (2014): The influence of fit on the distribution of glue in oval tenon mortise joint. *Wood Res-Slovakia* 59(2):297–302
- [5] Eckelman CA (2003): Textbook of product engineering and strength design of furniture. Purdue University Press, West Lafayette, Indiana
- [6] Forest Products Laboratory (2021): Wood handbook wood as an engineering material. General Technical Report FPL-GTR-282. Madison, WI: U.S. Department of Agriculture, Forest Service, Forest Products Laboratory. 543 p.
- [7] Gawronski, T., 2006: Rigidity-strength models and stress distribution in housed tenon joints subjected to torsion. *Electronic Journal of Polish Agricultural Universities* 9(4)
- [8] GOST 6449-76 - Product of woods and wooden materials. Limits and fits
- [9] Gruevski Gj. (2007): Istrazuvanja na jakosta sostavite vo konstrukciite na stolovi izraboteni od kostenovo drvo, Doktorska disertacija, Sumarski fakultet – Skopje.
- [10] Hajdarevi , S., and Martinovi , S. (2014). “Effect of tenon length on flexibility of mortise and tenon joint,” *Procedia Engineering* 69(2014), 678-685. DOI: 10.1016/j.proeng.2014.03.042.
- [11] Haviarova, E., Eckelman, C., and Erdil, Y. Z. (2001): “Design and testing of wood school desk frames suitable for production by low technology methods from waste wood residues,” *Forest Products Journal* 51(5), 79-88. WOS:000168740700011.
- [12] Henzold, G. (2006). *Geometrical Dimensioning and Tolerancing for Design, Manufacturing and Inspection: a Handbook for Geometrical Product Specifications Using ISO and ASME Standards*. Butterworth-Heinemann.
- [13] ISO 10360-2:2009 - Geometrical product specifications (GPS) — Acceptance and reverification tests for coordinate measuring machines (CMM) — Part 2: CMMs used for measuring linear dimensions
- [14] ISO 1101:2017 - Geometrical product specifications (GPS) — Geometrical tolerancing — Tolerances of form, orientation, location and run-out
- [15] ISO 12781-2:2011 - Geometrical product specifications (GPS) — Flatness — Part 2: Specification operators
- [16] ISO 14638:2015 - Geometrical product specifications (GPS) — Matrix model
- [17] ISO 14978:2018 - Geometrical product specifications (GPS) — General concepts and requirements for GPS measuring equipment
- [18] ISO 17450-3:2016 - Geometrical product specifications (GPS) — General concepts — Part 3: Toleranced features
- [19] ISO 1938-1:2015 - Geometrical product specifications (GPS) — Dimensional measuring equipment — Part 1: Plain limit gauges of linear size
- [20] ISO 22081:2021 - Geometrical product specifications (GPS) — Geometrical tolerancing — General geometrical specifications and general size specifications
- [21] ISO 286-1:2010 - Geometrical product specifications (GPS) — ISO code system for tolerances on linear sizes — Part 1: Basis of tolerances, deviations and fits
- [22] ISO 286-2:2010 - Geometrical product specifications (GPS) — ISO code system for tolerances on linear sizes — Part 2: Tables of standard tolerance classes and limit deviations for holes and shafts
- [23] ISO 5459:2011 - Geometrical product specifications (GPS) — Geometrical tolerancing — Datums and datum systems

- [24] ISO 8015:2011 - Geometrical product specifications (GPS) — Fundamentals — Concepts, principles and rules
- [25] JCGM 200:2011 – International vocabulary of metrology Basic and general concepts and associated terms (VIM)
- [26] Jivkov V, Marinova A (2006): Ultimate bending strength and stiffness under compression test of end corner miter joints constructed of solid wood. In: Paper presented at the International Symposium: “Furniture”. Technical University in Zvolen, pp 1–7. ISBN 80-228-1577-2
- [27] Mackerle, J., (2005): Finite element analyses in wood research: A bibliography. *Wood Science and Technology* 39(7): 579–600.
- [28] Ogawa K, Sasaki Y, Yamasaki M (2016): Theoretical estimation of the mechanical performance of traditional mortise-tenon joint involving a gap. *J Wood Sci* 62:242–250
- [29] Potrebi , M., (1970): Joint tolerance as effecting factor on strength of mortise joint. Master thesis, Belgrade University, Faculty of Forestry. Pp 105-107
- [30] Prekrat, S. i Smardzewski, J. (2010). Effect of Glueline Shape on Strength of Mortise and Tenon Joint. *Drvena industrija*, 61 (4), 223-228
- [31] Riegel, A., "Geometric tolerancing of furniture", (2018): Proc. 8th International conference on Production Engineering and Management (PEM), F.-J. Villmer, and E. Padoano, eds., Hochschule Ostwestfalen-Lippe.
- [32] Skaki , D., Jani ijevi , S., (2000): Effect of type of joint, machining precision, and type of fit on the strength of the joints in chairs. (Uticaj vrste spoja, ta nosti obrade i vida naleganja na vrsto u spojeva stolica). *Drvarski glasnik* 9(35/36): 21-25
- [33] Smardzewski, J., Papuga, T., (2004): Stress distribution in angle joints of skeleton furniture, *Electronic Journal of Polish Agricultural Universities* 7(1)
- [34] Sydor, M., Majka, J., and Langová, N. (2021): "**Effective diameters of drilled holes in pinewood in response to changes in relative humidity**," *BioResources* 16(3), 5407-5421, DOI: 10.15376/biores.16.3.5407-5421
- [35] Tankut, N. 2007. The effect of glue and glueline thickness on the strength of mortise and tenon joints. *Wood Res.* 52:69–78.
- [36] Tkalec S. (1990): Ispitivanje cvrstoce spojeva zaoblenim cepom, *Drvena industrija* 41(1-2) 3-8 6663-6676. DOI: 10.15376/biores.10.3.6663-6676.
- [37] Tkalec, S.; Prekrat, S., (2000): Konstrukcije proizvoda od drva – osnove drvnih konstrukcija – Sumarski fakultet, Zagrebu, 1-310.
- [38] Turba ski, W., Sydor, M., Matwiej, Ł., & Wiaderek, K. (2021): Moisture swelling and shrinkage of pine wood versus susceptibility to robotic assembly of furniture elements. *Annals of WULS, Forestry and Wood Technology*, DOI:10.5604/01.3001.0015.5274
- [39] Wärmefjord, K, Söderberg, R, Lindkvist, L, & Dagman, A. (2019): "Non-Rigid Variation Simulation for Ready-to-Assemble Furniture." *Proceedings of the ASME 2019 International Mechanical Engineering Congress and Exposition. Volume 2B: Advanced Manufacturing*. Salt Lake City, Utah, USA.
- [40] Xie, Q., Zhang, B., Zhang, L. *et al.* Normal contact performance of mortise and tenon joint: theoretical analysis and numerical simulation. *J Wood Sci* 67, 31 (2021). <https://doi.org/10.1186/s10086-021-01963-x>

## LOADBEARING STRUCTURES FROM RECLAIMED WOOD – STRATEGIES, DESIGN PARAMETERS AND REFLECTIONS

Olga Popovi Larsen<sup>1</sup>, Xan Browne<sup>1</sup>

<sup>1</sup>Royal Danish Academy: Architecture, Design, Conservation,  
Institute for Architecture and Technology,  
e-mail: Olga.Larsen@kglakademi.dk; xbro@kglakademi.dk

### ABSTRACT

It is a well-known fact that the building sector is one of the largest polluting and CO<sub>2</sub> emission contributing sectors. In addition, what Nature has created over millennia as material resources is used up very fast with some materials already becoming scarce. The climate emergency we are facing calls for better and more sustainable approaches for the building sector.

This is the motivation and starting point for this paper that presents three different strategies for building load bearing structures in wood. Through three full-scale prototypes we put forward strategies, design parameters and reflections about the opportunities and challenges of utilizing second-hand wood for load bearing structures. The three projects all seek to investigate the viability of wood cascading, giving wood a longer life in its solid form by offering a load-bearing structural design that can be reused several times. Furthermore, *The ReciPlyWood*, *Waste Wood Canopy* and the *Wood ReFramed* test different strategies for structural safety through robustness as well as simple connection systems. Optimising usability, buildability, and aesthetics and waying them out has been important in all three projects. The paper ends with a reflection of the process and results and points to steps needed for wood to be accepted as a multigenerational material for load-bearing structures.

**Keywords:** wood cascading, reclaimed wood loadbearing structures, full-scale prototypes

### 1. INTRODUCTION

In response to major environmental challenges, wood is regaining attention as a material that can solve some of our climate damaging practices. Once a material that made up a significant portion of our material culture, its use in building design has been subsided by the rapid development of other materials over the last centuries, such as steel and concrete.

The procurement of timber invokes complex challenges surrounding availability and biodiversity, both parameters have created strong critique of different types of forestry practice. Optimum stand rotation, diversity of species, and cutting methods are topics that struggle to find consensus (Liu et al., 2018). As well as this, a changing climate leads to uncertainties in how prediction models calculate wood availability, due to forest vulnerability to fire and insect attack- both expected to increase with a changing climate (Seidl et al., 2017).

The majority of timber today experiences a short lifespan, and where longer lifespans are made possible - such as timber used in buildings – most material is single use (Husgafvel et al., 2018). Energy recovery is typically the most common second application for timber, and where timber is reused, it is most often downcycled into particle-based products (Cristescu et al., 2020). Extending the lifetime of wood can contribute with many benefits. The most significant is the increased availability of timber that reduces pressure on virgin wood sources. Furthermore, extended timber lifetimes offer increased anthropogenic carbon storage, where the reuse of timber is essential for this to be most effective (Churkina et al., n.d.). As well as this, aesthetic opportunities emerge from the layers of exposure captured by used timber. In addition, material reclaimed from old existing buildings was harvested during a period when forests grew more slowly, creating timber of a higher density, often an indicator suggesting longevity and higher quality.

A key framework for conceptualizing extended uses of wood is biomass cascading. It is a system of material flows, that instead of focusing on product lifetimes, focuses on material lifetimes (Vis et al., 2016). For effective cascading, a series of sequential applications of timber are required, each utilising the highest proportion of material possible. Current challenges for scaling cascading strategies in the building sector include knowledge gaps and issues surrounding quality criteria, where contaminants such as fastenings inhibit secondary timber's use in current production methods (Sakaguchi et al., 2017). Furthermore, timber has been neglected during the development of legislation and building regulations, leaving reclaimed timber further ostracised from legal building practice (Niu et al., 2021).

The paper investigates some of the emergent challenges of effective timber utilisation, as well as realizing theoretical material flow strategies - in this case biomass cascading – by finding opportunities in unusual material forms. Each project asks how design can work towards extended timber lifetimes, by investigating symbioses between the vast library of structural typologies and emergent parameters describing timber less commonly used in building design. The three projects, *The ReciPlyWood*, *Waste Wood Canopy* and *Wood ReFramed* each offer an optimal utilisation of timber, albeit in different ways. They have been developed with their own strategies for extending the lifetime of the wood into multiple utilisations. Also, all three projects focus on material optimization, as well as novel approaches to designing for disassembly. The projects aim to motivate alternatives to current wasteful material flows and explore the structural potential of timber that is today regarded as waste. As demonstrators, they are each developed as design projects that lead to matured full-scale inhabitable structures.

## 2. RECIPLYDOME – BENDING ACTIVE PLYWOOD MODULAR KIT OF PARTS

*ReciPlyDome* is a prototype of a minimal structure designed for disassembly as a kit of parts. It is a spherical gridshell consisting of 45 double-layered beam members based on Reciprocal Frame principles.



*Figure 1: The ReciPlyDome pavilion*

The minimal plywood beam members form a grid – a self-supporting loadbearing structure that spans 5 meters using plywood of only 12 mm thickness. The double beam members are curved, providing the required rigidity and stiffness.

## 2.1 Strategy

The ReciPlyDome is a spherical gridshell consisting of 45 double-layered beam members. As a starting point, the *ReciPlywood pavilion* was designed as a structure from new-virgin material. The approach was to design a minimal, optimized by weight structure, spanning a long distance, that after its first use could be dismantled, possibly reconfigured, and re-erected for a new application. Thus, the two main strategies were: 1. Material optimization and 2. Design for disassembly (DfD) and reuse.

In order to minimize wood use by weight, a decision was taken to utilize plywood for the loadbearing system, a considerably lighter alternative to solid wood, that required a design approach to accommodate the challenges of working with a thin plate/sheet material (instead of the common longitudinal wood beam members) and also establishing and embracing the opportunities that it could offer.

## 2.2 Design approach: Reciprocal Frame principles and bending active beam members

The ReciPlyDome as a design was developed as a kit of parts based on Reciprocal Frame (RF) principles (Popovic Larsen, 2008) using bending active beam members. RF structures are three-dimensional grid structures consisting of mutually supporting beams, forming closed stable circuits of closed polygons with mutually supporting beams. The connections between the beams are made so that no more than two beams are being attached at a time, adding to the simplicity both design and construction. A decision was brought that all members and all connections are designed as geometrically identical offering further uniformity. This also enabled developing simple connections utilizing a single bolt forming the connection between two beam members. The identical single bolt connections further promoted reversibility of the structure.



**Figure 2:** *The ReciPlyDome pavilion was built with bending active plywood beams*

Working with a plywood sheet material posed challenges as well as opportunities. The thin sheets of plywood with only 12 mm thickness offered a truly materially minimal structure. However, loadbearing structures as beams that resist bending stresses require structural depth. Thus, a double bending active beam member was developed, that could resist efficiently the combination of axial forces and bending that the structure was subjected to. The lightweight plywood kit-of-parts dome, was created by overlaying the RF configuration onto a dome resulting in kit of parts with high level of repetition, further enhancing the ease of construction. One of the main drivers for this project was *handling of complexity through uniformity*.

### 2.3 Construction aspects

The *ReciPlyDome* structure was a fully reversible design made for DFD. It could be fully reconfigured and re-erected in a new form (within the geometrical boundaries). Actually, a design with “universal” beams was also designed, so that domes of different member density and size could be built in the subsequent material lives of the structure.

The construction was meant to be for untrained people, who with a set of instructions could both fabricate and erect the structure themselves. The *Domes of transition* study investigated the potential for an emergency shelters application, where untrained people could both fabricate and construct temporary structures out of local materials. Research suggests that involving the disaster affected in rebuilding their homes and community helps the healing process. (Larsen, 2019)

The overall dome design, geometry definition and detail design required teamwork and specialist knowledge whilst the fabrication, assembly, and disassembly apart from a set of instructions did not require any special skills. The *ReciPlyDome* was fabricated out of plywood sheet plates that were first cut into strips and then were prefabricated into the prefabricated bending active beams. The kit of parts required only few days to fabricate and few hours to assemble for 3-4 lay people. Because of the lightness of the members no specialist equipment was required.

### 2.4 Reflections

The *ReciPlyWood* project investigated the implementation of bending-active components in reciprocal grids. The project demonstrated that the mutually supporting RF beam structures, with their weave-like patterns that in each node connect only two beams despite the large number of connections, are simple to fabricate, construct, reconfigure and utilize in multiple further applications. The plywood beam members in this project were utilized for several exhibitions, concerts, workshops and they clearly demonstrated that the (ply)wood had the potential for multiple applications.

The integrated connections, by cut-outs or simple bolts, can however be complicated by the different beam inclinations. Moreover, the curvature of the grids depends on the eccentricity of the connections, and thus the cross-sectional height of the members. This, along with the bending forces that are imposed through the intermediate connections along the beams, often requires large cross-sections. Using bending-active components allows to employ the flexibility of the components to overcome the difference in beam inclinations and produce the cross-sectional height. While the flexibility of the components allows further reducing the technical complexity of the structure, it is often more challenging to produce adequate load-bearing behaviour in the bending-active case. (Brancart et al. 2019).

Perhaps the biggest challenge for the *ReciPlyDome* was developing a cladding system that is prefabricated and as high performing as the structure, yet low-tech in fabrication and construction. One development in that direction was the *ReciPlySkin*, a fully enclosed structure with a lightweight membrane. This was a waterproof solution that offered speed and simplicity of construction; however, it was not insulated. Further design and development need to be carried out to find alternatives of inexpensive, insulated façade systems. (Larsen, 2022)

From a point of view of wood cascading and investing the potential for multiple applications of reclaimed wood in loadbearing structures the *ReciPlyDome* structure reconfirmed that wood offers the potential for minimal, material optimized structures that can be (re)used several times.

## 3. WASTEWOOD CANOPY – RECIPROCAL FRAME (RF) GRID STRUCTURE FROM SHORT LENGTHS

*WasteWood Canopy* is a small gridshell inhabitable structure. It is a shelter and has been conceived as a demonstrator testing the viability of utilizing reclaimed timber for an inhabitable load-bearing structure.

### 3.1 Strategy

The strategy for making a case for wood as material that can have multiple use and reuse potentials was done in testing the viability of designing a building a loadbearing structure out of short lengths reclaimed wood. The technical/safety related aspects of the loadbearing structure were not the only requirements. Usability (architecture and aesthetic aspects) as well as buildability (ease of construction) were tested in parallel. By waying out the different objectives and developing a design that achieved the best of the combined criteria through an iterative multi objective criteria optimization (instead of the usual single objective optimization) the canopy was usable, safe, and easy to build. By achieving a highly optimized holistic design, it is project that presents the holistic potential for wood cascading in building design.

### 3.2 Design principles - Geometry and structural configuration

The structure is shaped like a vault, open at both ends. The ends provide access for visitors to the interior of the structure. The structure acts as a gridshell carrying the load via arch action.

The canopy's geometry is based on a Reciprocal Frame geometry with offset joints between the beam members. The members are all identical and are arranged in diamond shapes in a repeated pattern. They are connected at four-members nodes via a specially developed connector plate. This plate clamps the four members together and prevents them from sliding in the connection. The structure is assembled from prefabricated beams and connectors.

The structure can be either supported directly on an existing concrete floor, or on a wooden floor.



*Figure 3: WasteWood Canopy, exhibition at the Royal Danish Academy 2020*

### 3.3 Members, connections and construction aspects

When building with reclaimed wood, typically we are confronted with using shorter lengths of wood member than in conventional structures. That also means that we have many connections.

The timber members are 100x50mm in cross section and are made of reclaimed (waste) wood. The clamp connection developed for this project with plates that connect the main members are made from plywood that is CNC carved to fit the shape and angles of the incoming four members. The clamp plates are held together with a steel bolt and nut. This considerably reduces the number of the

connections and simplifies the construction. Due to the tight fit of the members in the clamp plates and the bolts, the connections have a high stiffness and safety against failure. The assembly was simple and did not require any specialist equipment.

### 3.4 Reflections

The overall stability of the structure is secured via the vault shape in the transverse direction and with the stiff connectors in the longitudinal direction. The structure is highly statically indeterminate, which means that there are alternate load paths taking the self-weight down to the floor. Removing one or more timber members will not cause the whole structure to fail. Likewise, the failure of a single clamp plate or bolt will not lead to overall failure of the structure. This ensures a safe and robust design secured against disproportional collapse.



**Figure 4:** The WasteWood Canopy's clamp connections rely on a single bolt connection,

Designing robust structures is one good way to work with reclaimed materials where there is a level of uncertainty about the material quality. The structure has been constructed and taken down several times and still can be used many more times, showing that wood can be a multi-generational material. Further work, especially in the connection design using higher strength materials, will enable longer spans and greater longevity of the structure.

## 4. WOOD REFRAMED

*Wood ReFramed* is a pavilion that investigates the potential utilizing reclaimed timber of different origins in structural applications. The design is based on a series of portal frames, made up of trusses that each integrate a variety of tones and geometries. These frames' structural capacity is demonstrated by a hanging amphitheatre where the public are invited to interact with the structure.

### 4.1 Strategy

The *Wood ReFramed* pavilion project, developed from concept to completion over a 6-month period with a primary aim of the project to demonstrate the structural potential of reclaimed timber at scale. The project departs from the idea of a building segment, featuring genuine loads, a relatable form, and components that could be integrated into buildings today. This strategy was to create a project that the many stakeholders of the building industry can relate to, whether they be craftspeople, urban planners, contractors, demolition workers, or policy makers. In short, the project aims to



convince; to mediate between the current disregard for reclaimed timber and propose a future alternative for timber structures. Exhibited during the World Architectural Congress (UIA) 2023, the pavilion also served to kick-start discussion around how we might (re)frame timber construction, as well as drawing upon the verb ‘framing’ - an activity associated with the assembly of timber buildings.



*Figure 5: Completed pavilion structure with 5 frames and a hanging amphitheatre.*

A core challenge regarding the effective utilisation of timber is yield, a metric that determines the quantity of source material ending up in a component. The larger the quantity that can be included reduces the overall material footprint, and therefore the burden on resource availability. Recent research has highlighted the significant variation of yield across component types in how effective they can utilise reclaimed timber streams. Based on this, a truss-like component typology was selected, that also succeeds in exposing the surfaces of reclaimed timber. Many common timber components today rely on planing timber surfaces, leading to relatively homogeneous timber surfaces compared to the varied aesthetic present in timber. In this project, the traits that have emerged as a result of the timber’s origins remain exposed, leading to new relations between new building components and material origins they rely on.

The trusses offer a unique opportunity to assimilate the many forms inherited from timber waste streams into components of standard rectilinear geometries. This works to mediate between the diversity inherent to reclaimed timber, and the construction industry’s preference of standards. Furthermore, material can be allocated within the trusses to create optimised topologies for specific load conditions, enabling an efficient distribution of material within a repeatable rigid boundary.

Many of the previously mentioned barriers for using reclaimed timber, such as contaminants (nails, screws, paints, treatments) and geometric deficiencies (cupping, wane, twist) lead to the material being rejected from production. *Wood ReFramed* works towards utilising materials with these traits, where the typical barriers associated with reclaimed timber are incorporated as a key part of the structural design.

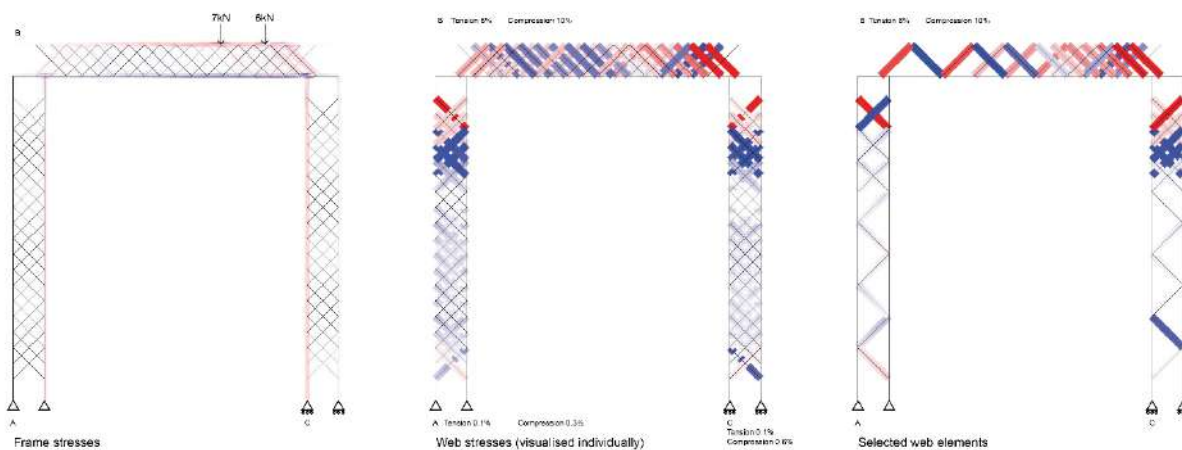
## 4.2 Design

*Wood ReFramed* comprises of two main parts, a series of 5 frames and a suspended amphitheatre. Each of the frames consist of 3 trusses, all uniform in exterior geometry, with varied distribution of material according to the loads of the amphitheatre. The amphitheatre, constructed from glulam beams, is the central interactive component of the structure, where members of the public can sit. It also initiates the main design challenge, requiring the frames to demonstrate their load bearing performance.

The arrangement of the glulam elements in the amphitheatre at 45 degrees creates an intimate space for hosting talks, and for visitors to experience the load bearing capacity of the trusses. The bottom step floats just a few centimetres above the floor, and the entire amphitheatre oscillates gently, limited only by 3 wires in the floor to prevent it from swinging uncontrollably. The dimensions of the glulam beams vary, creating unequal intersection points between the centre line of the glulam beams and the centre lines of the trusses. Their varied cross section dimensions and length also creates highly varied self-weight, resulting in a range of loads on the beams.

The trusses have uniform exterior geometry of 5x0.6m, and a varying allocation of material within this boundary. Figure x (main photo) describes the core components of the structure, and the connections between them. The location of the amphitheatre creates a gradient from one end of the structure to the other, where frame 5 is subject to the smallest loads, and frame 1 the highest.

The full frame is modelled in Rhinoceros 3D, Grasshopper and plug-in Karamba 3D as a wireframe, with supports, and point loads based on the intersection with the glulam beams. At first, the frames are filled completely with web elements, that can be progressively removed based on the axial stressed reported by the calculation.



**Figure 6:** Process of calculating the material allocation for frame 3. The frame on the right shows the final material allocation.

Frames x and x are designed using the same method, however the material quantity is arguably overallocated in the horizontal elements. This is due to the load distribution being relatively uniform, leading to symmetrical allocation, and presenting an opportunity to integrate structural redundancy. Structural redundancy is typically applied to the design of a global structure to avoid progressive collapse and has been implemented in the design of spatial structures that utilise reclaimed materials, including the *ReciPlyDome* and *Waste Wood Canopy* presented previously. *Wood ReFramed* applies redundancy at a component level, aiming to inhibit the progressive collapse of the truss if one of the web elements were to fail. An overallocation of web elements also has an impact on failure modes.

Failure modes are one of the most important considerations when designing load bearing structures (ref DOTS). Ductile failures are considered optimal over brittle failures, which is often achieved using steel connections, a material that is highly ductile. The shear connections between the web and chords are made with birch timber dowels. This brittle connection makes redundancy more relevant, as a component would progressively deflect via a series of brittle failures, mimicking the performance of a ductile failure. Mechanical joints also offer effective material utilisation as the uneven surfaces of reclaimed timber would otherwise need to be processed in order to create the accurate interfaces required by glued connections.

### 4.3 Construction- Material sourcing and fabrication

The project strived to be fabricated from only reclaimed timber materials and therefore was developed in close collaboration with a demolition contractor. The demolition sector is not a traditional source of material for construction projects and although many recent initiatives aim to change this, challenges remain in terms of material procurement. A major barrier is the unsynchronised material flows of demolition and new construction, leading to the mass discarding of resources that do not have immediate value. Whilst this can be attributed to flaws in our current value system and logistical challenges, the project aimed to solve this during the design process.

Already during the early design development of the pavilion, an evolving set of requirements for materials was being established. This culminated into a simple search criterion that could be distributed to all current demolition sites, and any material that met the criteria could be set aside for the pavilion with confidence that it can be used on a project. Very clear requirements were defined, stating a domain of permissible cross sections and minimum length, that metal fastenings and paint are allowed, and elements with signs of rotting or significant quantities of expanded foam should be avoided.



*Figure 7: Steel connections that support the hanging amphitheatre*

Enough material for the pavilion was gathered in a short time, that would otherwise have been discarded. A range of floorboards and beams from different demolition sites were delivered to the demolition contractor's main warehouse, which was also the site of fabrication.

This method enabled comparatively short supply chains relative to the typical procurement methods of structural timber in Denmark today. All the material required for the project was sourced within a 30km radius, reducing transportation distances that can have a high impact in sourcing wood in global supply chains. Fabricating all the parts for the entire pavilion took 2 persons 4 weeks, using

no specialist tools or digital fabrication technology. The fast production time is achieved due to the minimal processing of reclaimed feedstock and the uniform external geometries of the trusses. This meant that a single assembly jig could be used for all 15 trusses. The structure was assembled on site in a single day, a short period achieved due to the simplicity of connections and relatively lightweight structural frames.

#### 4.4 Reflections

The project is successful in demonstrating the load bearing potential of reclaimed timber and offers a clear reference point for developing the strategies further. Both the *design* and *construction* methods are novel, offering an alternative to the current practices of material allocation and construction. These methods initiate close dialogue between material availability and material allocation alongside new constellations of industry stakeholders. *Wood ReFramed* demanded significant design time relative to the project's scale. However, the methods could be adapted to the building scale by optimising groups of components rather than individuals. And developing projects in closer collaboration with demolition contractors would enable better utilisation of materials that are imminently available.

#### 5. CONCLUSIONS

The paper presented three different projects investigating the viability of building loadbearing structures from reclaimed wood. *The ReciPlyWood*, *Waste Wood Canopy* and the *Wood ReFramed* through full scale demonstrators all tested different strategies for structural safety through robustness as well as simple connection systems. The projects have in common that they all show that there is a great potential for using reclaimed timber for loadbearing structures. For all three projects, optimising usability, buildability, and aesthetics and waying them out was important; however, they all presented different approaches for achieving them. Each project offered reflections about the opportunities as well as challenges of each approach. Perhaps more projects through full scale demonstrators should continue the investigations and continue making the case for re-claimed wood. It is hoped that the presented learning from *The ReciPlyWood*, *Waste Wood Canopy* and the *Wood ReFramed* together with new studies will impact further research and building regulations to enable reclaimed wood to become a common occurrence in building design. This will be a huge step in resources optimization and help in addressing the climate crisis. It will also give rise to new ways of creating architecture through material agency.

#### REFERENCES

- [1] Brancart, S., Popovic Larsen, O., De Laet, L. & De Temmerman, N. (2019) Rapidly Assembled Reciprocal Systems with Bending active components: The ReciPlyDome Project, 30 Mar 2019, In: International Association for Shell and Spatial Structures. Journal. Vol. 60 (2019) No. 1 March n., 199, p. 65-77 13 p.
- [2] Castriotto, C., Tavares, F., Celini, G., Popovic Larsen, O. & Browne, X., (2021) Clamp links: A novel type of Reciprocal frame connection, 22 Nov 2021, In: International Journal of Architectural Computing. November 2021, 22 p.
- [3] Churkina, G., Organschi, A., Reyer, C. P. O., Ruff, A., Vinke, K., Liu, Z., Reck, B. K., Graedel, T. E., & Schellnhuber, H. J. (n.d.). Buildings as a global carbon sink. <https://doi.org/10.1038/s41893-019-0462-4>
- [4] Cristescu, C., Honfi, D., Sandberg, K., Sandin, Y., Shotton, E., Walsh, S. J., Cramer, M., Ridley-, D., Arana-fernández, M. D., Llana, D. F., Barbero, M. G., Nasiri, B., & Krofl, Ž. (2020). Design for deconstruction and reuse of timber structures – state of the art review Design for deconstruction and reuse of timber structures – state of the art review. <https://doi.org/10.23699/bh1w-zn97>
- [5] Husgafvel, R., Linkosalmi, L., Hughes, M., Kanerva, J., & Dahl, O. (2018). Forest sector circular economy development in Finland: A regional study on sustainability driven

- competitive advantage and an assessment of the potential for cascading recovered solid wood. *Journal of Cleaner Production*, 181, 483–497. <https://doi.org/10.1016/j.jclepro.2017.12.176>
- [6] Larsen, O (2008) *Reciprocal Frame Architecture*, Elsevier
- [7] Liu, C. L. C., Kuchma, O., & Krutovsky, K. V. (2018). Mixed-species versus monocultures in plantation forestry: Development, benefits, ecosystem services and perspectives for the future. *Global Ecology and Conservation*, 15, e00419. <https://doi.org/10.1016/j.gecco.2018.e00419>
- [8] Niu, Y., Rasi, K., Hughes, M., Halme, M., & Fink, G. (2021). Resources , Conservation & Recycling Prolonging life cycles of construction materials and combating climate change by cascading: The case of reusing timber in Finland. *Resources, Conservation & Recycling*, 170(November 2020), 105555. <https://doi.org/10.1016/j.resconrec.2021.105555>
- [9] Sakaguchi, D., Takano, A., & Hughes, M. (2017). The potential for cascading wood from demolished buildings: Potential flows and possible applications through a case study in Finland. *International Wood Products Journal*, 8(4), 208–215. <https://doi.org/10.1080/20426445.2017.1389835>
- [10] Seidl, R., Thom, D., Kautz, M., Martin-Benito, D., Peltoniemi, M., Vacchiano, G., Wild, J., Ascoli, D., Petr, M., Honkaniemi, J., Lexer, M. J., Trotsiuk, V., Mairota, P., Svoboda, M., Fabrika, M., Nagel, T. A., & Reyer, C. P. O. (2017). Forest disturbances under climate change. *Nature Climate Change*, 7(6), 395–402. <https://doi.org/10.1038/nclimate3303>
- [11] Vis, M., Mantau, U., & Allen, B. (2016). *CASCADES. Study on the optimised cascading use of wood: Vol. No 394/PP/.*

#### **The Authors' Addresses:**

Professor PhD MSc Architect MAA Olga Popovic Larsen,  
PhD Candidate, Architect MAA Xan Browne1

Royal Danish Academy: Architecture, Design, Conservation, Institute for Architecture and  
Technology, Copenhagen, Denmark, Phillip De Langes Alle 10, 1435 Copenhagen K, Denmark

## THE SOUND SIGNAL PROCESSING AND DEEP LEARNING NETWORK AS A TOOLS FOR DETERMINING THE CIRCULAR SAW BLADE SPEED

Srdjan Svrzi , Mladen Furtula, Marija Jurkovi ,  
Vladislava Mihailovi , Aleksandar Dedi

*University of Belgrade, Department of Wood Science,  
Faculty of Forestry, Belgrade, Serbia  
e-mail: srdjan.svrzic@sfb.bg.ac.rs*

### ABSTRACT

Rotation of a saw blade presents one of the most important cutting parameter, often regarded as cutting speed. The purpose of this paper was to determine the discrete values of the circular saw blade speed by means of the deep learning network. During idle rotation of the saw blade certain sounds are produced which were recorded and later processed in MatLab software making them suitable for further analysis and training the deep learning network. For the chosen values of the circular saw blade rotational speed, set at 2000, 3000 and 4000 rpm, totally 600 recordings were made (200 for each speed) in the form of wave format. All of them were converted in power spectrum by Fast Fourier Transformation (FFT) in order to determine spectral areas of the most importance, and later the spectrograms were made using Short Time Fourier Transform (STFT), as magnitude squared of STFT. The obtained spectrograms formed the data base for training and testing deep learning network. Pre-trained network shows the accuracy of 100%.

**Keywords:** sound signal, signal processing, FFT, SFFT, spectrogram, deep learning, machine learning

### 1. INTRODUCTION

Intelligent machining presents inevitable step in shaping computer-integrated manufacturing as a logical advance to industry 4.0. Process monitoring by implementation of different types of sensors, data acquisition and data processing obtains precondition for intelligent machining (Mishira et al. 2018.). Apart from commonly used force measuring approach (Li et al. 2018; Liu et al. 2018; Su et al. 2013; Zhou et al. 2018) or vibration monitoring (Fu et al. 2019) the sound and acoustic analysis are also of a great interest for cutting process monitoring (Cao et al. 2017; Kothurn et al. 2018; Kishawy et al. 2018).

Machine learning and its implementation becomes unavoidable in the novel technological processes in the sense of elevating process performances and thus its quality. So far different techniques were developed in order to achieve these tasks such as: decision trees, support vector machine, regression analysis, Bayesian networks, K-nearest neighbor classifier, deep learning etc. Deep learning itself presents a part of wider field of machine learning which is a piece of wider area of artificial intelligence.

During the cutting process where the circular saw blade is involved different parameters of the process are to be monitored e.g. power, force, surface quality, circular saw blade factors. This paper is dealing with one of the circular saw blade features – saw blade rotation speed. Saw blade rotation produces a certain sound also known as whistling that is generated by the teeth geometry and blade vibrations during machining (Agilera 2011; Kminiak et al.

2015; Kvietkova et al. 2015; Svrzic et al. 2021). Design of the optimal cutting system in respect to saw blade factors could be achieved by sound signal analysis and decision making. If the circular saw blade is idling the sound is generating only due to saw blade movement. This sound could be recorded and analyzed, hopefully giving useful information of present rotational speed. However, machining system also produce a certain amount of noise attached to its engine and transmission. Such sound signal is to be processed and subjected to deep learning process making it possible for machine decision making and process monitoring.

## 2. EXPERIMENTAL

The experiment took place at the Laboratory for Machines and Apparatus at the Faculty of Forestry, University of Belgrade (Beograd, Serbia). The machining system used for cutting the wood samples was a Minimax CU 410K combined machine (SCM, Rimini, Italy) equipped with a 3 kW three-phase asynchronous electrical motor. The rotational speed of the motor was set by custom made frequency regulator. For the speeds of 2000, 3000 and 4000 rpm the corresponded frequencies were 25.3, 38 and 50.5 Hz, respectively. The saw blade used in the experiment was FREUD LU2B 0500 with dimensions of 250 (diameter) x3.2 (width) x30 mm (inner diameter) and 48 saw teeth (fig. 1). The saw blade is, according to manufacturer, intended for cross and rip cutting of soft and hardwood species up to 50mm and for chipboards up to 60mm thickness. Measurement equipment consisted of: dbx RTA-M Measurement microphone with back electret-condenser, placed on anti-vibrational rack, Focusrite Scarlet SOLO USB audio interface and personal computer (fig. 2a,b).



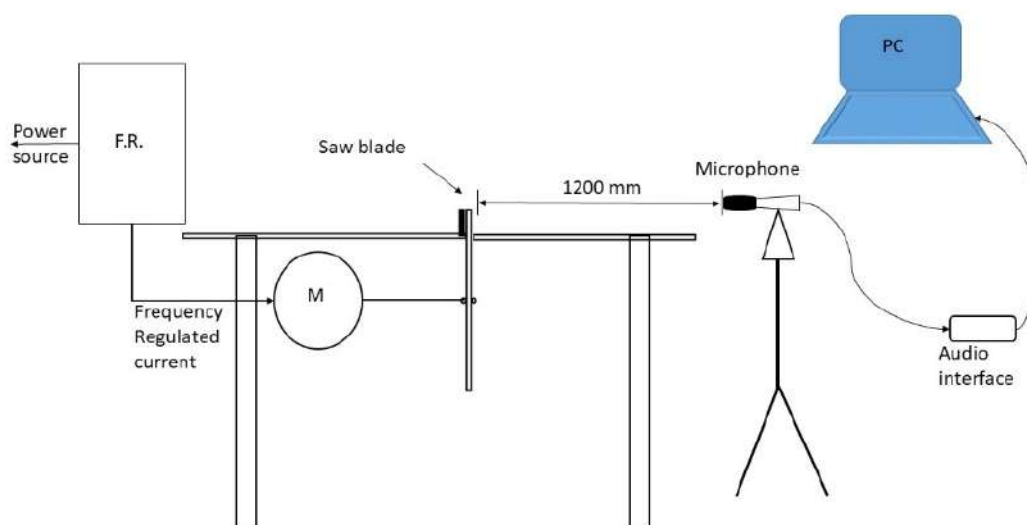
*Figure 1: FREUD LU2B 0500 saw blade*

The softer used for recording sound signals was Audacity, open source, cross-platform audio software. Slicing and trimming of the signals obtained was done by WavePad Sound Editor developed by NCH software. Measurements were performed at 44100 Hz sampling rate.



*Figure 2a: RTA-M Measurement microphone*    *Figure 2b: Scarlet SOLO audio interface*

Experimental setup is presented at figure 3.



**Figure 3: Experimental setup**

The sounds generated throughout the experiment originate from moving machine parts (electromotor, bearings, spindles etc.) and from saw blade whistling. Those sounds were detected by the microphone and recorded on PC as wave files. Originally the length of wave files were 4 minutes for each saw blade rotational speed. On these recordings spectral analysis were performed by means of FFT and STFT. The use of just FFT wasn't enough for detailed analysis because the obtained power spectrum involved lots of noise or parasitic frequencies. Further implementation of STFT, involving Hann's window function, thus obtaining spectral density graph, significantly smoothed the spectral line thus pointing to which spectral areas is to be carefully observed. This is particularly important for creating inputs to data base for deep learning network. Generally, there are some rules concerning raw data preparation: 1) Making data suitable for network architecture; 2) Dimensionality reduction – making patterns more obvious and 3) Data need to be so prepared to cover entire solution space.

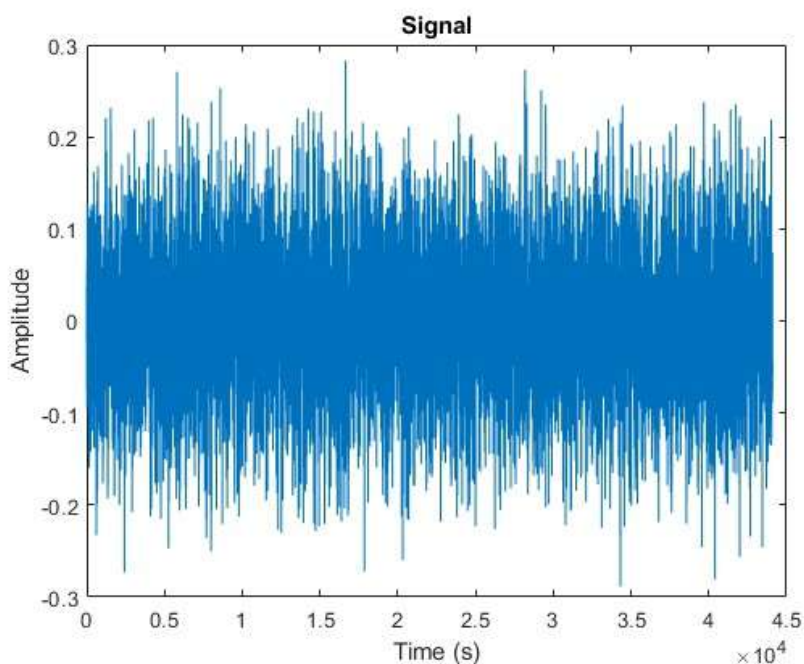
Further step was to slice entire recordings of 4 minutes into smaller even parts with length of 1 second, which was done by WavePad software. Now, it was possible to create data base for training deep learning network. First step was to import all of 240 short lasting recordings of sound signal for each saw blade speed and to transform them into 2D images of 3D spectrograms. Spectrograms are 3D (frequency-time-power) charts obtained by STFT or wavelet transform of original sound signals. 2D presentation involves RGB scale to present the power of certain peaks or spectral areas. These 2D spectrograms were saved in JPG format and presented training data for deep learning network which was GoogleNet transfer learning network specially designed for image recognition.

Some adjustments were made specific to the number of classes initial learning rate, that was set to 0.0001, validation frequency, maximal number of epochs and percentage of data used for validation.

### 3. RESULTS

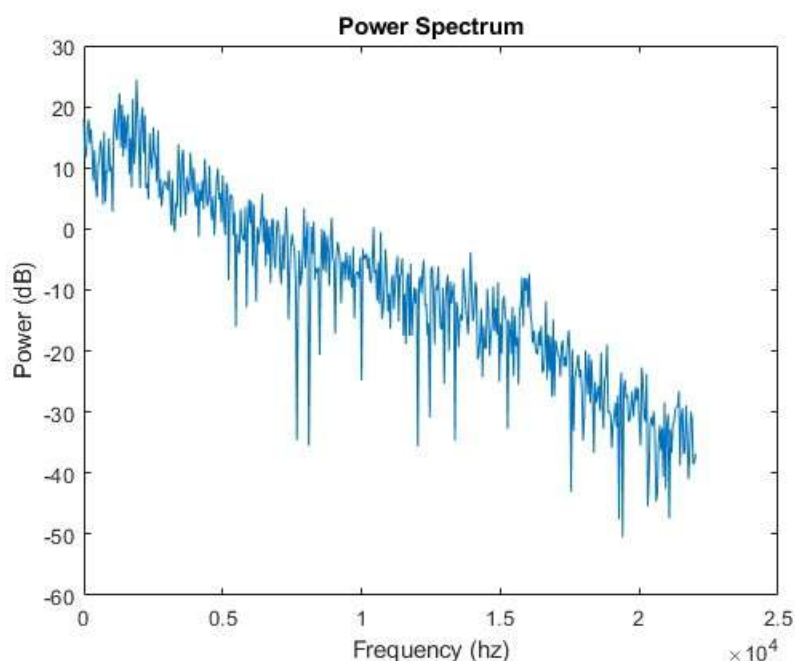
As the result of data recording a raw sound signal was acquired, which is presented in figure 4.





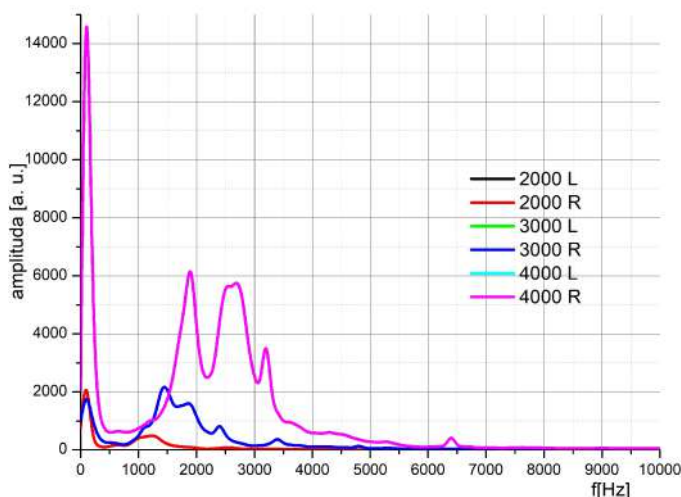
**Figure 4:** Sound signal of circular saw blade idling noise at 3000 rpm

It is impossible to extract any useful information from recording presented in figure 4. It is the same case with all other recorded signal so it was obvious that further signal processing is needed. First step was to perform FFT in order to extract characteristic spectral peaks.



**Figure 5:** Power spectrum of recorded sound signal

The power spectrum hasn't provided enough information for any decision concerning further steps of deploying deep learning network. The smoothening of power spectrum graph needed to be done introducing STFT. The spectrum of all tree recorded sets of data are presented in figure 6.

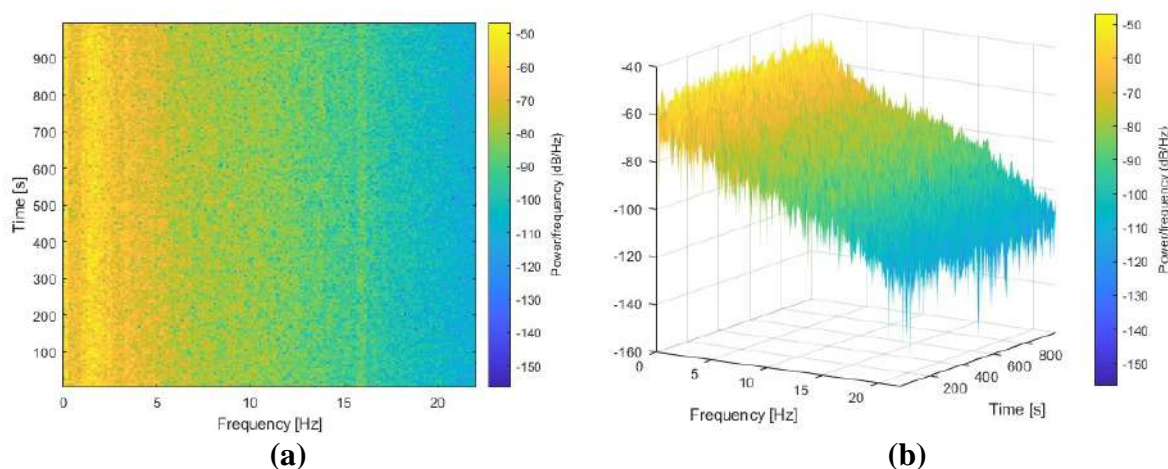


**Figure 6:** 2000, 3000 and 4000 rpm spectral density

The legend in figure 6 with L and R marks stands for left and right recording channels which are the same, so there are only three lines: purple for 4000, blue for 3000 and red for 2000 rpm. Now it is more clearly what was happening. Spectral areas between 0 and 500 Hz have very distinguished peaks for all speeds increasing with increasing speed of processing system. These peaks are addressed to the sounds created by the machine itself – rotation of electromotor, spindle and transmission. Another interesting spectral area is from 1000 up to 3500 Hz. There is obvious increase in magnitude of signal at those frequencies and they are subjected to the rotation of circular saw blade. This assumption is based upon simple mathematics: 2000 rpm is about 66 rps, multiplied by 48 saw blades gives frequency of about 1600 Hz, for 3000 rpm the frequency is at 2400 Hz and for 4000 rpm the value of frequency is 3168 Hz.

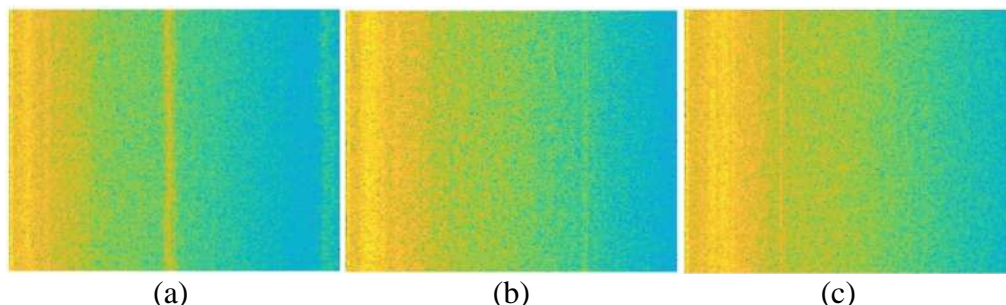
It is logically to conclude that both spectral areas are affected by processing system dynamics and that they will have influence on spectrograms to be obtained, so according to rules of data preparation for deep learning procedure it was decided to keep the whole spectrum for further steps of analysis.

As already said spectrograms presents 2D image of frequency change in time with belonging values of power, where the power is determined by color according to RGB scale (the hotter the color the greater the power).



**Figure 7:** Spectrograms presented in (a) 2D and (b) 3D

2D spectrograms in the JPG format present input data for deep learning network. Window length for STFT was set in accordance to the second rule of data processing – making patterns more obvious. In that sense the number of samples per window was set to 512 and overlapping of windows were 50%. According to the same rule all axes, legends, color bars and ticks were removed from acquired spectrograms.



**Figure 8:** Adjusted spectrograms for (a) 2000 rpm (b) 3000 rpm and (c) 4000 rpm

Deep learning data base was consisted of three directories: Spec2000, Spec3000 and Spec4000 each containing 200 JPG spectrograms.

GoogleNet network performed learning and validation process for more than two and a half hours.



**Figure 9:** Deep learning process report

The process was conducted through 20 epochs and 960 iterations. Accuracy validation was calculated after each 20 iterations.

According to the deep learning process report the accuracy rate of obtained was 100%, meaning that there is no doubt whether the signals would be properly recognized and therefore decision made was correct.

From the report it was obvious that the maximum accuracy was reached and didn't change at about 500<sup>th</sup> iteration. This practically means that fewer input data were needed than originally set, but also that signal processing and spectrogram preparation were made in satisfactory manner.

## 4. CONCLUSIONS

Based on all previously said it is possible to conclude that:

- This research presents an entry level paper for a possible use of a sound signal identification as a tool for a process monitoring in woodworking practice;
- The experimental setup proved to be adequate for this kind of research providing satisfactory data for further steps of analysis;
- Proposed software packages offered rather good signal management and transformation;
- STFT proved to be exceptional tool for investigation of frequency spectrum enabling easy insight in areas of the greatest interest concerning implementation of deep learning network;
- Spectrogram pictures were the right choice as input data for the deep learning process;
- The GoogleNet transfer learning process proved to be adequate for this type of investigation giving the perfect score in validation process;
- According to everything presented it was possible to exactly determine the rotational speed of circular saw blade and processing system;
- There is a broad field of future researches concerning process identification and process monitoring such as: determination of cutting parameters when tool is in interaction with material, assessment of the tool sharpness during cutting, process power consumption etc.

## REFERENCES

- [1] Aguilera, A. (2011b) Cutting energy and surface roughness in medium density fiberboard rip sawing. *European Journal of Wood and Wood Products*, 69(1), 11-18.
- [2] Cao, H., Yue, Y., Chen, X., and Zhang, X. (2017) Chatter detection in milling process.
- [3] Fu, Y., Zhang, Y., Gao, H., Mao, T., Zhou, H., Sun, R., and Li, D. (2019) Automatic feature constructing from vibration signals for machining state monitoring. *Journal of Intelligent Manufacturing*, 30(3): 995-1008.
- [4] Kishawy, H. A., Hegab, H., Umer, U., and Mohany, A. (2018) Application of acoustic emissions in machining processes: analysis and critical review. *The International Journal of Advanced Manufacturing Technology*, 98(5-8), 1391-1407.
- [5] Kminiak, R. and Kubš, J. (2016) Cutting Power during Cross-Cutting of Selected Wood Species with a Circular Saw. *BioResources*, 11(4), 10528-10539.
- [6] Kothuru, A., Nooka, S. P., and Liu, R. (2018). Application of audible sound signals for tool wear monitoring using machine learning techniques in end milling. *The International Journal of Advanced Manufacturing Technology*, 95(9-12), 3797-3808.
- [7] Kvietková, M., Gaff, M., Gašparík, M., Kminiak, R. and Kriš, A. (2015) Effect of number of saw blade teeth on noise level and wear of blade edges during cutting of wood. *BioResources*, 10(1), 1657-1666.
- [8] Li, H., Qin, X., Huang, T., Liu, X., Sun, D., and Jin, Y. (2018). Machining quality and cutting force signal analysis in UD-CFRP milling under different fiber orientation. *The International Journal of Advanced Manufacturing Technology*, 98(9-12), 2377-2387.
- [9] Liu, C., Li, Y., Zhou, G., Shen, W. (2018) A sensor fusion and support vector machine based approach for recognition of complex machining conditions. *Journal of Intelligent Manufacturing*, 29(8): 1739-1752.

- [10] Mishra, D., Roy, R. B., Dutta, S., Pal, S. K., and Chakravarty, D. (2018). A review on sensor based monitoring and control of friction stir welding process and a roadmap to Industry 4.0. *Journal of Manufacturing Processes*, 36, 373-397.
- [11] Nasir, V., Cool, J., and Sassani, F. (2019). “Acoustic emission monitoring of sawing process: Artificial intelligence approach for optimal sensory feature selection,” *The International Journal of Advanced Manufacturing Technology* 102, 4179-4197.
- [12] Su, H., Wu, C. S., Pittner, A., and Rethmeier, M. (2013). Simultaneous measurement of tool torque, traverse force and axial force in friction stir welding. *Journal of Manufacturing processes*, 15(4), 495-500.
- [13] Svrzic, S., Djurkovic, M., Danon, G., Furtula, M., and Stanojevic, D. (2021). "On acoustic emission analysis in circular saw cutting beech wood with respect to power consumption and surface roughness," *BioResources* 16(4), 8239-8257.
- [14] synchrosqueezing transform of sound signals. *The International Journal of Advanced Manufacturing Technology*, 89(9-12): 2747-2755.
- [15] Zhou, J., Mao, X., Liu, H., Li, B., Peng, Y. (2018) Prediction of cutting force in milling processsing vibration signals of machine tool. *The International Journal of Advanced Manufacturing Technology*, 99(1-4): 965-984.

## SPATIAL FLEXIBILITY IN TRADITIONAL MACEDONIAN ARCHITECTURE FROM THE 19<sup>TH</sup> CENTURY

**Branko Temelkovski**

*Faculty of Design and Technology of Furniture and Interior – Skopje,  
Ss. Cyril and Methodius University in Skopje  
e-mail: branko.tt@gmail.com*

### ABSTRACT

Intricate concepts of spatial organization characterize the traditional Macedonian architecture of the 19<sup>th</sup> century. The limitations imposed by specific materials and technological constraints during that era stimulated the development of intelligent and versatile spatial models. This research seeks to investigate the qualities of spatial flexibility and their practical application.

The study will begin by defining the concepts of flexibility and polyvalence of space as sustainable architectural properties. It will then systematically analyze these properties within traditional Macedonian architecture, focusing on elementary spatial units such as rooms, as well as communicative spaces. The study will examine approximately 200 houses from this period. Finally, a comparative analysis will be conducted, drawing examples from contemporary architecture to illustrate these concepts further.

**Keywords:** flexibility, polyvalence, spatial configuration, traditional architecture

### 1. INTRODUCTION

According to Charles J. Kibert (2016), vernacular architecture embeds cultural wisdom and an intimate knowledge of place in the built environment. It comprises technology, or applied science, that has evolved by trial and error over many generations all over the planet as people designed and built the best possible habitat with the resources available to them (Kibert, 2016).

Humanity is currently facing rapid and profound technological improvements within a short timeframe. In contrast, architecture as a discipline, demands a longer period to materialize from idea to reality due to its intricate complexity and material considerations. Additionally, the substantial costs associated with constructing architectural structures require extended periods of their use. The contradiction between technological and cultural advancements on the one hand, and permanence as one of the key attributes of architecture on the other hand, is imposed as a challenge in the discourse of sustainability in architectural design. Traditional architecture, particularly the Macedonian traditional architecture embodies sustainable principles that effectively address fundamental issues concerning spatial flexibility, permanence, and rationality. By studying the traditional architecture, which has stood the test of time and incorporated sustainable principles, architects and designers can learn from the past and apply those lessons to contemporary designs. Thus, this study aims to investigate the principles of flexibility and polyvalence of space in traditional Macedonian architecture of the 19<sup>th</sup> century.

### 2. METHODS

The research conducted in this study employed various methods to explore and analyze the architectural aspect on the concept of spatial flexibility in traditional Macedonian architecture. The research incorporates the historical method, collecting data from primary and secondary sources and examining theoretical views of various authors. Additionally, the normative method identifies recurring features and establishes standards. Field observations provide practical insights, while the comparative method is used for exploring notable examples of contemporary architecture with similar

spatial models. These combined approaches offer a comprehensive understanding of spatial flexibility and its relevance in modern contexts.

### 3. FLEXIBILITY AND POLYVALENCE OF SPACE

Flexibility and polyvalence are two crucial and interrelated concepts in architecture. Flexibility refers to the property of objects or spaces to adapt to different functions and activities during their use, rather than becoming outdated or requiring significant reconstruction efforts. The capacity for long-term adaptability of structures to accommodate changing needs and evolving conditions over time, as opposed to designing for specific and singular functions and purposes, represents a fundamental aspect of creating sustainable and flexible buildings and environments. Polyvalence, in the context of architecture, relates to the ability of an object or space in general, to serve multiple purposes simultaneously. It involves the ease with which the object or space can be reconfigured to accommodate various needs at the same time.

The renowned Dutch architect and influential theorist Herman Hertzberger, known for his humanistic approach in architecture, introduces the concept of a polyvalent form, which can be put into different uses without having to undergo changes itself, so that a minimal flexibility can still produce an optimal solution, in contrast to the collective prescription of uniformity and predetermined functional arrangements inherent in the functionalist doctrine of modernism (Hertzberger, 2001). According to him, collective interpretations of individual living patterns must be abandoned. What we need is a diversity of space in which the different functions can be sublimated to become archetypical forms, which make individual interpretation of the communal living pattern possible by virtue of their ability to accommodate and absorb, and indeed to induce every desired function and alteration thereof (Hertzberger, 1962). By the architectural design of Diagoon Houses in Delft where split levels evolve around an inner patio and are functionally neutral, he introduced two prototypical design concepts: a) polyvalence: the ability of spaces to be interpreted in multiple ways and absorb different functions with minimal intervention without losing their architectural identity, and b) the half-product: the houses were given an incomplete, raw aesthetic, that ought to inspire the inhabitants to adapt their house to their own personality (Karamalakis, 2015).

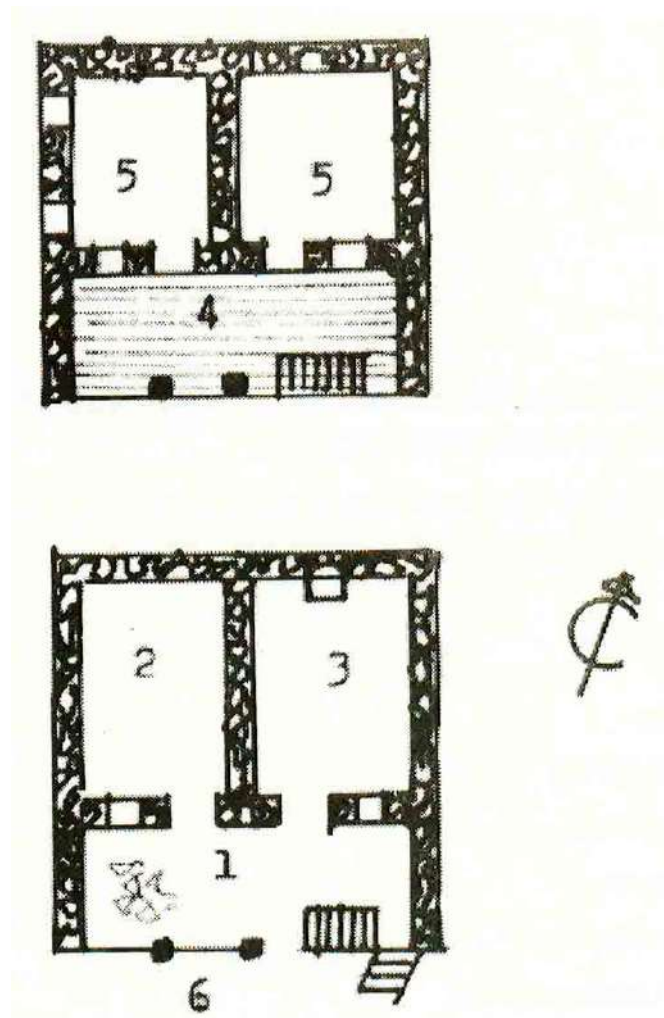
According to Bernard Leupen, designing for the unknown, the unpredictable, is the new challenge facing architects today. 'Form follows function' is giving way to concepts like polyvalence, changeability, flexibility, disassembly and semi-permanence. The design is becoming an innovative tool for developing new spatial and physical structures that generate freedom (Leupen at all, 2005). Leupen develops the concept of frame and generic space, which refers to the idea of flexibility in architecture. He argues that taking not the changeable but the permanent as a departure-point opens up new perspectives. The permanent, or durable component of the house, constitutes the frame within which change can take place and which defines the space for change; the frame itself is specific and has qualities that determine the architecture for a long period of time, and the space inside the frame is general, its use unspecified; this space Leupen has called generic space (Leupen, 2006). Generic space is not defined by its specific use or form, but rather by its ability to respond to changing needs and functions over time.

Gérald Ledent examines the 4x4 meter room as an original archetype within traditional houses and as the smallest functional unit whose inherent permanence allows for diverse functional, technical, and aesthetic adaptations, and which is capable of accommodating a variety of uses and design variations, spanning from multipurpose living areas to bedrooms. He explains that the most prominent characteristic of a type is that it is the result of a long and constant sedimentation process of uses and techniques in order to attain the quintessence of local dwelling needs. Therefore, through their constant improvement process, traditional types leave aside contingent elements to retain only the essential, the underlying structure of housing (Ledent, 2017). Archetypes can be regarded as a degré zero of architecture. They form a resilient frame within which change can occur on a functional, technological and formal level referring directly to the three founding principles of Vitruvius (Ibid.). The basic room - a cell with those dimensions, is optimal and sufficiently flexible to create a functional and adaptable space that could easily be reconfigured according to the changing needs of the residents. Its properties, such as modularity, adaptability, and efficiency, determine its sustainable character.

#### 4. FLEXIBILITY IN THE TRADITIONAL MACEDONIAN ARCHITECTURE

The internal form of the traditional Macedonian house derives from three compositional principles of structuring: 1. establishing typified functional groups organized according to a single purpose, with a clear distinction of primary (residential) and secondary (economic and representational) functions, 2. vertical growth - superimposition of functionally typified groups and 3. arranging the units from the groups around a core (chardak<sup>1</sup>, porch) as a result of the need for spiritual integration of people (Hadzieva Aleksievska, 1986).

According to Petar Mulichkoski, the elementary Macedonian rural house presents an archetypal model that he considers an authentic prototype - a nucleus composed of a porch and basements on the ground floor, and a chardak and rooms on the upper level [Fig.1]. He believes that this architectural prototype has evolved over a continuous tradition of 2000 years, adapting to changing needs, incorporating advancements in construction techniques and expanding its functionalities. As a result, this residential culture evolved further, transforming itself into an urban house model with multiple floors. The incorporation of "chardak" structures on various floors led to a distinctive and recognizable architectural expression, adding to the authenticity of these urban houses (Mulichkoski, 2000).



*Figure 1: Elementary Macedonian rural house - image from Mulichkoski, P. (2000).  
The Spirit of Macedonian House*

<sup>1</sup> Chardak is a multipurposed closed or open space, like a veranda, that connects the rooms of the house.

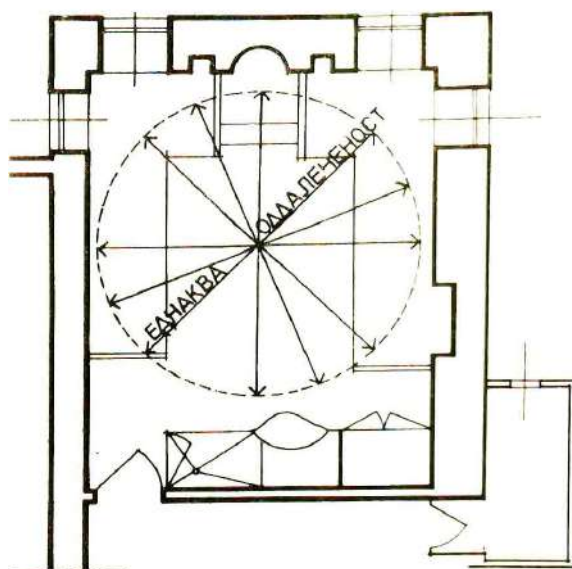


The spatial configuration of traditional Macedonian architecture is primarily based on a compositional system of elementary square or rectangular spatial units with a central character. Despite the spaces often being irregularly shaped, they strive to become rectangular and are arranged in an orthogonal structure. The room [Fig.2] serves as the primary living unit, accommodating various functions, including living room, dining room, guest room, bedroom, etc. It strives for a square form, as a result of anthropomorphic selection in choosing the most suitable shape. It appears with typical dimensions that often recur, with rare exceptions, as elaborated in the research by Jasmina Hadzieva Aleksievska (1985), where repetitive dimensions have been identified with the following values<sup>2</sup>:

- (5 6)AR=(3.8 4.5)meters,
- (6 6) R=(4.5 4.5) meters,
- (5 5) R=(3,8 3.8) meters,
- (4 5)AR=(3.0 3.8) meters,
- (6 7) R=(4.5 5.3) meters,
- (5 7) R=(3.8 5.3) meters.

Alternatively, deviations from whole arshin units occur as a result of specific programmatic requirements, site conditions, and conflicts arising from the dimensioning approach - axial or tangential:

- (5.5 6) R=(4.2 4.5) meters,
- (5.25 6) R=(4.0 4.5) meters,
- (4.5 5.5) R=(3.4 4.2) meters,
- (5.5 5.5) R=(4.2 4.2) meters.



**Figure 2:** Elementary room in traditional Macedonian house - image from Hadzieva Aleksievska, J. (1985). *Measures, Anthropomorphism...*

<sup>2</sup> In the research conducted by Hadzieva Aleksievska, the measurements are presented in the "arshin" measure unit (AR). Considering that the most commonly used arshin unit in Macedonian architecture is approximately 76 centimeters, the dimensions are converted in meters accordingly.

In the spatial design of traditional Macedonian architecture, the communicative space assumes another vital role beyond its function as a mere corridor connecting primary living areas. Instead, it evolves into a central gathering area around which these spaces are arranged. While facilitating movement and access to other rooms, the communicative space also becomes a destination in itself, encouraging social interaction and connection. The architecture exhibits a clear differentiation between open and enclosed spaces, with fluid elements like porches, chardaks, and staircases, referred to as transitory spaces according to Grabrijan (1986) on one hand, and well-defined, enclosed rooms on the other. These rooms, with similar dimensions and flexible functions, are strategically positioned in relation to the communicative space. This design concept is based on a dichotomy, emphasizing the contrast between private and social realms, and resulting in a harmonious composition of enclosed volumes and open areas with various interconnections.

Similarly, the German architect Oswald Mathias Ungers in his works often divided spaces into two categories: the bodies (matters) and spaces, or positives and negatives, determinants and determined, conceiving compartments according to simple and recognizable geometric shapes even through differentiation in the design plan, and consequently, the positive forms (opaque, filled) retain their formal integrity, while the negative ones, suffer the insertion of the constructive bodies, losing their figurative identity (Giancipoli, 2016). This concept is widely prevalent in contemporary architecture. A floor plan may also articulate an apartment as a “space of social interactions”, in which case the spaces are assessed on a scale from highly communicative (social) to extremely private, which could result in a largely balanced mix or a type that gives priority to privacy, or to the communicative aspect of cohabitation; these social interactions naturally influence how every floor plan is organized, but since they cannot be assumed to be constant or universal in nature, new attempts are always being undertaken to render floor plans modifiable, open to multiple interpretations (flexible floor plans or neutral spaces) or even involve the future user in the design process from the beginning (Heckman and Schneider, 2017).

In this regard, the transformative potential of space in the configuration of traditional Macedonian houses can be observed from two key aspects:

#### **4.1 Flexibility of a single room**

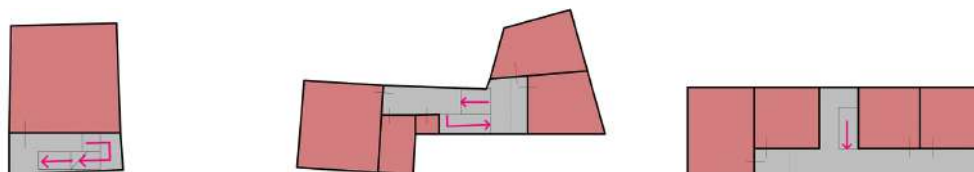
This category implies flexibility in determining the purpose of the fundamental spatial and functional unit - the room with dimensions approximating 4x4 meters, as an original polyvalent structure. The space with these dimensions and proportions does not suggest a specific function but rather embodies an archetype of human basic needs (as an individual and as part of a smaller group) and can serve various purposes, such as living space, workspace, sleeping area, play area, adaptable space with versatile day and night regimes, etc. This concept enables easy reconfiguration in response to lifestyle changes, such as family growth, changes in living habits, or variable work conditions. Due to its dimensions and compactness, this type of room enables the optimal use of available space. As a three-dimensional module, it allows easy spatial combinations, groupings, and articulations of the overall architectural expression of the entire structure. In traditional Macedonian houses, this type of room, with rare exceptions, is accessed exclusively through the chardak, and it represents the final destination in the spatial movement structure, obtaining a character of autonomy and privacy. The continuous use of this type of room indicates its capacity to adapt to changes at various levels, as this design has withstood the test of time, so in this sense, this archetypal room can be considered a key element for the sustainability of architectural design in future residential objects (Ledent, 2017).

#### **4.2 Flexibility of the chardak**

The chardak, a typical communicative space, displays a variety of dimensions, forms, and configurations within the overall spatial arrangement. Its design is influenced by climatic conditions, leading to possibilities of being open, semi-open, or enclosed, thereby acting as a physical barrier with the external environment. The Chardak serves multiple purposes, like providing a sheltered area for communication, social gatherings, and diverse interactions among the occupants. Additionally, it acts as an observation point to appreciate the surrounding landscape, facilitating natural ventilation and daylight penetration into the dwelling. Its role extends to enhancing spatial flow and circulation

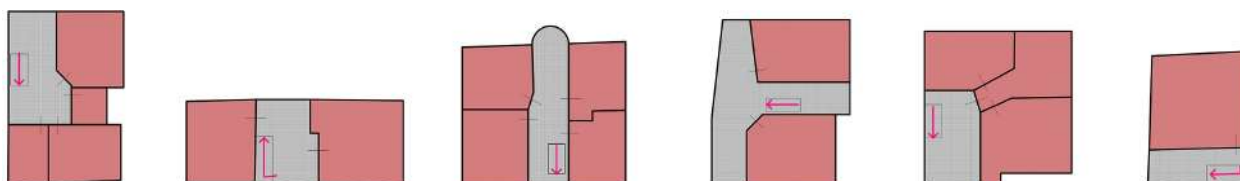
throughout the entire structure, acting as a connecting element. Furthermore, the chardak serves as a practical storage area for agricultural produce, household belongings, tools, or other materials, ensuring efficient space utilization. Its adaptability to accommodate various functions and the way it is integrated into the design of traditional Macedonian houses exemplify its significance as a fundamental element contributing to a coherent and sustainable architectural composition. In terms of size, it may range from a small area, resembling a typical room, to becoming a dominant surface within the comprehensive architectural composition. Depending on its size, the function of the chardak can be defined as follows:

In rare instances when the chardak occupies a small area, it assumes a transit-oriented character, primarily serving as a communicative space [Figure 3].

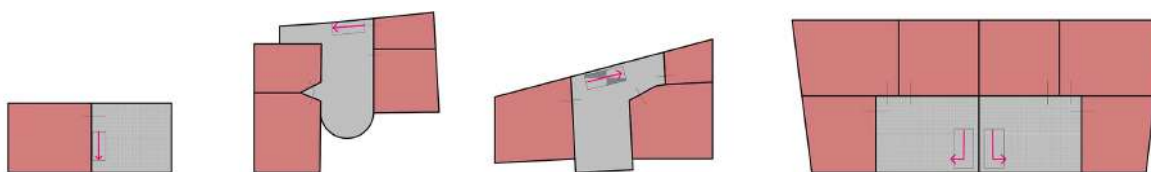


**Figure 3:** Chardak with minimal dimensions, as communicative space

When the chardak's dimensions and form resemble those of a typical room, it can acquire an expanded communicative character [Figure 4]. Besides its transit-oriented function and connection to other floors by positioning of the staircase space as an integral part, the chardak may accommodate an additional function that does not occupy significant space, such as a small working area or seating space. However, its transit-oriented nature limits the possibility of housing multiple functions. If the main communication links are strategically grouped or located at the edges, the chardak can assume multiple functions and acquire a multipurpose character, with an increased focus on communicative and social aspects over intimacy typically associated with individual rooms [Figure 5].



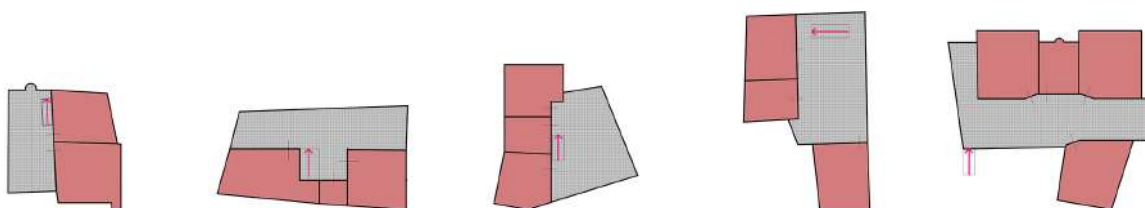
**Figure 4:** Chardak as an expanded communication



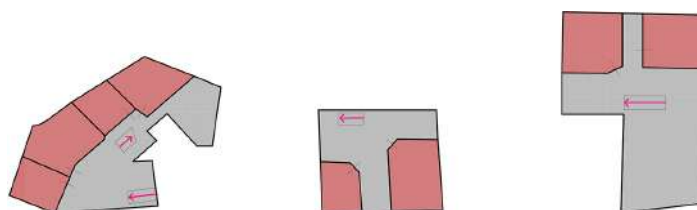
**Figure 5:** Chardak with the form and dimensions of a typical room

In cases where the chardak occupies a substantial portion of the building's footprint, it acquires an integrative role, being positioned within a system of communicative spaces that exhibit remarkable fluidity and flexibility in terms of purpose [Figure 6]. The chardak may occupy an entire floor area at the top level, or it may be compositionally fragmented [Figure 7]. This architectural model allows for the simultaneous organization of multiple activities within one continuous space. Furthermore, it enables seamless transitions between different areas, or overlapping of different spatial domains, as well as diverse setting of functions in order to establish distinct levels of separation or connection

based on the user's needs and preferences. This layout provides ample opportunities for space reconfiguration and accommodating various activities, facilitating interior modifications in response to changing needs by adding or removing functional elements. Such a flexible space encourages unrestricted and dynamic utilization. As a generic space, it opens up possibilities for organic and adaptable development of the structure, responsive to specific circumstances, and is linked to the concept of programmatic indeterminacy, where the architect does not predetermine the specific purpose of the space but enables free interpretation. The concept represents a social context founded on humane interaction, proximity, and socialization, offering a model that transforms static structures into dynamic spaces. The social aspect of this model, alongside its dynamism and integrative nature, is manifested through its ability to regulate the infiltration of public space into the intimate realm of the building. This complex juxtaposition of a dual concept—a fluid and fixed space, communicative space as a connective tissue, and room as an elementary structural core—becomes evident, culminating in a harmonious blend of social and private spaces.



**Figure 6:** Chardak as a dominant space



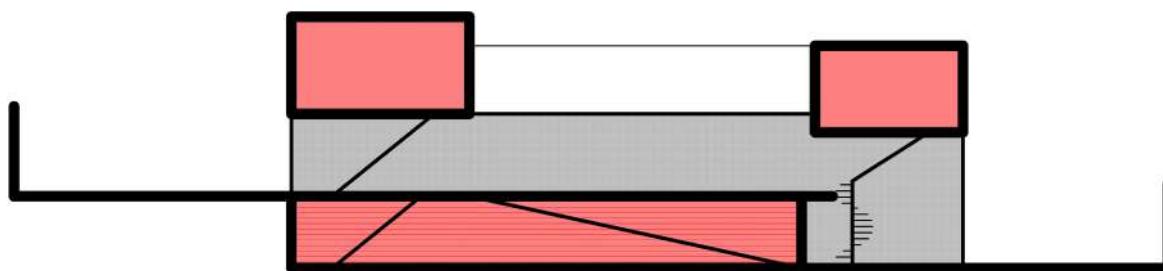
**Figure 7:** Chardak with a complex form

Chardak as a space, often with dominant facade exposure, rich views, and penetrations, which in traditional architecture acquires various forms in terms of physical openness to the external world, also acts as a powerful generator of dynamic connection with the surroundings and nature, commonly blurring the boundary with the exterior space.

Similar to the principles inherent in traditional Macedonian architecture, contemporary buildings also adopt such dualistic models. They embrace this approach, resulting in dynamic spaces that effectively blend social and private realms. Further in this study, we will examine some notable examples of the contemporary architecture:

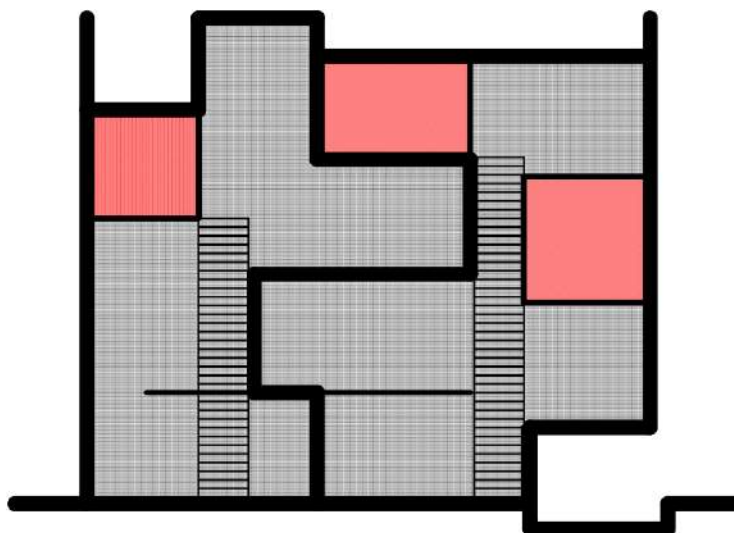
The Villa Dall'Ava in Paris, designed by the renowned architectural studio OMA, exemplifies the dualistic concept at a higher level with a profound integration of architecture and technology. This canonical masterpiece incorporates advanced technological systems, such as automated glass doors with varying levels of transparency and translucency, as well as featuring a rooftop swimming pool. Carefully developed on a sloping terrain, the spatial arrangement demonstrates intricate horizontal and vertical relationships, showcasing the meticulous attention to detail in its design. The architectural design revolves around an ingenious composition, where open fluid spaces elegantly interact with two distinct and prominently articulated closed cubes above, which house the private areas [Figure 8]. The expression of a glass cube as an open space creates a sense of passive volume, seamlessly embracing the surrounding environment rather than resisting it. This open space includes a double-height hall at the lower entrance level, seamlessly transitioning to the main living area situated at the middle level.

The living area establishes a flexible connection with nature, harmoniously blending with the courtyard. Through the skillful combination of transparency, fluidity, and adaptability, the Villa Dall’Ava exemplifies the concept of dynamic spaces that continuously interact with their surroundings. The architectural design brilliantly integrates technology, embracing the interplay between openness and enclosure, while maintaining a harmonious dialogue between the social and private aspects of the villa’s spaces. This innovative model successfully demonstrates the potential for sustainable and responsive architecture that remains adaptable to changing needs and environments, signifying a profound connection between human interaction and the built environment.



**Figure 8:** The flexible fluid concept of Villa Dall’Ava, section

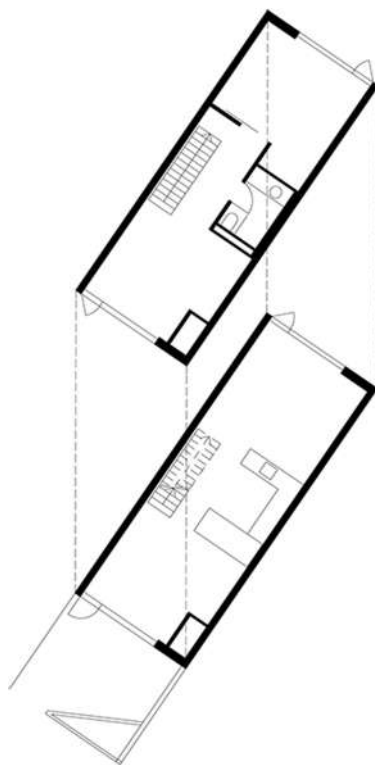
The Villa KBWW in Utrecht, designed by the Dutch studio MVRDV, presents a duplex with an innovative and unconventional approach to spatial design. The primary complexity is expressed through the meandering boundary between the two residences. Fluid spaces in both units circulate vertically around centrally positioned linear staircase spaces in a series of intertwined volumetric elements, among which closed and defined spaces are alternately distributed [Figure 9]. The use of lightweight materials rejects tectonic expression, emphasizing the abstraction of the form. The development of space is dynamically represented in the expression of the cubic monolithic form.



**Figure 9:** The flexible fluid concept of Villa KBWW, section

The apartments in the 8-Tallet housing complex in Copenhagen, designed by the architectural studio BIG, feature a spatial configuration based on a system of elementary square or rectangular spaces dictated by the primary construction. Their flexibility arises from the form, dimensions, and arrangement of these spaces [Figure 10]. The elementary spatial units are based on an almost uniform modular matrix in an immensely complex structure and strive for equal treatment in terms of form and dimensions. Flexibility is expressed in the versatile potential of spaces, where the communication areas are seamlessly incorporated into the living spaces, but also offering opportunities for various

modes of isolation or integration of spaces. In the fluid concept of space, the structure, bathrooms, and kitchens are imposed as fixed determinants that provide specific directions in defining the primary function. However, the concept allows for a degree of freedom and individual interpretation within a certain framework, which is more flexible than usual.



**Figure 10:** The flexible concept of an apartment in the housing complex 8-Tallet, plan

## 5. CONCLUSION

The research encompasses the polyvalence of space in the traditional Macedonian architecture of the 19th century, through detecting the significance of two important aspects: 1. the archetype of the approximately 4x4 meter room, which stands out as an original polyvalent structure that remains highly adaptable to changing lifestyle needs and preferences, and 2. the chardak, which serves as both communicative and living space, and plays a vital role in enhancing spatial flow and facilitating social gatherings.

Based on the research conducted on approximately 200 objects, it can be concluded that traditional Macedonian architecture exhibits distinct dynamic features and is defined by complex concepts of spatial organization based on duality in approach: a combination of open and closed, fluid and fixed spaces, extroverted and introverted, social and intimate models. All investigated parameters suggest an exceptionally flexible approach in functional solutions for architectural spaces. The spatial configuration, based on a system of elementary square or rectangular spatial modules, exhibits a strong potential for flexibility due to the polyvalence as a property of each individual unit and the possibilities for its multiplication, grouping, and combination. Flexibility is also observed in the potential for simultaneous organization of multiple activities within single continuous open space, as well as in the possibilities for spatial configurations with different degrees of isolation or integration in such structures. The fluid concept allows for the reconfiguration of space and accommodates different activities while enabling modification of the internal layout according to changing needs. Specific functional elements can be added, subtracted, or recombined as required.

Flexible concepts of programmatic indeterminacy, social and communicative nature of space, and dynamic connection with the surroundings represent an open source of ideas and spatial solutions that remain relevant in contemporary contexts. These traditional architectural concepts offer valuable

insights for modern design by facilitating interaction with the environment and addressing diverse social needs.

## REFERENCES

- [1] Giancipoli, G. (2016). *Matter and Space. Compositional Theory in the Work of Oswald Mathia Ungers*, FAmagazine n.36, pp43-51
- [2] Grabrijan, D. (1986). *Macedonian House or a Transition from an Old Oriental to a Modern European House* (in Macedonian), Mislra, Skopje
- [3] Hadzieva Aleksievska, J. (1986). *Architectural Composition of the Old Macedonian House – PhD Thesis* (in Macedonian), Ss. Cyril and Methodius University in Skopje, Faculty of Architecture Skopje
- [4] Hadzieva Aleksievska, J. (1985). *Measures, Anthropomorphism and Modular Proportions of the Old Macedonian House* (in Macedonian), Studentski zbor, Skopje
- [5] Heckman, O. and Schneider, F. (2017). *Floor Plan Manual Housing*, Birkhäuser
- [6] Hertzberger, H. (2001). *Lessons for Students in Architecture*, 010 Publishers, Rotterdam
- [7] Hertzberger, H. (1962). *Flexibility and Polyvalency*, Ecistics no.8, 1963, pp238-239
- [8] Karamalakis, A. (2015). *Case Study #1: Diagoon Houses – andreas krmilks* (wordpress.com)
- [9] Kibert, C. (2016). *Sustainable Construction Green Building Design and Delivery*, John Wiley & Sons Inc., Hoboken New Jersey, .521
- [10] Ledent, G. (2017). *Permanence to allow change. The archetypal room: The persistence of the 4×4 room*. The 10th EAAE/ARCC International Conference, pp339-344. DOI: 10.1201/9781315226255-54.
- [11] Leupen B. at all (2005). *Time-Based Architecture*, 010 Publishers
- [12] Leupen, B. (2006). *Frame and Generic Space*, 010 Publishers, Rotterdam,
- [13] Mulichkoski, P. (2000). *The Spirit of Macedonian House* (in Macedonian), AEA Izdavaci, Mislra, Skopje

## HARDNESS OF PLYWOOD REINFORCED WITH FIBERGLASS PREPREG

Violeta Jakimovska Popovska<sup>1</sup>, Borche Iliev<sup>1</sup>

<sup>1</sup> *Ss. Cyril and Methodius University in Skopje, R. of North Macedonia,  
Faculty of design and technologies of furniture and interior-Skopje  
e-mail: jakimovska@fdtme.ukim.edu.mk; iliev@fdtme.ukim.edu.mk*

### ABSTRACT

Improvement of plywood properties can be done by reinforcing plywood with non-wood materials in their structure.

The aim of this research is to study the Janka hardness of plywood reinforced with fiberglass prepreg sheets inserted in plywood structure. These reinforcement sheets are made of fiberglass fabric that is pre-impregnated with phenol-formaldehyde resin. Plywood is consisted of eleven veneer sheets with thickness of 1,5 and 1,85 mm that are bonded with the same resin used for fiberglass fabric pre-impregnation.

By changing the position of fiberglass prepreg sheets in plywood structure, four different models of plywood were made.

Tests for plywood hardness according to Janka were done on each plywood model.

The obtained results showed that the values of Janka hardness are affected by the use of fiberglass prepreg sheets in plywood structure.

**Keywords:** plywood, reinforcement, fiberglass, prepreg, pre-impregnated, phenol-formaldehyde resin, Janka hardness.

### 1. INTRODUCTION

Because of its high strength to weight ratio, plywood is good material for use in transport industry where it is a key material for floors in the construction of transport equipment. Thanks to its light weight, strength and hardness, plywood competes in the application area such as light metals (Lukkaroinen, Metsa wood, 2008). Plywood is characterized with decreased anisotropy compare to solid wood, as well as possibility to receive and distribute loads, which is why it is used in many applications in construction, such as: siding, roofing, shear walls, as well as for production of engineered wood flooring.

When plywood is used as flooring material as well as in transport industry, its hardness is an important property that has to be considered.

Improvement of plywood properties can be done by reinforcing plywood with non-wood materials in their structure (Jakimovska Popovska and Iliev, 2019, Davalos et al., 2000; Hardeo and Karunasena, 2002; Choi et al., 2011; Z ke and Kalni š, 2011, Xu et al., 1996, Xu et al., 1998, Brezovi et al., 2002, Brezovi et al., 2003, Brezovi et al., 2010, Biblis and Carino, 2000, Hrázský and Král, 2007, Mani š and Z ke, 2011).

Fiberglass fabrics pre-impregnated with resin (fiberglass prepregs) are efficient for plywood reinforcement. Application of these materials in plywood structure increase the bending strength and modulus of elasticity in bending (Jakimovska Popovska, Iliev, 2019).

The aim of the research is to study the Janka hardness of experimental plywood reinforced with fiberglass fabrics pre-impregnated with methyl alcohol-soluble phenol-formaldehyde resin.



## 2. EXPERIMENTAL METHODS

Four experimental eleven-layered beech plywood were made for the realization of the research. The thickness of the veneers was 1.5 mm and 1.85 mm, with moisture content of 9.77 %. The orientation of adjacent veneers in plywood structure was at right angle.

Each model was made by inserting reinforcements made of pre-impregnated fiberglass fabric (fiberglass prepreg) into the adhesive layer of plywood.

In three experimental models, each reinforcement layer is consisted of four sheets of fiberglass prepreg placed one above the other and inserted into the panel structure symmetrically on both sides with respect to its axis of symmetry. The compositions of plywood models are shown on Figure 1.

In the first model (F1), the reinforcements are positioned next to the central veneer sheet, respectively in the fifth and sixth adhesive layer, while in the structure of the second model (F2) they are inserted into the third and eighth adhesive layer. In the third model (F3), the reinforcements represent the surface layers of plywood. The fourth experimental model of reinforced plywood (F4) was made by inserting single sheets of fiberglass prepreg in each adhesive layer of the panel.

In all models of reinforced plywood, the orientation of the wrap of the fabric is parallel to grain direction of the surface veneers.

The fiberglass prepreg was made from fiberglass fabric that was pre-impregnated with methyl alcohol soluble phenol-formaldehyde resin in quantity of 140 g/m<sup>2</sup>. Resin with 51 % dry matters content was used. The same resin was used for veneer bonding, applied on the veneers in quantity of 180 g/m<sup>2</sup>. The thickness of the pre-impregnated fabric was 0.22 mm.

The technical characteristics of the fiberglass fabric, the resin characteristics and the impregnation process are described in other paper (Jakimovska Popovska and Iliev, 2019).

The thickness of non-impregnated fiberglass fabric was 0.173 mm. After impregnation, the thickness of the prepreg was 0.22 mm.

Plywood compositions of all four models were pressed under same conditions: specific pressure of 18 kg/cm<sup>2</sup> at 155°C for 30 minutes. Models were made in the following dimensions: 1180×910×d mm. The moisture content of the panels was 8.3 %.

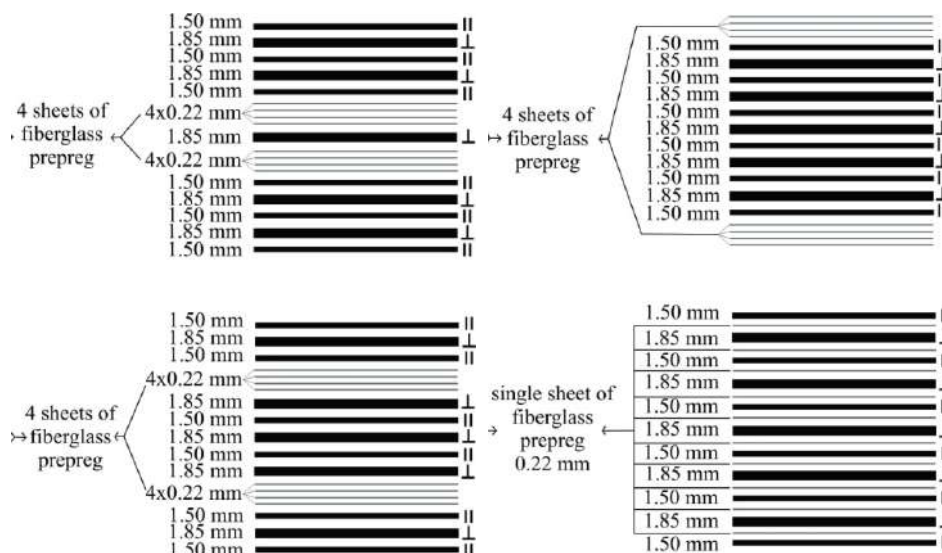


Figure 1: Composition of plywood models

The Janka hardness of the experimental plywood models was tested on the test specimens with dimensions of 100×100 mm. The tests were performed at two measuring points, positioned diagonally in the corners of the face and the back of the test specimens. Thereby, the measuring points on the back of the test specimens are positioned in opposite angles in relation to the measuring points on the face of the test specimens. The hardness was tested by pressing a stainless hemisphere on the surface of the test specimen, which when entering the surface of the test specimen leaves an impression in the form of a calotte with an area of 1 cm<sup>2</sup> (Figure 2). The ratio between the force used and the surface of the calotte represents the hardness of the panel.

The obtained data were statistically analyzed. One way ANOVA was used to determine the significance of the effect of the fiberglass prepreg reinforcements on plywood hardness. Tukey's test was applied to evaluate the statistical significance between the mean values of Janka's hardness of plywood with different layouts of reinforcement (different plywood models). The tests were conducted at 0,05 probability level. Statistical software SPSS Statistic was used for statistical analysis of the obtained data.

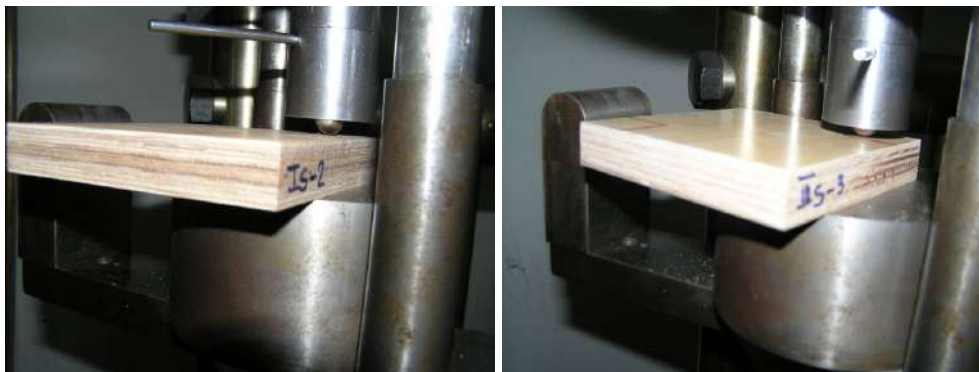


Figure 2: Testing of Janka hardness

### 3. RESULTS AND DISCUSSION

The thickness and the density of experimental reinforced plywood models are shown in table 1.

Table 1: Thickness and density of reinforced plywood models

Plywood model	Thickness (mm)	Density (kg/m <sup>3</sup> )
F1	16.69	929.01
F2	16.15	934.88
F3	16.38	939.67
F4	17.32	959.33

The obtained results from the tests of Janka hardness of the experimental plywood models are shown in table 2. The results from ANOVA and Tukey's test are shown in tables 3 and 4.

The highest value of hardness is achieved in model F1 in which the reinforcements are positioned next to the central layer of plywood. The difference between this value and the hardness of model F4 is not statistically significant, as well as the difference between models F2 and F3. The lowest value of this property is obtained in model in which the reinforcement layers are positioned as surface layers of plywood (model F3).

Compare to the mean values of hardness in models F2, F3 and F4, the highest obtained value in model F1 is higher for 14,6 %, 14,7 % and 1,4 %, respectively. There is almost no difference in the hardness of models F2 and F3.

Table 2: Statistical values for Janka hardness of reinforced plywood models

Model	N	Mean (N/mm <sup>2</sup> )	Std. Deviation (N/mm <sup>2</sup> )	Std. Error (N/mm <sup>2</sup> )	95% Confidence Interval for Mean (N/mm <sup>2</sup> )		Min (N/mm <sup>2</sup> )	Max (N/mm <sup>2</sup> )
					Lower Bound	Upper Bound		
F1	5	173.78 <sup>a</sup>	5.07	2.27	167.49	180.08	166.89	179.52
F2	5	151.61 <sup>b</sup>	14.42	6.45	133.71	169.52	134.64	173.27
F3	5	151.49 <sup>b</sup>	13.74	6.14	134.44	168.55	141.14	167.26
F4	5	171.45 <sup>a,b</sup>	8.54	3.82	160.86	182.05	162.85	184.92

The mean values with the same letters are not significantly different at 0,05 probability level

**Table 3:** Anova for significance of the effect of the fiberglass prepreg reinforcements on plywood hardness

ANOVA					
Janka Hardness	Sum of Squares	df	Mean Square	F	Sig.
Between Groups	2232.696	3	744.232	6.011	0.006
Within Groups	1980.870	16	123.804		
Total	4213.565	19			

**Table 4:** Tukey's test for the statistical significance between the mean values of Janka's hardness of different plywood models

Model	N	Subset for alpha = 0.05		
		1	2	
Tukey	F3	5	151.49	
HSD <sup>a</sup>	F2	5	151.61	
	F4	5	171.45	171.45
	F1	5		173.78
	Sig.		0.052	0.987

Means for groups in homogeneous subsets are displayed

a. Uses Harmonic Mean Sample Size = 5

The obtained values of Janka hardness of reinforced plywood panels are higher compare to the value of this property of unreinforced control plywood made from the same veneers and resin and under the same pressing conditions (127,41 N/mm<sup>2</sup>) (Jakimovska Popovska and Iliev, 2021). Compared to that control model, the mean value of Janka hardness of model F1 is higher for 36,4 %.

The same authors give the values of Janka hardenss of reinforced plywood with cotton prepreps in the limits of 144,26 to 207,06 N/mm<sup>2</sup>).

#### 4. CONCLUSIONS

The application of fiberglass preperg in plywood structure as reinforcement increases plywood hardness.

The position of the reinforcements in the plywood structure has significant impact on the plywood hardness.

By positioning the reinforcements next to the central veneer layer of plywood, the hardness is increased by 36 % compared to non-reinforced plywood. This kind of reinforcement compared to the other reinforced models is most favorable regarding the plywood hardness.

Moving the reinforcement layers to the surface of the plywood decreases the values of plywood hardness.

The choice of certain reinforced plywood model will depend on other physical and mechanical properties that should be considered, depending on the application area and exposure to different type of loads.

#### REFERENCES

- [1] Biblis, .J.; Carino, H.F., 2000: Flexural properties of southern pine plywood overlaid with fiberglass-reinforced plastic. Forest Prod J., 50 (1): 34-36.

- [2] Brezovi , M.; Jambrekovi V.; Kljak, J., 2002: Utečaj karbonskih vlakana na neka relevantna svojstva furnirskih plo a. *Drvna ind.*, 53 (1): 23-31.
- [3] Brezovi , M.; Jambrekovi , V.; Pervan, S., 2003: Bending properties of carbon fiber reinforced plywood. *Wood Research*, 48 (4): 13-24.
- [4] Brezovi , M.; Kljak, J.; Pervan, S.; Antonovi , A., 2010: Utjecaj kuta orientacije sintetskih vlakana na savojna svojstva kompozitne furnirske plo e. *Drvna ind.*, 61 (4): 239-243.
- [5] Choi, S.W.; Rho, W.J.; Son, K.J.; Lee, W.I., 2011: Analysis of buckling load of fiber-reinforced plywood plates for NO 96 CCS. *Proceedings of the Twenty-first International Offshore and Polar Engineering Conference*, 2011, Maui, Hawaii, USA, pp: 79-83.
- [6] Davalos, J.F.; Qiao, P. Z.; Trimble, B.S., 2000: Fiber-reinforced composite and wood bonded interfaces: Part 1. Durability and shear strength. *Journal of Composites Technology & Research*, 22 (4): 224–231. <https://doi.org/10.1520/ctr10544j>.
- [7] Hardeo, P.; Karunasena, W., 2003: Buckling of fiber-reinforced plywood plates. *Proceedings of Second International Conference on Structural Stability and Dynamics*, 2002, Singapore, pp. 442-447. [https://doi.org/10.1142/9789812776228\\_0062](https://doi.org/10.1142/9789812776228_0062).
- [8] Hrázský, J.; Král, P., 2007: A Contribution to the properties of combined plywood materials. *J For Sci*, 53 (10): 483-490. <https://doi.org/10.17221/2087-jfs>.
- [9] Jakimovska Popovska, V., Iliev, B. 2019: Bending Properties of Reinforced Plywood with Fiberglass Pre-impregnated Fabrics, *Proceedings of 30th International Conference on Wood Science and Technology - ICWST and 70th anniversary of Drvna industrija Journal “Implementation of wood science in woodworking sector”*, 12th -13th December, Zagreb, 2019: 77-85.
- [10] Jakimovska Popovska, V., Iliev, B. 2021. Janka hardness of plywood reinforced with pre-impregnated cotton fabrics, *Proceedings of the 5<sup>th</sup> International conference „Wood technology and product design“*, 14-17<sup>th</sup> September, Ohrid, 2021: 7-14.
- [11] Joni Lukkaroinen, *Metsa Wood* (2008): Plywood carries the transportation vehicle industry (<https://www.globenewswire.com/news-release/2008/01/31/123874/0/en/Plywood-carries-the-transportation-vehicle-industry.html>)
- [12] Kohl, D.; Million, M.; Böhm, S., 2013: Adhesive bonded wood-textile-compounds as potentially new eco-friendly and sustainable high-tech materials. *Proceedings of the Annual Meeting of the Adhesion Society 2013*, Florida, USA, pp: 27-29.
- [13] Mani š, M.; Z ke, S., 2011: Textile fabrics reinforced plywood with enhanced mechanical properties. *Abstracts of the International Scientific Conference „Civil Engineering’11”*, 2011, Latvia, pp: 35.
- [14] Rowlands, R.E.; Van Deweghe, R.P.; Launferbeg, T.L.; Krueger, G.P., 1986: Fiber-reinforced wood composites. *Wood and Fiber Science*, 18 (1): 39-57.
- [15] Sillanpää, M. (2018): The industrial manufacturing of plywood is based on several generations of experience and know-how. Article in: <https://www.woodproducts.fi/articles/industrial-manufacturing-plywood-based-on-several-generations-experience-and-know-how>.
- [16] Xu, H.; Tanaka, C.; Nakao, T.; Nisano Y.; Katayama, H., 1996: Flexural and shear properties of fiber reinforced plywood. *Mokuzai Gakkaishi*, 42: 376-382.
- [17] Xu, H., Nakao, T., Tanaka, C., Yoshinobu, M., Katayama, H., 1998: Effects of fiber length orientation on elasticity of fiber-reinforced plywood. *Journal of Wood Science*, (44): 343-347. <https://doi.org/10.1007/bf01130445>
- [18] Z ke S.; Kalni š K., 2011: Enhanced impact properties of plywood. *Proceedings of the 3rd International Conference Civil Engineering’11*, 2011, Latvia, pp: 125-130.

## IN-PLANE COMPRESSIVE STRENGTH OF PLYWOOD REINFORCED WITH COTTON PREPREG

Violeta Jakimovska Popovska<sup>1</sup>, Borche Iliev<sup>1</sup>

<sup>1</sup> Ss. Cyril and Methodius University in Skopje, R. of North Macedonia,  
Faculty of design and technologies of furniture and interior-Skopje  
e-mail: jakimovska@fdtme.ukim.edu.mk; iliev@fdtme.ukim.edu.mk

### ABSTRACT

The aim of this research is to study the in-plane compressive strength of eleven-layered beech plywood reinforced with non-wood material in its structure.

Plywood reinforcement was made by inserting certain numbers of sheets of pre-impregnated cotton fabric (cotton prepreg). Methyl alcohol soluble phenol-formaldehyde resin was used for fabric pre-impregnation, as well as for veneer bonding. The thickness of the veneers used in plywood structure was 1,5 and 1,85 mm. Different models of plywood were made by changing the position of cotton prepreg reinforcements in plywood structure. One control model of plywood without reinforcement was made.

In-plane compressive strength of plywood models was tested in five directions: parallel to the face grain, perpendicular to the face grain, at the angles of 22,5°, 45° and 67,5° to the face grain of the plywood panel.

The obtained results showed that the application of cotton prepreg in plywood structure has impact on the values of in-plane compressive strength of plywood.

**Keywords:** plywood, reinforcement, cotton fabric, prepreg, pre-impregnated, phenol-formaldehyde resin, compressive strength.

### 1. INTRODUCTION

Plywood is a material that is often used in construction in many applications because of its good strength characteristics, high strength to weight ratio, good dimensional stability and decreased anisotropy compared to solid wood. It is widely used for siding, roofing, flooring, shear walls and production of engineered wood products.

Plywood properties can be improved by reinforcing plywood with non-wood materials. Significant improvement of mechanical properties can be achieved by overlaying plywood with fiber reinforced polymers (Hardeo and Karunasena, 2002; Choi *et al.*, 2011, Z ke and Kalni š, 2011). Beside reinforcement of plywood with different types of fibers and matrixes (Xu *et al.*, 1996, Xu *et al.*, 1998, Brezovi *et al.*, 2003, Brezovi *et al.*, 2010, Biblis and Carino, 2000, Hrázský and Král, 2007, Mani š and Z ke, 2011), possibilities to reinforce wood with pre-impregnated materials-prepregs were also explored (Rowland *et al.*, 1986).

The study of Kohl *et al.* (2013) showed that the application of pre-impregnated glass, carbon and aramid fiber materials results in a significant reduction in deflection and an increase in carrying capacity.

The study of Jakimovska Popovska and Iliev (2019) showed that using pre-impregnated fiberglass fabric (fiberglass prepreg) can increase the plywood bending strength and modulus of elasticity in bending.

Other research (Jakimovska Popovska and Iliev, 2021) showed that the application of pre-impregnated cotton fabric in the structure of plywood significantly increases its hardness.

The aim of the research is to study the in-plane compressive strength of plywood reinforced with cotton fabrics pre-impregnated with methyl alcohol-soluble phenol-formaldehyde resin.

## 2. EXPERIMENTAL METHODS

For the realization of the research, four experimental eleven-layered beech plywood were made. The thickness of the veneers was 1,5 mm and 1,85 mm, with moisture content of 9,77 %. The orientation of adjacent veneers in plywood structure was at right angle.

Each model has inserted reinforcement sheets of pre-impregnated cotton fabric (cotton prepreg) in its adhesive layers. In three models, each reinforcement layer is consisted of four sheets of pre-impregnated cotton fabric placed one above the other and inserted symmetrically on both sides with respect to its axis of symmetry. In the first model (CP-1), the reinforcements are inserted in the fifth and sixth adhesive layer, while in the second model (CP-2) they are inserted into the third and eighth adhesive layer. In the third model (CP-3), the reinforcements are positioned as surface layers of plywood. The fourth model of plywood (CP-4) was made by inserting single sheets of cotton prepreg in each adhesive layer of the panel. One control model (C) of plywood without reinforcement was made for comparison of the results. The pattern and cross-section of experimental plywood models are given in previous research paper (Jakimovska and Iliev, 2021).

In all models of reinforced plywood, the orientation of the wrap of the fabric is parallel to grain direction of the surface veneers.

The cotton prepreg was made from cotton fabric that was pre-impregnated with methyl alcohol soluble phenol-formaldehyde resin with 51 % dry matters content, in quantity of 300 g/m<sup>2</sup>. The same resin was used for veneer bonding, applied on the veneers in quantity of 180 g/m<sup>2</sup>. The thickness of the cotton fabric before impregnation was 0,22 mm, while the thickness of the cotton prepreg was 0,6 mm.

The technical characteristics of the cotton fabric, the resin characteristics and the impregnation process of the fabric, as well as the parameters of the pressing process of plywood models are described in other research (Jakimovska and Iliev, 2021).

The in-plane compressive strength of plywood was tested according to the national standard MKS D.A8.070/85 on test specimens with dimensions of 50-6d-d (mm). This property is tested in five directions, i.e. parallel to the face grain, perpendicular to the face grain, at the angles of 22,5°, 45° and 67,5° to the face grain of the plywood panel.



*Figure 1: Test specimen during testing the compressive strength of experimental plywood*

For statistical analysis of the obtained data SPSS Statistic software was used. One way ANOVA was used to determine the significance of the effect of the cotton prepreg reinforcements on plywood in-plane compressive strength. Tukey's test was applied to evaluate the statistical significance between the mean values of compressive strength of plywood with different layouts of reinforcement. The tests were conducted at 0,05 probability level.

## 3. RESULTS AND DISCUSSION

The obtained results for the in-plane compressive strength of experimental plywood models are shown in table 1 and figure 2.

The analysis of the obtained data showed that in all tested directions, reinforced plywood models have higher values of compressive strength compared to the control model made without

reinforcements. In all tested directions the highest value of this property is achieved in model CP-2. Compared to the control model C, the value of compressive strength in model CP-2 is higher for 29,4 % in parallel direction, 33,3 % in perpendicular direction, 39,7 % at the angle of 22,5°, 34,6 % at the angle of 45° and 35,4 % at the angle of 67,5° to the face grain of the panel. Within the reinforced models, the lowest value of compressive strength in all tested direction is achieved in model CP-3 where the reinforcements are positioned as surface layers of plywood.

*Table 1: Statistical values for compressive strength of experimental plywood*

Compressive strength	Model	N	Mean (N/mm <sup>2</sup> )	Std. Deviation (N/mm <sup>2</sup> )	Std. Error (N/mm <sup>2</sup> )	95 % Confidence Interval for Mean		Min (N/mm <sup>2</sup> )	Max (N/mm <sup>2</sup> )
						Lower Bound	Upper Bound		
Parallel to the face grain	CP-1	5	68.12 <sup>a</sup>	4.00	1.79	63.15	73.09	62.73	72.73
	CP-2	5	76.52 <sup>b</sup>	5.69	2.54	69.45	83.58	67.49	82.43
	CP-3	5	66.69 <sup>a</sup>	3.03	1.36	62.93	70.46	61.46	68.75
	CP-4	5	69.63 <sup>a,b</sup>	3.39	1.51	65.43	73.84	66.20	73.71
	C	5	59.12 <sup>c</sup>	2.10	0.94	56.52	61.72	56.65	61.61
Perpendicular to the face grain	CP-1	5	73.11 <sup>a</sup>	3.10	1.39	69.26	76.96	69.17	76.57
	CP-2	5	77.65 <sup>a</sup>	3.37	1.51	73.46	81.83	74.21	83.11
	CP-3	5	69.84 <sup>a</sup>	4.82	2.15	63.86	75.82	64.68	74.62
	CP-4	5	76.46 <sup>a</sup>	7.84	3.51	66.71	86.20	62.70	81.65
	C	5	58.27 <sup>b</sup>	1.75	0.78	56.10	60.44	55.72	60.23
22,5° to the face grain	CP-1	5	68.66 <sup>a</sup>	1.81	0.81	66.40	70.91	66.66	71.48
	CP-2	5	73.19 <sup>b</sup>	0.64	0.29	72.40	73.99	72.49	74.20
	CP-3	5	64.64 <sup>c</sup>	0.89	0.40	63.53	65.75	63.53	65.90
	CP-4	5	70.01 <sup>a,b</sup>	1.86	0.83	67.70	72.32	67.73	72.19
	C	5	52.39 <sup>d</sup>	2.62	1.17	49.15	55.64	48.56	54.44
45° to the face grain	CP-1	5	58.93 <sup>a,b</sup>	1.27	0.57	57.36	60.50	57.10	60.62
	CP-2	5	64.71 <sup>c</sup>	3.83	1.71	59.96	69.47	59.05	68.91
	CP-3	5	56.36 <sup>a</sup>	0.88	0.39	55.27	57.45	55.41	57.43
	CP-4	5	61.86 <sup>b,c</sup>	1.19	0.53	60.38	63.34	60.61	63.38
	C	5	48.06 <sup>d</sup>	2.01	0.90	45.57	50.56	45.02	49.86
67,5° to the face grain	CP-1	5	66.54 <sup>a</sup>	1.37	0.61	64.84	68.25	65.17	68.80
	CP-2	5	72.41 <sup>b</sup>	1.38	0.62	70.70	74.12	70.33	73.88
	CP-3	5	62.65 <sup>c</sup>	0.89	0.40	61.54	63.75	61.16	63.53
	CP-4	5	68.82 <sup>a</sup>	1.45	0.65	67.02	70.62	66.57	70.14
	C	5	53.46 <sup>d</sup>	1.65	0.74	51.42	55.51	51.24	55.82

\*The mean values with the same letters are not significantly different at 0.05 probability level

The analysis of variance of the obtained data for compressive strength parallel to the face grain (ANOVA:  $F(4, 20) = 13,26$ ;  $p = 0,001$ ) showed that the differences between the mean values of this property of at least two plywood models are statistically significant. The conducted post-hoc Tukey's test for multiple comparison between models showed that there are statistically significant differences in the mean values of compressive strength parallel to the face grain between the control model and all reinforced models. Within the reinforced models, there are no statistically significant differences between models CP-1, CP-3 and CP-4 where the differences are small and do not exceed 2,93 N/mm<sup>2</sup>. The differences between the values of models CP-2 and CP-4 are also not statistically significant.

Compared to the values of compressive strength parallel to the face in models CP-1, CP-2 and CP-3, the highest value of this property obtained in model CP-2 is higher for 12,3 %, 14,7 % and 9,9 %, respectively.

Regarding the compressive strength perpendicular to the face grain, the analysis of the variance (ANOVA:  $F(4, 20) = 13,886$ ;  $p = 0,001$ ) and post-hoc Tukey's test showed that there is statistically significant differences between the value of the control model and values of all reinforced models. The differences within the reinforced models are not statistically significant, which shows that position of the cotton prepreg reinforcement does not have significant impact on the values of compressive strength perpendicular to the face grain of the panel.

Compared to the highest obtained value in model CP-2, the values of models CP-1, CP-3 and CP-4 are lower for 5,8 %, 10,1 % and 1,5 %, respectively.

The analysis of the obtained results for compressive strength at the angle of  $22,5^\circ$  to the face grain showed that the position of the multilayer reinforcements in plywood structure (models CP-1, CP-2 and CP-3) has significant impact on the values of compressive strength in this direction of the panel (ANOVA:  $F(4, 20) = 110,57$ ;  $p = 0,001$ ). The lowest value is achieved when the reinforcements are positioned as surface layers of plywood. The values between model CP-4 and CP-1, as well as between CP-4 and CP-2 are not statistically significant. The values of all reinforced models statistically differ from the value of the control model without reinforcements.

Results from the tests of compressive strength at the angle of  $45^\circ$  to the face grain of plywood also showed that all reinforced models have higher values of this property compared to the control model C. The differences in the values of all reinforced models and control model are statistically significant (ANOVA:  $F(4, 20) = 45,118$ ;  $p = 0,001$ ). Within the reinforced models, the highest value achieved in model CP-2 is higher for 9,8 %, 14,8 % and 4,6 % compared to models CP-1, CP-3 and CP-4, respectively.

At the angle of  $67,5^\circ$  to the face grain of plywood, the mean values of models CP-1, CP-3 and CP-4 are lower for 8,1 %, 13,5 % and 5 %, respectively, compared to the highest obtained value in model CP-2. The analysis of the variance (ANOVA:  $F(4, 20) = 262,863$ ;  $p = 0,001$ ) and post hoc test showed that the values of all reinforced models statistically differ from the value of the control model. Within the reinforced models, the value of model CP-2 statistically differs from the values of other three models.

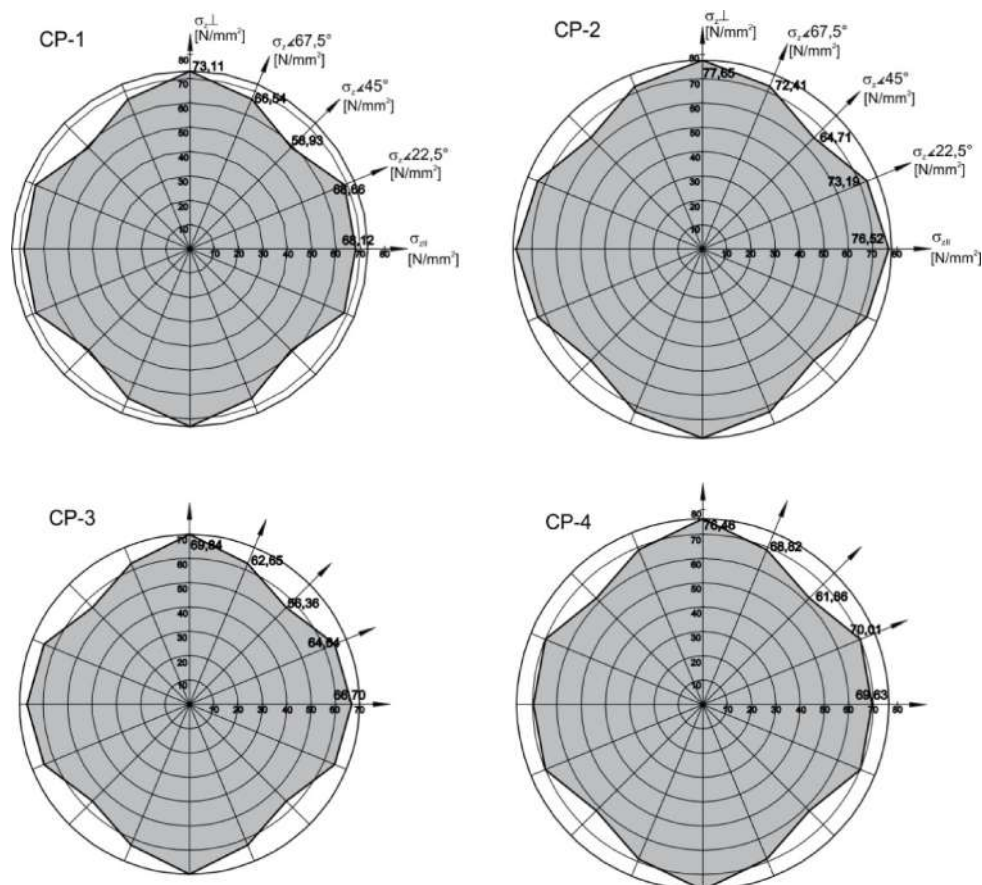


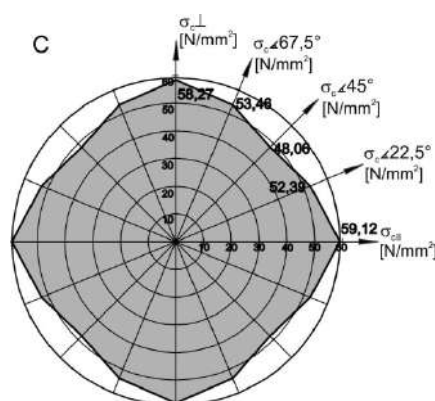
Figure 2: Polar diagrams of compressive strength of plywood reinforced with cotton prepreps



In all reinforced plywood models the highest value of compressive strength is achieved in direction perpendicular to the face grain, while the lowest value is achieved at the angle of 45° to the face grain of plywood. The biggest difference between the values of compressive strength parallel and perpendicular to the face grain is achieved in model CP-4 ( $\sigma_{\perp} > \sigma_{\parallel}$  for 9,8 %). In other models, the difference between these values is smaller i.e., in models CP-1, CP-2 and CP-3, the mean value of compressive strength perpendicular to the face grain is higher compared to the mean value of compressive strength parallel to the face grain for 7,3 %, 1,5 % and 4,7 %, respectively.

The mean value of compressive strength at the angle of 45° to the face grain is lower compared to the value of compressive strength perpendicular to the face grain of plywood for 19,4 % in model CP-1, for 16,7 % in model CP-2, for 19,3 % in model CP-3 and for 19,1 % in model CP-4.

The values of compressive strength at the angle of 22,5° and 67,5° are similar to each other, where the value of compressive strength at the angle of 22,5° are higher compared to the values of compressive strength at the angle of 67,5° for 3,2 % in model CP-1, 1 % in model CP-2, 3,2 % in model CP-3 and 1,7 % in model CP-4.

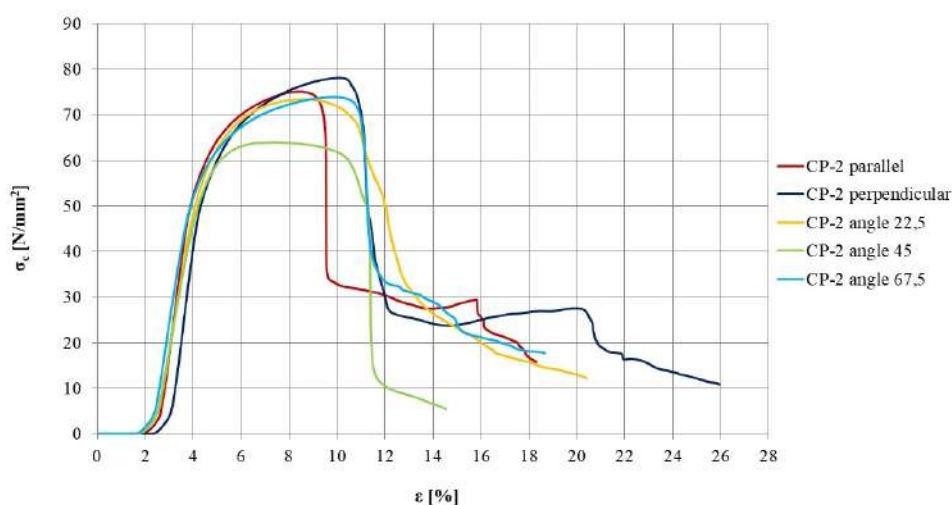


**Figure 3:** Polar diagram of compressive strength of control model of plywood without reinforcements

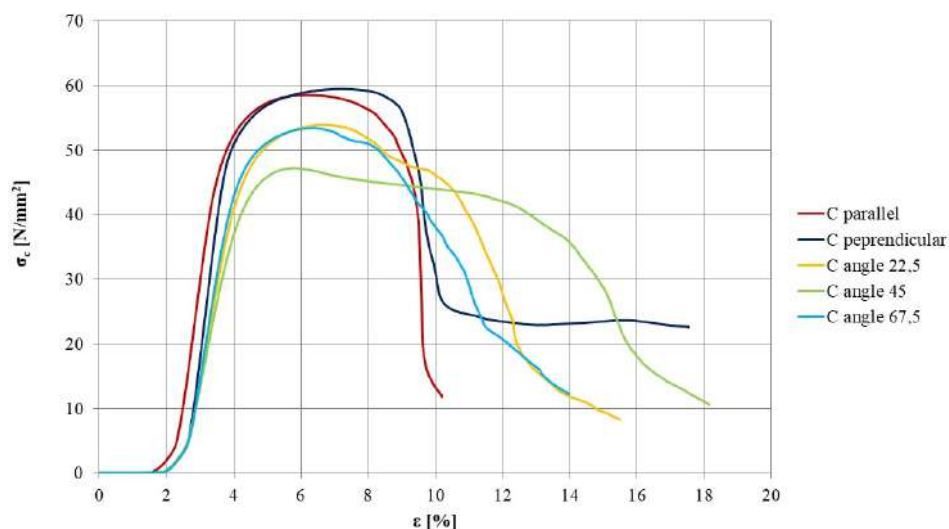
In the control model of plywood without reinforcements the difference between the values of compressive strength parallel and perpendicular to the face grain is very small and it is 1,5 % ( $\sigma_{\parallel} > \sigma_{\perp}$ ). Compared to the mean value of compressive strength parallel to the face grain, the values of this property at the angle of 22,5°, 45° and 67,5° are lower for 11,4 %, 18,7 % and 9,6 %, respectively.

On figures 4 and 5 are presented the stress-strain diagrams during testing compressive strength for model CP-2 and the control model C. The stress-strain diagrams for other reinforced models are similar to those for model CP-2.

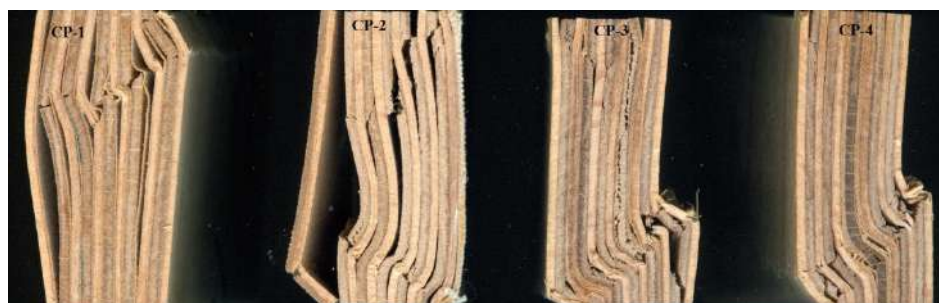
The analysis of the stress-strain diagrams of experimental plywood models showed that the failure of the material happens after pronounced plastic deformations.



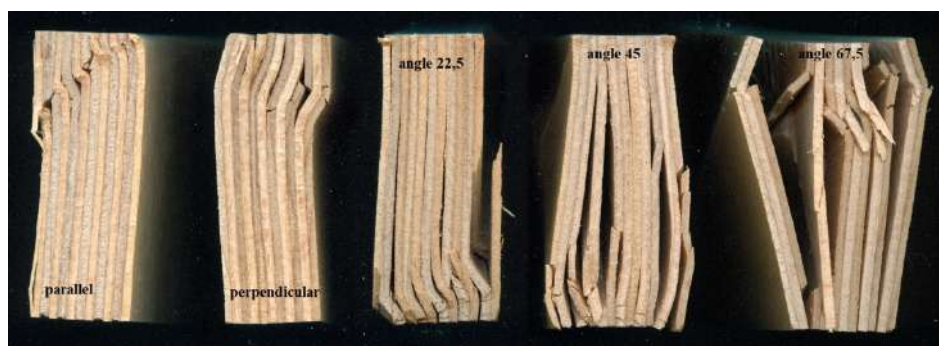
**Figure 4:** Stress-strain diagram during testing compressive strength of model CP-2



**Figure 5:** Stress-strain diagram during testing compressive strength of the control model C



**Figure 6:** Failure mode of the test specimens of reinforced models during testing the compressive strength parallel to the face grain



**Figure 7:** Failure mode of the test specimens of control model during testing the compressive strength

All experimental plywood models in all tested direction, exceed the minimal value of compressive strength defined in the national standard D.C5.043 for load-bearing panels for use in construction.

#### 4. CONCLUSIONS

The application of cotton prepreg in the structure of plywood significantly increases its compressive strength in all tested directions.

Application of cotton prepreg sheets as reinforcement of plywood structure lead to increasing of compressive strength up to 29 % in direction parallel to the face grain, up to 33 % perpendicular to the face grain, up to 40 % at the angle of 22,5° to the face grain and up to 35 % at the angle of 45° and 67,5° to the face grain.

Different positioning of the cotton prepreg reinforcements in the plywood structure has impact on the plywood compressive strength in all panel directions.

Regarding the reinforcement position, the best results are achieved with application of multilayered cotton prepreg inserted in the third and in the eight adhesive layer of plywood (model CP-2). Moving the reinforcement layers to the surface of the plywood decreases the values of plywood compressive strength.

## REFERENCES

- [1] Biblis, J.; Carino, H.F., 2000: Flexural properties of southern pine plywood overlaid with fiberglass-reinforced plastic. *Forest Prod J.*, 50 (1): 34-36.
- [2] Brezovi, M.; Jambrekovi, V.; Pervan, S., 2003: Bending properties of carbon fiber reinforced plywood. *Wood Research*, 48 (4): 13-24.
- [3] Brezovi, M.; Kljak, J.; Pervan, S.; Antonovi, A., 2010: Utjecaj kuta orientacije sintetskih vlakana na svojstva kompozitne furnirske ploče. *Drvna ind.*, 61 (4): 239-243.
- [4] Choi, S.W.; Rho, W.J.; Son, K.J.; Lee, W.I., 2011: Analysis of buckling load of fiber-reinforced plywood plates for NO 96 CCS. *Proceedings of the Twenty-first International Offshore and Polar Engineering Conference, 2011, Maui, Hawaii, USA*, pp: 79-83.
- [5] Hardeo, P.; Karunasena, W., 2003: Buckling of fiber-reinforced plywood plates. *Proceedings of Second International Conference on Structural Stability and Dynamics, 2002, Singapore*, pp. 442-447. [https://doi.org/10.1142/9789812776228\\_0062](https://doi.org/10.1142/9789812776228_0062).
- [6] Hrázský, J.; Král, P., 2007: A Contribution to the properties of combined plywood materials. *J For Sci*, 53 (10): 483-490. <https://doi.org/10.17221/2087-jfs>.
- [7] Jakimovska Popovska, V., Iliev, B. 2019: Bending Properties of Reinforced Plywood with Fiberglass Pre-Impregnated Fabrics, *Proceedings of 30<sup>th</sup> International Conference on Wood Science and Technology-ICWST and 70<sup>th</sup> anniversary of Drvna industrija Journal “Implementation of wood science in woodworking sector”, 12<sup>th</sup> -13<sup>th</sup> December, Zagreb, 2019: 77-85.*
- [8] Jakimovska Popovska, V., Iliev, B. 2021. Janka hardness of plywood reinforced with pre-impregnated cotton fabrics, *Proceedings of the 5<sup>th</sup> International conference „Wood technology and product design“, 14-17<sup>th</sup> September, Ohrid, 2021: 7-14.*
- [9] Kohl, D.; Million, M.; Böhm, S., 2013: Adhesive bonded wood-textile-compounds as potentially new eco-friendly and sustainable high-tech materials. *Proceedings of the Annual Meeting of the Adhesion Society 2013, Florida, USA*, pp: 27-29.
- [10] Maniš, M.; Žuke, S., 2011: Textile fabrics reinforced plywood with enhanced mechanical properties. *Abstracts of the International Scientific Conference „Civil Engineering’11”, 2011, Latvia*, pp: 35.
- [11] Macedonian standards.
- [12] Rowlands, R.E.; Van Deweghe, R.P.; Launferbeg, T.L.; Krueger, G.P., 1986: Fiber-reinforced wood composites. *Wood and Fiber Science*, 18 (1): 39-57.
- [13] Xu, H.; Tanaka, C.; Nakao, T.; Nisano Y.; Katayama, H., 1996: Flexural and shear properties of fiber reinforced plywood. *Mokuzai Gakkaishi*, 42: 376-382.
- [14] Xu, H., Nakao, T., Tanaka, C., Yoshinobu, M., Katayama, H., 1998: Effects of fiber length orientation on elasticity of fiber-reinforced plywood. *Journal of Wood Science*, (44): 343-347. <https://doi.org/10.1007/bf01130445>
- [15] Žuke S.; Kalniš K., 2011: Enhanced impact properties of plywood. *Proceedings of the 3rd International Conference Civil Engineering’11, 2011, Latvia*, pp: 125-130.

## BENDING STRENGTH AND MODULUS OF ELASTICITY IN BENDING OF BEECH AND BLACK PINE PLYWOOD

Violeta Jakimovska Popovska<sup>1</sup>, Borche Iliev<sup>1</sup>

<sup>1</sup> Ss. Cyril and Methodius University in Skopje, R. of North Macedonia,  
Faculty of design and technologies of furniture and interior-Skopje  
e-mail: jakimovska@fdtme.ukim.edu.mk; iliev@fdtme.ukim.edu.mk

### ABSTRACT

The research presented in this paper includes the study of bending properties of plywood made from beech and black pine veneers. For this purpose, four experimental plywood models were made. Two of the models were made from peeled beech veneers and other two models were made from peeled black pine veneers. Water-soluble phenol-formaldehyde resin was used as plywood binder.

The bending strength and modulus of elasticity in bending of the experimental plywood were tested in two directions, parallel and perpendicular to the face grain. According to the values of bending strength and modulus of elasticity in bending, plywood models can be used for structural application in construction. Production of plywood with different number of veneers in panel structure, as well as plywood with the same number of the veneers but from different wood specie, gives opportunities for production of panels that can meet different application requirements.

**Keywords:** plywood, veneer, beech, black pine, phenol-formaldehyde resin, bending strength, modulus of elasticity in bending

### 1. INTRODUCTION

The performance of wood composite materials is characterized by wide range of engineering properties. Mechanical properties are mostly used to evaluate wood-based composites for structural and nonstructural applications. Elastic and strength properties are the primary criteria to select materials or to establish design or product specifications (Cai and Ross 2010).

Plywood panels have significant bending strength in both length and width direction of the panel, whereas the differences in strength and stiffness along the length of the panel versus across of the panel are smaller compared to those one in solid wood (Stark et al. 2010). Bending properties of plywood are important for their adequate use in construction as structural panels. Plywood panels are exposed to bending load in numerous applications, such as floor constructions in buildings, floors of vehicles, formwork etc. Bending strength can be affected by using veneers produced from various wood species, by various thicknesses of veneers and direction of fibers (Hrásk and Král, 2006).

Research on technical characteristics, including bending properties of plywood made from veneers from several wood species in different combinations was conducted by Örs et al. (2002). Research on plywood bending strength and modulus of elasticity in bending in relation to their structure was carried out by Hrásk and Král (2005). Trough combining the veneers with different thickness, plywood with adequate characteristic for its application can be obtained (Hrásk and Král, 2006).

Change of the position of the layers in the structure of the plywood panel around the central axis, without changing the number and the thickness of the veneers provide different strength characteristics of plywood that are important for their application (Jakimovska Popovska, 2011). Study of flexural properties of plywood made from different wood species was carried out by Vasileiou et al. (2011), as well as by Bal and Bekta (2014).

The aim of the research presented in this paper is to determine the bending strength and modulus of elasticity in bending of seven-layer and nine-layer plywood panels made from beech and black pine veneers.

## 2. EXPERIMENTAL METHODS

For the realization of the research four experimental plywood models were made. Two of the models were made as seven-layer plywood, while the other two as nine-layer plywood. Peeled beech and black pine veneers with thickness of 1,5; 2,2 and 3,2 mm were used for plywood manufacturing. The seven-layer plywood models were made with two veneer sheets with thickness of 1,5 mm, two veneer sheets with thickness of 2,2 mm and three veneer sheets with thickness of 3,2 mm. The nine-layer plywood models were made with the same number of veneers with thickness of 1,5 and 3,2 mm and four veneer sheets with thickness of 2,2 mm.

The orientation of adjacent layers in plywood structure is at right angle, whereas in all models, the grain direction of the surface layers is parallel to the longitudinal axis of the panel. The central layer of each model represents a veneer sheet with thickness of 3,2 mm, oriented perpendicular to the face grain of the seven-layer plywood panel and parallel to the face grain of the nine-layer plywood panels.

In all models the veneers with thickness of 1,5 mm represent the surface layers of the panel. The compositions of the experimental plywood models are shown on figure 1.

Water-soluble phenol-formaldehyde resin with concentration of 48 % was used as plywood binder.

Wheat flour was used as filler and 20 % solution of NaOH as catalyst. The binder was applied in quantity of 180 g/m<sup>2</sup> on both sides of the veneers with thickness of 3,2 mm in seven-layer models and on the veneers with thickness of 2,2 mm in nine-layer models.

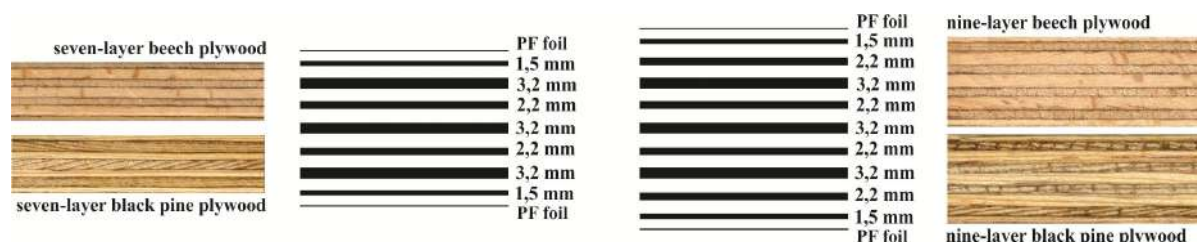
The plywood compositions were pressed in a hot press under specific pressure of 15 kg/cm<sup>2</sup> at temperature of 155° for time of 20 minutes for seven-layer models and 25 minutes for nine-layer models.

The panels were overlaid with phenol-formaldehyde resin impregnated paper that was bonded during the hot pressing process. Plywood overlaying with this paper is made in order to improve the water resistance of plywood, having in consideration the fact that these plywood panels are intended for application in construction where can be exposed to high humidity conditions.

The plywood models were made with dimensions of 540×540 mm<sup>2</sup>. The moisture content of the panels was 10 %.

According to this methodology four models of plywood were made:

- model B7: seven-layer plywood made with beech peeled veneers (panel thickness of 15 mm; density of 751,90 kg/m<sup>3</sup>);
- model B9: nine-layer plywood made with beech veneers (panel thickness of 19 mm; density of 758,38 kg/m<sup>3</sup>);
- model BP7: seven-layer plywood made with black pine veneers (panel thickness of 13 mm; density of 758,72 kg/m<sup>3</sup>);
- model BP9: nine-layer plywood made with black pine veneers (panel thickness of 16 mm; density of 760,55 kg/m<sup>3</sup>).



**Figure 1:** Composition of the experimental seven-layer and nine-layer plywood models

The bending strength and modulus of elasticity in bending of experimental plywood were tested according to EN 310. These properties were tested in two directions, i.e., parallel and perpendicular to the face grain of the plywood panel.

The obtained data were statistically analyzed. One way ANOVA was used to determinate the significance of the effect of type and number of the veneers in plywood composition on the bending properties of the plywood panels. Shapiro-Wilk test for normality of the obtained data was applied and Levene's test for homogeneity of variances was applied. Tukey's test was applied to evaluate the

statistical significance between mean values of the properties of different plywood models. Statistical software SPSS Statistic was used for statistical analysis of the obtained data.

### 3. RESULTS AND DISCUSSION

The test results for the bending strength and modulus of elasticity in bending of plywood panel are shown in tables 1 and 2.

*Table 1: Statistical data for bending strength of experimental plywood*

Bending strength	Model	N	Mean [N/mm <sup>2</sup> ]	Min [N/mm <sup>2</sup> ]	Max [N/mm <sup>2</sup> ]	95% Confidence Interval for Mean		Std. Dev. [N/mm <sup>2</sup> ]	Std. Error [N/mm <sup>2</sup> ]
						Lower Bound	Upper Bound		
Paralell to the face grain	B7	6	96,12 <sup>a</sup>	84,82	104,02	87,74	104,50	7,98	3,26
	B9	6	123,54 <sup>b</sup>	120,02	128,85	119,99	127,10	3,39	1,38
	BP7	6	92,51 <sup>a</sup>	81,02	102,27	84,65	100,36	7,49	3,06
	BP9	6	98,55 <sup>a</sup>	85,01	108,53	89,11	107,99	9,00	3,67
Perpendicular to the face grain	B7	6	89,63 <sup>a</sup>	78,43	100,82	78,43	100,82	10,67	4,36
	B9	6	64,92 <sup>b</sup>	59,59	70,24	59,59	70,24	5,08	2,07
	BP7	6	97,59 <sup>a</sup>	95,42	99,76	95,42	99,76	2,07	0,84
	BP9	6	66,28 <sup>b</sup>	62,83	69,72	62,83	69,72	3,28	1,34

The mean values with the same letters are not significantly different at 0,05 probability level

The highest value of bending strength parallel to the face grain of plywood is achieved in nine-layer model of plywood made with beech veneers (model B9). Compared to other plywood models, this model has higher mean value of this property up to 33,54 %. Nine-layer plywood models made with beech and black pine veneers (B9 and BP9) have higher values compared to the seven-layer plywood models (B7 and BP7).

In cross-grain direction, the highest value of bending strength is achieved in seven-layer model of plywood made with black pine veneers (model BP7). Compared to other plywood models, this model has higher mean value of this property up to 50,32 %. Seven-layer plywood models made with beech and black pine veneers (B7 and BP7) have higher values compared to the nine-layer plywood models (B9 and BP9).

The higher values of bending strength parallel to the face grain of nine-layer plywood models compared to the seven-layer models are attributed to the orientation of the veneers in plywood composition regarding the span of the loaded panel. In these two models (B9 and BP9) a bigger percentage of plywood thickness is occupied by the veneers oriented parallel to the span (parallel to the length of the test specimen) which contribute in higher values of bending strength, compared to the seven-layer models, where the bigger percentage of plywood thickness is occupied by the veneers oriented perpendicular to the span of the loaded panel. According to the so-called “Parallel ply theory”, veneers with grain direction parallel to the span, carry all of the bending from the applied load to the supports, while the veneers with grain direction perpendicular to the span are assumed not to contribute to the strength (EWPAA, 2009).

For the same reason, the values of bending strength in cross-grain direction of seven-layer plywood models are higher compared to the nine-layer models in which bigger percentage of plywood thickness is occupied by the veneers oriented perpendicular to the span of the loaded panel.

The analysis of variance of the obtained data for bending strength parallel to the face grain (ANOVA:  $F(3; 20) = 22,58$ ;  $p = 0,001$ ) and perpendicular to the face grain of plywood (ANOVA:  $F(3;20) = 42,29$ ;  $p = 0,001$ ) showed that the differences between the mean value of this properties of at least two models are statistically significant. The conducted post-hoc Tukey’s test for multiple comparison between models showed that there are statistically significant differences in the mean value of bending strength parallel to the face grain of model B9 and all other models. The values of bending strength parallel to the face grain of models B7, BP7 and BP9 are in similar limits, whereas the differences between them are not statistically significant.

The post-hoc Tukey's test for bending strength perpendicular to the face grain showed that there are statistically significant differences in the mean values of this property between seven-layer and nine-layer plywood models from the two types of veneers (beech and black pine). The differences in the values between model B7 and BP7, as well as between model B9 and BP9 are not statistically significant, which means that when plywood is made with the same number of veneers, the type of veneer (beech or black pine) used for plywood production does not cause significant differences in the value of bending strength perpendicular to the face grain of plywood.

**Table 2: Statistical data for modulus of elasticity in bending of experimental plywood**

Modulus of elasticity in bending	Model	N	Mean	Min	Max	95% Confidence Interval for Mean		Std. Dev.	Std. Error
			[N/mm <sup>2</sup> ]	[N/mm <sup>2</sup> ]	[N/mm <sup>2</sup> ]	Lower Bound	Upper Bound	[N/mm <sup>2</sup> ]	[N/mm <sup>2</sup> ]
Paralell to the face grain	B7	6	19137,93 <sup>a</sup>	16134,67	21917,62	16791,25	21484,61	2236,13	912,90
	B9	6	22266,10 <sup>b</sup>	19743,58	24685,70	20152,63	24379,57	2013,91	822,17
	BP7	6	16461,46 <sup>a,c</sup>	14698,44	18500,00	14720,55	18202,37	1658,90	677,24
	BP9	6	15032,55 <sup>c</sup>	14306,57	16063,45	14196,07	15869,02	797,07	325,40
Perpendicular to the face grain	B7	6	18221,68 <sup>a</sup>	14527,94	20787,86	15706,48	20736,89	2396,72	978,46
	B9	6	11240,16 <sup>b</sup>	10077,54	11906,46	10538,70	11941,62	668,42	272,88
	BP7	6	10997,81 <sup>b</sup>	9853,16	12914,96	9695,38	12300,25	1241,08	506,67
	BP9	6	11917,81 <sup>b</sup>	10162,64	13262,62	10614,53	13221,09	1241,89	507,00

The mean values with the same letters are not significantly different at 0,05 probability level

The highest mean value of modulus of elasticity in bending parallel to the face grain of plywood is achieved in nine-layer beech plywood model (B9). Plywood models made from beech veneers (B7 and B9) have higher mean values of this property compared to plywood made from black pine veneers (models BP7 and BP9). Model B9 has higher value of modulus of elasticity in bending parallel to the face grain for 48,12 % compared to nine-layer black pine plywood (model BP9), while the seven-layer beech plywood has higher value for 16,26 % compared to the seven-layer black pine plywood.

The analysis of variance of the obtained data for the modulus of elasticity in bending parallel to the face grain of plywood (ANOVA:  $F(3; 20) = 19,587$ ;  $p = 0,001$ ) showed that the differences between the mean value of this property of at least two models are statistically significant. The conducted post-hoc Tukey's test for multiple comparison between models showed that there are statistically significant differences between nine-layer beech plywood (model B9) and all other plywood models, which means that the number and the type of the veneers have significant impact on the values of this property.

The highest mean value of modulus of elasticity in bending in cross-grain direction is achieved in seven-layer beech plywood (model B7) and this value is higher for 62,11 %, 65,68 % and 52,89 % compared to nine-layer beech plywood (model B9), seven-layer black pine plywood (model BP7) and nine-layer black pine plywood (model BP9), respectively. The analysis of variance of the obtained data and post-hoc Tukey's test (ANOVA:  $F(3;20) = 30,631$ ;  $p = 0,000$ ) showed that there are statistically significant differences in the mean values of this property between model B7 and all other plywood models. The values of modulus of elasticity in bending in cross-grain direction of models B9, BP7 and BP9 are in similar limits, whereas the differences between them are not statistically significant.

The differences in the values of bending strength in both panel's directions in seven-layer plywood models (B7 and BP7) are smaller compared to the nine-layer models. Nine-layer plywood have significantly lower values of bending strength perpendicular to the face grain compared to the values obtained when the panels are stressed parallel to the grain direction. The reason for this is the percentage of the panel thickness occupied by the veneers that run parallel to the span of the loaded panel. When plywood panels are stressed parallel to the face grain, 44,83 % of the thickness of seven-layer plywood models is occupied by the veneers that run parallel to the span, while when panels are stressed in cross-grain direction, 55,2 % of the panel thickness is occupied by parallel veneers. In nine-layer plywood models, the differences in the percentage of plywood thickness that is occupied by the veneers that run parallel to the span when panels are stressed parallel and in cross-grain direction is bigger than in seven-layer models. Nine-layer models have 58,8 % of the panel thickness occupied by

parallel veneers when the panels are stressed parallel to the face grain and 41,12 % of the panels thickness occupied by parallel veneers when plywood are stressed in cross-grain direction.

The failure mode of the test specimens of experimental plywood models is shown on figure 2. During the testing of bending strength the failure of the specimens happened at once, which justified the assumption that plywood material can be considered elastic up to failure.



**Figure 2:** Failure mode of the test specimens of the experimental panels

The obtained values of bending strength and modulus of elasticity in bending of the experimental plywood are within the limits of the values for these properties listed in available literature. Iliev (2000) for bending strength parallel to the face grain gives a value of 84,25 N/mm<sup>2</sup> for seven-layer and 96,51 N/mm<sup>2</sup> for nine-layer beech plywood. The same author for seven-layer and nine-layer black pine plywood gives the values of 85,21 N/mm<sup>2</sup> and 86,22 N/mm<sup>2</sup> respectively. Hrásk and Král (2005) give the values of 75,81 N/mm<sup>2</sup> for bending strength and 18456 N/mm<sup>2</sup> for modulus of elasticity in bending parallel to the face grain of nine-layer beech plywood and the values of 55,68 N/mm<sup>2</sup> and 9775 N/mm<sup>2</sup> in cross-grain direction. The same authors for eleven and thirteen-layer beech plywood give the values of 86,74 and 78,07 N/mm<sup>2</sup> for bending strength and 21969 and 21015 N/mm<sup>2</sup> for modulus of elasticity in bending parallel to the face grain of the plywood panels. In cross-grain direction, the same authors give the values of 70,71 and 65,62 N/mm<sup>2</sup> for bending strength and 14053 and 13774 N/mm<sup>2</sup> for modulus of elasticity in bending of eleven and thirteen-layer beech plywood, respectively. Kljak et al. (2006) give the values of 92,35 and 9924,29 N/mm<sup>2</sup> for bending strength and modulus of elasticity in bending parallel to the face grain of multi-ply beech plywood and the values of 89,45 and 9333,31 N/mm<sup>2</sup> for bending strength and modulus of elasticity in bending perpendicular to the face grain. Hrásk and Král (2006) give the values in the range from 85,32 to 109,83 N/mm<sup>2</sup> for bending strength parallel to the face grain of seven-layer beech plywood panels and from 49,83 to 61,21 N/mm<sup>2</sup> for bending strength in cross-grain direction. For the same plywood panels, the authors give the values in the limits of 8139,34 to 9695,86 N/mm<sup>2</sup> for the modulus of elasticity in bending parallel to the face grain and from 3970,18 to 4870,09 N/mm<sup>2</sup> for the modulus of elasticity in cross-grain direction. Dieste et al. (2008) for bending strength and modulus of elasticity in bending parallel to the face grain of five-layer beech plywood give the values of 87,46 and 10000 N/mm<sup>2</sup> respectively. The same authors for bending strength and modulus of elasticity in bending in cross grain direction give the values of 50 N/mm<sup>2</sup> and 3000 N/mm<sup>2</sup> respectively. Jakimovska Popovska (2011) gives the values within the limits of 64,16 N/mm<sup>2</sup> to 99,71 N/mm<sup>2</sup> and in the limits of 6405,22 N/mm<sup>2</sup> to 10157,91 N/mm<sup>2</sup> for bending strength and modulus of elasticity in bending parallel to the face grain of nine-layer beech plywood. The same author for bending strength and modulus of elasticity in bending in cross-grain direction gives the values in the limits of 43,79 N/mm<sup>2</sup> to 83,87 N/mm<sup>2</sup> for bending strength and from 3368,25 N/mm<sup>2</sup> to 8028,55 N/mm<sup>2</sup> for the modulus of elasticity. For five-layer beech plywood Bal and Bekta (2014) give the values of 80,2 N/mm<sup>2</sup> and 8258 N/mm<sup>2</sup> for bending strength and modulus of elasticity in bending parallel to the face grain and 39,4 N/mm<sup>2</sup> and 2640 N/mm<sup>2</sup> for bending strength and modulus of elasticity in bending in cross-grain direction. Zdravkovi et al. (2014) give the values of 89,87 N/mm<sup>2</sup> and 66,18 N/mm<sup>2</sup> for bending strength parallel and perpendicular to the face grain of nine-layer beech plywood.

According to the obtained data for bending strength and modulus of elasticity in bending and related to the requirements of the standard EN 636, plywood models can be classified as follows:



seven-layer beech plywood model (B7) as class F60/50 E140/140, nine-layer beech plywood model (B9) as class F80/40 E140/100, seven-layer black pine plywood model (BP7) as class F60/60 E140/100 and nine-layer black pine plywood model (BP9) as class F60/40 E140/100.

#### 4. CONCLUSIONS

On the basis of the conducted research it can be concluded that different number of the veneers and different veneer specie used in plywood structure has significant impact on plywood bending properties.

The highest value of bending strength and modulus of elasticity in bending parallel to the face grain is achieved in nine-layer beech plywood.

Nine-layer plywood models have higher values of bending strength parallel to the face grain compared to the seven-layer models, which is a result of a bigger percentage of plywood thickness that is occupied by the veneers oriented parallel to the span of the loaded panel.

The orientation of the veneers regarding the span of the loaded panel also is a reason for higher values of bending strength perpendicular to the face grain of seven-layer plywood models compared to the nine-layer models.

Veneer specie (beech or black pine) used for plywood production does not cause significant differences in the value of bending strength perpendicular to the face grain of plywood, when plywood is made with the same number of veneers.

The production of plywood with different number of veneers in panel structure, as well as plywood with the same number of the veneers but from different wood specie, gives opportunities for production of panels that can meet the different application requirements. The choice of particular plywood configuration will depends on the application area, i.e., the type of loads on which the panel is exposed during the exploitation period.

#### REFERENCES

- [1] Bal, B.C., Bekta , . 2014: Some mechanical properties of plywood produced from eucalyptus, beech and poplar veneers. *Maderas. Ciencia y tecnologia* 16 (1): 99-108.
- [2] Cai, Z.; Ross, R.J. 2010: Wood handbook - Wood as engineering material, Chapter 12: Mechanical properties of wood-based composite materials. USDA, Forest Product Laboratory, General Technical Report-190: 12-1 - 12-12.
- [3] Dieste, A.; Krause, A.; Bollmus, S.; Militz, H. 2008: Physical and Mechanical Properties of Plywood Produced with 1,3-dimethylol-4,5-dihydroxyethyleneurea (DMDHEU)-Modified Veneers of *Betula sp.* and *Fagus sylvatica*. *Holz Roh Werkst* 66: 281–287.
- [4] EN 310. Wood-based panels - Determination of modulus of elasticity in bending and bending strength.
- [5] EN 636. Plywood - Specifications.
- [6] EWPA-Engineered Wood Products Association of Australasia. 2009: Structural plywood & LVL design manual, <http://www.ewp.asn.au>.
- [7] Hrázský, J.; Král, P. 2005: Assessing the bending strength and modulus of elasticity in bending of exterior foiled plywoods in relation to their construction. *J For Sci* 51(2):77–94.
- [8] Hrázský, J.; Král, P. 2006: Effects of the Thickness of Rotary-Cut Veneers on Properties of Plywood Sheets. Part 2. Physical and Mechanical Properties of Plywood Materials. *Journal of Forest Science* 52 (3): 118-129.
- [9] Iliev, B. 2000. Comparative researches between water resistant combined wood based panels and water resistant multilayer plywood. Doctoral dissertation, Skopje.
- [10] Jakimovska Popovska, V. 2011: Comparative researches of the properties of laboratory plywood and some industrial manufactured wood-based panels. Master thesis. Skopje.
- [11] Kljak, J.; Brezovic, M.; Jambrekov, V. 2006: Plywood stress optimization using the finite element method. *Wood Research* 51 (1): 1-10.
- [12] Örs, Y.; Çolako lu, G.; Aydin, .; Çolak, S. 2002: Comparison of some technical properties of plywood produced from beech, okume and poplar rotary cut veneers in different combinations. *Journal of Polytechnic* 5 (3): 257-265.

- [13] Stark, N.M.; Cai, Z.; Carll, C. 2010: Wood handbook - Wood as engineering material, Chapter 11: Wood-based composite materials. USDA, Forest Product Laboratory, General Technical Report-190: 11-1 - 11-28.
- [14] Vasileiou, V.; Barboutis, I.; Kamperidou, V. 2011: Properties of thin 3-ply plywood constructed with three-of-heaven and poplar wood. Proceeding of the International Conference “Wood Science and Engineering in the Third Millennium” - ICWSE 2011, Brasov, 2011: 323-329.
- [15] Zdravkovi , V.; Lovri , A.; Todorovi , N. 2014: Some characteristics of beech plywood for floors of the city buses. Proceedings of the 10th International Symposium - Research and Design for economy, Belgrade, 2014: 185-191.

## DETERMINATION OF THE HEAT ENERGY FOR HYDROTHERMAL TREATMENT OF ASHWOOD (*Fraxinus excelsior*) BY LOG SOAKING

Ana Marija Stamenkoska, Goran Zlateski

Ss. Cyril and Methodius University in Skopje, North Macedonia,  
Faculty of Design and Technologies of Furniture and Interior-Skopje  
e-mail: stamenkoska@gmail.com; zlateski@fdtme.ukim.edu.mk

### ABSTRACT

The treatment of logs by soaking is a complex technological and thermal procedure, in which logs and prisms are used as raw material for the production of peeled and sliced veneers. Such treatment of logs is carried out in pools or pits constructed in the ground. By log soaking two significant changes to the wood are achieved, its coloring and the inevitable plastification of the wood fibers. During this procedure, the time required for air drying is significantly reduced. The soaking medium is fresh water or previously used water at an elevated temperature. This soaking treatment is particularly suitable for logs for the production of peeled and sliced veneer, from which resin must be removed. Soaking is also used when treating wood species that are sensitive to steaming.

This paper provides an analysis of the thermal energy required for hydrothermal treatment by log soaking of ashwood (*Fraxinus excelsior*). The logs were intended for the production of peeled veneer. The log treatment was done in a reinforced concrete pool built in the ground. The total amount of heat for log soaking ( $Q$ ) consists of effective heat ( $Q_{pv}$ ) and heat loss ( $Q_{zv}$ ). The procedure was conducted by the strong treatment mode, with a temperature interval in the range of 70 to 90 °C. The treated logs had a minimum mean diameter of 35,0 cm and a minimum length of 1,8 m. Log soaking was used as a method for defrosting of the logs, due to their low initial temperature, which was – 15 °C.

**Keywords:** hydrothermal treatment, log soaking, temperature, heat energy, effective heat, heat loss

### 1. INTRODUCTION

Wood thermal treatment implies heating the wood in its raw state, under the influence of a medium. The heating medium is usually saturated water vapor or hot water. The aim of thermal treatment, as a part of the primary processing, is to change the physical, mechanical and aesthetic properties of the wood. The main task of this kind of treatment is to change the heat of the wood, with the smallest increase or decrease of moisture in the wood. The purpose of this technological operation is closely related to technological processes in industrial wood processing. Representative process of the thermal treatment is sawn lumber steaming, with the aim of equalizing the color between the sapwood and heartwood, plastification of the wood for bending and veneer pressing, reducing the internal stresses in the wood and reducing its hygroscopic properties. It is commonly used for veneer and plywood production, as it increases the bonding properties of the wood.

Log soaking is a technological procedure that is carried out with hot water, usually in pools or pits constructed in the ground, made of reinforced concrete and baked bricks in combination with steel sheets. Pools are built in an open or closed space. In an open space, they are structurally covered with a canopy to protect against atmospheric influences (snow, rain, frost). The main purpose of log soaking is the plastification of the wood material, the logs or prisms, for the production of rotary cut and plain sliced veneers. The inevitable plastification of the wood fibers and coloring of the wood is achieved by soaking. Soaking mainly takes place for the purpose of decreasing the time required for the air drying of the wood material (decrease up to three weeks), thus decreasing the cracks occurred from manipulations with the material, and as the wood itself is sanitized, the phytopathological destructors are destroyed.

The soaking medium (water) can be fresh or previously used with an elevated temperature. Because of the resins and fats that are secreted by the wood and absorbed into the water, alkali (sodium) is added for its repeated use. Frozen logs are soaked in fresh water with a moisture content below the saturation point of the wood fibers. Soaking in previously used water, compared to fresh water, takes less time, however, due to the content of acids from the previous round of soaking, a change in the color of the wood occurs. Raw material is best for the purpose of soaking and the process takes place until the established temperature of the wood is higher than the optimal temperature for mechanical processing (example: peeling logs for rotary cut veneers).

Rabadziski and Zlateski (1998) researched the optimal temperature for heating the wood during soaking, for the production of rotary cut veneer from some wood species, and some of the obtained temperatures were: for beech from 40 to 60 °C, birch from 30 to 50 °C, poplar from 30 to 45 °C, larch from 50 to 65 °C and fir/spruce from 40 to 55 °C. The authors provide data on the soaking of beech logs, for the production of rotary cut veneer. In the winter period, according to the mild mode of soaking, the maximum temperature of wood heating was 52 °C, and the minimum temperature was 29 °C. In the summer period, the maximum temperature was 58 °C, and the minimum was 44 °C.

Kolin (2000) gives data for soaking beech prisms for the purpose of production of rotary cut veneer. The data from this author suggests that the plastification time in the summer period is 36 h, at a maximum water temperature of 90 °C.

Beech logs intended for the production of rotary cut veneer, which were treated by soaking at a temperature of 70 °C, showed better peeling properties than logs treated in the same way at a temperature of 20 °C. Logs treated at a temperature of 70 °C result in better adhesion properties of the peeled veneer. (Dupleix *et al.*, 2013)

Log soaking has a direct impact on the quality of veneers and plywood, but the full mechanism behind the improvement of the adhesive properties of plywood cannot be fully understood due to insufficient data regarding this phenomenon. The soaking temperature is the same as the peeling temperature. The peeling of the logs takes place immediately after soaking, because the time required for cooling the logs is more than 12 h, which adversely affects the technological process. The prolonged time of soaking has a direct impact on the chemical composition of the wood. Therefore, it is not known whether the improvement in the adhesive properties of the rotary cut veneers is a result of the softening of the wood fibers due to the previously elevated temperature of the logs from the soaking process, or as a result of the altered chemistry of the wood. (Rohumaa *et al.*, 2016)

Log soaking is carried out according to certain modes, which differ from one another. There are mild and strong modes for log soaking. Mild modes are defined by a temperature interval of 40 to 50 °C. The strong modes are defined by a temperature interval between 70 and 90 °C. By applying these modes, veneers with lighter tones in color are obtained from prisms and logs, which is difficult to achieve by direct and indirect steaming of the sawn lumber. The soaking time of the logs, with the use of strong modes is decreased by about 30 %, compared to the mild modes.

After the plastification of the wood and the process of soaking, the change in the properties of the wood mainly depend on the species, the initial moisture content of the wood, the temperature of the water, as well as the soaking time. As a result of the temperature of the water and the soaking time, changes occur in the physical and mechanical properties of the wood. Most of the changes are desirable and positive, as they improve the properties of the wood, positively influencing the density, color, hygroscopicity, and reduce internal stresses, which results with sawn lumber less prone to cracks. As a result of the subtraction of some substances from the wood, the density decreases in small, insignificant limits. Depending on the wood species, if the wrong mode of soaking is applied, internal stresses usually appear in the final stages of the soaking process, when the raw material is cooled. Hygroscopicity changes with the changes in equilibrium moisture content, caused by kinematic changes of sorption and desorption. The color change is due to the pigments, which materialize in all parts of the wood at a water temperature of 60 °C and above. As a result of the soaking, commonly pentosans of hemicellulose are hydrolyzed, as well as pectins, which transform into a soluble state. These chemical changes result in the creation of phosphoric ( $H_3PO_4$ ), acetic ( $CH_3COOH$ ) and formic ( $CH_2O_2$ ) acid. After soaking, in relation to mechanical processing, the plastic and elastic properties of the wood increase, the rotary cut and plain sliced veneers are characterized with smoother surface, the forces during cutting and peeling processes are reduced, the life of the tool

is extended, the consumption of electricity is reduced and therefore it leads to the increase of the production capacity.

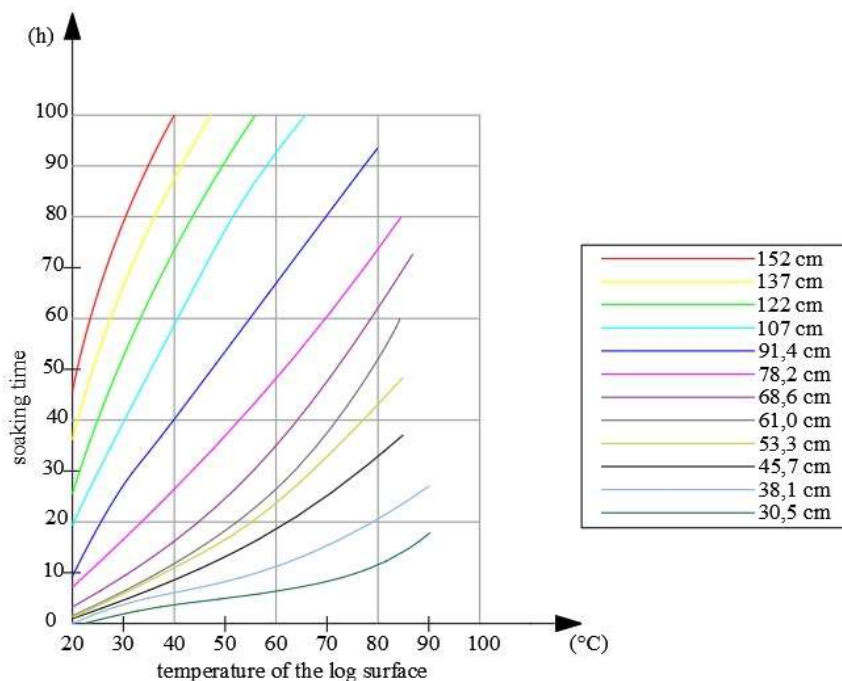
The paper presents methods for determining the amount of heat energy used for wood thermal treatment by soaking of ash logs. The logs are intended for the production of rotary cut veneers. The paper aims to analyze the effective heat, as well as heat loss, to determine the profitability of the technological soaking process. The soaking process is not always a necessity, but it can significantly improve the quality of the wood material.

## 2. MATERIAL AND METHODS

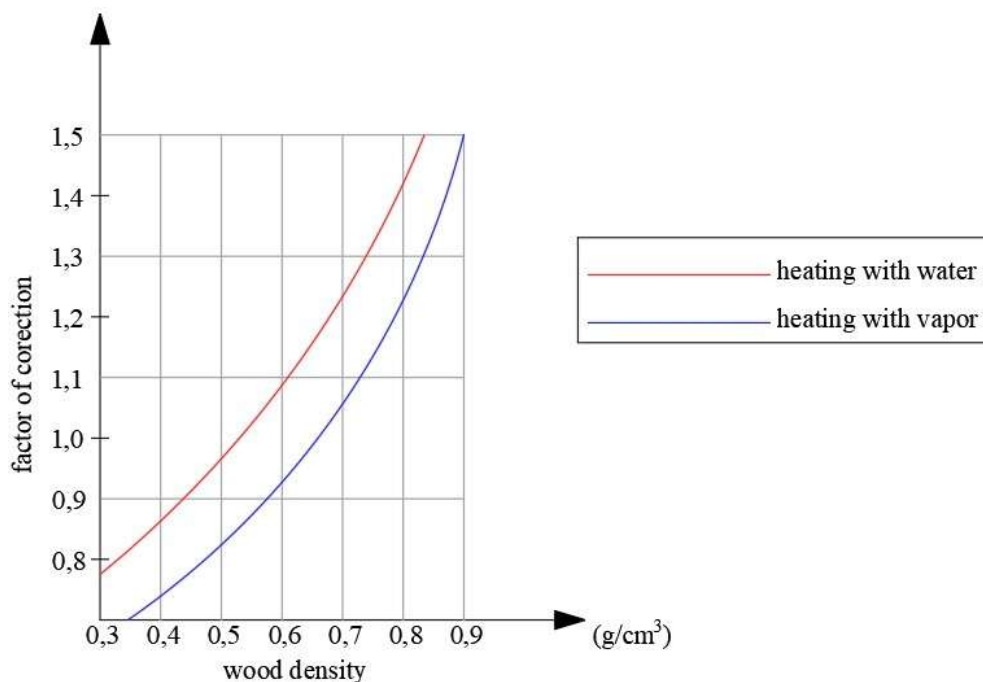
As a forest assortment, the raw material is in the form of logs, from which, after mechanical processing, rotary and plain sliced veneer is obtained. The logs, which are intended for the production of rotary cut veneer, are marked with the marking "L". In terms of diameter, the smallest mean diameter ranges from 25 to 35 cm. The smallest allowed length of logs, without considering the shrinking allowance, is 20 cm, and this length depends on the opening of the peeling machine.

The water, as a medium for soaking, can be in a fresh state or previously used, with an elevated temperature. Because of the resins and fats that are secreted by the wood and absorbed into the water, alkali (sodium) is added for its repeated use. Soaking in fresh water is used for frozen logs and logs with a moisture content above the saturation point ( $W > 30\%$ ). Soaking in previously used water, compared to soaking in fresh water, takes a shorter time, but due to the presence of acids from the previous round of soaking, a change in the color of the wood occurs. The best and fastest results are obtained from soaking raw material and the process continues until the established temperature in the wood is higher than the optimal temperature for mechanical processing of the logs.

The paper analyzes the heat energy for soaking ash logs. Ash, as a wood species, is characterized by a uniform color and a regular grain of wood fibers, which makes it extremely favorable for use in furniture manufacturing. The density of ash is  $\rho = 590 \text{ kg/m}^3$ . The logs have a diameter  $d = 50 \text{ cm}$ . The specific heat of wood is  $C_d = 1,35 \text{ kJ/kg } ^\circ\text{C}$ . The logs are in a frozen state and the initial temperature of the wood for soaking was  $t_{pv} = -15 \text{ } ^\circ\text{C}$ . The heating temperature of the wood was  $t_{spv} = 50 \text{ } ^\circ\text{C}$ . For determining the soaking time and achieving the optimal temperature, charts were used for the purpose of production of rotary cut veneer (Figure 1, Figure 2), according to Fleischer (1963).



**Figure 1:** Correlation between the log heating time and log diameter



**Figure 2:** Corelation between the factor of corection and wood density

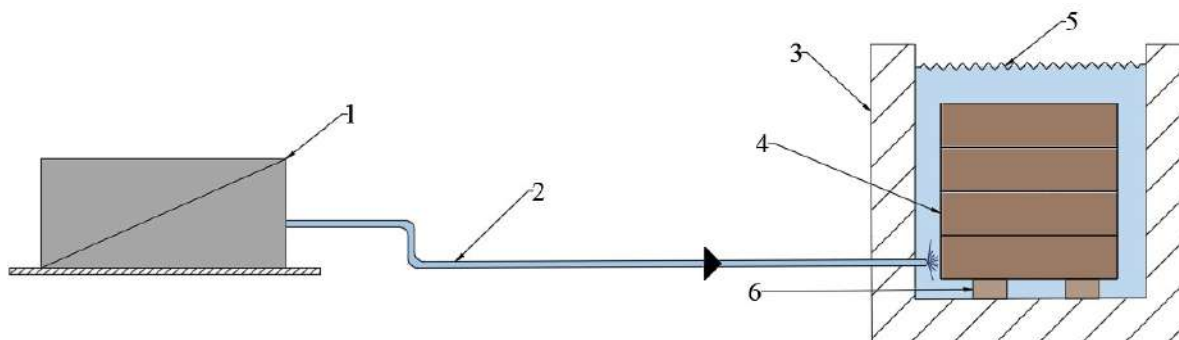
The logs heating time is calculated according to the formula:

$$Z_6 = Z_7 \cdot f_k (h)$$

where  $Z_6$  – heating (h),  $Z_7$  – soaking time (h),  $f_k$  – factor of correction for heating wood with water.

If the log diameter, the heating temperature and the density of the wood are known, according to figure 1, the soaking time is  $Z_7 = 15$  h, and according to figure 2, the correction factor is  $f_k = 1,1$ . The calculated time of logs heating, according to the given formula, is 16,5 h.

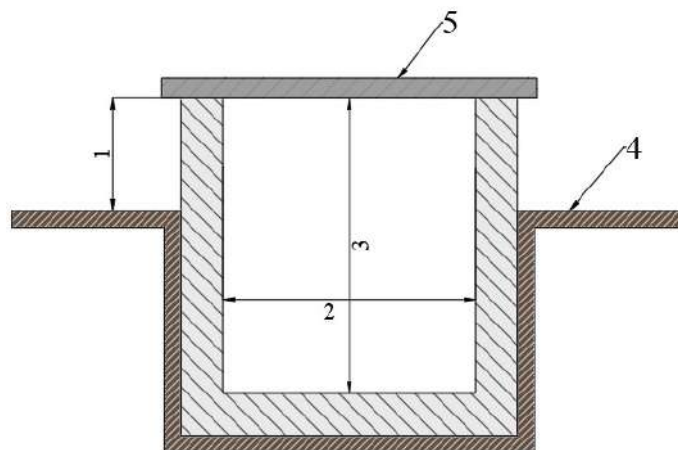
Logs were soaked according to the direct method (Figure 3). Water vapor from the heat source was transferred to the pool through the steam pipeline. The logs were placed on wooden beds. The pool was made of reinforced concrete with specific mass  $\gamma = 2\,400$  kg/m<sup>3</sup> and specific heat  $C = 0,922$  kJ/kg°C. The thermal conductivity of reinforced concrete is  $\lambda = 7,33$  kJ/m°C. The temperature of the soaking medium (water) was  $t_{vv} = 80$  °C, and the temperature of the steam for heating the water was  $t_{ip} = 100$  °C. The length of the steam supply installation was  $l_i = 60$  m, and the coefficient of heat conductivity of the water heating medium installation is  $K = 6,0$  kJ/m2h°C.



**Figure 3:** Direct method of log soaking, 1.heat source, 2.steam pipeline, 3.pool, 4.logs, 5.water, 6.wooden beds

Figure 4 shows a cross section of a log soaking pool. The length of the pool was  $l_b = 4,0$  m, the width  $s_b = 2,0$  m, and the height  $h_b = 2,5$  m. The thickness of the walls and bottom of the pool was  $t =$

0,3 m, the height of the wall of the pool above the ground was  $l_{vn} = 0,5$  m. The factor of pool fullfilment was  $f_v = 0,75$ . The value for the continuous working time of the pool was  $Z_v = 120$  h. The temperature of the inner surface of the cooled walls of the pool was  $t_{zdv} = 15$  °C. The pool lid was made of a combination of wood and aluminum and its mass was  $G_{kv} = 450$  kg, and the specific heat is  $C_{kv} = 1,28$  kJ/ kg°C. The maximum heating temperature of the lid was  $t_{kvmax} = 70$  °C, and the minimum cooling temperature of the lid was  $t_{kvmin} = -15$  °C. The heat transfer coefficient of non-boiling water from the wall to the soil is  $\alpha_1 = 45$  kJ/m<sup>2</sup>h°C. The temperature on the outside of the wall was  $t_{v1} = 30$  °C, the temperature of the soil around the pool was  $t_{vp} = 12$  °C.



**Figure 4:** Cross section of a log soaking pool, 1.wall above the pool ground, 2.pool width, 3.pool height, 4.ground, 5.lid

### 3. RESULTS AND DISCUSSION

The amount of heat  $Q$  for hydrothermal treatment of the raw material by soaking was calculated according to the general formula:

$$Q = Q_{pv} + Q_{zv} \text{ (kJ)}$$

where  $Q_{pv}$  – effective heat (kJ),  $Q_{zv}$  – heat loss (kJ).

The effective heat  $Q_{pv}$  was calculated according to the formula:

$$Q_{pv} = Q_{vv} + Q_{zdv} + Q_{dv} + Q_{kv} \text{ (kJ)}$$

where  $Q_{vv}$  – heat for water heating (kJ),  $Q_{zdv}$  – heat for heating the walls and the bottom of the pool (kJ),  $Q_{dv}$  – heat for heating of the wood(kJ),  $Q_{kv}$  – heat for heating the pool lid (kJ).

The heat loss was calculated according to the formula:

$$Q_{zv} = Q_{zzv} + Q_{ziv} + Q_{zhv} \text{ (kJ)}$$

where  $Q_{zzv}$  – heat loss through the pool walls and bottom (kJ),  $Q_{ziv}$  – heat loss through the installation for the water heating (kJ),  $Q_{zhv}$  – heat loss due to poor sealing of the pool lid (kJ).

According to the given known parameters, the amount of effective heat for soaking ash logs will be shown below.

$$Q_{vv} = 4190 (V_{bv} - V_{dv})(t_{vv} - t_{pv}) \frac{1}{Z_v} \text{ (kJ/h)}$$

$$V_{bv} = s_b \cdot h_b \cdot l_b \text{ (m}^3\text{)}$$

$$V_{bv} = 2,0 \cdot 2,5 \cdot 4,0 = 20,0 \text{ m}^3$$

$$V_{dv} = V_{bv} \cdot f_k \text{ (m}^3\text{)}$$

$$V_{dv} = 20,0 \cdot 0,75 = 15,0 \text{ m}^3$$

$$Q_{vv} = 4\,190 (20,0 - 15,0)(80 - 14) \frac{1}{120} = 11\,522,5 \text{ kJ/h}$$

$$Q_{zdv} = V_{zdv} \cdot C_{zdv} \cdot \left( \frac{t_{vv} - t_{zdv}}{2} \right) \cdot \frac{1}{Z_v} \text{ (kJ/h)}$$

$$V_{zdv} = V_{dno} + V_c + V_s \text{ (m}^3\text{) – volume of pool walls and bottom}$$

$$V_{dno} = s_{b1} \cdot l_{b1} \cdot h_{b1} \text{ (m}^3\text{) – volume of the pool bottom}$$

$$V_{dno} = 2,6 \cdot 4,6 \cdot 0,3 = 3,59 \text{ m}^3$$

$$V_c = (h_b \cdot s_{b1}) \cdot 2 \text{ (m}^3\text{) – front wall volume}$$

$$V_c = (0,3 \cdot 2,5 \cdot 2,6) \cdot 2 = 3,9 \text{ m}^3$$

$$V_s = (s_{b1} \cdot l_{b1} \cdot h_{b1}) \cdot 2 \text{ (m}^3\text{) – lateral sidewall volume}$$

$$V_s = 0,3 \cdot 2,5 \cdot 4,0) \cdot 2 = 6,0 \text{ m}^3$$

$$V_{zdv} = 3,59 + 3,9 + 6,0 = 13,5 \text{ m}^3$$

$$Q_{zdv} = 13,5 \cdot 590 \cdot 1,28 \cdot \left( \frac{80 - 14}{2} \right) \cdot \frac{1}{120} = 2\,803,68 \text{ kJ/h}$$

$$Q_{dv} = V_{dv} \cdot C_d \cdot (t_{srv} - t_{pdv}) \cdot \frac{1}{Z_v} \text{ (kJ/h)}$$

$$Q_{dv} = 590 \cdot 15,0 \cdot 1,35 \cdot (55 + 15) \cdot \frac{1}{120} = 6\,969,37 \text{ kJ/h}$$

$$Q_{kv} = G_{kv} \cdot C_{kv} \cdot (t_{kvmax} - t_{kvmin}) \cdot \frac{1}{Z_v} \text{ (kJ/h)}$$

$$Q_{kv} = 450 \cdot 1,28 \cdot (70 + 15) \cdot \frac{1}{120} = 408 \text{ kJ/h}$$

$$Q_{pv} = 11\,522,5 + 2\,803,68 + 6\,969,37 + 408 = 21\,703,55 \text{ kJ/h}$$



- Heat for water heating
- Heat for heating the walls and the bottom of the pool
- Heat for heating of the wood
- Heat for heating the pool lid

**Figure 5: Effective heat**

The effective amount of heat consumed for soaking of ash logs includes the heat for heating the water with a partition of 53,09 %, the heat for heating the walls and bottom of the pool with a partition of 12,92 %, the heat for heating the bottom of the pool with a partition of 32,11% and the heat for heating the pool lid with a partition of 1,88 %. It can be observed that the most amount of heat was spent on heating the soaking water, which was due to the low initial temperature of the water. The greater percentage of heat for heating of the wood was consumed due to the fact that the logs were in a frozen state before the start of the soakig process.

For the given time of 120 h:

$$Q_{pv} = 21\,703,55 \cdot 120 = 2\,604\,426 \text{ kJ}$$

The amount of heat loss used for the hydrothermal treatment by soaking of the ash logs will be shown below.



$$Q_{zzv} = F \cdot K \cdot (t_{vm} - t_{vp}) \cdot \frac{1}{Z_v} \text{ (kJ/h)}$$

$F = 2 \cdot l_b \cdot h_b + 2 \cdot s_{b1} \cdot h_{b1}$  ( $m^2$ ) – surface of the wall through which the heat is lost

$$F = 2 \cdot 4,0 \cdot 2,8 + 2 \cdot 2,6 \cdot 2,8 = 36,96 \text{ m}^2$$

$$K = \frac{1}{\frac{1}{\alpha_1} + \frac{\delta}{\lambda} + \frac{1}{\alpha_2}} \text{ (kJ/m}^2\text{h}^\circ\text{C)} \text{ – coefficient of heat conduction}$$

$\alpha_2 = [8,5 + 0,06 \cdot (t_{v1} - t_{vp})] \cdot 4,19$  ( $\text{kJ/m}^2\text{h}^\circ\text{C}$ ) – heat transfer coefficient from the wall to the soil

$$\alpha_2 = [8,5 + 0,06 \cdot (30 - 12)] \cdot 4,19 = 39,72 \text{ kJ/m}^2\text{h}^\circ\text{C}$$

$$K = \frac{1}{\frac{1}{45} + \frac{0,08}{7,88} + \frac{1}{39,72}} = 10,62 \text{ kJ/m}^2\text{h}^\circ\text{C}$$

$$Q_{zzv} = 36,96 \cdot 10,62 \cdot (80 - 12) \cdot \frac{1}{120} = 222,42 \text{ kJ/h}$$

For the given time of 120 h:

$$Q_{zzv} = 222,42 \cdot 120 = 26\,691,03 \text{ kJ}$$

$$Q_{ziv} = l_i \cdot K \cdot (t_{ip} - t_{pv}) \cdot \frac{1}{Z_v} \text{ (kJ/h)}$$

$$Q_{ziv} = 60,0 \cdot 3,14 \cdot 6,0 \cdot (100 + 15) \cdot \frac{1}{12} = 1\,083,3 \text{ kJ/h}$$

For the given time 120 h:

$$Q_{ziv} = 1\,083,3 \cdot 120 = 129\,996 \text{ kJ}$$

Heat loss due to poor sealing of the pool lid was calculated as 10 % of the effective heat  $Q_{pv}$ , and according to the calculations,  $Q_{zhv} = 260\,442,6 \text{ kJ}$ .

$$Q_{zv} = 26\,691,03 + 129\,996 + 260\,442,6 = 417\,129,63 \text{ kJ}$$



- Heat loss through the pool walls and bottom
- Heat loss through the installation for the water heating
- Heat loss due to poor sealing of the pool lid

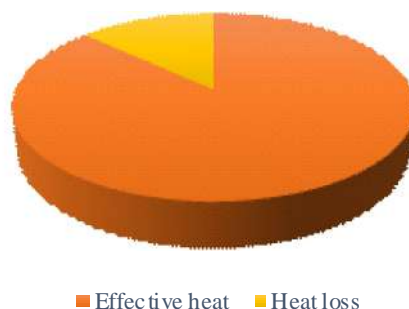
**Figure 6:** Heat loss

Heat loss through the walls and bottom of the pool participated with 6,4%, heat loss in the installation of the water heating medium account for 31,16 % and heat loss through the installation for the water heating participated with 63,44 %. It can be noted that the highest percentage of loss was due to poor lid sealing, which cannot be avoided, but certain actions can take occurrence for the their reduction to ensure the best possible sealing of the pool with the lid. Losses through the installation for water heating had a high participation due to the length of the pipeline for supplying water vapor to the pool. The percentage of losses in the installation would be higher by 30 % in the case of a treatment with indirect log soaking.

According to the obtained results for effective heat and heat loss, the amount of total consumed heat for soaking of ashlogs was:

$$Q_v = 2\,604\,426 + 417\,129,63 \text{ (kJ)}$$

$$Q_v = 3\,021\,555,63 \text{ kJ}$$



**Figure 7:** Heat energy used for ashlogs soaking

In the total percentage of heat, heat loss was 13,808 %, and effective heat was 86,192 %. Heat loss is an inevitable occurrence during the soaking treatment, and in order to reduce this kind of loss, it needs to be aimed towards the best choice of materials for the construction of the soaking pool. In the given case, the heat loss was within small limits, which can be attributed to the good sealing of the pool lid and the direct soaking method of treatment.

#### 4. CONCLUSIONS

The hydrothermal treatment of wood by soaking is an important technological operation that is carried out in order for the plastification of the wood. The soaking medium is hot water, and the process takes place in pools or pits. The purpose of the soaking process is the plastification of the wood fibers, sterilization and improvement of the properties of the rotary cut and plain sliced veneer. Species with a high Janka hardness, species sensitive to steaming and species from which resin and fat should be removed are treated by soaking. The moisture content of the raw material should be above the saturation point. Soaking has also proven effective as a way to defrost logs. Soaking softens the wood fibers and improves the peeling quality of the rotary cut veneers, through the improved mechanical properties of the wood material. Soaking is done according to two modes, depending on the temperature of the water, mild and strong. This process takes place by the methods of direct or indirect soaking, depending of the construction of the pool or the pit.

The paper presented data on the determination of the total amount of heat for hydrothermal treatment of ash logs by soaking. The logs were intended for the production of rotary cut veneer. The soaking process takes place according to the strong mode, by the direct method. The pool, in which the soaking process was carried out, was made of reinforced concrete, and the pool lid was made of a combination of concrete and aluminum. The total amount of heat for this treatment consists of effective heat and heat loss. According to the calculations, based on the given input parameters, the effective heat for soaking treatment of the ash logs was 2 604 426 kJ, and the heat loss was 417 129,63 kJ. The total heat required for hydrothermal treatment by soaking, during the time of 120 h, is 3 021 555,63 kJ. Of the total amount of heat consumed, effective heat was in a partition of 86,192%, and heat loss with a partition of 13,008 %. The most amount of heat was used for water heating, and the most amount of heat was lost due to the poor sealing of the pool lid. The results showed relatively low heat loss, which was due to the direct method of soaking of the wood material and the simplicity of the heating installations of the pool.

#### REFERENCES

- [1] Ali, R., Abdullah, U. H., Ashaari, Z., Hamid, N. H., & Hua, L. S. (2021). Hydrothermal Modification of Wood: A Review. *Polymers*, 13(16). doi:<https://doi.org/10.3390/polym13162612>
- [2] Barbero-López, A., Vek, V., Poljanšek, I., Virjamo, V., López-Gómez, Y. M., Sainio, T., . . . Haapala, A. (2022). Characterisation, Recovery and Activity of Hydrophobic Compounds in Norway Spruce Log Soaking Pit Water: Could they be Used in Wood Preservative

- Formulations? *Waste and Biomass Valorization*, 13, 2553-2564. doi: <https://doi.org/10.1007/s12649-022-01676-2>
- [3] Dupleix, A., Denaud, L.-E., Bleron, L., Marchal, R., & Hughes, M. (2013). The effect of log heating temperature on the peeling process and veneer quality: beech, birch, and spruce case studies. *European Journal of Wood and Wood Products*, 71(2), 163-171. doi: <https://doi.org/10.1007/s00107-012-0656-1>
- [4] Fleischer, H. (1963). *Heating veneer logs electrically*. USA: Lab. Madison.
- [5] Kolin, B. (2000). *Hidrotermi ka obrada drveta* (2). Šumarski fakultet Univerzitet u Beogradu.
- [6] Kollmann, F. (1951). *Technologies des Holztes und der Holzwerkstoffe* (2). Berlin: Springer, Berlin, Heidelberg.
- [7] Rabadziski, B., & Zlateski, G. (1998). *Optimalna temperatura za plastifikacija na drvoto pri dobivanje na furniri*. Skopje: Šumarski fakultet, Univerzitet „Sv. Kiril i Metodij“.
- [8] Rabadziski, B., & Zlateski, G. (2015). *Hidrotermi ka obrabotka na drvoto, II del, Plastifikacija na drvoto*. Skopje: Fakultet za dizajn i tehnologii na mebel i enterier, Univerzitet „Sv. Kiril i Metodij“.
- [9] Rohumaa, A., Viguier, J., Girardon, S., Krebs, M., & Denaud, L. (2018). Lathe check development and properties: effect of log soaking temperature, compression rate, cutting radius and cutting speed during peeling process of European beech (*Fagus sylvatica* L.) veneer. *European Journal of Wood and Wood Products*, 76(6), 1653-1664. doi:10.1007/s00107-018-1341-9
- [10] Rohumaa, A., Yamamoto, A., Hunt, C., Frihart, C., Hughes, M., & Kers, J. (2016). Effect of Log Soaking and the Temperature of Peeling on the Properties of Rotary-Cut Birch (*Betula pendula* Roth) Veneer Bonded with Phenol-Formaldehyde Adhesive. *BioResources*, 11(3), 5829-5838. doi:10.15376/biores.11.3.5829-5838

#### **The Authors' Address:**

Ana Marija Stamenkoska, MSc, PhD candidate at the Department of Primary Wood Processing, Faculty of Design and Technologies of Furniture and Interior-Skopje, Ss. Cyril and Methodius University, 16-ta Makedonska brigada 3, 1000, Skopje, Republic of North Macedonia.

Goran Zlateski, PhD, full professor at the Department of Primary Wood Processing, Faculty of Design and Technologies of Furniture and Interior-Skopje, Ss. Cyril and Methodius University, 16-ta Makedonska brigada 3, 1000, Skopje, Republic of North Macedonia.

## IMPACT OF FEED RATE ON ROUGHNESS OF THE CUT SURFACE, DURING CUTTING DRY BEECH WOOD WITH A CIRCULAR SAW

Anastasija Temelkova

*Ss. Cyril and Methodius University in Skopje, R. of North Macedonia,  
Faculty of design and technologies of furniture and interior-Skopje  
e-mail: temelkova@fdtme.ukim.edu.mk*

### ABSTRACT

The feed rate during mechanical processing of wood is one of the factors that has a high influence on the roughness of the cut surface.

The roughness of the cut surface caused by traces of the cutting tool (the main and secondary blades of the teeth) has an influence on the hydrothermal treatment and all other mechanical treatments of the wood. Greater roughness, due to faster evaporation of moisture from the wood, increases the percentage of drying errors. On the other hand, higher roughness reduces the utilization rate of the wood.

For this purpose, in this paper, the dependence of the feed rate on the roughness of beech wood during cutting of dry wood with a circular saw is investigated, with the intention of determining the optimal cutting conditions for obtaining lower values of the roughness.

In this research, three different feed rates were applied ( $U_1=12 \text{ mm min}^{-1}$ ,  $U_2=16 \text{ mm min}^{-1}$  and  $U_3=20 \text{ mm min}^{-1}$ ) for a constant cutting height of 45 mm in dry beech wood with humidity  $W=10\pm 1\%$ . The measurements were made with a circular saw with diameter of  $D=250 \text{ mm}$ , number of teeth  $Z=40$  and width of the cut  $b=3,2 \text{ mm}$ . The number of revolutions is  $n=5500 \text{ min}^{-1}$ .

Roughness measurements were taken with a digital comparator, according to the  $R_{\max}$  criterion. The obtained results show a pronounced significance, i.e. directly proportional dependence of the roughness of the cut surface on the feed rate.

**Keywords:** beech wood, circular saw, roughness, the feed rate

### 1. INTRODUCTION

In order to ensure quantity and quality when processing wood with circular saws, it is of great importance to make the right choice of cutting tool. Tool manufacturers on the market offer different types of saws with different diameters and different number of teeth. Circular saws are commonly used tools in mechanical processing of wood and wood based materials, including all production phases. Circular saws are also used for cutting other materials such as: plastic, metal, ceramics, different types of construction materials etc [7]. When processing on circular saws with equal diameter and equal peripheral cutting speed, the number of teeth that actively participate in the process of cutting per time is different. This has a significant impact on the thickness of wood chips, as well as the pressure on the kerf, especially at the rear surface of the blade [5]. The choice of the number of teeth for the same diameter of the saw depends on the required quality of processing of the cut surface, that is, a saw with a larger number of teeth provides better processing and vice versa. In the process of wood cutting, cutting force and cutting power are the main output parameters, while the chip length, chip thickness, feed per tooth, teeth pitch, average kinematic cutting angle, cutting speed, average pressure on front side, fictive specific force on back side are secondary parameters [3]. Cutting height and number of teeth affect cutting resistance with a circular saw. Greater cutting resistance leads to increased vibration and distortion of the cutting tool. This results in the appearance of a crooked and rough cut. The contact surfaces of tools in the machining process are exposed to high pressures and friction, which results in tool wear. Tool wear is one of the important factors in mechanical wood processing since it directly affects surface quality, cutting forces, cutting power and energy

consumption [8]. The criteria that characterize the quality of the treated surface are surface roughness, accuracy of processing and resistance. Traces of the processing from the vibration of the machine and the cutting tool, the structure and volume of the material being processed, are part of the reasons for the appearance of roughness. The roughness of the cut surface caused by traces of the cutting tool (the main and secondary edges of the teeth) has an influence on the hydrothermal treatment and all other mechanical treatments of the wood. The feed rate during mechanical processing of wood is one of the factors that has a high influence on the roughness of the cut surface.

## 2. THE AIM OF THE RESEARCH

The aim of the research of this paper is to determine the dependence of the feed rate on the roughness in beech when cutting dry wood with a circular saw, with the intention of determining the optimal cutting conditions for obtaining lower roughness values.

## 3. MATERIAL AND METHOD OF WORK

### 3.1 Material

For testing was taken sawn lumber from beech (*Fagus Sylvatica* L.) without defects with dimension 1500 x 150 x 15mm. All lumber is dried and conditioned. The measured humidity of the beech is 9,32 % on average.

Samples were cut from the planks with a constant cutting height of 45mm. The research of the samples was carried out on a circular saw machine type NIKOLAIDIS TEMA 3800 in „KI-PAR“ from Strumica (Figure 1). The main feature of this machine is that both the main and auxiliary movements are performed by the cutting tool. During cutting, the object to be processed is pressed with a pneumatic pressure beam. The technical characteristics of the machine are given in table 1.



**Figure 1:** Circular saw machine type NIKOLAIDIS TEMA 3800

**Table 1:** Technical characteristics of the format circular saw machine type Nikolaidis TEMA 3800

Technical characteristics	
External length	5500 mm
External width	4400 mm
Cutting length	3800 mm
Cutting height	55 mm
Dimensions of the circular saw	200 3,3 30 mm 250 3,2 30 mm
Power of the main electric motor	4,5 kW
Power of the electric motor to move the main electric motor	1,75 kW
Number of revolutions of the circular saw	5500 min <sup>-1</sup>
Pressure on the pressed beam	6-7 bar
Feed rate	5-30 mmin <sup>-1</sup>



**Figure 2:** Circular saw with diameter  $D=250\text{mm}$ , number of teeth  $Z=40$  and thickness  $b=3,2\text{mm}$

### 3.2 Metod of work

In this research were applied three different feed rates ( $U_1=12\text{mmmin}^{-1}$ ,  $U_2=16\text{mmmin}^{-1}$  and  $U_3=20\text{mmmin}^{-1}$ ). The measurements were made with a circular saw with a diameter of  $D=250\text{mm}$ , number of teeth  $Z=40$  and width of the cut  $b=3,2\text{mm}$ . The number of revolutions is  $n=5500\text{min}^{-1}$ . The cutting length of each sample is 1,2m.

The roughness data is measured with a digital comparator, type Shane, according to the  $R_{\max}$  criterion. For each sample (3 in total), 100 measurements were taken at a length of 1,0m, with a reference flange of 100mm length (Figure 3).



**Figure 3:** Digital comparator for measuring roughness type Shane

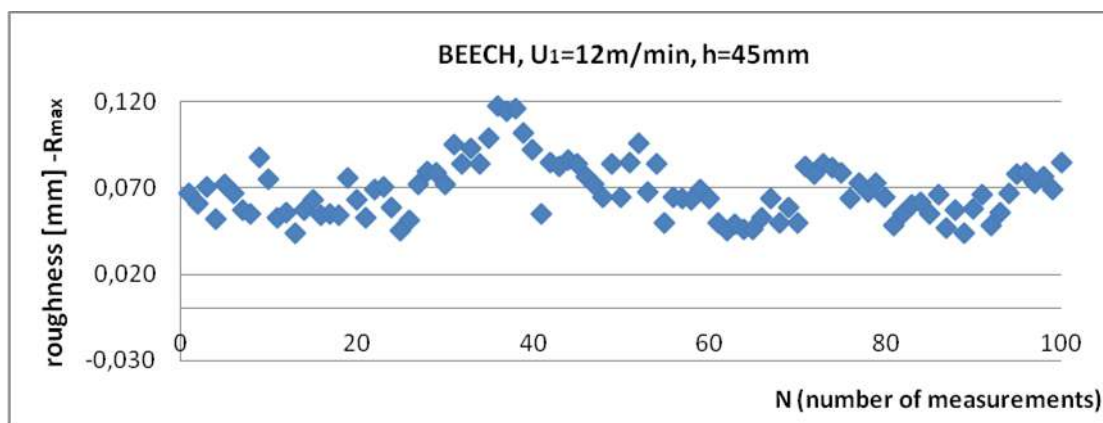
#### 4. RESULTS

The results of the roughness measurement values according to the  $R_{max}$  criterion are shown in Table 2.

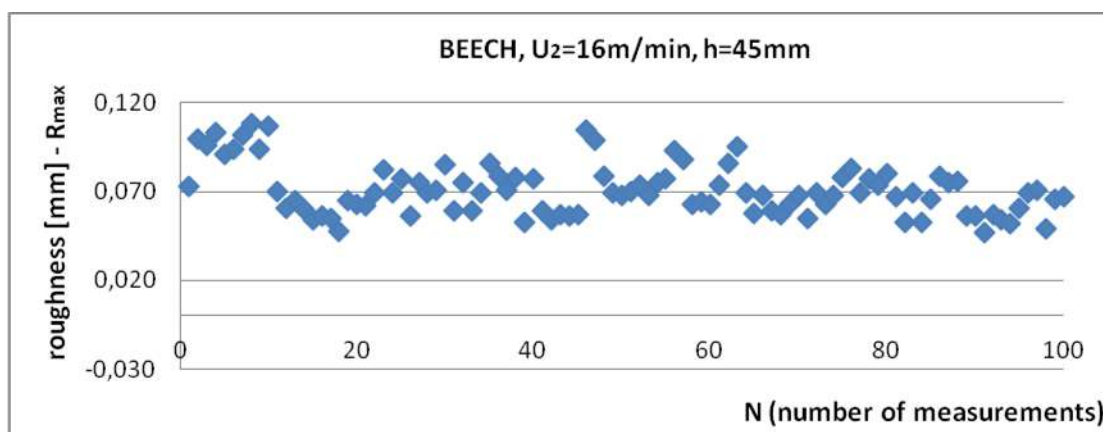
**Table 2:** Results of testing the roughness of beech samples at different feed rates ( $U_1=12\text{mmmin}^{-1}$ ,  $U_2=16\text{mmmin}^{-1}$  and  $U_3=20\text{mmmin}^{-1}$ ), according to the  $R_{max}$  criterion

1	displacement speed (U), for number of teeth Z = 40 and diameter D=250mm									BEECH
	U <sub>1</sub> = 12 m/min			U <sub>2</sub> = 16 m/min			U <sub>3</sub> = 20 m/min			
	cutting height [mm]			cutting height [mm]			cutting height [mm]			
	h=45			h=45			h=45			
	ROUGHNESS [mm]			ROUGHNESS [mm]			ROUGHNESS [mm]			
	1	2	3	4	5	6	7	8	9	
1	0.067	0.055	0.082	0.073	0.059	0.067	0.079	0.064	0.089	
2	0.061	0.085	0.079	0.100	0.054	0.053	0.069	0.091	0.076	
3	0.071	0.083	0.064	0.096	0.057	0.069	0.087	0.113	0.068	
4	0.052	0.086	0.073	0.103	0.056	0.053	0.092	0.104	0.069	
5	0.072	0.084	0.068	0.091	0.057	0.066	0.099	0.084	0.071	
6	0.067	0.077	0.073	0.094	0.105	0.079	0.068	0.077	0.078	
7	0.057	0.072	0.099	0.102	0.099	0.075	0.073	0.094	0.068	
8	0.055	0.065	0.118	0.108	0.079	0.076	0.083	0.102	0.097	
9	0.088	0.084	0.115	0.094	0.069	0.056	0.079	0.080	0.088	
10	0.075	0.065	0.116	0.107	0.068	0.056	0.086	0.083	0.102	
11	0.053	0.085	0.102	0.070	0.070	0.047	0.082	0.066	0.097	
12	0.056	0.096	0.092	0.061	0.074	0.057	0.093	0.065	0.099	
13	0.044	0.068	0.048	0.065	0.068	0.054	0.073	0.063	0.101	
14	0.057	0.084	0.055	0.060	0.075	0.052	0.102	0.090	0.074	
15	0.063	0.050	0.060	0.054	0.077	0.061	0.085	0.064	0.081	
16	0.054	0.065	0.062	0.056	0.093	0.069	0.099	0.074	0.081	
17	0.055	0.064	0.055	0.055	0.088	0.071	0.085	0.079	0.079	
18	0.054	0.063	0.066	0.048	0.063	0.049	0.089	0.084	0.093	
19	0.076	0.069	0.047	0.065	0.064	0.066	0.074	0.089	0.091	
20	0.063	0.064	0.057	0.063	0.063	0.067	0.068	0.081	0.096	
21	0.053	0.050	0.044	0.062	0.074	0.078	0.072	0.069	0.069	
22	0.069	0.045	0.058	0.069	0.086	0.083	0.081	0.064	0.067	
23	0.071	0.049	0.066	0.082	0.095	0.069	0.069	0.068	0.081	
24	0.059	0.046	0.048	0.069	0.069	0.077	0.103	0.064	0.097	
25	0.045	0.046	0.056	0.077	0.058	0.074	0.084	0.074	0.081	
26	0.051	0.053	0.067	0.056	0.068	0.080	0.076	0.072	0.091	
27	0.072	0.064	0.078	0.075	0.059	0.086	0.083	0.083	0.079	
28	0.080	0.050	0.079	0.069	0.057	0.079	0.074	0.079	0.099	
29	0.079	0.059	0.073	0.071	0.063	0.071	0.086	0.069	0.088	
30	0.072	0.050	0.077	0.085	0.068	0.078	0.074	0.076	0.079	
31	0.095	0.083	0.069	0.059	0.055	0.053	0.083	0.076	0.098	
32	0.084	0.078	0.085	0.075	0.069	0.077	0.100	0.069	0.089	
33	0.093	0.084		0.059	0.063		0.086	0.072		
34	0.084	0.065		0.069	0.068		0.077	0.066		
average value	<b>0.06864</b>			average value	<b>0.0708</b>			average value	<b>0.0818</b>	
standard deviation	<b>0.01636</b>			standard deviation	<b>0.0143</b>			standard deviation	<b>0.0116</b>	
coefficient of variation	<b>23.835</b>			coefficient of variation	<b>20.261</b>			coefficient of variation	<b>14.182</b>	
minimum value	<b>0.044</b>			minimum value	<b>0.047</b>			minimum value	<b>0.063</b>	
maximum value	<b>0.118</b>			maximum value	<b>0.108</b>			maximum value	<b>0.113</b>	

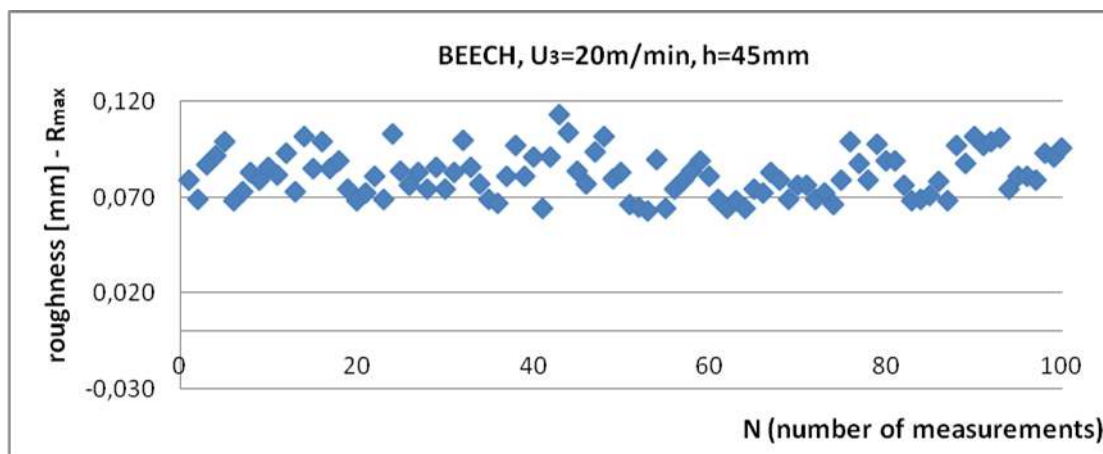
The mean values of the measurements show an increasing trend with increasing feed rate. The standard deviation and the coefficient of variation show sufficient uniformity of the measurement data.



**Graph 1:** Roughness of the cut surface of the beech samples at a feed rate  $U_1=12\text{mm}^{-1}$  according to the  $R_{max}$  criterion



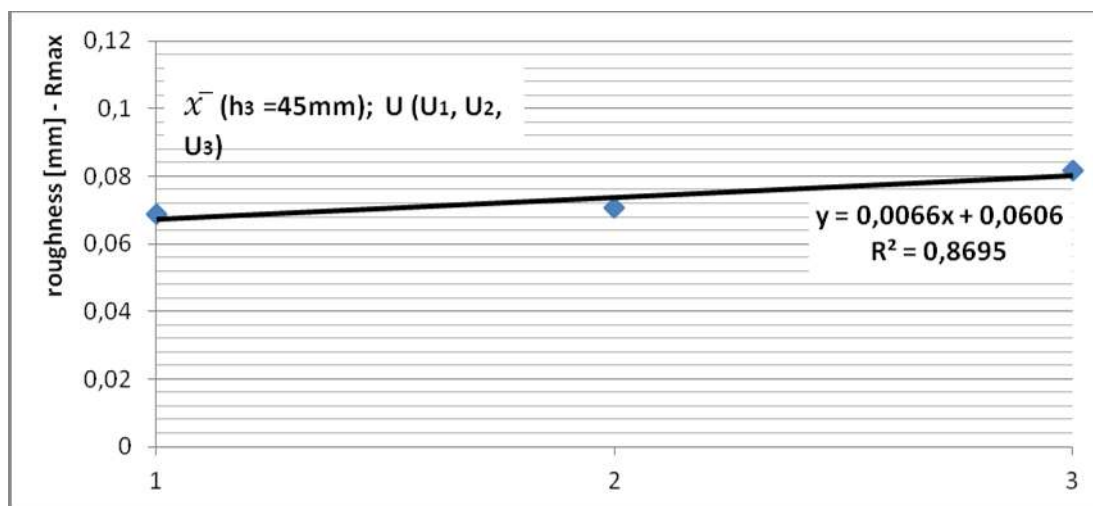
**Graph 2:** Roughness of the cut surface of the beech samples at a feed rate  $U_2=16\text{mm}^{-1}$  according to the  $R_{max}$  criterion



**Graph 3:** Roughness of the cut surface of the beech samples at a feed rate  $U_3=20\text{mm}^{-1}$  according to the  $R_{max}$  criterion

Graphs 1, 2 and 3 show the measurement data from the measurements. In graph 1, a greater deviation of the values is observed.





**Graph 4:** Regression analysis of mean values of roughness at all three feed rates ( $U_1=12\text{mmmin}^{-1}$ ,  $U_2=16\text{mmmin}^{-1}$  and  $U_3=20\text{mmmin}^{-1}$ )

Regression analysis showed that the measurements were best fitted to a line equation. Graph 4 shows the regression line of the mean values from the measurement data. The correlation coefficient shows high dependence.

From the results shown (table 2, graphs 1, 2, 3 and 4), we can state that with an increase in the feed rate, the roughness of the cut surface increases directly. The dependence is expressed mathematically by the regression law  $y=0,0066x+0,0606$  and the correlation coefficient  $R^2=0,8695$ .

## 5. DISCUSSION AND CONCLUSIONS

The reviewed professional and scientific literature, which was available to us, showed that all authors agree in the statement that with the increase in the feed rate, the roughness of the cut surface increases, regardless of the type of mechanical processing.

The reasons for the depth of unevenness are also mentioned: the geometric characteristics of the cutting tool, the type of wood, the vibration and dullness of the tool, the humidity of the wood, the temperature of the wood, the thickness of the sawdust per tooth, etc. [1,6,9]

Preparation of the cutting tool is also essential. It is enough for just one tooth to fall out and cause deeper traces to appear. Also, with a greater bevel of the side blades (larger angle), deeper traces (bumps) appear. Deeper marks (grooves) must be removed in subsequent machining operations. At the same time, the loss of wood mass is greater, and because of this, it often happens that the dimensions of the final product deviate from the required dimensions. In extreme cases, errors appear in the final product.

Low feed rates compared to high feed rates give a better quality of the cut surface, but the productivity of the machine decreases. It is very important to determine the optimum feed rate value to obtain favorable productivity and surface quality. [2,4]

In this research, the dependence of the feed rate on the roughness of the cutting surface was confirmed. The mean values of the relations increase with increasing feed rate.

## REFERENCES

- [1] Klinarov, R., Trposki, Z., Koljozov, V., (2000): Teorija na reženje na drvoto, Skopje.
- [2] Koljozov V., Trposki Z., Rabadziski B., Zlateski G., (2012): Influence of feed rate on cutting force and cutting power during wood processing on band saw, Wood - Design and Technology, Journal of wood science, design and technology, Vol.1 No.1, Pg.52-56, Skopje.
- [3] Koljozov V., Trposki Z., Rabadziski B., Zlateski G., Karanakov V., (2019): „Research on the effects of the cutting speed on cutting force and the cutting power in the process of milling“, 4<sup>th</sup> International Scientific Conference „Wood Technology & Product Design“, Pg. 278-283, Ohrid.

- [4] Paralidov, K., (2014): Istraživanja na vlijanieto na brojot na zabi i viso ina na reženje vrz otporot na reženje so kružna pila, Magisterska rabota, Fakultet za dizajn i tehnologii na mebel i enterier, Skopje.
- [5] Paralidov K., Koljozov V., Trposki Z., Karanakov V., (2015): Research on kerf number influence on cutting power during woodprocessing on circular saw, Second International Scientific Conference "Wood Technology & Product Design", Pg. 221-225, Ohrid.
- [6] Trposki Z., Klincarov R., Koljozov V., (1999): The influence of cutting kinematics of bandsaw on production effects“, 2-nd International conference "Machine-Tool-Workpiece", Technical, University of Zvolen, Nitra.
- [7] urkovi M., Danon G., Svrzi S., Trposki Z., Koljozov V., (2017): A justification of the use of specialized circular saws for wood, 3<sup>rd</sup> International Scientific Conference "Wood Technology & Product Design", Pg. 61-66, Ohrid.
- [8] urkovi M., Milosavljevi Miric M., Mihailovi V., Danon G., (2019): Tool wear impacts on cutting power and surface quality in peripheral wood milling, 4<sup>rd</sup> International Scientific Conference "Wood Technology & Product Design", Pg. 110-118, Ohrid.
- [9] Hutton S. G., (1991):The dynamics of circular saw blades, Munchen: Holz als Roh-und Werkstoff 49105-10.

## ANALYSIS OF THE INFLUENCE OF CONSUMERISM ON THE EPHEMERALITY OF THE INTERIORS OF PUBLIC FACILITIES

**Edona Arifi Sadiku**

*Ss. Cyril and Methodius University in Skopje, North Macedonia,  
Faculty of Design and Technologies of Furniture and Interior-Skopje,  
e-mail:edona.arifi@gmail.com*

### ABSTRACT

The purpose of the research is to confirm the is the verification of the indications of consumerism and architecture, specifically in the sphere of interiors for trade and sales. The properties of consumerism that contribute directly and indirectly through the social factor to ephemerality in architecture, interiors and design are analyzed and detected.

Consumerism in the period of postmodernism, as a more specific research area of this paper, is an immanent occurrence. The social -economic conditions that determine the social-economic conditions indicate a strong rise of consumerism in more significant spheres of human life, and especially and undoubtedly in the spheres that are connected to direct profit, such as public interiors with salesoccupation.

The architectureand interior design are applied multidisciplinary sciences, always under the influence of political, sociological and economic developments. Today's post-industrial period – the rapid development of technologies and materials, fast and unlimited production, leads to endless consumption and changes in the appearance of the product, thereby indirectly and directly to changing the architecture and design in public buildings.

Ephemeral architecture and design become the key answer. Through the research of commercial public facilities - from the City Trade Center to some newer shopping centers in R.N. Macedonia, in this paper we practically come to conclusions which characteristics, processes and influences of consumerism as a phenomenon have contributed to today's appearance in the architecture and design of public commercial buildings over the years. Through architectural recording, analysis and comparison of existing interiors,the ways and methods of organizing the public interior are also clarified, which in conditions of frequent consumerism become ephemeral - temporary, transient, short-lived.

**Keywords:** social - economic conditions, cultural - social conditions, consumerism, internationalism, ephemerality, interior, architecture, design, furniture, public facilities

### 1. INTRODUCTION

The topic of research and analysis in this paper is the frequent change of architecture and interior as a consequence of consumerism. An analysis is made of the architecture and interior of some of the shops within the City Shopping Center, how it was in the years when it started working and how it looks today, with a further comparison with the first and last sales points in R.N. Macedonia, more specifically Skopje.

The researches of the economic and commercial context in which the Republic of Macedonia existed, first as a Socialist Republic, part of the SFRJ, then from independence onwards as an independent Republic of Macedonia, and today the Republic of North Macedonia indicate permanent economic problems in the economy, low incomes and earnings, and a series of others social and sociological problems arising from the long transition period.

The transition period in R. N. Macedonia, as in the republics in the region, is not finished, on the contrary, it has a tendency to deepen and confirm depending on the political situation of the country. After the earthquake in 1963, Skopje was desperate, with human and material losses, which contributed to its becoming a "city of international solidarity" when many countries built it and helped

rebuild the city (Naumovska, Shopov 2014:185 ). The construction of Skopje begins on the basis of the urban plan, worked by the world architect Kenzo Tange and his team. Due to the large percentage of destroyed buildings, Skopje is being built massively, under the spirit of modern architecture, especially brutalism.

The execution of the new urban plan and the building of the city were crucial for further economic development. However, the implementation of the urban plan was not fully implemented, in the 80s, especially in the 90s, the Republic of Macedonia suffered a great economic stagnation due to the wars from the former Yugoslavia, the collapse of the common market, economic sanctions, the embargo from Greece, etc. Construction in this period was the lowest in the country. Growth in the economy of our country took place in 2010, with an increase in the trade balance through agricultural and food products and industry. The new economic trends with the promotion of state benefits in foreign countries encouraged foreign investments, which positively contributed to raising the standard of living. Consequently, in recent decades, the construction of more commercial modern facilities has begun , a fact that has brought a different kind of consumerism and a new commercial culture to our society.

One of the consequences of globalism is excessive consumerism , which reaches our culture through new formats of commercial facilities and chain stores. These stores, in conjunction with marketing and international brands, contributed to the formation of store prototypes and thus, perfecting the architecture and interior design of the stores.

In what way does consumerism, architecture, interior and design contribute to the emergence of short-lived and often changing shops, which is that constant circle of consumer+product +space, what is the interaction and indications between these elements and what were the processes of changes in the field of trade in our country over half a century, will be the subject of research in this paper.

## **2. PURPOSE OF RESEARCH**

The purpose of this paper is to research the factors that contributed to interior design and architecture becoming ephemeral, under the influence of today's consumerism. Since the architecture and interior design of a shopping center is a combination of many complex components, special attention is paid to consumerism as an important factor that directly acts in the organization of a shopping center, a store and sales process.

## **3. RESEARCH METHODS**

The research methods will focus on the theoretical part - the sociological, philosophical and economic aspects of people as consumers; today's way and purpose of consumption, consumerism as a phenomenon and the connection of consumerism with architecture and interior design.

The second way, the analytical method - through real photos, a comparison is made of the public interior as it was and as it is today in R. N. Macedonia ,it is clarified how much the public interiors of shopping centers have changed. A qualitative table explains the key factors of design that influence consumerism and vice versa. The rapid change of commercial environments does not lead us to an explanation of the public interior, which in conditions of frequent consumerism become ephemeral - temporary, transient, short-lived.

## **4. HISTORICAL AND ECONOMIC REVIEW OF COMMERCIAL FACILITIES IN R. N. MACEDONIA**

Historically speaking, Ethnic Macedonia was under the Ottoman influence for five hundred years, the time when the country also had minimal economic development. After the end of the Second World War, during the Kingdom of Serbia and then in the former Yugoslavia, in Macedonia, specifically in Skopje, urbanization and the construction of several important buildings began. During this period, the socialist modernization begins, then the period of industrial development, when there is a mass migration of the inhabitants of the entire country to the cities, especially Skopje.

Consequently, the largest reconstruction of the city of Skopje begins after the overflowing of the Vardar river and after the catastrophic earthquake (1962 and 1963), when 80% of the city was

destroyed (Arsovski, 1981:25). Parallel to the construction of the City Trade Center in Skopje, many residential buildings and towers, public buildings were built, the old bazaar was being reconstructed, massive growth of Skopje follows. Urban plans failed to be fully implemented due to the transition period – a time when various conversions and upgrades take place, the reign of urban chaos due to individual gains. The political indication follows, when the appearance of Skopje underwent major changes after the implementation of the "Skopje 2014" project.

From an economic perspective, under the Ottoman rule in Skopje, in the 19th century, there were 50-60 different trades working in the old bazaar. "The bazaar as a whole is getting stronger and, as a unique trade and craft center, it is starting to directly influence the development of the city as a whole" (Arsovski, 1981:19). The bazaar continues to expand, especially after the construction of the railway station in 1873, when a more intensive development of trade begins. The construction of a new city axis – Marshal Tito Street, brought new commercial buildings: Ristic and Krang Palace, where many textile shops were opened. Otherwise, after the end of the Second World War, great economic stagnation was emphasized in Skopje (Arsovski, 1981:19).

The development of the economy in R. Macedonia (today's RN Macedonia) initially started with the creation of preconditions, which period started from 1940-1970 (Klusev, 2002:10-14). Then, until 1989, the development of the economy in Macedonia was slightly higher - 0.3 percent of the growth than that of SFRJ. This is also the time when "Architects in Macedonia spontaneously accept functionalism and the international style, which in conditions of low economic development are in full accordance with the preferred rational system of building" (Tokarev, 2006:77).

During the SFRJ, several shopping centers were built, some of them were on the ground floor of residential complexes, and then also department stores. Home of the Chamber of Commerce, designed by the architect Milan Zlokovikj, later got the function and the name of Stokovna Kukja, located in the square of Skopje and adapted to the movement of the context (Arsovski, 1981:23). Next is the Skopje Fair, which was recently destroyed.

After the earthquake and the permanent increase in the number of residents in the capital, from the analyzes made by the Urban Planning Administration of the city of Skopje and the Chamber of Commerce of R.M. and professionals, resulted in the construction of GTC, as the main and most important commercial building in Skopje, which exists and is actively functioning today. The department stores "NAMA", "BEKO", "SKOPJE" (later "TIPO"), "ILINDEN", "JULY 26th", "MARCH 8th", and "BRIDGE". These public buildings were in a location close to the old bazaar and the city center, thus creating an urban central city (Naumovska, Shopov 2014:187)

R. Macedonia in the transition period at the end of the 80s "... collides with the biggest problems and dilemmas, with the biggest uncertainties and social upheavals precisely in the domain of the transformation of social, that is, state property..." (Kljusev, 2002 :103-104). There is an uncontrolled opening of all kinds of shops throughout the city, while former Yugoslav industries failed to privatize and ceased to exist.

The law on privatization in R. Macedonia was adopted in June 1993 (Kljusev, 2002:103-104). The privatization of GTC at this time stagnated the work temporarily, for the benefit of the following commercial facilities: "Mavrovka" (1993), then "Skopjanka", "Beverly Hills", "Bunjakovec", "Leptokaria", "Aluminka", "Biser", etc. The functioning of these facilities today is partial.

Under the influence of globalism and internationalism, with an increase in the standard, Viktor Gruen's architecture appears in Macedonia, i.e. super markets, hyper markets and new closed shopping facilities. In 1994, the first modern supermarket "Tinex" was opened, a state-owned chain store, which in a short time opened several sales points throughout Macedonia. In 1997, McDonald's - a world-famous food store - was opened, followed by the "Vero Plus" supermarket. By the way, the first modern shopping center with global standards is "Ramstor Mall", put into operation on June 11, 2005, located in the city center, with 25,000 m<sup>2</sup> and 90 different shops. After "Ramstor Mall", Skopje and other cities in R.N.Macedonia are full of modern closed shopping centers, which were built according to international standards and most of them are active.

## 5. CONSUMERISM AND EPHEMERALITY IN ARCHITECTURE AND DESIGN

The term consumerism describes a state of advanced industrial society, in which the buying and selling of products and services is carried out (Cambridge dictionary . org). Consumerism began with the exchange of materials and products between people, in the ancient age. From the Greek agora and the Roman forum, continuing in the arcaded squares , the old bazaars, to the shopping malls and the modern closed shopping malls, today's postmodern trade and consumption becomes a multifunctional and comprehensive area, which affects in a very complex way the city, the society, parallel to architecture and design.

Consumerism has been prominent since the industrialization period. Today "-Information production leads the post-industrial society, theoretical knowledge becomes the new goal, not economic development as in the industrial society" (Tonovski, 2008:59). Digitization, good infrastructure, surplus of labor force, easy transportation of products enables huge consumption and facilitation of service activities. Out of mass production and competition, branding and marketing appeared– which creates a hierarchy of producers and products. "-All are equal before objects such as use value, but not at all before objects such as "brands" and differences, which are deeply hierarchical." (Baudrillard , 1970 :133 ).

Another influential factor, social media today has created a hyper-real world.” - Simulated digital life takes on an autonomous status and being a simulation does not make it less real, but rather makes it more real than the real in terms of the weight it gets in the human life. As a result, it is not only reality, but hyperreality." (Baudrillard, 1970 :17). We are what we buy, what we have. This is where the differences appear, which make us dominant over our competitors. "-visible connection or evidence of this connection are the social self and the material or extended self, as well as the primary orientation towards others, the external." (Janakov:39).Janakov explains about the objective appearance with which each individual in a society strives to present himself, through the possession of things, an appearance with which it is subjectively connected, an appearance that it interprets in front of the world and allows social integration in the modern world.

This phenomenon is very inherent in postmodernism or transmodernism as Baudrillard says. Due to this phenomenon, architecture and design are undergoing major changes. Sociologist Tonovski explains that change means modernization of social life, and that changes are complex and multidimensional (Tonovski , 2008:54). The professor also explains about the possible factors that influence the creation of changes: the class struggle, science, religion, ideological and technological factors, the demographic factor, the political system, etc.

Changes and innovations that create attraction, in addition to consumerism, people look for in sales premises. Many indoor shopping centers around the world have closed due to lack of attraction among consumers (Chandler 1995:39). Great competition leads to specific closed modern shopping centers, which before opening determine the thematic content, according to which all other elements should correspond. Today's consumers are not completely focused on the product or the purchase, but on the search for a unique and unforgettable experience ( Yuan et al, 2021) and "lifestyle" ( Boustani, 2020 :34 ).

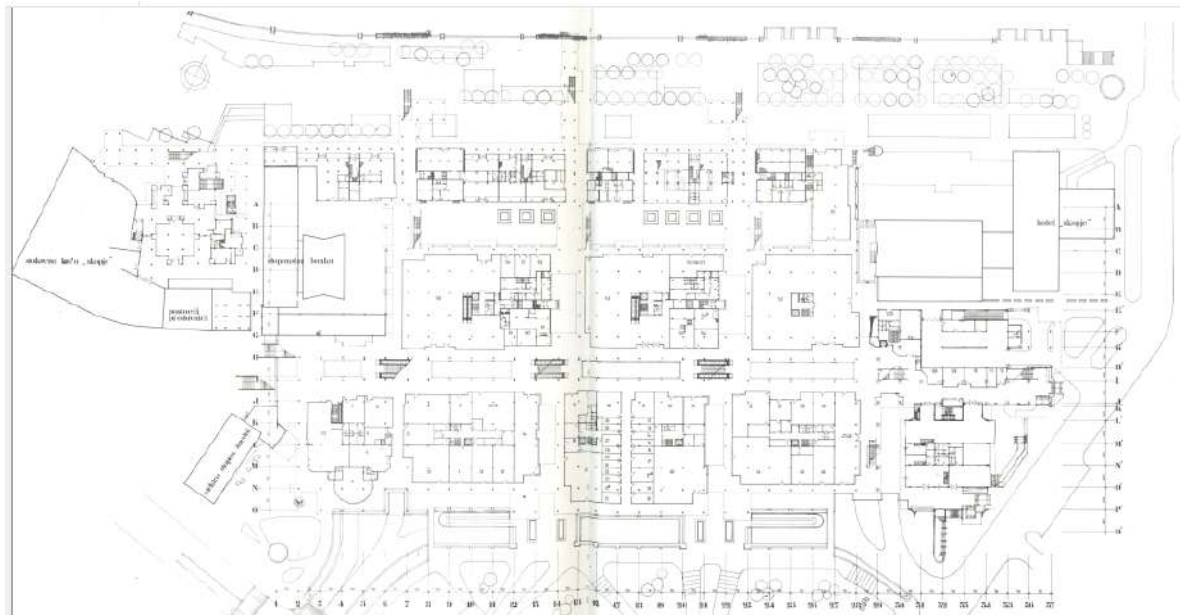
The store is a space where the interaction between the consumer and the product takes place (Boustani 2020:38 ), and such places need to be constantly renewed due to the rapid aging of their attraction (Boustani2020 :34). Consequently, these stores due to attractiveness become temporary, transient and short-lived, more concisely ephemeral.

Today's postmodern store formats can be interpreted as an experiential marketing format, a synthesis between communication and sales, an interactive and narrative place (Boustani2021:64) . According to Pomodoro, "ephemeral stores are recent formats that respond to postmodern society" (Pomodoro 2013:341-352).

## **6. TRADE FACILITIES IN SKOPJE**

City Trade Center in Skopje (hereinafter only: GTC)is one of the most important buildings of the city of Skopje, the only one with this name, built in the city center by the Vardar river in 1973, as an open shopping center. Integrated into “Makedonija” Square on the east-west axis, it has a linear architectural form, located between the five existing residential towers with excellent incorporation into the context - the square and the existing buildings - the Skopje Department Store, residential towers, catering facility, hotel, etc. It was built with two underground floors, a ground floor and two

above-ground floors, with spaces that have commercial and service activities."Pedestrian movements, according to the urban concept of the central city area, are solved with emphasized floor walkways, with a balanced relationship and an emphasized longitudinal axis in the east-west direction" (Arsovski1981:32).



**Figure 1:** Foundation of GTC (arch. Arsovski, Tihomir1981: City Shopping Center)



**Figure 2:** Perspective of GTC (arch. Arsovski, Tihomir 1981: City Shopping Center

Since this paper investigates the impact of consumerism on architecture and design, the construction of the GTC happened because of the great needs of the city, the state and the people to have a shopping center that would also satisfy regional needs. Among the main reasons for this phenomenon are the changes of the city after the earthquake: the construction of residential buildings in this part and the increase of the population, the development of industry, the growth of the standard of living, etc. After the earthquake, Skopje was built according to the new urban plan, which provided for new commercial contents due to the demolition of the former ones. - were basic elements to update the construction of new commercial spaces, in conditions of reduced capacities after the demolition of the buildings and due to the clearing of the commercial spaces for the realization of the urban plan in the central city area." (Arsovski 1981: 32) .

GTC was officially put into function on April 27, 1973 year. It has a total area of 149,530 m<sup>2</sup>, of which 30,966 m<sup>2</sup> are for trade, 2743 m<sup>2</sup> for hospitality and other contents. Over the years, the type and size of the stores have undergone several changes, especially the privatization of parts of GTC.

In 2005, "Ramstore Mall" was built in our country, the first indoor shopping center with world standards, of a closed type, which creates new neoliberal habits in society. Since it is the first of its kind in the entire country, society has accepted it as a luxurious, extravagant, futuristic, post-modern facility with high standards. The facility was visited by people from outside Macedonia as much as possible. This modern shopping facility works towards modernizing retail and changing the concept of consumerism in society, a phenomenon that could not happen during socialism. From the old bazaar, in the department stores, GTC to the new closed shopping facilities, the transitional changes are clearly noticeable. From controlled production and premises, to uncontrolled production, trade and purchase, i.e. consumption.

The proliferation of modern indoor commercial facilities in R.N. Macedonia continued its rapid emergence throughout the last decades. "Vero Center", a new commercial building opened in 2010 in Skopje, with an area of 40,000 m<sup>2</sup>. The next large shopping center "Skopje City Mall" opened in 2012 in the city of Skopje, among the large shopping centers in the region, and the newest "East Gate Mall" with international standards, with 168,000 m<sup>2</sup>, put into function in 2021.

## 7. THE INTERACTION BETWEEN CONSUMERISM AND ARCHITECTURE - RESULTS

This research will analyze the impact of consumerism on public interiors, which become ephemeral over time. Under the theoretical perspective and academic research done so far, there are several factors in design and architecture, which are a response to consumerism and current changes and current events.

The main factors that make a shopping center more visited are the visual atmosphere, physical comfort in that environment, spatial structure and business plan (Yuan et al, 2021). Based on several studies and researchers, Yuan lists specific influencing elements that create interaction between consumers and interior design: focus on a theme focus, variety of products and services, space ratio, visibility through space, space accessibility and identification in space. Next elements that are also important are music and fragrance, lighting and internal optimal temperature. Consciously or unconsciously, when people visit closed shopping centers, they are influenced by the architecture and interior design. Especially the design of the interior atmosphere, which includes elements such as decoration, color, materials, signs through signs for information and marketing (Andreu et al, 2006:559-578).

The mentioned factors, through a qualitative table, show the real situation and the changes from the 70s to today in the public interiors in Skopje.

**Table 1:** Qualitative comparison table of GTC and postmodern shopping facilities in Skopje

<b>Ord. No.</b>	<b>Factors</b>	<b>GTC (1973)</b>	<b>GTC (2023)</b>	<b>Modern shopping facilities in RSM</b>
1	Theme focus	There is not <b>no</b>	There is not <b>no</b>	There is <b>yes</b>
2	Variety of products (services)	Yugoslav and European trademarks <b>yes</b>	Several international brands <b>partly yes</b>	There is <b>Yes</b>
3	Spatial ratio (width, length, height in stores)	Yes <b>yes</b>	Stores have been resized multiple times for current and individual needs <b>partly yes</b>	There is <b>Yes</b>
4	Visibility through space	There is <b>yes</b>	There is <b>yes</b>	There is <b>Yes</b>
5	Appropriate approaches and	6 approaches, the center is open	6 approaches, the center is open	2 to 3 entrances <b>partly yes</b>



	communications	Yes	Yes	
6	Identification in space – landmarks, marketing	In the entrance name of the store, less through the promenade <b>7Partly yes</b>	With the opening of new chain stores, advertisements and signs are added in front of the store and along the promenade <b>Yes</b>	There is <b>Yes</b>
8	Decoration, color, materials	Concrete and white color, partially or fully glazed windows, seating tables and greenery in the terraces <b>Partly yes</b>	Concrete and white paint, partially or fully glazed windows, tables for sitting and greenery in the terraces, tables for sitting in the walkway, kiosks, points, ATMs, etc. <b>Partly yes</b>	Clean walls with light colors, high transparency, fully glazed windows, with urban equipment, greenery, decorative installations, kiosks, stalls, etc. <b>yes</b>
9	Lighting	Artificial lighting in the shop windows and interior of the shops, natural lighting from the gallery and the open roof <b>yes</b>	Artificial lighting in the windows and interior, natural lighting in the promenades, the gallery and the open roof <b>yes</b>	Organized amount of natural and artificial lighting, above promenades and gallery natural lighting, artificial lighting inside stores <b>Yes</b>
10	Internal optimum temperature	GTC is an open facility, it has built-in air conditioning in the shops, natural ventilation and lighting in the walkways. Cool in summer, cool in winter. <b>Partly yes</b>	GTC is an open facility, it has built-in air conditioning in the shops, natural ventilation and lighting in the walkways. Cool in summer, cool in winter. <b>Partly yes</b>	Closed facilities, with built-in air conditioning and internal optimal temperature control <b>Yes</b>

*Yes, mostly yes, partly yes, no, mostly no, partly no*

Description of key factors:

**Factor 1 – Theme focus**– we are talking about a content topic towards which the architectural project, the interior design and the overall management organization are moving. GTC is an older facility that today does not have a specific theme, but each space/store functions independently. The administration manages the letting of shops that are under their authority (30%), maintenance of the building as a whole, but the majority of the premises have private owners. GTC from before the construction is planned to be incorporated into the landscape of the city and to satisfy the basic shopping needs of the citizens, but also beyond. In contrast to modern closed shopping facilities, they are built for profit, with pre-organized managerial and business plans, with specifics of certain target groups, eg: organizing various events for the purchase of certain items for a certain group, by establishing a time period.

**Factor 2 – Variety of products and services** – GTC has mixed content. On floor -1 opposite the very busy Vero supermarket, there is a smaller old grocery store which is also very busy! There are old leather shops, an old traditional patisserie that always has loyal customers, small shops with specific clothes, which still attract certain social groups! The ground floor is more active, with older stores and new chain stores, but also empty. The first floor is partially used and the last floor less used, there are more empty rooms in the last floor. Modern indoor shopping centers have a wide variety of products and services, specially arranged by content and location.

**Factor 3 – Spatial ratio** – The internal spaces in the GTC have undergone changes in terms of sizes from the moment of construction until today. The promenade was open and clean in the 70s, today it is full of advertisements of chain stores, ATMs have been established, content has been established "not in its place", details that affect the overall aesthetics and function. The premises range from 3 m<sup>2</sup> to 5000 m<sup>2</sup>, i.e. 3 department stores, 1 hypermarket, 1 carpet fashion house, several larger or smaller specialized shops for textiles, clothing, children's clothing, sports equipment, shoes, leather goods, furniture, appliances, etc., catering spaces, service crafts, banks and representative offices, rest and recreation area, bowling alley, cinema, disco club, etc. (Tihomir 1981:64). Big changes are seen when closing old and opening new stores, changing windows and interior design, dividing a larger room into several smaller rooms, etc. Changes have also taken place in modern closed shopping facilities, but in the form of a change of owner and supermarket brand, opening of a new store due to the closing of an old one, changing of windows and renovations.

**Factor 4 – Visibility through the space** – GTC is an open facility, with natural ventilation and lighting. The windows are fully glazed, with 10 cm glass. In addition to lateral natural lighting, there are lighted atriums overlooking the promenades on all floors. The closed shopping facilities have the same concept, with central openings or atriums, with wider views towards larger lighted rooms. Modern indoor contemporary shopping centers have wider rooms, horizontally and vertically.

**Factor 5 – Adequate accesses throughout the space** – GTC has 6 main entrances throughout the facility. This configuration allows people to pass through the GTC without the intention of purchasing, but only passing from one side to another. Such a benefit increases the possibilities of high frequency and increasing economic benefits. Over time, additional doors have been added to the shops, so that they can have an exit to both promenades! In a parallel analogy, closed shopping centers have a different concept - consumers visit them with a prior plan! Such closed facilities usually have fewer entrances, in order for consumers to stay inside for a longer time and spend more.

**Factor 6 - Identification in Space - Features and Marketing** - Marketing is the most important component in labor, especially in capitalism. In 1973, GTC had no other advertising material except in front of the entrance to the store. Today, there is advertising material in front of stores, in large quantities in chain stores and in smaller quantities in private individual stores. In GTC, there are advertisements and signs in exact locations in certain places and rooms, but they differ in format, design and appearance, which still creates disorientation and avoids a holistic aesthetic. The closed shopping centers in Skopje have a preconceived organization of marketing in the interior and in the entire facility. The locations of the premises are marked by brand or function, which allows consumers to move easily.

**Factor 7 – Decoration, Color, Materials** – the architectural concept of GTC is the clean, modern, straight form, realized with concrete. The concrete is painted white, in some places blue. The decoration follows in the windows, almost every store has its own trademark and concept. Decorative elements are the concrete stairs, greenery on the terraces, tables for sitting on the terraces and the promenade, glass windows, etc. The floor is with gray tiles, through the walk you can see certain advertisements of the existing novelty shops. Closed shopping centers as a decorative element have certain three-dimensional installations, greenery, urban equipment and thematic temporary decorations – novelties, for example a new product, a new installation, new characters at specific temporary events, etc.

**Factor 8 – Lighting** – the GTC is more dominated by natural lighting, due to the fact that it is open and there is a breakthrough of natural lighting and ventilation. It is also used overnight until 24 hour, and for safety reasons every floor must be lit at night. The new indoor malls close at 10pm to the public and are not accessible until the next morning. They are always illuminated during work, with natural and artificial lighting. Special attention is paid to the type of lighting, as a key detail for increasing luxury and attractiveness.

**Factor 9 – Indoor Optimum Temperature** – GTC has an indoor common air conditioner, which operates in every space/store. The air conditioner does not work in the walkways, because they are open. In GTC there is no optimal temperature throughout the four seasons due to the openness of the facility. Otherwise, during the summer you feel a fresh temperature, during the winter a cooler temperature. The new closed shopping centers have built-in air conditioners to maintain an optimal temperature in every season and time.

## 8. RATIO BETWEEN STOREFRONT AND INTERNAL CONTENT

The presence of modern trade in Skopje can be found before the world wars, and in addition to domestic goods, there were also industrial and European goods in the city, with a significant turnover. After the Second World War, the massive construction of the city begins, GTC confirms the presence of beautiful modern architecture.

The shop window represents an aesthetic facade where the first contact between the product and the customer is created. The aesthetic arrangement of the shop window "proves the novelty and innovation of the consumer culture of that period" (Lasc et al, 2018:22). The rapid expansion of retailing creates a variety of products and competition. The famous shops with their glamorous windows were in the promenades under the arcades along the city squares. The old bazaars in the east also have a different configuration, but the storefront was always developed under the same concept: artistic and aesthetic arrangement with the aim attraction of consumers for more sales.



*Figure 3: Promenade GTC 1976*



*Figure 4: Promenade GTC 2023*



*Figure 5: Promenade in a shopping mall*

The shop windows in GTC were specially maintained. Each sales and service space had a transparent glass facade, with a detail of glass prisms by the entrance door. Today in GTC, the glass of the shop windows has been replaced with new, more sophisticated glass hanging in aluminum frames,

and the glass prisms have been removed. The window decoration was simple with less products on it, less decoration and lighting, clean lines and not overloaded. Advertising material compared to today, was in much smaller quantity. In picture no. 6 you can see the prisms by the door, picture no. 7 crystal shop window and picture #8 window of a children's store. The window in the crystal store had glass shelves in a metal structure, on which products were displayed. In the children's window, a "sequence of a children's story" is shown, behind which you can see the products arranged in metal/plastic shelves. The technology and materials used to make the public furniture of GTC after opening, was simpler compared to today's technology. Attention at that time was devoted to the product.



*Figure 6: Interior in GTC 1976*



*Figure 7: Shop window 1976*



*Figure 8: Children's shop window 1976*

The furniture in the interior of the GTC when it opened was made of wood made of panel wood material, chipboard with a veneer finish, for easier maintenance the wood was covered with glass in the upper surface. The glass in the role of transparent shelves was used that hung on a metal or wooden structure. Apart from the role of construction, the metal also appears in the pictures as a decoration.



**Figure 9:** Interior of a jewelry store GTC 1976



**Figure 10:** Interior of a jewelry store 1976



**Figure 11:** Interior of a homeware store GTC 1976

The lighting in the interior of the shops in the GTC was of the type of ceiling mounted led, waterproof lamp usually in the walkways, led panels, lamps built into rails and lamps. The lamps were mostly placed near the windows and internal shelves where the products were arranged (fig. 10 and 11).

Today in GTC the interior has been completely changed, from the glass of the window and completely inside. With the opening of new chain stores that have their own authentic concept of products, advertisements and interior decoration, the interior rooms of the stores are designed under postmodern standards. Otherwise, there are also individual retail stores with a simpler look of the interior. The differences can be seen in pictures number 12 and 13.



**Figure 12:** GTC 2023 retail store window



**Figure 13:** Shop window of the GTC 2023 chain store

Today, the lighting in the GTC above the promenades remains the same, and in the shops, postmodern lighting concepts follow. The internal public interior today is the most different and completely replaced by a new one. Chain stores have their authentic furniture, as in each of their branded stores, and other ordinary retail stores pay less attention to furniture and more to products.

Closed modern shopping centers today in Skopje are full of branded stores, whose interior has a unique concept that follows in every store all over the world. You can also notice the rapid time change of the same trademark, when the windows change very often, the order of the products as well, and two stores with a year difference in opening, although designed in the same concept, always introduce novelties.

Closed shopping centers have several types of lighting, depending on the space where they are placed and the function they perform. Above the walkways there is natural lighting and additional moderate artificial lighting built into the suspended ceilings. The shop windows are more intensively lit.



**Figure 14 and 15:** Interior of a shop in a contemporary square center,



**Figure 16:** Shop window in a contemporary trade centre

The architecture and design of public buildings has obviously changed over time. Today's image is a symbiosis of the rapid development of technology that enables the realization of beautiful details in the interior; advance planning of multidimensional management of public commercial premises and creation of a theatrical, hedonic atmosphere. Perfection, harmony and futuristic environments provide great pleasure when visiting, a person feels part of that "show". In parallel, the architecture and design developed with the standard and the possibilities to reach the top - increase in profit and sales.

Store design has been linked to consumerism as one of its "...key engines" ( Thorpe 2012:2). Because design and architecture are promoters of improvement and advancement of society. The definition of ephemerality in architecture is as follows: "A class of building designed to be distinguished by impermanence, and its physical departure from the site" (Chappell 2004: 4). Since the definition refers to an architectural object, would the same apply to interior design, remains to be confirmed.

The term "ephemera" or "ephemerality" is an international term used in literature in several languages. The word comes from the Greek language which means "lasting only one day" (Merriam-Webster dictionary). Time always encourages changes and the process of defining the duration of an architectural space is complex. Time taken from an objective sense would be the physical duration of the object/product, or the "warranty". But time measured in a subjective sense would be more difficult to define. Chappell says that no one can say with authority what constitutes the 'short life' of an object. The determination of time in ephemeral architecture depends more on the expectations and intentions for which it was created, consequently, "... ephemeral means a short existence in terms of our expectations and the intention of the designers." (Chappel2004 :16).

## 9. CONSUMERISM AND HUMANITY

So far, a lot of research has been done regarding the emotional side of consumers, which is connected to all important economic developments and benefits of buying and selling. Shopping is no longer a short act of exchange, but much more than that – a pleasurable experience. It is a mental behavior of an acquired experience of consumption that can be positive or negative, the nature of which can involve a symbolic, cognitive, utilitarian or social dimension (Boustani, 2020:88).

Boustani also describes the interaction that is created during the buying process. "- Experience is a set of results whose memory is generated by an interaction between a person and a consumed object, in a given situation: person + object + situation ." (Boustani 2020:88). Consequently, the person and the individual "I", which is changeable throughout the course of life; the object or product is diverse and the situation is created in the space, which inevitably affects the consumer. Here the complex relationship between consumption, architecture and design is concluded.

But the individual "I" is also under the impact of society: under the effect of social networks, it is difficult to imagine the consumer as a "rational individual", and the choice in the market is not completely free ( Thorpe 2012:21) .Man was always under pressure from that wide circle of society where he acted, and today he is under pressure from the whole world! "- Social media has changed the way people communicate, collaborate, exchange and connect with others." (Boustani 2021: 94).

As a result of all the benefits, Thorpe gives the following thought: “-Increasing consumption in this respect improves satisfaction, but only up to point A, and maintaining satisfaction requires moving to new areas of stimulation and novelty. This constant escalation really indicates gluttony.” (Thorpe 2012: 60). Subjective well-being is an internal emotion that has no measure, and creates a contradiction with material reality, which does not actually lead to real economic well-being. In the growth of economic well-being, a person moves from one position of society to another position with higher standards, and as a result, "...in the face of positional consumption, high-quality public goods and public spaces are a central component of "development" (as opposed to just "growth") in affluent countries where there are no shortage of goods, and "positional consumption" is the dominant form of consumption." (Thorpe 2012: 61) . Sociologists use the sentence "from a society without reason to a society without a heart", a sentence that describes the transition from a system with a non-market economy to a system with a market economy (Aceski 2002: 30).

## 10. DISCUSSION

The quantity of consumerism in Macedonia in the former Yugoslavia was standardized. Organic production, guided by norms and standards, created organic and one-way consumption, while society was monotonous.

GTC is a landmark of the city with half a century of existence, through which a large number of people pass daily, who do not always make an act of purchase. When walking through this building, you can see empty shops waiting for a new owner. The object is active and as a result of the above qualitative table, it contains all the components of a modern shopping center, and its open configuration allows GTC to be "... an integral element of the new city pedestrian axis traced by the plan of Tange" (Vaseva, Jovanovski 2014: 26-27).

GTC got a different image due to the privatization of the majority of the premises, when the owners independently manage their retail space for their individual profit, with minimal obligations to the management of the facility. The appearance of GTC begins to lose its original weight: the components of privatization, globalization, actuality and competitiveness meet here! These components, derived from today's current economy, are inappropriately stacked on top of each other within the same spatial boundaries, creating disharmony.

On the other hand, the new closed shopping centers in Skopje brought a new shopping culture. As the city grows, there is an additional need for the proliferation of commercial content, and globalism is inevitable. Trade facilities in Skopje do not only meet the needs of that city, but reach a regional dimension. The new commercial facilities remained a great attraction for the citizens; the luxurious premises are aesthetic, the innovations in technology and production, and due to the various organized events, consumers go through euphoria and great attraction, which acts to forget the daily tension.

The phenomenon of ephemerality in the interior of retail stores is a new phenomenon in recent decades in the world, especially in RN Macedonia. Contact with global brands and Macedonian society gives a sense of belonging in the postmodern world. The aesthetic appearance and the opportunities to be a part of it result in a positive and beautiful feeling, which is why they are often visited especially by teenagers and middle-aged people. The ephemeral in public architecture is also a spatial element of the marketing of a branded commercial store with a profit goal.

## 11. CONCLUSION

Ephemeral architecture has become a very immanent topic in recent decades. In particular, it is becoming very common and through the interior as the most important tool of marketing, for ultimate economic benefits. It appears through architectural objects, which last for a short time and have a specific purpose, and it also appears in marketing stores, which also last for a short time with a pre-determined mainly economic purpose.

Man was created toward beauty and aesthetics, he feels it with his all senses, always seeking to become a part of it. This format of stores has long been present in Europe, mostly in shopping facilities. With globalism, the often changing public interior has also appeared here, in closed commercial buildings, a phenomenon that has brought a new era of consumerism in our society.

The research is based on an analysis of GTC, as the first modern shopping center in Skopje, its architecture and interior once and today, with a parallel comparison with today's new shopping centers. The qualitative table, the images of the interior public arrangement in 1973 and today, in addition the comparison of the new shopping facilities, once again brings us to the conclusion that today's modern closed shopping centers are an imitation of the square, the promenade and the arcades. The storefront and the interior design of public spaces move under the same concept, with an effort to create a beautiful human experience with the environment, the storefront and the product.

Over the years, the process of interior public decoration has been raised to a higher level, due to the development of technology, various building materials and the possibilities of interior decoration. The feeling created in a person when visiting these environments becomes great and strong, which makes a person make unreasonable purchases, regardless of the value of the object. Unreasonable spending is a consequence of excessive production, which in recent times often destroys all norms and standards.



Consumerism is becoming the most important tool for economic development in the 21st century. Architecture and design are highly affected by this phenomenon, which manifests itself in society through major changes. With frequent "timeless" changes (because changes happen much more often than the real need), architecture and interior design become ephemeral - temporary, transient and short-lived.

Architecture together with design are multifunctional applied sciences, which create and arrange the space for life and work. Since buying and selling in the past was done in a simpler way compared to today, it can be concluded that the architecture of commercial spaces is eclectic. Zevi interprets eclecticism from a social and economic aspect as an architecture of industrial expansion (Zevi 2013:175). Zevi explains about the necessary comfort of the societies from the architecture throughout different centuries, which comfort has not essentially changed from the aspect of human subjectivity.

The positive effect of this subsequent phenomenon is enthusiasm, casualness, multi-functionality and well-spent leisure time in aesthetic architectural mediums. While, the negative effect is that consumption knows no more boundaries, people spend senselessly and the value of material goods is lost.

If it is concluded that voracious consumerism creates problems on value and identity, from the perspective of architecture and design, are frequently changing interiors benevolent? Or what would a non-commercial design look like? Would it even exist? With the over-indulgence of luxury stores, new groups of people have come up with new ideas of using recycled and sustainable materials. Such materials have appeared in the interior design in a short time, as details through covering walls with sustainable materials! New environmental design norms have even been added. And whether this will contribute to stopping excessive consumption and returning to true values, remains a new field of future research.

## REFERENCES

- [1] Adam, Robert. (2012): *The Globalization of Modern Architecture. The Impact of Politics, Economics and Social Change on Architecture and Urban Design since 1990*. Cambridge Scholars Publishing. Newcastle, UK.
- [2] Baudrillard, Jean. (2020): *Shoqëria e Konsumit. Mitet dhe strukturat e saj*. Logos A. Shkup.
- [3] Coleman, Petar (2006): *Shopping environments: Evolution, planning and design*. Architectural Press, Oxford.
- [4] Chappel, Bryan (2004): *Ephemeral Architecture – towards definition 3*.
- [5] Petermans, Ann & Anthony, Kent (2017): *Retail Design. Theoretical Perspectives*. Routledge. New York.
- [6] Boustani, Ghalia (2020): *Ephemeral retailing. Pop-up stores in postmodern consumption era*. Routledge Taylor and Francis Group. New York, USA.
- [7] Boustani, Ghalia (2021): *Pop-up Retail..The evolution, application and future of ephemeral stores*. Routledge Taylor and Francis Group. New York, USA.
- [8] Zevi, Bruno (2013): *Si ta kuptosh arkitekturën. Shtëpia botuese DITURIA, Tiranë*.
- [9] Tonovski, Gjorgji (2008): *Sociologija, FON - Univerzitet, Skopje*
- [10] Yuan, Ye., Gang, L., Dang, R., Lau, S.S.Y., Qu, G.(2021): *Architectural Design and consumer experience: an investigation of shopping malls throughout the desing process*. Asia Pacific Journal of Marketing and Logistics. China.
- [11] Pomodoro, Sabrina (2013): *Temporary retail In fashion system: An explorative study*. Journal of fashion marketing and Management: An International Journal, pp.341-352.
- [12] Janakov, Blagoja: *Za vlijaniето na potrošuva koto opštество vrz li nosta*, Univerzitet Sv. Kiril i Metodij, Filozofski fakultet, Skopje
- [13] Nikola, Kljusev (2002): *Ekonomijata na Makdonija vo tranzicija (Problemi, Dilemi, celi), Makedonska akademia na naukite i umetnostite, Skopje*
- [14] Tokarev, Mihail (2006): *100 godini moderna arhitektura, Pridonesot na Makedonija i Jugoslavija (1918-1990)*
- [15] Chandler, S. (1995): "Where Sears wants America to shop now", *Business Week*, Vol. 12, p. 39

- [16] Andreu, L., Bigne, E., Chumpitaz, R. and Swaen, V. (2006), “How does the perceived retail environment influence consumers’ emotional experience evidence from two retail settings”, *International Review of Retail Distribution and Consumer Research*, Vol. 16 No. 5, pp. 559-578.
- [17] Mau, Gunnar; Schweizer, Markus (2006): *Multisensory in Stationary Retail. Principles and Practice of Customer-Centered Store Design*. Springer, Germany.
- [18] Arsovski Tihomir, Gavruk Gavrilski, Stojkov Trajko, (1981): *Gradski Trgovski Centar, Osnovna zaednica za deloven prostor*, Skopje
- [19] Thorpe, Ann (2012): *Architecture design versus Consumerism. How design consumerism confronts growth*. Routledge, London & New York.
- [20] Petermans, Ann & Kent, Anthony (2016): *Retail Design: Theoretical Perspectives*. RoutledgeTaylor and Francis Group. New York, USA.
- [21] I. Lasc, Anca; Betancourt-Lara P.; Maile Petty M (2018): *Architecture of Display. Department Store and Modern Retail*. Routledge, Abingdon, Oxon and New York.
- [22] Vaseva Ivana, Jovanovski Filip, (2014): *111 Tezi za GTC*, Skopje
- [23] Aceski Ilija, (2002): *Opšttestvoto i ovekot vo tranzicija (tret del)*, Filozofski fakultet, Skopje
- [24] Naumovska Senka, Šopov Ivan, (2014): *50 godini od zemjotresot vo Skopje*, Skopje Anti ko ili moderno, Nacionalna Univerzitetska Biblioteka Sv. Kliment Ohridski, Skopje

## THE INFLUENCE OF PARTICLEBOARD SQUARENESS ON THE EDGE BONDING QUALITY

Igor Džini, Tanja Palija,

University of Belgrade, Faculty of Forestry, Serbia  
e-mail: igor.dzincic@sfb.bg.ac.rs; tanja.palija@sfb.bg.ac.rs

### ABSTRACT

This paper shows the influence of the squareness of wood-based panels on the quality of edge bonding. Edge bonding of wood-based panels can be done by applying different types of adhesives and using different types of edge materials. The number of factors that affect the quality of bonding is large. Analysis of wood-based panels squareness after processing by pre-cutters, as well as the position of the roller for applying glue to the panels, was analyzed. The static analysis showed that there is a significant influence of the measured parameters on the strength of the edge bonding quality. Variation of the observed factor, leads to a change in the quality of the bonding quality. The highest strength of the glued joint was shown by the samples with the smallest angular deviation of the edge to the wider side of the panel. The minimum strength that the edge bonding should require are not defined by the standard.

**Keywords:** wood-based panels, edge bonding, squareness, internal bond

### 1. INTRODUCTION

Edge bonding refers to the process of gluing of edge material to the narrow sides of wood-based panels. Covering the narrow sides with edging material can be done before or after covering the wider sides of the panels (by coating or lamination processes), depending on the aesthetic effect that should be achieved. In the modern wood industry, the process of covering the narrow sides of wood-based panels is carried out on automatic edge banding machines using hot-melt adhesives. The basic characteristic of hot-melt adhesives, which qualifies them for this type of bonding, is the lack of evaporative components, so hotmelt adhesives harden by cooling, which makes them suitable for joining different types of the materials. The gluing process set up this way is very effective both from productivity point of view of, as well as from aesthetic requirements and achieved durability during the use of the product. Depending on the shape of the board and its profile of the narrow side, we distinguish the covering of: boards with a prismatic base, linear line and flat surfaces, boards with a curved base, linear line and flat surfaces, and the boards with a prismatic base, linear line and profiled surfaces (soft forming procedure). The technological process of covering the narrow sides of the boards can be carried out on all types of wood-based boards: solid wood panels, fibre and chip wood panels (chipboards, fiber boards and composite boards), layered wood panels (panel panels, plywood panels). The edging material that covers the narrow sides can be of natural or synthetic origin. The edges can be covered with solid wood up to 25 mm thickness, veneer, PVC, ABS, HPL and CPL tapes. Depending on the type of base (panel), the type of edging material, as well as the resistance requirements during exploitation, three types of adhesives can be applied: ethyl-vinyl-acetate adhesives (EVA), polyphenol-based adhesives (PO), isocyanate adhesives known as reactive polyurethane binders (HMPUR).

The quality of edge banding depends on a large number of factors that have been investigated by a number of authors. According to Jianhua et al (2017), as well as according to Miškinite, , Juknelevi ius, (2021), the quality of the glued connection is influenced by the following factors: properties of the panel, properties of the glue, properties of the edging material, angularity of the bords and gluing parameters. According to previous researches (Iuanet al, 2011; Ven, et al, 2012), bonding quality is influenced by the gluing parameters (glue temperature and method of application), panel

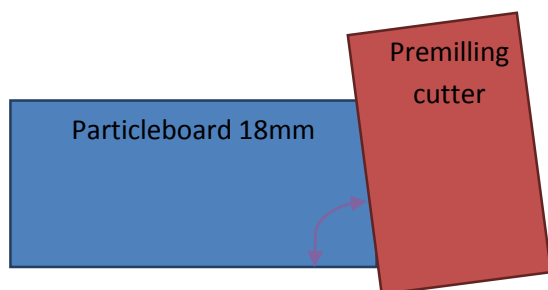
moisture (Sacli 2015), as well as the feed speed of the panel in edge banding machines. In their work (Tankut Tankut, 2010) explained the correlation between pressure and tension forces on adhesive tapes and quality of furniture. The paper proved that a clear correlation between the thickness of the tape edge and the joint strength could not be determined.

In MMS (micro-medium-small) companies, because of deformation of the boards due to inadequate storage conditions (cold flow of the boards), as well as the lack of levelling of the machines, the loss of squareness and edge straightness can affect the quality of the gluing between edging material and panel. A part of these problems is addressed in the work of Zhang et al (2007), where the permissible size of angularity deviation is not clearly defined. On the other hand, the standard that regulates this subject (EN 324-2) defines the method of measurement, while the permitted deviations are only partially defined. Namely, the standard defines permitted deviations in terms of squareness on the wider side, but not in relation to the thickness of the board. In order to better understand the influence of this parameter on the quality of the glued connection, the influence of the squareness of the board on the quality of the glued connection was analysed when lining the narrow sides of the particle board. The subject of his research particleboards coated with melamine foil and aligned with PVC edge band, these are the most commonly used materials in MMS companies.

### 3. MATERIAL AND METHODS OF WORK

The test was carried out on samples made of three-layer particleboard (18mm thickness) covered with melamine foil, from a renowned manufacturer. According to Jianhua et al (2017) the quality of the edge bonding will depend on the density of the board (EN323), moisture content (EN322) and delamination strength of the layers (EN319). The properties of the particleboard from which the samples were made were not investigated, but the properties of the material were considered to correspond to the data provided by the manufacturer (Freehart, and Hunt 2010). The samples were taken from the manufacturer's warehouse fifteen days after the production process, so that longer storage of the samples in the warehouse space was avoided.

Before edge bending process, the samples were cut to certain dimensions on the beam saw. The samples for this test were taken from the middle of the boards and their dimensions were controlled according to the EN 324-2 standard. The test was performed on samples with dimensions of 600x300x18mm. Before edge bending process, the samples and the edge material were conditioned for 7 days in controlled conditions of relative air humidity ( $50\pm 5\%$ ) and temperature ( $20\pm 2^\circ\text{C}$ ). In order to simulate the loss of squareness of wood-based panels, the premilling cutters on the edge ender machine were excluded from processing. Before gluing the edge material, the samples were processed on a moulders joinery machine, where the  $90^\circ$  angle was reduced by 2 or 4 degrees, figure 1. The processing was carried out using a DP tipped cutterhead with alternate shear angle at the following processing parameters :feed speed of 12m/min; cutting depth of 2mm; revolutions per minute of 9000 rpm..



**Figure 1:** Inclination of the edge towards the wider side

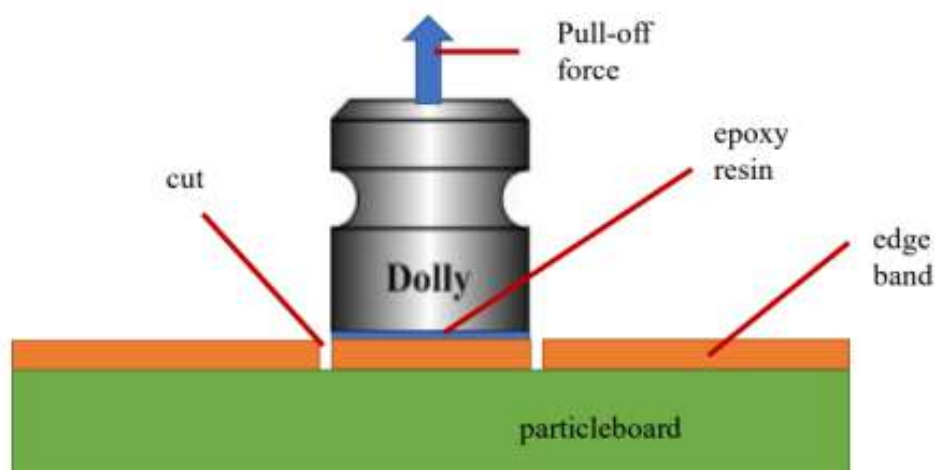
Table 1 shows the angles, the size of the resulting gap, as well as the processing accuracy class according to DIN 68101.

**Table 1:** Overview of samples by groups

Group label	Angle deflection	Gap size	Accuracy class acc DIN68101	No.of samples by group
1	2	3	4	5
group 1	90°	0	/	20
group 2	88°	0.6mm	TD40	20
group 3	86°	1.3mm	TD100	20

After processing on a moulders joinery machine, a ABS edge band, with dimensions 22x3mm, was glued to the samples, using Kleberit's EVA glue (HotMelt 774.4). Gluing was performed on an automatic edge banding machine with roller application manufactured by Biesse at the following gluing parameters: glue temperature: 210°C; application quantity: 110g/m<sup>2</sup>; feed speed: 15m/min). Within each group, 20 samples were made, a total of 60 samples for the entire test.

After gluing the edge material, the samples were conditioned for 5 days under the same conditions as before processing. Methods of testing the strength of the glued connection between the panel and the edge material can be divided into two groups: tests that can be applied directly in production, and tests that must be conducted in laboratories. As part of this research, the samples were tested in laboratory conditions in accordance with the standard EN ISO 4624:2017. A pull off test was performed verifying the force required to detach the edge band from the panel. In addition to this part of the test, the effect caused by the pull-off stress on the edge band is also monitored. After conditioning, dollies were attached to the samples using a two-component epoxy adhesive. Dollies were placed 200mm from the face of the board to avoid undulations during milling, which could affect the test result, Figure 2.



**Figure 2:** The sample with the dolly

The dollies was placed on each sample (two dollies). Considering that the diameter of the dolly was 20mm, and the thickness of the plate was 18mm, the contact surface under the dolly was recalculated (from full circle) to the surface of narrow side of the board covered by dolly. The samples were tested for tension on a universal tearing machine by applying a force that was constantly and evenly increased to the point of separation of the edge material from the board. The load speed on the device was about 0.5N/sec.

#### 4. RESULTS AND DISCUSSION

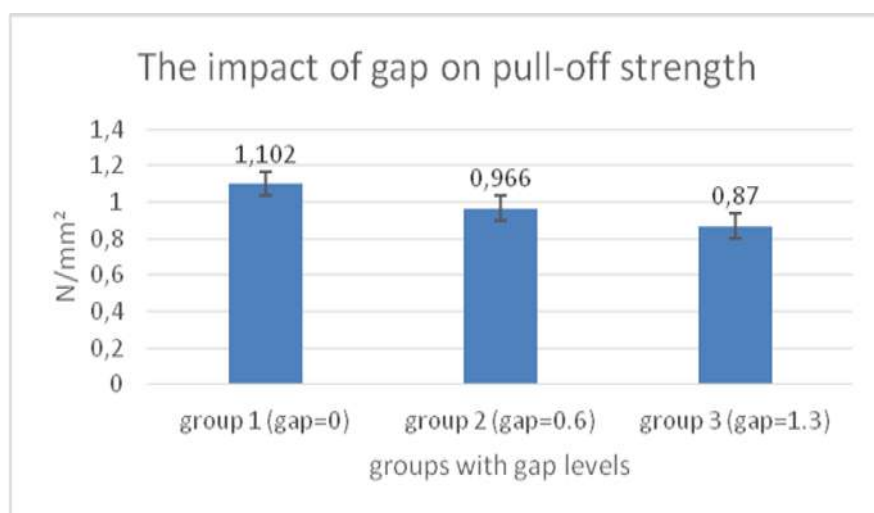
The samples were divided into three groups. The first group represents the control group where there was no deviation of the angle in relation to the wider sides of the board. During the statistical analysis of the given data, the SPSS v.20 program with the basic data package was used. Table 2 provides some basic data of descriptive statistics for the mentioned samples.

*Table 2: Descriptive statistics by sample groups*

group label	Average (N/mm <sup>2</sup> )	Max/min (N/mm <sup>2</sup> )	Standard deviation	Variance
1	2	3	4	5
group 1	1.102	1.21/0.05	0.055	0.00045
group 2	0.966	1.05/0.88	0.03	0.0018
group 3	0.87	0.95/0.8	0.02	0.0008

By analysing the normal distribution, the Shapiro-Wilk test showed that all groups met the basic requirement of normality, which enables further statistical tests (. After confirming that not all groups are subject to a normal frequency distribution, an analysis was performed using a t-test to determine whether there is a significant difference in the variances between the groups, i.e. whether the size of the gap (loss of squareness) affects the final strength of the glued connection. Further analysis revealed that there was a difference in the variances between the groups. Using Levene's Test for Equality of Variance, it was established that there is an Equal variances assumption.

Based on the obtained results of the size of the strength of the glued connection, it can be seen that the highest mean tear value was obtained by control group 1, where there was no slope between the narrow and wide sides. The average value is 1.1N/mm<sup>2</sup>. A slightly lower value was shown by the samples of the second group, where the gap was made at a 2° slope. It is interesting to note that an inclination of 2° creates a gap of about 0.6 mm on average. According to the manufacturer of the glue, EVA glues allows a greater layer thickness and can fill the resulting gap without any problems. However, from the point of view of joint strength, the joints of the second group gave less strength by about 12%. The lowest value of the strength of the glued connection was obtained from the samples of 3 groups where the joint was made at an inclination of 4°, i.e. with a gap of 1.3 mm on average. The joints of this group gave lower strength by about 30% compared to the first control group, figure 3.



*Figure 3: Mean values of adhesion strength of glued edge band according to groups of samples*

Characteristic damage after testing is shown in figure 4. In the case of samples of the first group, it is clearly visible that the damaged glued joint occurred along the gluing line. Within sample of first group during removing the dolls, the whole edge band was removed together with some chips from the panel. In contrast to the samples of the first group, on the samples of the second and third groups, you

can see uneven layers of glue, which are caused by the size of the gap between the edge material and the application roller. Damages recorded on the samples of the second group (where gap was around 0.6mm from one edge of the panel) shown that there are some tracks of the hot-melt adhesive, together with chips and stripes of the panel. Samples of the third group revealed even more tracks of hot-meld adhesive where quantity and position of hot-melt adhesive differed from sample to sample.



**Figure 4:** Characteristic damage of the samples after the test  
(from left to right, samples of group 1 to group 3)

Looking at the results presented on the graph in Figure 3, the influence of the factors on the gluing strength are clearly visible. With the increase of the gap and the angle under the slope between the narrow and wide sides, the strength of the joint decreases. The comparison of the obtained results with the data obtained by other researchers is hardly applicable due to the different values in which the results were expressed, and different testing methods. For example, the work of Miškinyte and Juknelevi ius (2021) conducted research using the peel-off test and expressed the results in N, while Jianhua et al, (2017), Zhang et al (2007), Yuan et al (2010, 2011), expressed their results in N/m although they also tested the samples through the peel-off test. In addition to this, the standard does not define the methods that regulate this area, nor are there any recommendations on the values that the joint should fulfil in the works. Also, this information is not available in the technical data presented by the manufacturer of glues for edge banding machines. Considering the lack of results, it can be concluded that this segment of the wood industry is not fully examined.

#### 4. CONCLUSION

This paper shows the influence of the squareness of wood-based panels on the quality of edge bonding. The number of factors that affect the quality of edge bonding is large. Analysis of wood-based panels squareness after processing by pre-cutters, as well as the position of the roller for applying glue to the panels, was analysed. The standard does not define methods that can be used to test the strength of the glued connection between edge band and wood-based panel, so the test was performed by pull off test according to EN ISO 4624:2017. A review of the available literature did not show much data on this type of adhesive bond.

The static analysis showed that there is a significant influence of the measured parameters on the strength of the edge bonding. Variation of the observed factors, leads to a change in the quality of the bonding strength. The highest strength of the glued joint was shown by the samples with the smallest angular deviation of the edge to the wider side of the panel. In real production conditions, the deviation of the squareness can occur with boards of larger dimensions if the auxiliary work table is further away from the of the edge machine, inadequate pressure of the upper conveyor or in the situation when the machine is not levelled. These factors should be the subject of a additional analysis.

The minimum strength required for the edge bonding of bands to narrow sides of wood-based panels is not defined by the standard.

## REFERENCES

- [1] Frihart, R.C., Hunt, G.C. (2010): Adhesives with Wood Materials, Centennial Edition, Forest Product Laboratory.
- [2] Jianhua, L., Li, J., Ming, C. (2017): Influence of Temperature of Applying Glue, Glue Dosage and Feed Rate on Peel Strength of Edge Band from Curved Edge Part. *Materials Science and Engineering* 274 012159 doi:10.1088/1757-899X/274/1/012159.
- [3] Miškinyte, U., Juknelevičius, R., (2021): Quality Research of Edge Banding of Unit Furniture. 16th International Conference: Mechanotonic Systems and Materials, doi:10.1088/1757-899X/1239/1/012014 .
- [4] Qi, Y., Xu, B. (2007): Effect of Lay-by Time on Panel Furniture Edge Banding Quality. *China Wood based Panel* (9) 16-18.
- [5] Sacli, C. (2015): The effect of time and edge banding type and thickness on the bending and tensile strength of melamine coated particleboard. *Research for Furniture Industry, Turkey/ Creative Commons Attribution*, p. 469–480
- [6] Tankut, A.N., Tankut, N. (2010): Evaluation the effects of edge banding type and thickness on the strength of corner joints in case-type furniture. *Materials and Design*, p. 2956–2963.
- [7] Yuan, N., Ding, W., Zhang, H., Zhu, Y.(2010): Peeling Properties of Edge Banded Parts of MDF. *Furniture China Forest Products Industry*. 37(6) 27-30.
- [8] Yuan N, Ding W, Wen W, Zhu Y, Zhang H (2011): Peeling Properties of Edge-banded Parts of Particleboard. *Furniture China Forest Products Industry* 38(1) 32-34.
- [9] Wen, C., Wu, Z., Zhang, J. (2013): New exploration of peeling method for plastic edge banding on panel furniture. *Furniture* 34(4) 22-25.
- [10] Zhang, J. Z.; Joseph, C.; Chen, E.; Kirby, D. (2007): Surface roughness optimization in an end-milling operation using the Taguchi design method. *Journal of Materials Processing Technology*. 184, pp. 233-239. DOI: 10.1016/j.jmatprotec.2006.11.029.
- [11] DIN 68101:2012: Fundamental deviations and tolerance zones for wood working and wood processing.
- [12] EN 324-2:1993: Wood based panels – Determination of dimensions of boards: Part 2: Determination of squareness and edge straightness
- [13] EN ISO 4624:2017: Paints and varnishes – Pull-off test



## INFLUENCE OF THE MATERIAL FROM WHICH THE PROFILE IS MADE ON THE FINAL QUALITY OF THE WINDOW

Elena Jevtoska, Gjorgji Gruevski

*Ss. Cyril and Methodius University in Skopje, North Macedonia,  
Faculty of Design and Technologies of Furniture and Interior-Skopje  
e-mail: jevtoska@fdtme.ukim.edu.mk; gruevski@fdtme.ukim.edu.mk*

### ABSTRACT

The window as a product used in construction aims to provide natural light and the possibility for ventilation in the building where it is placed but at the same time to protect the room from external influences such as wind and rain and to prevent uncontrolled cooling or heating of the building in which it is built-in. Given the purpose, a quality window is one that protects against air penetration, water penetration and provide wind resistance. The window is a complex product that is composed of different parts that can be made of different materials. As part of this research, windows constructed from profiles made of different materials (wood, PVC, aluminum) with approximately the same dimensions of the profiles will be tested. The same type of glass package will be built in every window. The goal is to prove whether the material which is used for making the window profile has an impact on the final quality of the window. To carry out the research, thirty windows will be tested of which ten are made of wooden profile, ten of aluminum profile and ten of PVC profile in accordance with European norms EN 1026:2016 (test method for air permeability), EN 1027: 2016 (water permeability test method), EN 12211:2016 (wind resistance test method).

**Keywords:** construction carpentry, window, air permeability, water permeability, wind resistance, PVC profiles

### 1. INTRODUCTION

The quality of one product is a characteristic worth being considered when it is proven that the same satisfies the needs for which it is produced. Having in mind that the purpose of one window is to provide light and desirable ventilation of a room, and, at the same time, to protect the object from external influences such as air permeability, water tightness and resistance to wind, we state that the window is of a higher quality as much as it can guarantee all these conditions. The window as a product is of complex content from diverse materials and parts. As different parts of the window we enlist the following below: Frame – the frame is a construction of the jamb and the construction of the side jamb.

Glass – the content of the construction that can be made of glass and glass packet.

Hinge – design, window handle, window lockers which offer the sliding of the window, meaning, the possibility for its opening and closing.

Throughout the production of window parts, different types of materials are used:

Frame – wood profiles from different types of wood, PVC profiles, aluminum profiles, as well as a combination of these materials.

Glass – one glass (4mm, 6mm), glass packet out of two, three or four glasses with different combinations of glasses layered with different protective paints.

Fittings – metal, plastic, rubber.


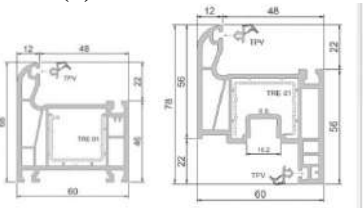

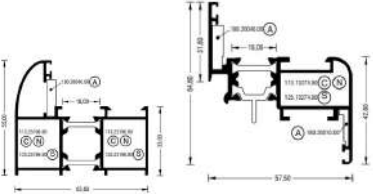


The field in which this research is directed is a current topic that is of great importance for analysis, especially in the field of the energetic efficiency. The heating and the cooling of one object is enabled through the energy consumption. The energy efficiency policy is an integral part of the politics in the field of energetics, economy, sustainable development and protection of the environment, and it is conducted through measures and activities for efficient energy use. When choosing windows, a great

attention is dedicated to how much they are going to protect the object from external influences and how much energy they are going to save.

**2. MATERIALS AND METHODS**

The samples which are subject of the research are 30 windows. Each group consisting of ten windows. All the samples’ dimensions are 800mm width and 1400 mm height. All the samples in the group are made of the same profile (Table 1). The samples that are the subject of this part of the research are 30 windows from 3 different types of materials. 10 windows are made of PVC profile, 10 windows are made of wooden profile and 10 windows are made of aluminum profile. The selection of profiles is made of approximately the same thickness and lower price. All windows are identical glazing with a double thermal insulation glass 4/16/4 mm.

**Table 1: Group of samples**  
Windows with dimensions 800/1400mm

Group	Picture of the sample	Profile of the sample
Group 1		<p>PVC profile KMG (1)</p> 
Group 2		<p>Aluminium profile ALUMIL M9650 (2)</p> 
Group 3		<p>Wooden profile</p> 

### 3. RESULTS

#### 3.1. Results of the air permeability

The testing of the air permeability is conducted with pressure and absorption of the different air pressure. The mean values for every group will be presented individually in a table and diagram, just as the class according to the EN 1026:2016 “Windows and doors - Air permeability - Test method” standard. [3]

**Table 2: Group 1 (PVC profile) – air permeability**

Pa normal		50	100	150	200	250	300	450	600	General class
Pa actual		50	100	150	200	251	302	450	605	
Air permeability	$\frac{m^3}{h}$	0.99	1.69	2.28	2.72	3.13	3.51	4.57	5.51	
Seam lenght	$\frac{m^3}{(h/m)}$	0.24	0.41	0.56	0.66	0.76	0.86	1.11	1.34	
Class		4	4	4	4	4	4	4	4	4
Window surface	$\frac{m^3}{(h/m^2)}$	0.88	1.51	2.04	2.43	2.80	3.14	4.08	4.92	
Class		4	4	4	4	4	4	4	4	4
										4

**Table 3: Group 2 ( aluminium profile) – air permeability**

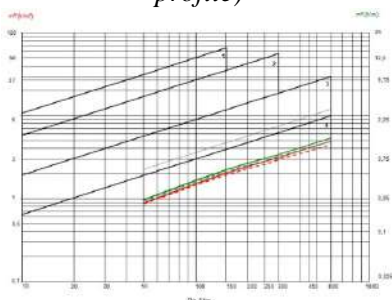
Pa normal		50	100	150	200	250	300	450	600	General class
Pa actual		50	100	150	200	215	300	449	600	
Air permeability	$\frac{m^3}{h}$	4.21	6.92	6.98	12.58	15.74	19.21	32.11	49.29	
Seam lenght	$\frac{m^3}{(h/m)}$	1.01	1.66	2.33	3.02	3.78	4.62	7.72	11.85	
Class		3	3	3	3	3	3	0	0	2
Window surface	$\frac{m^3}{(h/m^2)}$	3.76	6.18	8.64	11.23	14.05	17.15	28.67	44.01	
Class		3	3	3	3	3	3	0	0	2
										2

**Table 4: Group 3 (wooden profile)– air permeability**

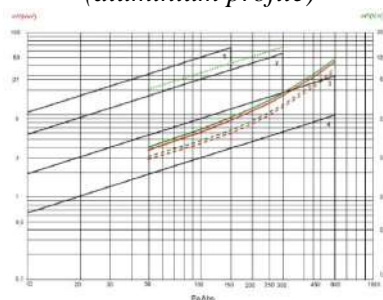
Pa normal		50	100	150	200	250	300	450	600	General class
Pa actual		50	100	150	200	251	302	452	603	
Air permeability	$\frac{m^3}{h}$	1.50	2.51	3.35	4.11	4.82	5.52	8.01	11.86	
Seam lenght	$\frac{m^3}{(h/m)}$	0.39	0.66	0.88	1.08	1.27	1.45	2.10	3.11	
Class		4	4	4	4	4	4	3	3	3
Window surface	$\frac{m^3}{(h/m^2)}$	1.34	2.24	2.99	3.67	4.31	4.93	7.15	10.59	
Class		4	4	4	4	4	4	4	3	3
										3

Diagrammatic representation of air permeability at average value of pressure and suction

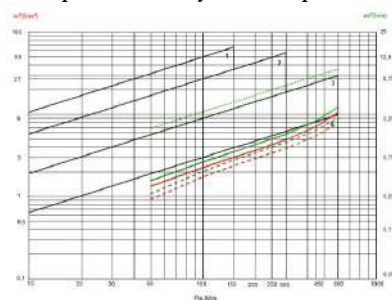
**Diagram 1: Air permeability – Group 1 (PVC profile)**



**Diagram 2: Air permeability – Group 2 (aluminium profile)**



**Diagram 3: Air permeability – Group 3 wooden profile)**



Legend 1, 2, 3

- Corner data classification
- $m^3/(h/m^2)$  Window surface 1<sup>st</sup> measuring
- $m^3/(h/m)$  Seam length 1<sup>st</sup> measuring
- - -  $m^3/(h/m^2)$  Window surface 2<sup>nd</sup> measuring
- - -  $m^3/(h/m)$  Seam length 2<sup>nd</sup> measuring
- ..... Limit 2<sup>nd</sup> measuring Window surface
- ..... Limit 2<sup>nd</sup> measuring Seam length

### 3.2. Results – water tightness

Class according to the EN 1027:2016 “Windows and doors - Water tightness - Test method” standard. [4]

**Table 5: Group 1 (PVC profile) – water tightness**

Class	Pressure in Pa		Time	Water entrance		Observation
	Normal	Actual		Dripping	Flowing	
A1	0	0	00:15:00	00:00:00	00:00:00	OK
A2	50	50	00:05:00	00:00:00	00:00:00	OK
A3	100	100	00:05:00	00:00:00	00:00:00	OK
A4	150	150	00:05:00	00:00:00	00:00:00	OK
A5	200	200	00:05:00	00:00:00	00:00:00	OK
A6	250	250	00:05:00	00:00:00	00:03:44	NOT OK

**Table 6: Group 2 (aluminium profile) – water tightness**

Class	Pressure in Pa		Time	Water entrance		Observation
	Normal	Actual		Dripping	Flowing	
A1	0	0	00:15:00	00:00:00	00:00:00	OK
A2	50	50	00:05:00	00:00:00	00:00:00	OK
A3	100	100	00:05:00	00:00:00	00:00:00	OK
A4	150	149	00:05:00	00:00:00	00:00:00	OK
A5	200	201	00:05:00	00:00:00	00:01:38	NOT OK

**Table 7: Group 3 (wooden profile) – water tightness**

Class	Pressure in Pa		Time	Water entrance		Observation
	Normal	Actual		Dripping	Flowing	
A1	0	0	00:15:00	00:00:00	00:00:00	OK
A2	50	50	00:05:00	00:00:00	00:00:00	OK
A3	100	100	00:05:00	00:00:00	00:00:00	OK
A4	150	148	00:05:00	00:00:00	00:00:00	OK
A5	200	201	00:05:00	00:00:00	00:00:00	OK
A6	250	251	00:05:00	00:00:00	00:00:09	NOT OK

### 3.3. Results – resistance to wind load

Class according to the EN 12211:2016 "Windows and doors - Resistance to wind load - Test method" standard. [5]

**Table 8: Maximum deflection to the classification at the base width**

Class	f (mm)
(a-c) 1250 mm	
A	(a-c)/150
B	(a-c)/200
C	(a-c)/300

**Table 9: Results of the frontal deflection in mm section/pressure – Group 1 (PVC profile)**

Pa	1(a)	2(b)	3(c)	f (mm)
2001 Pa	0.31	5.03	0.37	4.72
0 Pa	0.05	0.04	0.04	0.01
-2002 Pa	0.53	5.81	0.50	5.29
0 Pa	0.02	0.00	0.00	0.01

**Table 10: Results of the frontal deflection in mm section/pressure – Group 2 (aluminium profile)**

Pa	1(a)	2(b)	3(c)	f (mm)
2003 Pa	1.01	2.39	1.29	1.24
0 Pa	0.10	0.24	0.63	0.19
-2003 Pa	0.28	1.19	0.63	0.74
0 Pa	0.00	0.00	0.00	0.00

**Table 11: Results of the frontal deflection in mm section/pressure – Group 3 (wooden profile)**

Pa	1(a)	2(b)	3(c)	f (mm)
2000 Pa	0.58	1.98	0.45	5.54
0 Pa	0.17	0.14	0.00	0.06
-2002 Pa	0.00	0.64	0.12	0.58
0 Pa	0.00	0.00	0.00	0.00

## 4. CONCLUSION

From the analyzed results and their comparison of the individual samples, the following can be confirmed:

- The material from which the profile used to manufacture windows is made has a significant impact on air permeability. The tested samples that were made in were divided into three groups and each group had ten samples. All samples from one group had the same profile material. The results given by the windows varied considerably and they circulated in three classes of sustainability of air permeability.

- The material from which the profile used to manufacture windows is made has a significant impact on water tightness. The tested samples that were made in were divided into three groups and each group had ten samples. All samples from one group had the same profile material. The results given by the windows varied considerably and they circulated in three classes of EN 1027:2016 “Windows and doors - Water tightness - Test method” standard. [4]

- The material from which the profile used to manufacture windows is made has significant influence over the deformities of the window itself. The tested samples that were made in were divided into three groups and each group had ten samples. All samples from one group had the same profile material. The analysis of the results brought conclusion that the windows are made of profile which is strengthened with more steel making it more resistant to deformities when hit by wind load. The results given by the windows varied considerably and they circulated in two classes of EN 12211:2016 "Windows and doors - Resistance to wind load - Test method" standard. [5]

## REFERENCES

- [1] <https://www.altest-kmg.com/> (03-05-2023).
- [2] <https://www.alumil.com/> (03-05-2023).
- [3] EN 1026:2016 “Windows and doors - Air permeability - Test method” standard.
- [4] EN 1027:2016 “Windows and doors - Water tightness - Test method” standard.
- [5] EN 12211:2016 "Windows and doors - Resistance to wind load - Test method" standard.
- [6] Gruevski, T., Simakoski, N. (2002): Elementi na drvnite konstrukcii, Skopje: UKIM Shumarski fakultet.
- [7] Gruevski, T., Simakoski, N. (2003): Konstruiranje na mebel, Skopje: UKIM Shumarski fakultet.
- [8] Zakon za energetska efikasnost (2020): Sluzben vesnik na Republika Makedonija, br.32/2020 od 09-02-2020 god.
- [9] Zakon za gradezni proizvodi (2015): Sluzben vesnik na Republika Makedonija, br.104/2015 od 24-06-2020 god.
- [10] Ibrahimovic, E., Kljuno, H.A. Window frame materials and window size: parametesrs that influence enegy efficiency in buildings. Technics technologies education managment.
- [11] Kralj, A., Znidarsic, M., Fir, J.M., Lampic, P. Five and more – chamber, transparent, insulated panel Qbiss air. Znanstveni clanak.
- [12] Ma, L., Shao, N., Zhang, J., Zhao, T. The influence of Doores and Windows on the Indoor Temperature in Rular House. 9<sup>th</sup> Internacional Symposium on Heating, Ventilation and Ait Conditioning (ISHVAC) and the 3<sup>rd</sup> International Conference on Building Energy and Environment (COBEE).

## THE INFLUENCE OF COMPUTER SOFTWARE INTENDED FOR CONSTRUCTIVE PREPARATION ON THE TIME FOR THE PRODUCTION OF THE NECESSARY TECHNICAL DOCUMENTATION IN A MICRO-ENTERPRISE FOR THE PRODUCTION OF CUSTOM-MADE PLATE FURNITURE

**Marija Krstev**

*Ss. Cyril and Methodius University in Skopje, North Macedonia,  
Faculty of Design and Technologies of Furniture and Interior-Skopje,  
e-mail:ilievska\_11@yahoo.com*

### ABSTRACT

The research presented in this paper is part of an ongoing research intended for the preparation of the author's PhD dissertation. Its purpose is to see the impact of computer software intended for constructive preparation, on the time required to prepare the complete technical documentation during the launch of a new product within a micro enterprise for the production of custom-made plate furniture.

For that purpose, the time spent during standard constructive preparation was measured by drawing views, sections and details in AutoCAD of previously prepared 3D models of various pieces of furniture, and then dimensioning the constituent elements and creating a scheme for cutting the material in an appropriate software.

For the same pieces of furniture, time was measured during the preparation of the same documentation through several different software intended for constructive preparation, specifically in Corpus5 in the first part of the research, as well presented in this paper.

The results are showing that the computer software significantly shortens the constructive preparation time when we use ready-made pieces of furniture that already exist in their database.

**Keywords:** computer software, corpus, constructive preparation, custom-made

### 1. INTRODUCTION

Production preparation within a company engaged in the production of custom-made panel furniture requires particular attention and a precise approach, due to predicting all further steps in production and reducing the risk of unnecessary stoppages and bottlenecks.

The use of numerically controlled machines, not only during complex operations such as curved cutting or drilling, but also during the basic cutting of plate material, contributed to the entire planning process, starting from a 3D drawing, being carried out through a software solution that further generates all the necessary information to the machines for work.

There are several programs on our market that are actively used by manufacturers, namely: Corpus, PolyBoard, imos and HOLZHER CabinetControl.

The question arises, do these types of software make the process easier or more complicated, how do they affect the time required to prepare the necessary documentation, work errors or the use of material, when it is known that in the production of custom-made furniture, each element is special and unique?

When creating the design of the furniture, as well as when preparing the production order, computer programs such as Excel, AutoCAD, then Sketch Up, 3ds Max or other software for 3D visualization are used, but with their application we get only a part of the information that we need, e.g. only a front view, or only a visual and not a constructive solution, etc.

Based on the accurately drawn appearance in autocad, we can draw elevations and get the exact dimensions of the structural parts of the furniture we are designing, but further on we should write those dimensions in an excel table, note which side they are edged on, write name of the pieces, then

make a cutting pattern from that table in another software, so that pattern can serve when cutting the plate material.

Next, we should make a copy of those sections with inset drilling for the appropriate hardware: hinges, sliders, dampers, structural fasteners, etc. It already complicates the work and requires a lot of work experience of the designer, and further, during the production process, it also requires experienced operators and carpenters who will be able to read those drawings and carry out the required operations.

In contrast to this way of working, with the use of software that allows complete planning of the production process, by drawing and entering data for the furniture that we project only once and in one drawing, we have the opportunity to draw various data that we would need in each subsequent one phase. Apart from drawings in all respects, accurate drilling, edging and review of the material used, we also have insight into the purchase or sale price, and it is very simple and quick to change any part of the furniture, in terms of dimensions, selected material or used fittings used fittings and whereupon that change is generated in all reports.

The best part of this way of working is that the CNC machine receives complete data, and in addition to cutting the plate material, it also performs complete drilling for the necessary hardware and additional processing, such as cutting buckets under the ger or making grooves and semi-grooves for the ruhwand, further grooves for led profile, cuts for Gola profile, etc. What is more remarkable, the dimensions of such drillings are generated automatically, by just selecting the fitting that is already in the database. So, with a production order prepared in this way, the plant workers do not need to do any calculations and manual drilling, and with a simple tool such as a screwdriver or Allen key, they assemble the furniture. At the same time, each structural piece is numbered with a name and exact position within the assembly, and a detailed 3D drawing is available to them that is easy to read, together with a list of all the necessary components, as well as a list of the necessary hardware in the exact quantity.

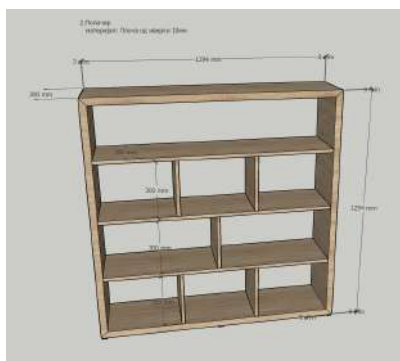
The advantages are numerous, and the possibilities are unlimited. The only condition that needs to be satisfied is an experienced and trained designer, with knowledge of the basic principles of design, as well as an insight into the operation of the machines and the possibilities of the structural fittings that will foresee it, and of course, an excellent knowledge of the software that uses it.

## 2. METHODS OF THE EXPERIMENTAL WORK

In order to carry out this research intended for the preparation of a doctoral dissertation, pieces of furniture were selected from concrete, made 3D projects and proceeded to their constructive preparation through the listed software, as well as through the classic way by drawing views and sections in autocad and measuring the time spent.

In this paper, only a part is shown, that is, the method of work and the results obtained through the Croatian software Corpus RC5, which is the most commonly used in our country, is covered, perhaps because it is available in a language that is close to us and easy to understand. This part of the research was conducted at Drvodekor Enterier Shtip, a company for the production of panel furniture, which performs the entire process of planning and launching new products through the mentioned software.

The following are pictures of some of the furniture for which we performed structural preparation and whose data are shown in this initial research.



**Figure 1:** 3D model of a free-standing shelves rack (position no. 2 in the element database)





Figure 2: 3D model of a work desk (position no. 8 in the element database)

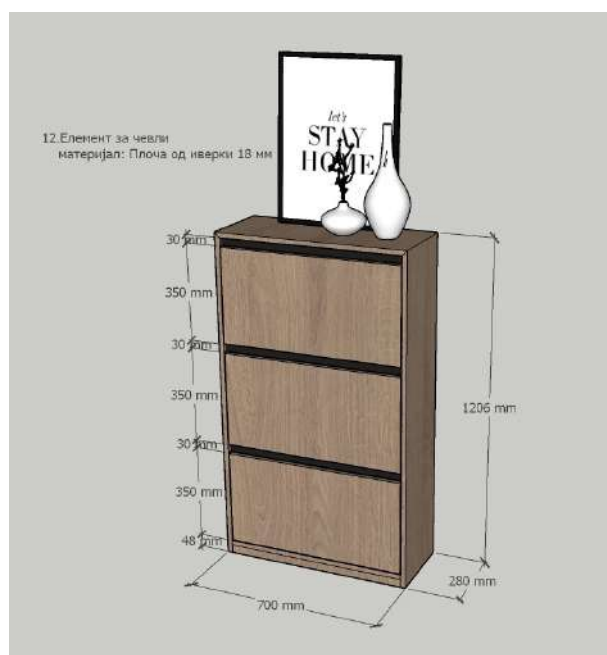


Figure 3: 3D model of a shoe rack (position no. 12 in the element database)



Figure 4: 3D model of a office storage cabinet (position no.17 in the element database)

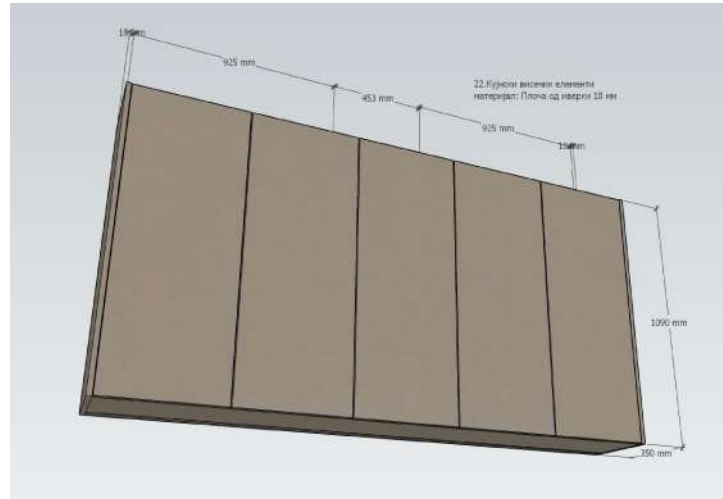


Figure 5: 3D model of kitchen hanging elements (position no. 22 in the element database)

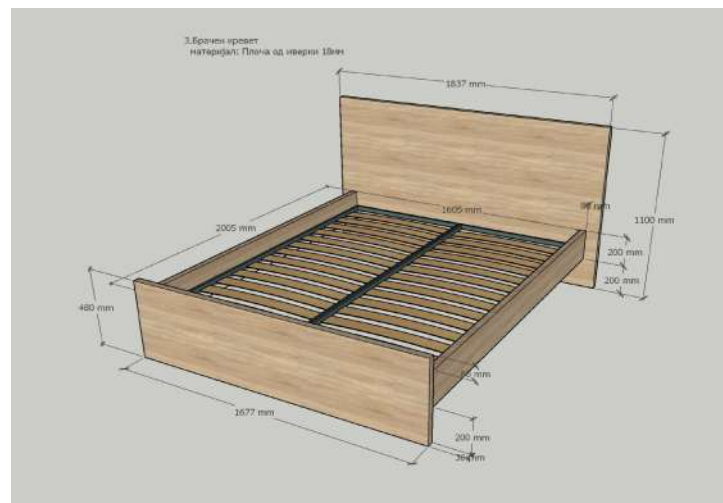


Figure 6: 3D model of a double bed (position no. 3 in the element database)



Figure 7: 3D model of kitchen base cabinets (position no.21 in the element database)

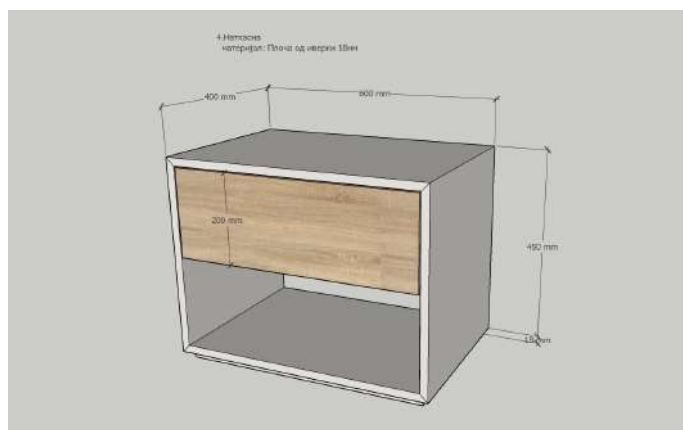


Figure 8: 3D model of night stand (position no.4 in the element database)

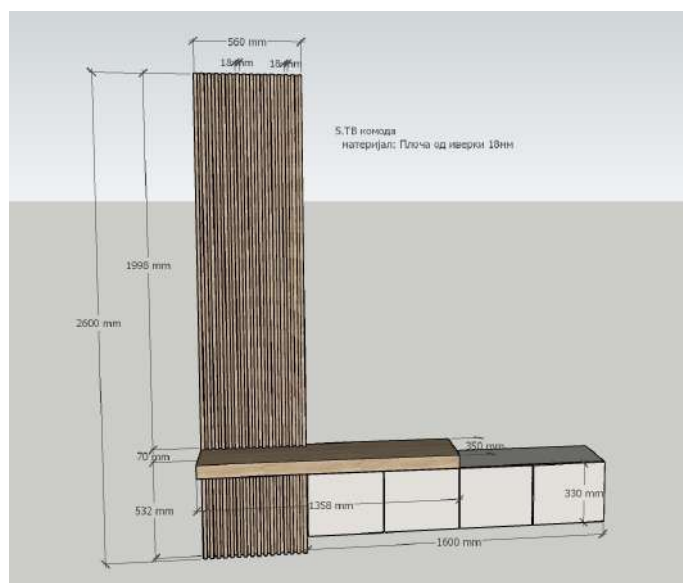


Figure 9: 3D model of a TV cabinet (position no.5 in the element database)

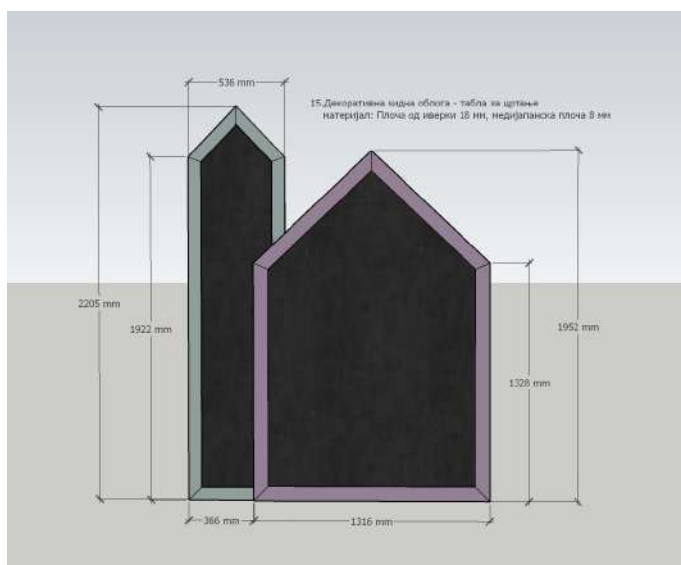


Figure 10: 3D model of decorative wall panel (position no.15 in the element database)

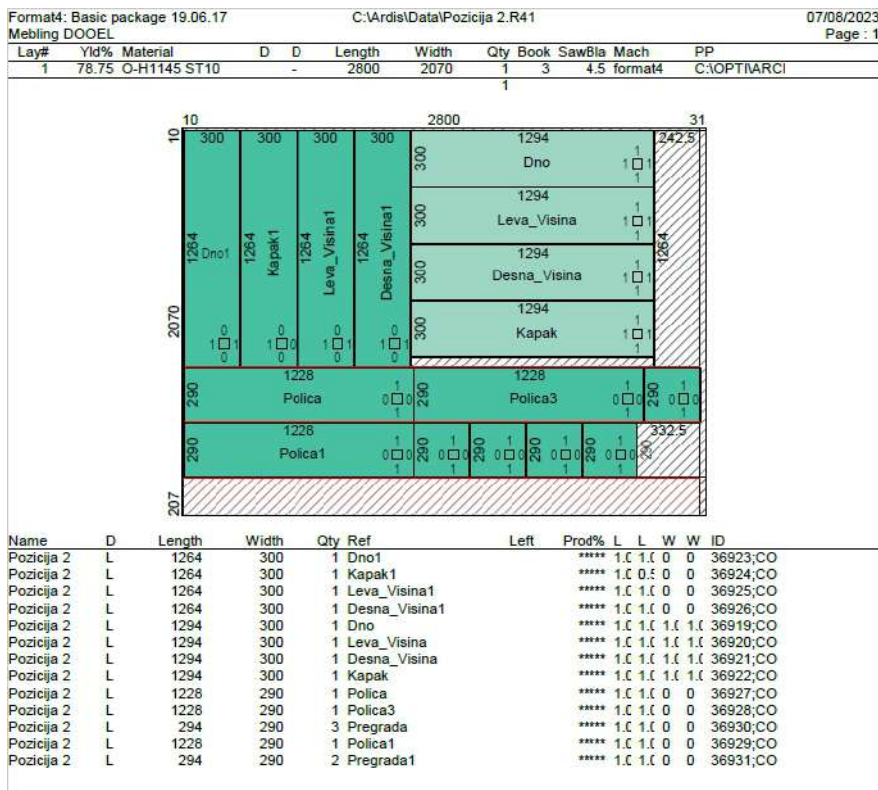
The way of working in specialized software differs significantly from the classical way of constructive preparation. When working in Corpus5, the drawing of the furniture is approached as a 3D model, at the same time the sides that are edged are marked, the method of joining, the material, its thickness, the necessary fittings and so on are selected. If there is additional processing on a component, such as beveling or gerig, that data is entered to be read by the CNC machine, selecting the correct tool and its path of movement. Furthermore, the data is transferred to a tailoring optimization program and we receive tailoring schemes for all the materials that are part of the furniture.

Automatically, we also receive all the reports that we would need in the further production process: 3D drawing, layouts, list with dimensions of all components, required fittings, and, if necessary, purchase and sale price. What is even more important, it is very simple to change the thickness of the material or the final overall dimension on already drawn furniture, and there is no room for errors in the production process because all the holes are already provided. Below is an example of one of the pieces of furniture.

**Report no. 1** 3D view, layouts, list of components and required furniture mechanism

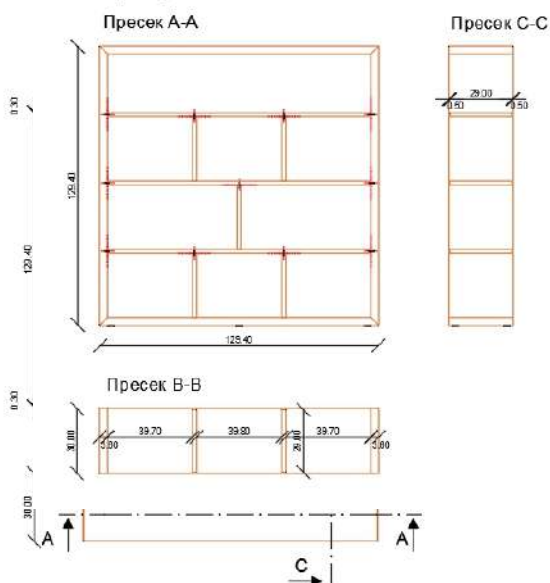
Id	Ime	Količina	Dimenzije	Material	Referenca
1	Dno	1 kom	1294 x 300	MBL_3201	11P8872323125Z
2	Leva_Visina	1 kom	1294 x 300	MBL_3201	12P19548354651
3	Desna_Visina	1 kom	1294 x 300	MBL_3201	11P0527903717Z
4	Kapak	1 kom	1294 x 300	MBL_3201	12P98822180805
5	Dno1	1 kom	1264 x 300	MBL_3201	11P8872323125Z
6	Kapak1	1 kom	1264 x 300	MBL_3201	11P8872323125Z
7	Leva_Visina1	1 kom	1264 x 300	MBL_3201	12P19548354651
8	Desna_Visina1	1 kom	1264 x 300	MBL_3201	12P19548354651
9	Polica	1 kom	1228 x 290	MBL_3201	
10	Polica2	1 kom	1228 x 290	MBL_3201	
11	Polica1	1 kom	1228 x 290	MBL_3201	
12	Pregrada	1 kom	294 x 290	MBL_3201	
13	Pregrada2	1 kom	294 x 290	MBL_3201	
14	Pregrada1	1 kom	294 x 290	MBL_3201	
15	Pregrada4	1 kom	294 x 290	MBL_3201	
16	Pregrada3	1 kom	294 x 290	MBL_3201	

**Report no. 2** Cutting pattern with bar codes of the components for drilling and additional processing



In contrast to this method, during classical construction preparation, we prepare everything we need as information in the further production process as a separate document, and also in a separate computer program: AutoCAD, Optimic, Excel, Word, etc. For the same piece of furniture, there are drawings and documents that we produce in a classic way.

**Report no. 3** Views and sections prepared in AutoCAD



**Report no. 4** Excel table with dimensions and material of the components

МАРИЈА АРСТЕВ ИНТЕРИОР КОНСАЛТ ДООЕЛ ШТИП  
m.arkinteriorconsult@gmail.com

MK interior consult		ПРОЕКТ:				ПОЗИЦИЈА 2				
MK interior consult		ПОЗИЦИЈА:				ПОЛИЧАР				
БР	МАТЕРИЈАЛ	ДОЛЖИНА	ШИРИНА	НОМ	КАНТИРАЊЕ				ОПИС	ЗАБЕЛЕШКА
					1	2	3	4		
1	Egger H11445 18 mm	1304	310	8					страници, дно, плафон	надмер, т.м. 1294*300*36 - 4 бр, кант 4 стр
2										2 нуси стр нагласен гер 3 мм
3	Egger H11445 18 mm	1228	290	3	1		1		фински полица	
4	Egger H11445 18 mm	300	290	5	1		1		вертикали	
5										
6										
7										
8										
9										
10										

**Report no. 5** Excel table with required furniture mechanism

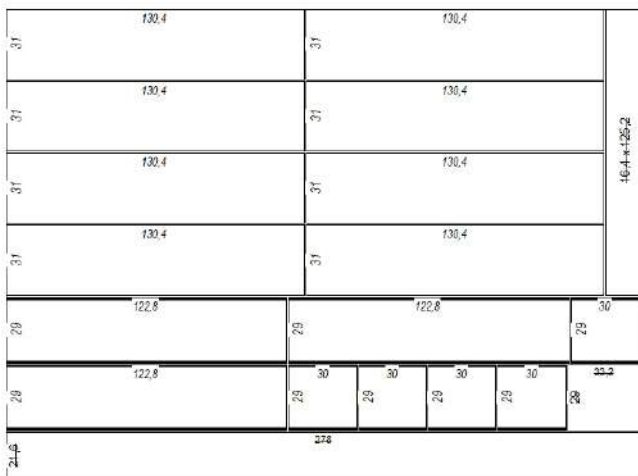
МАРИЈА АРСТЕВ ИНТЕРИОР КОНСАЛТ ДООЕЛ ШТИП  
mk.interiorconsult@gmail.com

MK interior consult		ПОЗИЦИЈА 2		
MK interior consult		ПОЛИЧАР		
БР	ТРЕБОВНИЦА			
	ОКОВ (ОПИС)	КОЛИЧИНА	БРЕНД	
1	Дрвени бискијти	22 бр	ЛАМЕЛО	
2	Пластични палуци	12 бр		
3				
4				
5				
6				
7				
8				
9				
10				

**Report no. 6** Cutting pattern prepared in Optimic



**Позиција 2 (H1145 18 mm)**  
278 x 206 cm (8) - iverka 18mm (18mm)  
MK interior consult  
© P1111111 © P1111111, 1999-2022 <http://www.optmk.com>  
DREAM TEAM 2022



**Boards**  
Job: Позиција 2 (H1145 18 mm)  
Material: iverka 18mm (18mm)  
MK interior consult  
© P1111111 © P1111111, 1999-2022 <http://www.optmk.com>  
DREAM TEAM 2022

Description / Pcs(s)	
130.4 x 31 cm	(P1) 8 pc(s)
122.8 x 29 cm	(P1) 3 pc(s)
30 x 29 cm	(P1) 5 pc(s)
	16 pc(s)

### 3. RESULTS AND DISCUSSION

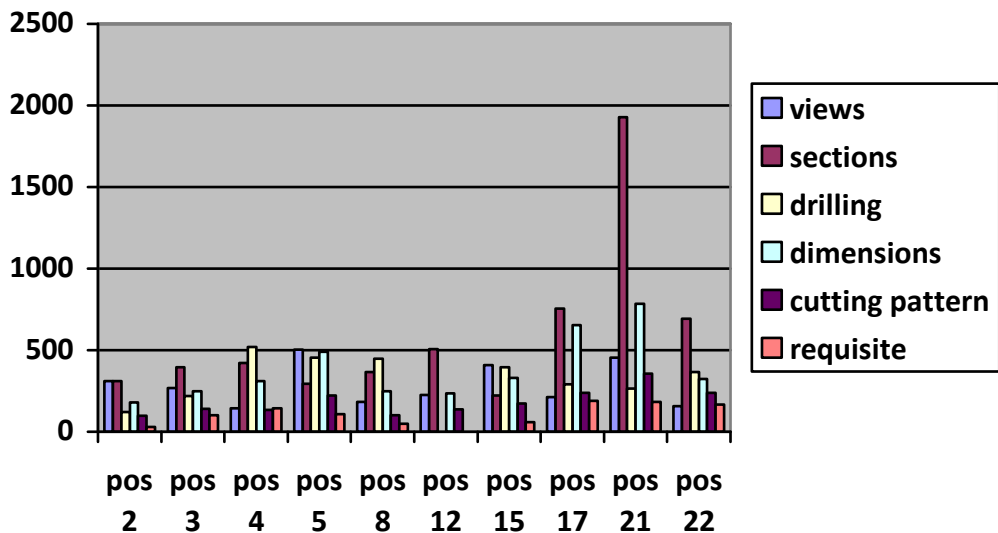
This research will include over 20 pieces of furniture, constructively prepared in 4 different softwares. The initial results for some of the furniture, obtained by measuring the time required to subfloor the furniture in Corpus5, compared to the time for classical construction preparation, are given in the tables and graphs that follow.

**Table 1: Time spent on constructive preparation in both ways**

No.	FURNITURE	Classical construction preparation / Time in seconds							CORPUS 5 / Time in seconds		
		VIEWS	SECTIONS	DRILLING	DIM	CUTTING PATTERN	REQUISITE	TOTAL	DRAWING	CUTTING PATTERN	TOTAL
1	Pos. No. 2 shelves rack	310	312	120	180	98	28	1048	1037	230	1267
2	Pos. No. 8 work desk	184	365	447	250	100	48	1394	800	184	984
3	Pos. No. 12 shoe rack	224	507		236	137		1104	865	197	1062
4	Pos. No. 17 office cabinet	214	754	292	652	240	191	2343	2475	205	2680
5	Pos. No. 22 kitchen cabinet	156	692	367	323	240	166	1944	2355	140	2495
6	Pos. No. 3 double bed	268	395	220	247	142	100	1372	700	140	840
7	Pos. No. 21 kitchen cabinet	454	1929	265	784	356	183	3971	1748	180	1928
8	Pos. No. 4 night stand	145	420	520	312	135	144	1676	1020	135	1155
9	Pos. No. 5 TV unit	504	294	455	490	221	107	2071	1114	170	1284
10	Pos. No. 15 Wall panel	408	222	395	330	173	60	1588			0

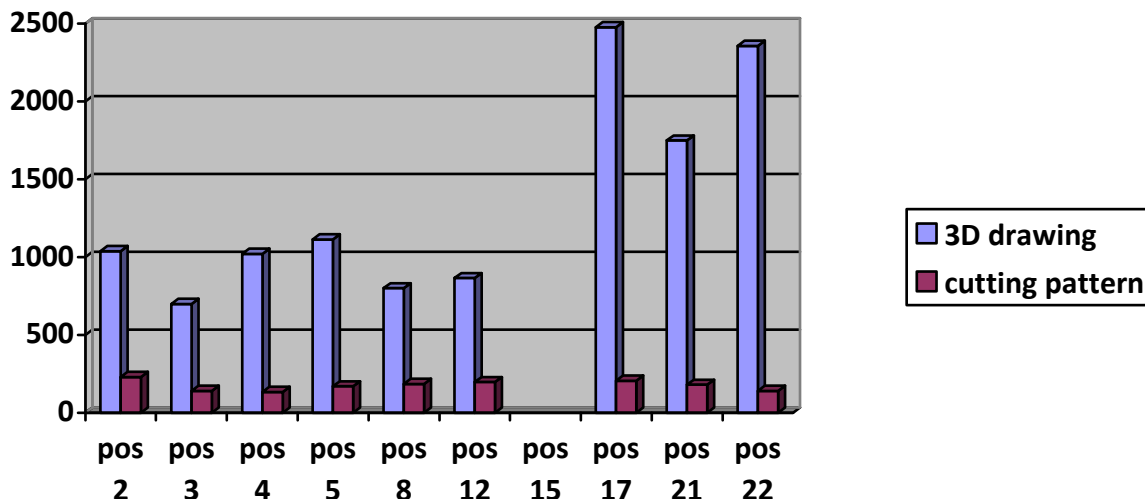
Table 1 shows the times expressed in seconds, individually for each piece of furniture, and for each step in the construction preparation process, both during the classic and during the preparation through Corpus5.

Graph 1 shows the time spent during classical construction preparation, where a comparison can be made in the length of time required for each individual step in the procedure. It can be seen that the drawing of sections and drilling is the longest step in time, and the shortest is the preparation of the list of consumables, as well as the cutting pattern in an optimization program.



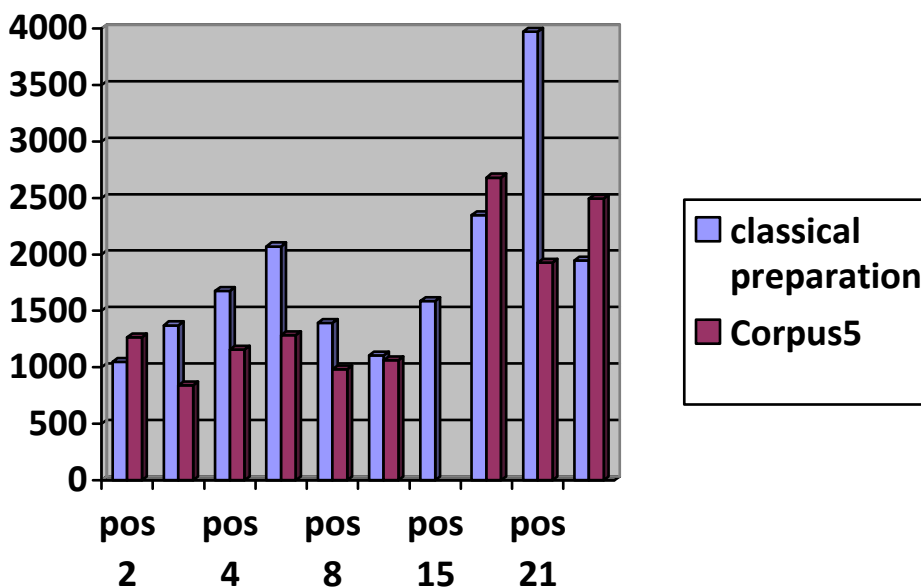
**Graph 1.**

Graph 2 shows the time spent on preparation in Corpus5. We can notice a significant reduction in preparation steps, because the program allows us automatically to create all the necessary reports with a single drawing of the furniture as a 3D shape.



Graph 2.

On Graph 3, a comparison is made between the total time spent for each piece of furniture, constructively worked out in a classical way and through the computer software Corpus5.



Graph 3.

As can be seen from the graph, in half of the measured pieces, the computer software has a shorter time for constructive preparation, and in the other half it has values close to the classic way or longer than it. Further research and measurement of more pieces of furniture will give us more precise insight and more data, to make a clear conclusion whether in small custom furniture productions, it is economically viable to install expensive software of this type.

#### 4. CONCLUSION

The data so far from this initial research do not make a big difference in the time period required to constructively prepare a piece of furniture in the classical way, compared to preparation through the computer software Corpus5. But the positive aspects in the further production process cannot be left



out, where by using computer software for preparation and machine drilling, it is possible to assemble the furniture by not very expert and experienced staff, which is a great advantage for the furniture industry which currently suffers from a lack of skilled labor.

## REFERENCES

- [1] Gruevski, T., (2000): Podgotovska na proizvodstvoto, Šumarski fakultet, UKIM, Skopje.
- [2] Grladinovic, T. (1999): Upravljanje proizvodnim sustavima u preradi drva i proizvodni namjestaja, Zagreb.
- [3] Mileusnic, N. (1977): Organizacija procesa proizvodnje, Beograd.
- [4] Vila, A. , Leicher, Z. (1983): Planiranje proizvodnje i kontrola rokova, Zagreb.
- [5] <https://corpus.hr>
- [6] <https://redcat.hr>
- [7] <https://www.corpus-software.com>

## IMPACT OF FEED RATE ON ROUGHNESS OF THE CUT SURFACE, DURING CUTTING DRY SPRUCE WOOD WITH A CIRCULAR SAW

Anastasija Temelkova

*Ss. Cyril and Methodius University in Skopje, R. of North Macedonia,  
Faculty of design and technologies of furniture and interior-Skopje  
e-mail: temelkova@fdtme.ukim.edu.mk*

### ABSTRACT

The feed rate during mechanical processing of wood is one of the factors that has a high influence on the roughness of the cut surface.

The roughness of the cut surface caused by traces of the cutting tool (the main and secondary blades of the teeth) has an influence on the hydrothermal treatment and all other mechanical treatments of the wood. Greater roughness, due to faster evaporation of moisture from the wood, increases the percentage of drying errors. On the other hand, higher roughness reduces the utilization rate of the wood.

For this purpose, in this paper, the dependence of the feed rate on the roughness of spruce wood during cutting of dry wood with a circular saw is investigated, with the intention of determining the optimal cutting conditions for obtaining lower values of the roughness.

In this research, three different feed rate were applied ( $U_1=12 \text{ m min}^{-1}$ ,  $U_2=16 \text{ m min}^{-1}$  and  $U_3=20 \text{ mmin}^{-1}$ ) for a constant cutting height of 45 mm in dry spruce wood with humidity  $W=10\pm 1\%$ . The measurements were made with a circular saw with diameter of  $D=250 \text{ mm}$ , number of teeth  $Z=40$  and width of the cut  $b=3,2 \text{ mm}$ . The number of revolutions is  $n=5500 \text{ min}^{-1}$ .

Roughness measurements were taken with a digital comparator, according to the  $R_{\max}$  criterion. The obtained results show a pronounced significance, i.e. directly proportional dependence of the roughness of the cut surface on the feed rate.

**Keywords:** spruce wood, circular saw, roghness, the feed rate

### 1. INTRODUCTION

In order to ensure quantity and quality when processing wood with circular saws, it is of great importance to make the right choise of cutting tool. Tool manufacturers on the market offer different types of saws with different diameters and different number of teeth. Circular saws are commonly used tools in mechanical processing of wood and wood based materials, including all production phases. Circular saws are also used for cutting other materials such as: plastic, metal, ceramics, different types of construction materials etc [7]. When processing on circular saws with equal diameter and equal peripheral cutting speed, the number of teeth that actively participate in the process of cutting per time is different. This has a significant impact on the thickness of wood chips, as well as the pressure on the kerf, especially at the rear surface of the blade [5]. The choice of the number of teeth for the same diemeter of the saw depends on the required quality of processing of the cut surface, that is, a saw with a larger number of teeth provides better processing and vice versa. In the process of wood cutting, cutting force and cutting power are the main output parameters, while the chip length, chip thickness, feed per tooth, teeth pitch, average kinematic cutting angle, cutting speed, average pressure on front side, fictive specific force on back side are secondary parameters [3]. Cutting height and number of teeth affect cutting resistance with a circular saw. Greater cutting resistance leads to increased vibration and distortion of the cutting tool. This results in the appearance of a crooked and rough cut. The contact surfaces of tools in the machining process are exposed to high pressures and friction, which results in tool wear. Tool wear is one of the important factors in mechanical wood processing since it directly affects surface quality, cutting forces, cutting power and energy

consumption [8]. The criteria that characterize the quality of the treated surface are surface roughness, accuracy of processing and resistance. Traces of the processing from the vibration of the machine and the cutting tool, the structure and volume of the material being processed, are part of the reasons for the appearance of roughness. The roughness of the cut surface caused by traces of the cutting tool (the main and secondary edges of the teeth) has an influence on the hydrothermal treatment and all other mechanical treatments of the wood. The feed rate during mechanical processing of wood is one of the factors that has a high influence on the roughness of the cut surface.

## 2. THE AIM OF THE RESEARCH

The aim of the research of this paper is to determine the dependence of the feed rate on the roughness in spruce when cutting dry wood with a circular saw, with the intention of determining the optimal cutting conditions for obtaining lower roughness values.

## 3. MATERIAL AND METHOD OF WORK

### 3.1 Material

For testing was taken sawn lumber from spruce (*Picea Abies*) without defects with dimension 1500 x 150 x 15mm. All lumber is dried and conditioned. The measured humidity of the beech is 10,22 % on average.

Samples were cut from the planks with a constant cutting height of 45mm. The research of the samples was carried out on a circular saw machine type NIKOLAIDIS TEMA 3800 in „KI-PAR“ from Strumica (Figure 1). The main feature of this machine is that both the main and auxiliary movements are performed by the cutting tool. During cutting, the object to be processed is pressed with a pneumatic pressure beam. The technical characteristics of the machine are given in table 1.



**Figure 1:** Circular saw machine type NIKOLAIDIS TEMA 3800

**Table 1:** Technical characteristics of the format circular saw machine type Nikolaidis TEMA 3800

Technical characteristics	
External length	5500 mm
External width	4400 mm
Cutting length	3800 mm
Cutting height	55 mm
Dimensions of the circular saw	200 3,3 30 mm 250 3,2 30 mm
Power of the main electric motor	4,5 kW
Power of the electric motor to move the main electric motor	1,75 kW
Number of revolutions of the circular saw	5500 min <sup>-1</sup>
Pressure on the pressed beam	6-7 bar
Feed rate	5-30 mmin <sup>-1</sup>



**Figure 2:** Circular saw with diameter  $D=250\text{mm}$ , number of teeth  $Z=40$  and thickness  $b=3,2\text{mm}$

### 3.2 Metod of work

In this research were applied three different feed rates ( $U_1=12\text{mmmin}^{-1}$ ,  $U_2=16\text{mmmin}^{-1}$  and  $U_3=20\text{mmmin}^{-1}$ ). The measurements were made with a circular saw with a diameter of  $D=250\text{mm}$ , number of teeth  $Z=40$  and width of the cut  $b=3,2\text{mm}$ . The number of revolutions is  $n=5500\text{min}^{-1}$ . The cutting length of each sample is 1,2m.

The roughness data is measured with a digital comparator, type Shane, according to the  $R_{\max}$  criterion. For each sample (3 in total), 100 measurements were taken at a length of 1,0m, with a reference flange of 100mm length (Figure 3).



**Figure 3:** Digital comparator for measuring roughness type Shane

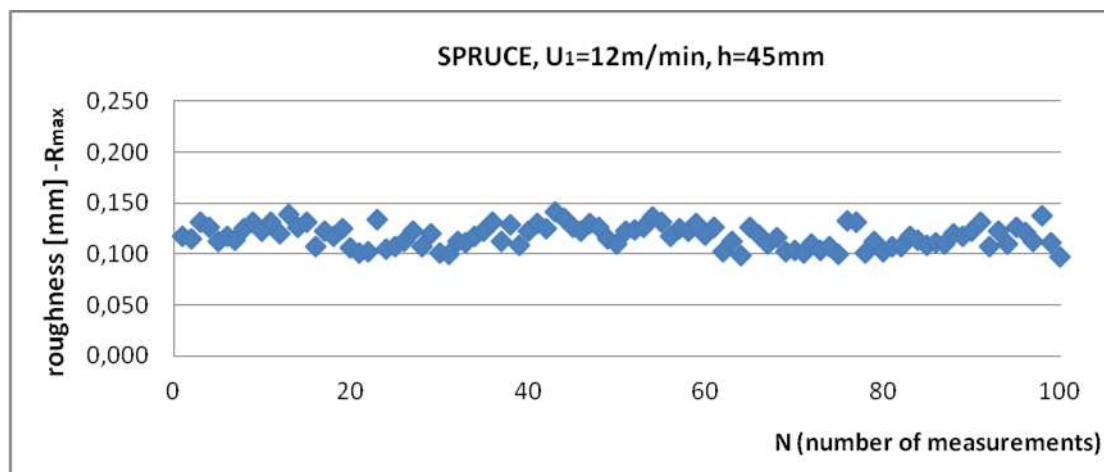
## 4. RESULTS

The results of the roughness measurement values according to the  $R_{\max}$  criterion are shown in Table 2.

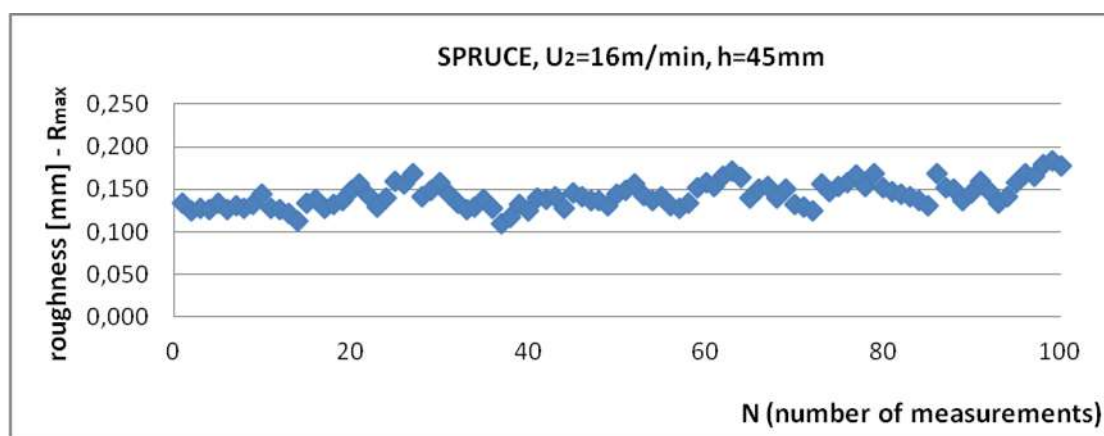
**Table 2:** Results of testing the roughness of spruce samples at different feed rates ( $U_1=12\text{mmmin}^{-1}$ ,  $U_2=16\text{mmmin}^{-1}$  and  $U_3=20\text{mmmin}^{-1}$ ), according to the  $R_{\max}$  criterion

1	displacement speed (U), for number of teeth Z = 40 and diameter D=250mm									SPRUCE
	U <sub>1</sub> = 12 m/min			U <sub>2</sub> = 16 m/min			U <sub>3</sub> = 20 m/min			
	cutting height [mm]			cutting height [mm]			cutting height [mm]			
	h=45			h=45			h=45			
	ROUGHNESS [mm]			ROUGHNESS [mm]			ROUGHNESS [mm]			
	1	2	3	4	5	6	7	8	9	
1	0.117	0.123	0.102	0.134	0.138	0.150	0.208	0.218	0.224	
2	0.115	0.132	0.104	0.124	0.127	0.132	0.222	0.223	0.221	
3	0.132	0.112	0.101	0.128	0.109	0.129	0.231	0.219	0.236	
4	0.126	0.129	0.110	0.126	0.117	0.125	0.228	0.221	0.230	
5	0.113	0.109	0.104	0.133	0.132	0.156	0.213	0.202	0.237	
6	0.118	0.123	0.107	0.126	0.124	0.147	0.199	0.207	0.139	
7	0.114	0.130	0.100	0.131	0.140	0.154	0.210	0.219	0.233	
8	0.125	0.125	0.133	0.127	0.138	0.158	0.200	0.223	0.227	
9	0.132	0.142	0.131	0.132	0.142	0.167	0.202	0.232	0.205	
10	0.122	0.135	0.101	0.144	0.127	0.153	0.207	0.230	0.211	
11	0.132	0.126	0.112	0.127	0.146	0.169	0.210	0.221	0.224	
12	0.120	0.122	0.103	0.126	0.141	0.152	0.198	0.230	0.238	
13	0.139	0.130	0.108	0.121	0.136	0.147	0.221	0.229	0.192	
14	0.127	0.127	0.107	0.112	0.137	0.145	0.204	0.227	0.203	
15	0.132	0.115	0.118	0.133	0.130	0.142	0.214	0.214	0.208	
16	0.107	0.110	0.114	0.139	0.144	0.136	0.218	0.235	0.199	
17	0.122	0.122	0.109	0.127	0.149	0.131	0.196	0.238	0.215	
18	0.118	0.124	0.111	0.132	0.157	0.169	0.212	0.228	0.233	
19	0.125	0.127	0.110	0.137	0.143	0.152	0.204	0.220	0.239	
20	0.106	0.137	0.120	0.149	0.136	0.150	0.222	0.230	0.234	
21	0.101	0.131	0.117	0.156	0.142	0.136	0.218	0.219	0.215	
22	0.102	0.117	0.123	0.143	0.131	0.146	0.211	0.233	0.237	
23	0.134	0.125	0.132	0.129	0.128	0.159	0.189	0.240	0.234	
24	0.105	0.122	0.107	0.140	0.134	0.148	0.198	0.208	0.236	
25	0.108	0.130	0.122	0.159	0.152	0.134	0.196	0.230	0.233	
26	0.113	0.119	0.110	0.157	0.158	0.141	0.204	0.223	0.238	
27	0.123	0.126	0.126	0.168	0.154	0.158	0.199	0.229	0.219	
28	0.107	0.102	0.121	0.141	0.166	0.168	0.194	0.203	0.236	
29	0.120	0.113	0.112	0.149	0.172	0.166	0.231	0.207	0.235	
30	0.101	0.099	0.138	0.158	0.164	0.179	0.214	0.233	0.215	
31	0.100	0.126	0.111	0.144	0.140	0.184	0.224	0.204	0.242	
32	0.112	0.119	0.098	0.133	0.151	0.177	0.195	0.218	0.219	
33	0.111	0.110		0.126	0.153		0.204	0.234		
34	0.117	0.116		0.129	0.140		0.225	0.214		
	average value	<b>0.118</b>		average value	<b>0.143</b>		average value	<b>0.218</b>		
	standard deviation	<b>0.0108</b>		standard deviation	<b>0.0151</b>		standard deviation	<b>0.0138</b>		
	coefficient of variation	<b>9.193</b>		coefficient of variation	<b>10.577</b>		coefficient of variation	<b>6.311</b>		
	minimum value	<b>0.098</b>		minimum value	<b>0.109</b>		minimum value	<b>0.189</b>		
	maximum value	<b>0.142</b>		maximum value	<b>0.184</b>		maximum value	<b>0.242</b>		

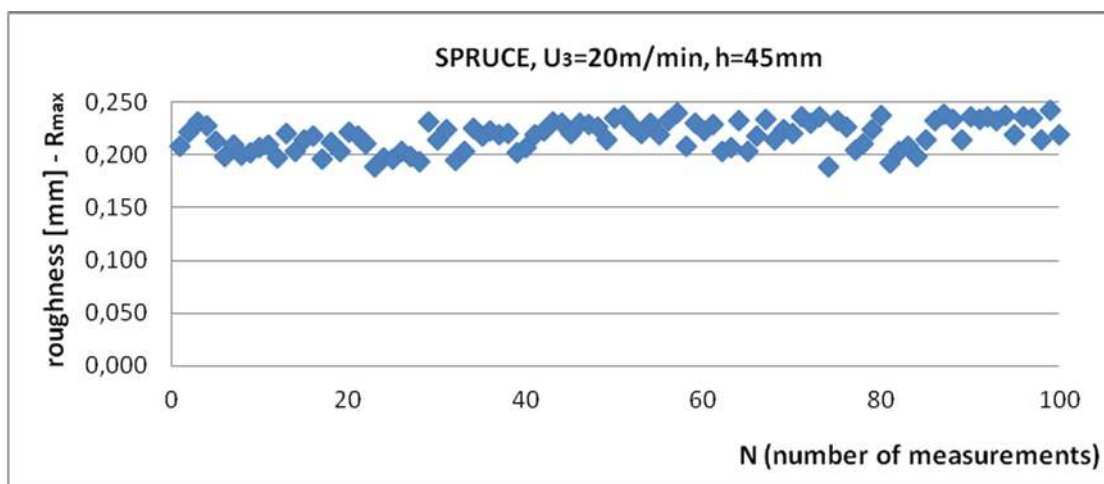
The mean values of the measurements show an increasing trend with increasing feed rate. The standard deviation and the coefficient of variation show sufficient uniformity of the measurement data.



**Graph 1:** Roughness of the cut surface of the spruce samples at a feed rate  $U_1=12\text{mmin}^{-1}$  according to the  $R_{max}$  criterion

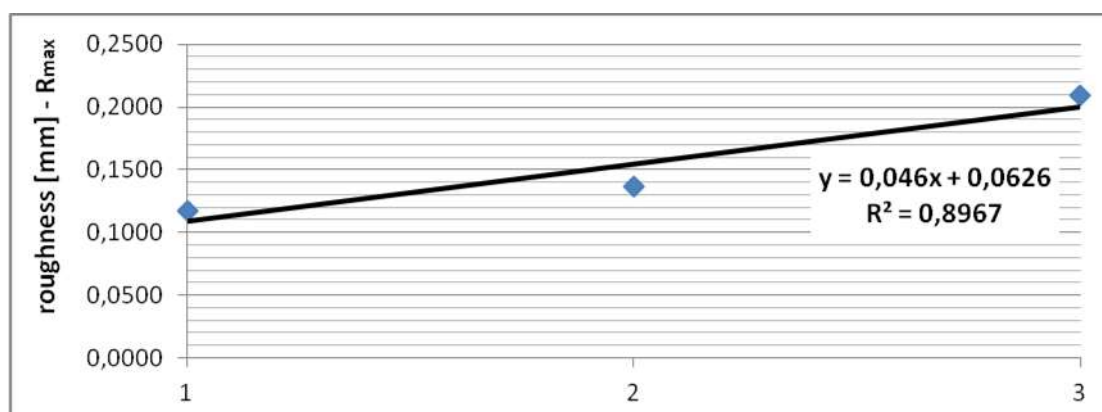


**Graph 2:** Roughness of the cut surface of the spruce samples at a feed rate  $U_2=16\text{mmin}^{-1}$  according to the  $R_{max}$  criterion



**Graph 3:** Roughness of the cut surface of the spruce samples at a feed rate  $U_3=20\text{mmin}^{-1}$  according to the  $R_{max}$  criterion

Graphs 1, 2 and 3 show the measurement data from the measurements. Data uniformity is observed in all graphs.



**Graph 4:** Regression analysis of mean values of roughness at all three feed rates ( $U_1=12\text{mmmin}^{-1}$ ,  $U_2=16\text{mmmin}^{-1}$  and  $U_3=20\text{mmmin}^{-1}$ )

Regression analysis showed that the measurements were best fitted to a line equation. Graph 4 shows the regression line of the mean values from the measurement data. The correlation coefficient shows high dependence.

From the results shown (table 2, graphs 1, 2, 3 and 4), we can state that with an increase in the feed rate, the roughness of the cut surface increases directly. The dependence is expressed mathematically by the regression law  $y=0,046x+0,0626$  and the correlation coefficient  $R^2=0,8967$ .

## 5. DISCUSSION AND CONCLUSIONS

The reviewed professional and scientific literature, which was available to us, showed that all authors agree in the statement that with the increase in the feed rate, the roughness of the cut surface increases, regardless of the type of mechanical processing.

The reasons for the depth of unevenness are also mentioned: the geometric characteristics of the cutting tool, the type of wood, the vibration and dullness of the tool, the humidity of the wood, the temperature of the wood, the thickness of the sawdust per tooth, etc. [1,6,9]

Preparation of the cutting tool is also essential. It is enough for just one tooth to fall out and cause deeper traces to appear. Also, with a greater bevel of the side blades (larger angle), deeper traces (bumps) appear. Deeper marks (grooves) must be removed in subsequent machining operations. At the same time, the loss of wood mass is greater, and because of this, it often happens that the dimensions of the final product deviate from the required dimensions. In extreme cases, errors appear in the final product.

Low feed rates compared to high feed rates give a better quality of the cut surface, but the productivity of the machine decreases. It is very important to determine the optimum feed rate value to obtain favorable productivity and surface quality. [2,4]

In this research, the dependence of the feed rate on the roughness of the cutting surface was confirmed.

## REFERENCES

- [1] Klinarov, R., Trposki, Z., Koljozov, V., (2000): Teorija na reženje na drvoto, Skopje.
- [2] Koljozov V., Trposki Z., Rabadziski B., Zlateski G., (2012): Influence of feed rate on cutting force and cutting power during wood processing on band saw, Wood - Design and Technology, Journal of wood science, design and technology, Vol.1 No.1, Pg.52-56, Skopje.
- [3] Koljozov V., Trposki Z., Rabadziski B., Zlateski G., Karanakov V., (2019): „Research on the effects of the cutting speed on cutting force and the cutting power in the process of milling“, 4<sup>th</sup> International Scientific Conference “Wood Technology & Product Design”, Pg. 278-283, Ohrid.
- [4] Paralidov, K., (2014): Istraživanja na vlijanje na brojot na zabi i viso ina na reženje vrz otporot na reženje so kružna pila, Magisterska rabota, Fakultet za dizajn i tehnologii na mebel i enterier, Skopje.

- [5] Paralidov K., Koljozov V., Trposki Z., Karanakov V., (2015): Research on kerf number influence on cutting power during woodprocessing on circular saw, Second International Scientific Conference "Wood Technology & Product Design", Pg. 221-225, Ohrid.
- [6] Trposki Z., Klincarov R., Koljozov V., (1999): The influence of cutting kinematics of bandsaw on production effects“, 2-nd International conference "Machine-Tool-Workpiece", Technical, University of Zvolen, Nitra.
- [7] urkovi M., Danon G., Svrzi S., Trposki Z., Koljozov V., (2017): A justification of the use of specialized circular saws for wood, 3<sup>rd</sup> International Scientific Conference "Wood Technology & Product Design", Pg. 61-66, Ohrid.
- [8] urkovi M., Milosavljevi Miric M., Mihailovi V., Danon G., (2019): Tool wear impacts on cutting power and surface quality in peripheral wood milling, 4<sup>rd</sup> International Scientific Conference "Wood Technology & Product Design", Pg. 110-118, Ohrid.
- [9] Hutton S. G., (1991):The dynamics of circular saw blades, Munchen: Holz als Roh-und Werkstoff 49105-10.



## DEVELOPMENT OF DISCOLORATION DURING CONVENTIONAL DRYING OF OAK TIMBER

Bogdan Bukara<sup>1</sup>, Goran Mili<sup>2</sup>

<sup>1</sup>*Gir ltd, Adrani - Kraljevo, Republic of Serbia  
e-mail: bogdan.bukara@gir.rs*

<sup>2</sup>*University of Belgrade – Faculty of Forestry,  
Department of Wood Science and Technology,  
Belgrade, Republic of Serbia  
e-mail: goran.milic@sfb.bg.ac.rs*

### ABSTRACT

This research aimed to examine the development of inhomogeneous colour changes in oak timber during conventional drying and its relation to moisture content distribution across the wood thickness. To explore this phenomenon, control boards (quarter-sawn and flat-sawn, 38 mm thick) were cut from two oak logs, one of the sessile oak (*Quercus petraea*) and one of the pedunculate oak (*Quercus robur*). The control boards were dried in a conventional kiln according to the common drying schedule, and at specific time intervals, samples were taken to determine the moisture content profile. During each cutting of the samples, the appearance of discoloration was controlled. The results of the study revealed that there is a connection between the moisture content distribution within the boards and the appearance of discoloration. Furthermore, it was found that sessile oak timber dries more slowly and with less intense discolourations than pedunculate oak timber. It is confirmed that quarter-sawn boards dry slower compared to flat-sawn boards and this applies to both wood species.

**Keywords:** conventional drying, oak timber, discoloration, moisture content profile

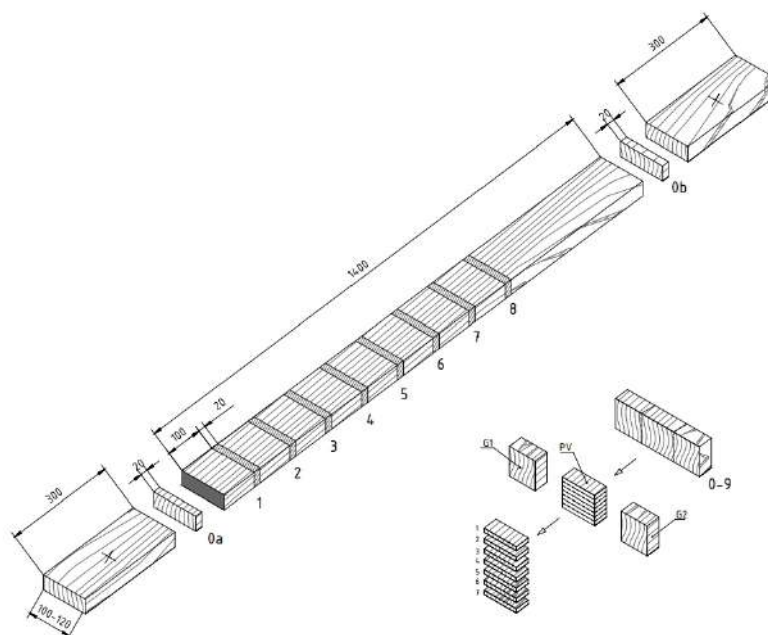
### 1. INTRODUCTION

The highly aesthetic texture of oak wood positions it among the most visually captivating and certainly the most high-priced hardwood species in Europe. Three oak species hold significant positions in Serbian forests: pedunculate oak (*Quercus robur*), sessile oak (*Quercus petraea*), and Turkey oak (*Quercus cerris*), with pedunculate oak and sessile oak finding broader technical applications. From the felled log to high-quality oak wood products, a series of processing steps must be undertaken, among which drying stands as one of the most critical. Drying involves removing a substantial amount of water from the wood while maintaining high quality and the wood's natural color, a challenge particularly pronounced in oak wood. It is known that oak wood undergoes a slight darkening during and after the drying process, frequently accompanied by sections that remain lighter than the surrounding wood. This phenomenon diminishes the visual quality of oak timber and leads to financial losses in the industry. These wood surfaces, characterized by a lighter hue than the surrounding wood after drying, are commonly known as "white clouds" and often manifest as discolorations in the form of irregular alternating brown and white strips (Mili, 2020). In researching of this problem, one direction focused on optimising the drying schedule to avoid the occurrence of discolorations, while another direction delved into the impact of wood extractives on discoloration development. Beyond the physiological processes that take place in living or freshly cut wood, it has been determined that these color changes are caused by chemical reactions of extractive substances (tannins) and cell wall components (Koch and Skarvelis, 2007). Conditions favorable for the development of these discolorations involve high wood moisture content (above 30%), drying temperatures exceeding 30°C, and air humidity around (or above) 70% (Fortuin et al., 1998). of extractive substances in these regions. This prevents the chemical reactions that lead to darkening.

The objective of this study was to examine the relation between drying rate, moisture content (MC) gradient across the thickness of quarter-sawn and flat-sawn boards of pedunculate oak and sessile oak, and the internal discoloration during conventional drying processes.

## 2. MATERIAL AND METHODS

For this study, one log of sessile oak (*Quercus peatrae* L.) and one log of pedunculate oak (*Quercus robur* L.) were selected, each with an average diameter of approx. 40 cm and a length of about 3.0 m. From each log, two quarter-sawn and two flat-sawn trimmed control boards were sawn, with a nominal thickness of 38 mm and a width of 100-120 mm. These boards were marked, and samples were taken from each end to determine initial MC gradient and density (Fig. 1). MC gradient samples were sliced into 7 lammellae, and MC of each lammella was determined by oven dry method. Density was determined on samples with dimensions of 38x38x20 mm. The end-grain of the control boards was protected with adhesive, and they were placed in a conventional kiln with a capacity of 200 m<sup>3</sup>, along with other oak boards of the same thickness. The drying schedule started with an initial temperature of 33°C and concluded at 62°C, while an initial EMC was 17.5%, eventually reaching a final value of 4%. Drying was controlled based on 4 (out of 10) of the wettest electrical probes, positioned at a depth of 1/3 of the board's thickness. Drying continued until the moisture content reached 8%. During the drying process, the control boards were periodically removed from the kiln. From one end, a 20 mm sample was cut to determine MC profile. The discarded 100 mm sections (Fig. 1) were used to assess the occurrence of internal discolorations. The end-grain was re-adhered, and the boards were returned to the kiln. A total of 9 samplings were conducted at specific time intervals: 0 hours (initial), 48 hours, 96 hours, 240 hours, 384 hours, 576 hours, 1008 hours, 1416 hours (end of the active drying phase), and 1440 hours (end of the conditioning phase). The entire drying process lasted 1440 hours (60 days).



**Figure 1:** Test samples for determination of MC profiles (7 lammellae) during drying

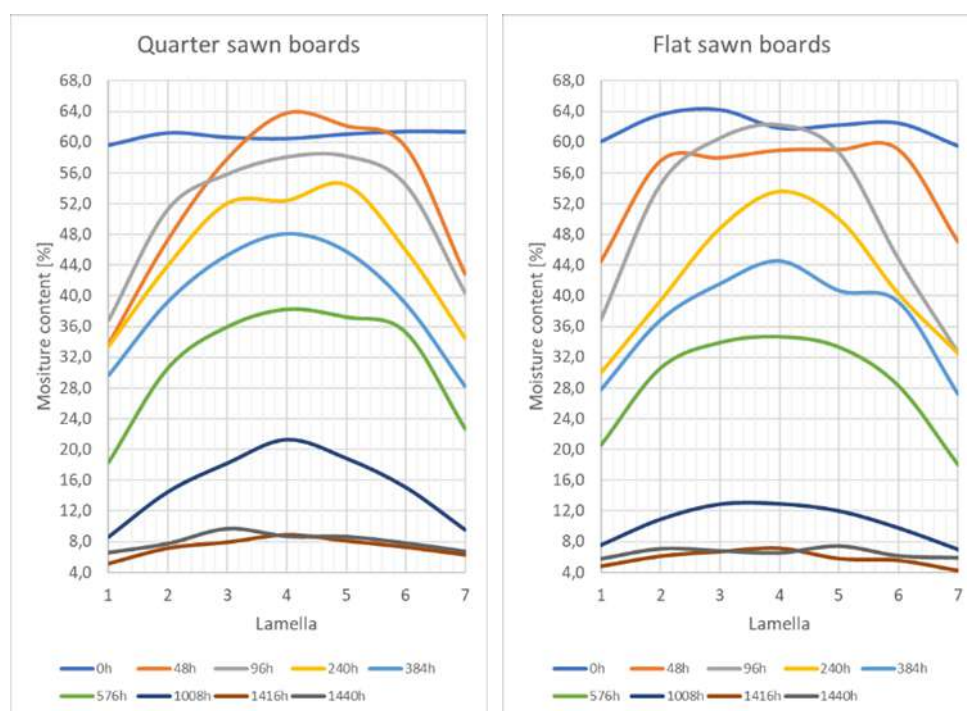
## 3. RESULTS

The average oven-dry density of sessile oak wood was 675 kg/m<sup>3</sup> (variations ranging from 630 to 732 kg/m<sup>3</sup>), which is in agreement with the literature data (Šoški et al. 2005, Deaconu et al. 2023). The pedunculate oak wood exhibited 40 kg/m<sup>3</sup> lower oven-dry density – 635 kg/m<sup>3</sup> (with variations between 620 and 647 kg/m<sup>3</sup>), slightly higher compared to values reported in the literature (Vavrík

and Gryc, 2012). The initial MC of the sessile oak and pedunculate oak boards was 60.8% and 61.7%, respectively.

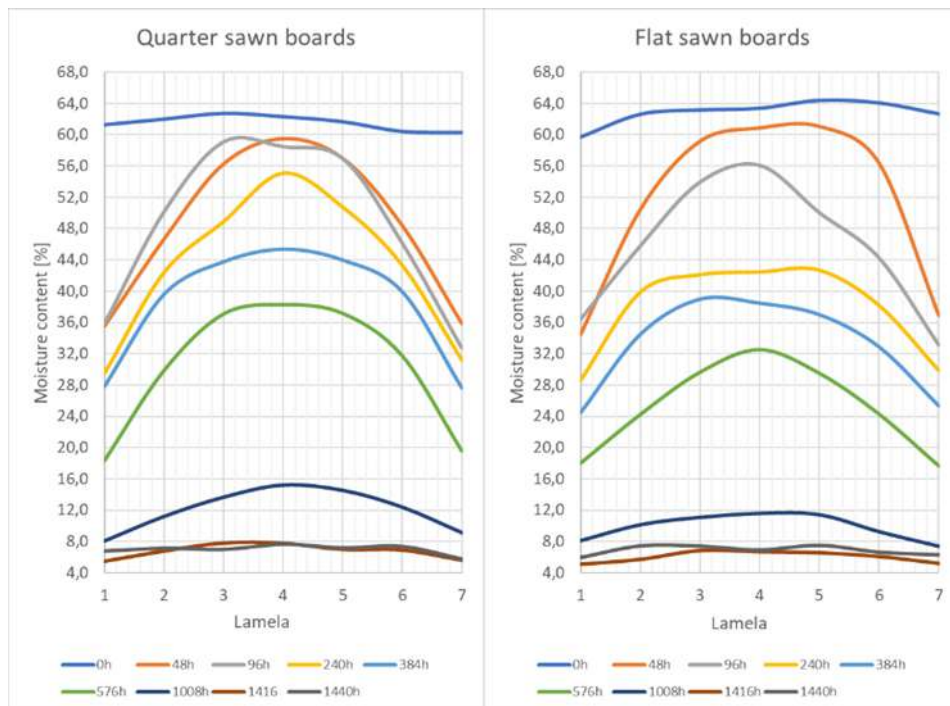
Fig. 2 illustrates the MC profiles across the thickness of sessile oak control boards during the drying process. As expected, the outer layers lost free water fast during the initial days of drying, causing a MC gradient that later prompted the movement of water from the central layers towards the surface. The highest MC difference across the thickness of 20.3% occurred after 48 hours of drying for quarter-sawn boards, while flat-sawn boards exhibited the highest difference of 22.6% after 96 hours of drying. From then on, the MC difference between central and outer layers gradually decreased, ultimately reaching minimal values (2.3-3.3%) at the end of drying.

The difference in drying rates between quarter-sawn and flat-sawn boards became noticeable after 10 days of drying. After 42 days of drying, quarter-sawn boards reached an average MC of 15.6%, while flat-sawn boards reached an average MC of 10.1%, indicating significantly faster drying of flat-sawn compared to quarter-sawn boards. Consequently, this difference led to overdrying of flat-sawn boards (6.4% and 6.5%).



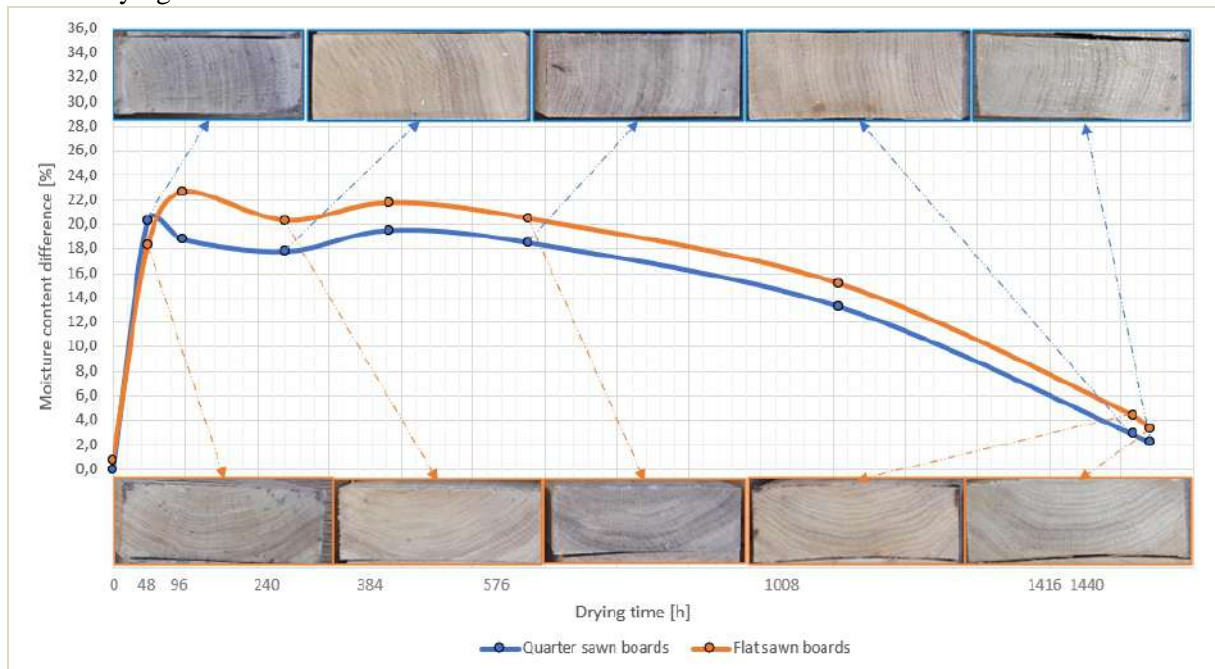
**Figure 2:** MC profiles across the thickness of sessile oak boards during drying

In terms of MC difference across the thickness during drying, a similar pattern was observed in pedunculate oak boards (Fig. 3). The highest MC difference was observed in quarter-sawn and flat-sawn boards after 240 hours (24.7%) and 48 hours of drying (25.1%), respectively. As drying progressed, the MC differences diminished, ultimately reaching minimal values of 0.8-1.4% at the end of the drying process. Again, significantly higher drying rate was found in flat-sawn compared to quarter-sawn boards. This disparity in drying rates became evident already after 96 hours of drying. After 42 days of drying, quarter-sawn and flat-sawn boards achieved average MCs of 12.0% and 9.9%, respectively.

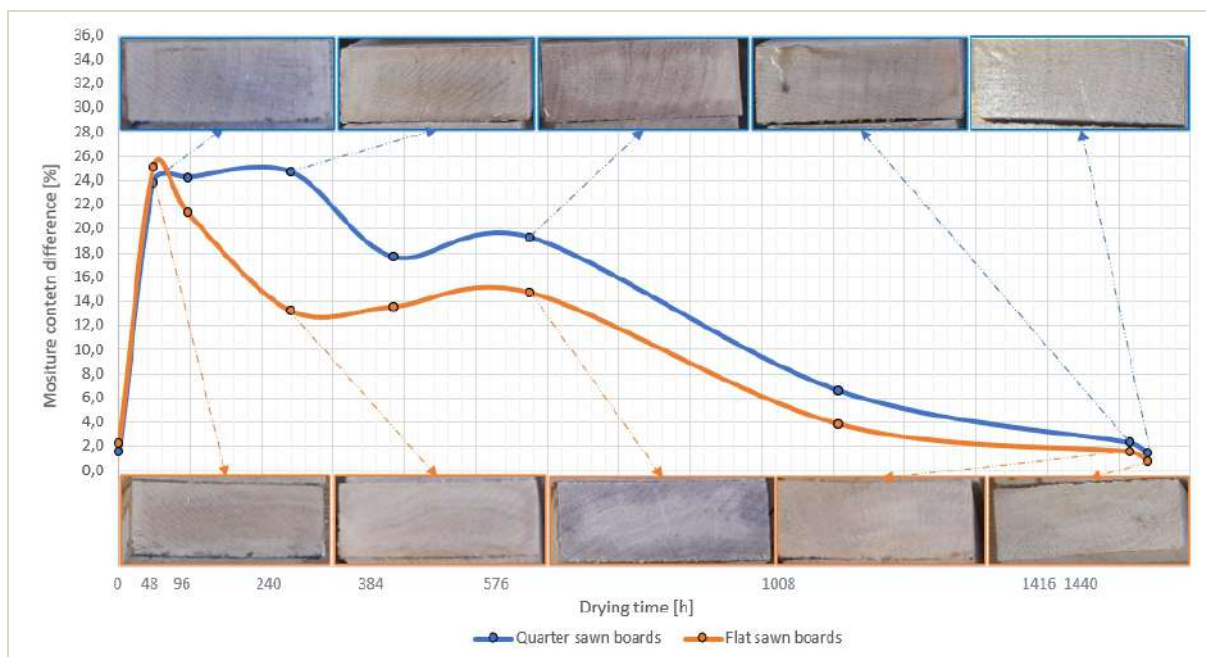


**Figure 3:** MC profiles across the thickness of pedunculate oak boards during drying

Figures 4 and 5 depict MC differences and photographs of board cross-sections taken at specific time intervals for both wood species. In the case of sessile oak, the emergence of cross-sectional discolorations in the form of a darker outer layer and a lighter inner layer is barely noticeable, only becoming apparent after 576 hours of drying (Fig. 4). These discolorations disappear entirely with further drying.



**Figure 4:** MC differences and discoloration progression for quarter-sawn and flat-sawn sessile oak boards



**Figure 5:** MC differences and discoloration progression for quarter-sawn and flat-sawn pedunculate oak boards

In the case of pedunculate oak boards, the occurrence of discoloration on the cross-section can be observed after 240 hours of drying (Fig. 5). These discolorations progressively intensify, with the darker outer layer extending towards the central portions and the inner lighter layer diminishing. At the end of the drying process, subtle irregularities remain visible on the board cross-sections. The more pronounced discolorations in pedunculate oak compared to sessile oak are likely the result of a combined effect of multiple factors. One of these factors is the somewhat differing drying behavior: e.g. higher maximum MC difference (i.e., higher moisture gradient) was observed in pedunculate oak, but this difference decreases significantly faster than in sessile oak during drying. After 42 days of drying, this difference for quarter-sawn and flat-sawn pedunculate oak boards was 7% and 4%, respectively, whereas for sessile oak, these values were as high as 13.5% and 15.5%. Nevertheless, the primary cause of the more pronounced discolorations in pedunculate oak could be the greater density variation within the boards of this species. Areas of higher density within the board retain water for a longer period than areas of lower density, behaving similarly to inner compared to outer layers of the board. This longer presence of free water leads to the accumulation of tannins, which further prevent the darkening of the wood (Felhofer et al. 2021, Hansmann et al. 2020). The irregular forms of discoloration in Fig. 5 also indicate potential density variation.

#### 4. CONCLUSIONS

In this study, an investigation was carried out to explore the behavior of pedunculate oak and sessile oak wood during the drying process, with a specific focus on moisture content (MC) gradients and the development of internal discolorations. The results shed light on the complex interactions between wood species, drying parameters and discoloration formation. The following conclusions can be drawn:

1. The drying behavior of sessile oak and pedunculate oak timber differs: pedunculate oak boards dry faster, with a somewhat higher MC gradient at the beginning of drying, but much lower in the later stages compared to sessile oak boards.
2. Both oak species demonstrated faster drying in flat-sawn boards compared to quarter-sawn boards, although the influence of grain orientation on discolorations remained unclear.
3. Pedunculate oak displayed more pronounced and persistent discolorations. While factors such as moisture content gradients and drying rates clearly influence discoloration, the density

variation within pedunculate oak boards could be a significant contributing element to the observed differences in discoloration intensity.

## REFERENCES

- [1] Deaconu, I., Porojan, M., Timar, M. C., Bedeleian, B., and Campean, M. (2023): Comparative research on the structure, chemistry, and physical properties of Turkey oak and sessile oak wood. *BioResources* 18(3), 5724-5749.
- [2] Felhofer, M., Bock, P., Xiao, N., Preimesberger, C., Lindemann, M., Hansmann, C., Gierlinger, N. (2021): Oak wood drying: Precipitation of crystalline ellagic acid leads to discoloration. *Holzforsch* 75:712–720.
- [3] Fortuin, G., Welling, J., Hesse, C., Brückner, G. (1988). Verfärbung von Eichenschnittholz bei der Trocknung (a). *HolzZentralblatt* 114: 1606–1608.
- [4] Hansmann C., Felhofer M., Preimesberger C., Widhalm B., Bock P., Gierlinger N., (2020): White clouds – Undesired discolouration of oak wood during kiln drying. 9th Hardwood Conference, Sopron, p. 95-98.
- [5] Koch G., Skarvelis M., (2007): Discoloration of wood during drying. *Advances in the drying of wood, COST E15*, p. 1–22.
- [6] Mili G. (2020): Hidrotermi ka obrada drveta, Univerzitet u Beogradu, Šumarski Fakultet Beograd.
- [7] Šoški B., Popovi Z., Todorovi N., (2005): Svojstva i mogu nost upotrebe drveta Hrasta kitnjaka. *Šumarstvo*, Jul – Septembar 2005.
- [8] Vavr ík, H., Gryc, V. (2012): Analysis of the annual ring structure and wood density relations in English oak and Sessile oak. *Wood research*, 57(4), 573-580.

### The Authors' Addresses:

Mili Goran, D.Sc., professor, University of Belgrade - Faculty of Forestry,  
Department of Wood Technology  
Kneza Višeslava 1  
11030 Belgrade, Republic of Serbia

Bogdan Bukara, B.Sc., GIR ltd.  
Jug Bogdanova 18  
Kraljevo, Republic of Serbia

## THE INFLUENCE OF THE QUALITY OF POPLAR LOGS ON THE YIELD IN THE PRODUCTION OF VENEER PACKAGING

Aleksandar Lovri <sup>1</sup>, Vladislav Zdravkovi <sup>1</sup>, Nebojša Todorovi <sup>1</sup>, Stefan Milovanovi <sup>2</sup>

<sup>1</sup>University of Belgrade – Faculty of Forestry  
email: [aleksandar.lovric@sfb.bg.ac.rs](mailto:aleksandar.lovric@sfb.bg.ac.rs); [vladislav.zdravkovic@sfb.bg.ac.rs](mailto:vladislav.zdravkovic@sfb.bg.ac.rs);  
[nebojsa.todorovic@sfb.bg.ac.rs](mailto:nebojsa.todorovic@sfb.bg.ac.rs);  
<sup>2</sup>e-mail: [stefanmilovanovic92@gmail.com](mailto:stefanmilovanovic92@gmail.com)

### ABSTRACT

Poplar logs of F, L, I and II quality classes were used in the research. The logs are first cut to the appropriate size and then rotary peeled into standard elements for veneer packaging. According to the results of the research, a significantly higher quantitative utilization (71.93% and 75.55%) was obtained with F and L class logs compared to quality class I and II logs (58.83% and 53.69% respectively). However, according to the corrected coefficients of economic profitability of processing, it was the least profitable to process logs of F class, followed by class I and finally class II, while logs of class L were the most profitable for processing.

**Keywords:** poplar, wooden crates for packaging, quantitative utilization and financial effect

### 1. INTRODUCTION

All types of product packaging are called by one name - packaging. The packaging protects the product from various mechanical, physical, chemical and microbiological, climatic and other influences. The current primacy on the market is held by wooden crates - as an ecological product that gives the best price-quality ratio compared to plastic and cardboard ones (Van Acker 2016). During the their production, the percentage of waste is very small and almost 100% of the raw material is utilized. Pellets can be produced from the waste (Pradhan et al. 2018), which are further used to obtain thermal energy to heat the production plant or dryer within the company. The waste also is often sold, which allows companies to make additional profit and consequently have a higher degree of self-sustainability. As wooden crates are organic pigs, they do not pollute nature when they get into it. Given that the world is increasingly turning to products that do not pollute the natural environment and tends to reduce the use of plastic, it is clear that wooden crates represent a solution that is optimal in the given circumstances.

In the Republic of Serbia, wooden crates are most often made from poplar wood, which has the appropriate mechanical, physical and chemical properties (Klašnja et al. 2007). The poplar wood has the appropriate toughness to withstand the load it carries for the transport of fruits and vegetables, and on the other hand, it is "soft" enough for quick and easy processing (Shu et al. 2017). The poplar wood also provides satisfactory aesthetics characteristics (Lovri et al. 2014) and, most importantly, does not retain odors that could affect the final quality of the product.

The aim of the research

The goal of this research was to determine the degree of utilization of different types of poplar logs in production of elements for crates. Due to the disproportionate difference in the price of logs among classes, the question arose: Which class is optimal for processing in sense of utilization and profitability? The assumption is that F or L class logs have a higher utilization than other classes, but this difference does not necessarily mean a better economic balance at the end.

The attention must be paid to this issue with over a longer period of time, where the market situation in terms of prices and availability of raw materials should be analyzed and monitored and compared with the price of the finished product. The current timber market is very volatile and that the situation changes from month to month, if not in shorter periods of time, this issue becomes more and more

important. Producers generally rely on bottom line profits while ignoring current market shifts and they are often late to adapt to new conditions.

#### Materials and methods

For the research poplar logs of F, L, I and II class poplar were sorted according to the SRPS D.B4.028 standard. Logs were brought from forest farms in Vojvodina and stored at the log storage facility of Banija-Pal DOO, Serbia. The reason for this type of control is to avoid potential errors during data collection in further research. The moisture content of the logs, as well as their mechanical properties, were not taken into account, because they did not significantly affect the final results. Since the goal of the research is to investigate utilization of raw materials, the measurements were related to the dimensions of the log (diameter, length, bark thickness). One specimen was selected from each log class (Figure 1) and the volume of each of them was measured before and after debarking. After measuring the volume, further logs processing and the produced assortments were monitored. The assortments were counted and their total volume was calculated, what was later compared to the initial volume of the log.



*Figure 1: Poplar logs*

## 2. LOGS VOLUME MEASURING

After logs selection, the length, mean diameter and bark thickness each log was measured before being sent to the debarker. The length was measured twice, because the bases are not clearly formed, so the length varied depending on the place of measurement. The length was measured using a regular tape measure. A large wooden caliper was used to measure the middle diameter, and the measurement was made in the middle and at the ends, at each point of measurement by cross-positioning the caliper. Bark thickness was measured at three positions from the base of the log to its end. For each dimension that was measured (length, diameter and bark thickness), the mean value of multiple measurements was taken at each point to obtain more accurate results.

After all necessary measurements were made, the logs were transported for debarking. Transport was carried out using a forklift. After removing the bark, on each log the places where the cutting should be done are marked with a marker. The length of the logs depended on the production needs. Logs marked in this way were transported by chain conveyor to the cutter. The volume of full length logs and cutted logs was calculated according to Rieke's (Newton's) formula:

$$V = \frac{(g_0 + 4g_s + g_n) \cdot L}{6}$$

(1)

$g_0$  – the base surface area at the thinner end of the log in  $m^2$

$g_s$  – the base surface area at the middle of the log in  $m^2$

$g_n$  – the base surface area at the thicker end of the log in  $m^2$

$L$  – log length in m.



The logs were further transported to the peeler where the elements for the crates were made. After rejecting the scrap, the elements that satisfy in quality were stacked on the cart (picture 2) until the complete log has been processed and the final number of elements was obtained. The elements were then manually counted. After they were counted, the elements were transferred to the line to form the bottom of the crates. The line consists of a series of molds and automatic guns for joining elements. The elements were placed on the line manually. The formed crate bottoms were then stacked and transported to the crate forming line. The elements that will make up the sides of the crates, as well as the elements that represent vertical reinforcements at the joints of the sides, are brought to the line. The entire methodology was aimed to monitor the acquisition of elements and counting them in order to obtain their quantity and their volume.



*Figure2: Elements after peeling of poplar logs*

## 4. RESULTS AND ANALYSIS

### 4.1 Logs and residue proportion

The lengths of the logs are determined by the needs of production, as well as by the maximum utilization of raw materials. In relation to production needs, ie. in relation to the production program of the company itself, the lengths of the logs vary. In the analyzed production period, lengths of 63 cm, 53 cm, 43 cm, 47 cm and 33 cm were represented. It is important to note that the class of raw material has no influence here and that it does not affect the determination of the dimensions for obtaining the elements, but they are determined by the needs of production.

*Table 1: Utilization of logs by classes*

Class	Log volume without bark (m <sup>3</sup> )	Number of cutted logs (pcs)	Volume of cutted logs (m <sup>3</sup> )	Utilization (%)
<b>F</b>	<b>0.846</b>	<b>5</b>	<b>0.820</b>	<b>96.95</b>
<b>L</b>	<b>0.515</b>	<b>8</b>	<b>0.502</b>	<b>97.47</b>
<b>I</b>	<b>0.157</b>	<b>4</b>	<b>0.152</b>	<b>97.10</b>
<b>II</b>	<b>0.656</b>	<b>9</b>	<b>0.567</b>	<b>86.34</b>

According to the results (Table 1), it can be seen that cutted logs have a much higher percentage of participation in the volume of logs in F, L and I class than in II class. The reason for this is the length of the logs of F, L and I class, what corresponded more to the length modules to they were cutted than was the case in the II class log. Another reason was the presence of cracks in Class II logs, so the log had to be shortened additionally. As a third reason that affected to the result, the curvature

of the Class II log prevented the entry of the log into the debarker, so it was necessary to cut off certain parts of the log in order to obtain the appropriate shape.

#### 4.2 Assortments and their share

After logs peeling, the main assortments for making elements for crates were obtained (Tables 2 and 3), so as secondary assortments for forms and cubes for pallets. (Table 4). The term assortments refers to elements that meet the quality and dimensions criteria required for the production of crates. Usable scrap refers to elements that could not be used in full, but their dimensions allowed us to shorten them to obtain an elements for shorter side of the crate. The shapes (rest rolls) represent the rest of the logs that could not be processed due to the technical characteristics of the machine. They are later processed into cubes that were used as pallet feet. After data collection and processing, the following results were obtained:

**Table 2:** Share of assortments (elements) for crates obtained from cutted logs

Class of log	Dimensions of elements			Volume of elements (m <sup>3</sup> )	Number of elements	Total volume of elements (m <sup>3</sup> )	Elements share (%)
	Length (m)	Width (m)	Thickness (m)				
F	0.291	0.056	0.0013	0.000021	27852	0.590	71.93%
L	0.494	0.053	0.004	0.000104	3620	0.379	75.55%
I	0.593	0.054	0.004	0.000128	700	0.090	58.83%
II	0.437	0.084	0.0016	0.0000587	5179	0.304	53.69%

**Table 3:** Share of usable scrap for the production of crate elements

Class of log	Dimensions of elements			Volume of elements (m <sup>3</sup> )	Number of elements	Total volume of elements (m <sup>3</sup> )	Scarp share (%)
	Length (m)	Width (m)	Thickness (m)				
F	0.291	0.056	0.0013	0.000021	5362	0.045	5.54%
L	0.494	0.053	0.004	0.000104	477	0.020	3.98%
I	0.593	0.054	0.004	0.000128	177	0.009	5.95%
II	0.437	0.084	0.0016	0.0000587	956	0.022	3.96%

**Table 4:** Share of shapes and cubes for pallets

Class of log	Volume of shapes (m <sup>3</sup> )	Shapes share (%)	Volume of cubes (m <sup>3</sup> )	Cubes share (%)
F	0.036	4.39	0.031	3.81
L	0.045	8.96	0.039	7.68%
I	0.028	18.42	0.025	16.39
II	0.052	9.17	0.041	7.17%

According to above table, it is obvious that the obtained elements participate in a much higher percentage in F and L class logs (71.93% and 75.55%), than in I and II class logs (58.83% and 53.69%). A number of factors contributed to obtaining such results:

1) The first factor and certainly the most important is the diameter of the log being processed. By increasing the diameter of the log, there is a reduction in the proportion of shapes, which results in

obtaining more elements for the production of crates. This effect is especially pronounced in the Class I log, which had the smallest diameter of all the tested logs;

2) The second factor is the log class, because F and L class logs have fewer errors in the structure of the log and have a more regular shape, which enables processing without the appearance of large gaps between the elements. In the II class log, cracks appeared on the log itself and for this reason the log could not be processed to an optimal extent. There were also errors in the structure of the wood, so the percentage of total scrap was high (21.91%);

3) The third factor refers to specified dimensions of the elements, because the smaller the dimensions of the elements, the greater the possibility of using usable scrap that appears during peeling.

### 4.3 Justification of using F and L logs in the production of crates

Logs buyers are conditioned by JP VOJVODINAŠUME in sense when purchasing I and II class they must also buy a certain part of F and L class logs, the question arises whether it is economically profitable to use F and L class logs in the production of crates. As Euro-American poplar is mostly used in production, for that reason their prices were also analyzed. According to the official price list of JP VOJVODINAŠUME (year 2022), the price of F class per cubic meter is 80.16 EUR per m<sup>3</sup>, L class 62.79 EUR per m<sup>3</sup>, I class 48.97 EUR per m<sup>3</sup>, and II 38.49 EUR per m<sup>3</sup>.

According to this price list, the prices of the examined logs are as follows:

1. F class log – EUR 69.50
2. L class log – EUR 31.96
3. First class log – EUR 9.31
4. Second class log – EUR 25.25

The elements obtained from L and I class logs are the elements that are most often used in the production of crates, so the profitability coefficient was calculated in relation to them. For this reason, a correction was made to the amount of elements obtained from F and II class logs, which are smaller in volume and are used exclusively for making paths or strengthening crates. The volume of elements obtained from L and I class logs is five times higher than volume of elements from F class, and twice than volume of elements obtained from II class. If we take into account that of 20 elements for one three-row crate in average is necessary, the number of crates obtained from each class of examined logs is as follows:

1. From the F class log, we obtained –  $27852/20 = 1393$  pieces

The elements obtained from F logs are 5 times smaller in volume than the elements obtained from L and I class logs and they were used only in the production of floors, so the amount obtained is divided by 5. So the amount of crates from F class logs is:  $1393/5 = 278$  pieces.

2. From L class logs, we obtained –  $3620/20 = 181$  pieces
3. From class I logs  $700/20 = 35$  pieces were obtained
4. From class II logs  $5179/20 = 259$  pieces were obtained

The volume of elements obtained from Class II logs is about 2 times smaller than the volume of L and Class I, so the amount obtained is divided by 2. The amount of crates obtained from Class II logs is:  $259/2 = 130$  pieces.

The average price of a three-row crate on the market for smaller quantities (smaller quantities means quantities less than 1500 pieces) is 1 EUR or 117.5 RSD. If take this into account, we get that the values of the obtained products, from each class, are as follows:

1. F class log – 278 EUR
2. L class log – 181 EUR
3. Class I log – 35 EUR
4. Class II log - 130 EUR

In order to determine whether some class is more or less profitable, we need to compare the market price of the log with the market price of the cost of the obtained products. This ratio shows us how many times money was earned on each log.

The F class log cost EUR 69.50, and the value of the obtained products is EUR 278. When we divide these two values, we get the following result:  $278/69.5 = 4.01$ . This shows us that the income was 4 times more money than the cost price of the log. For L class, the result is the following  $181/31.96 = 5.68$ . In class I it is  $35/9.31 = 3.76$ , and in class II it is  $130/25.25 = 5.16$ .

**Table 5: Profitability coefficients**

F class	4,01
L class	5,68
I class	3,76
II class	5,16

The results show that the highest profitability is in the processing of class L logs, and the lowest in class I logs. The characteristics of the logs should certainly be taken into account, primarily the diameter of the log. In the case of Class I log, the diameter of the log was significantly smaller, and thus the fewest elements were obtained. If we equalize volumes of I and II class logs and assume that the utilization of class I logs is the same, we would get the following result:

The volume of a Class II log is  $0.656 \text{ m}^3$  and 130 crates were obtained from it. The volume of a Class I log is  $0.157 \text{ m}^3$  and 35 crates were obtained from it.

If we assume that the utilization of class I logs remained the same, than the obtained elements participate in the same percentage (58.83%), which means approximately  $0.383 \text{ m}^3$  of elements from a class I log that has a volume of  $0.656 \text{ m}^3$ . One element has a volume of  $0.000128 \text{ m}^3$ , so we would get approximately 2992 elements from a Class I log. If we know that one crate is made of 20 elements, it can be concluded that from 2992 elements  $2992/20 = 150$  crates can be made.

The value of the crates obtained from such class I log would be EUR 150. A class I of poplar log, according to the official price list of JP VOJVODINAŠUME, costs 48.97 EUR/m<sup>3</sup>, so a log with a volume of  $0.656 \text{ m}^3$  would cost  $48.97 \cdot 0.656 = 32.12$  EUR. When we compare the market price of the log, and the selling price of the product, we get  $150/32.12 = 4.67$ .

**Table 6: Corrected profitability coefficients**

F class	4,01
L class	5,68
I class	4,67
II class	5,16

## 5. CONCLUSIONS

From all this, it can be concluded that the least profitable log is the F class. The results indicate that the L class is the most profitable, followed by the II class, despite the largest share of the total scrap (of 22.12%), because the price is lower compared to other classes, and yet a satisfactory amount of product is obtained that justifies its use. This results were obtained on the basis of a smaller sample that was examined, and a long-term and thorough examination of which class of logs is the most profitable in this type of production should certainly be undertaken.

### Conclusion

The production of veneer crates as an activity that deals with the production of an ecological product, with the maximum utilization of raw materials, perfectly fits into World trends. The trends are such that there is an aspiration towards as little pollution of nature as possible, and crates,

compared to other types of product packaging, have the possibility of recycling in a large percentage. And in the production process itself, all by-products that are obtained are used to the greatest extent possible, enabling a lower need for energy sources, while not polluting nature.

The justification for using F and L class logs in the production of veneer crates, from an economic point of view, most likely exists. However, the question arises, are veneer crates a product that should be made from F and L logs economically? Although the L class showed the highest profitability coefficient, it was not significantly higher than that of I and II class logs, while it was even the smallest in the case of F class logs. Other types of poplar based products should be considered from F and L grade logs that would be more cost effective than crates like plywood or similar.

Literature cited

## REFERENCES

- [1] Bao, F., & Liu, S. (2001). Modeling the relationships between wood properties and quality of veneer and plywood of Chinese plantation poplars. *Wood and fiber science*, 264-274.
- [2] El Haouzali, H., Marchal, R., Bléron, L., Kifani-Sahban, F., & Butaud, J. C. (2020). Mechanical properties of laminated veneer lumber produced from ten cultivars of poplar. *European Journal of Wood and Wood Products*, 78, 715-722.
- [3] Klačnja, B., Orlović, S., Drekić, M., Radosavljević, N., & Marković, M. (2007). Possibilities of using poplar wood for chemical and mechanical processing. *Topola*, (179-180), 3-13.
- [4] Kurt, R., & Cavus, V. (2011). Manufacturing of parallel strand lumber (PSL) from rotary peeled hybrid poplar I-214 veneers with phenol formaldehyde and urea formaldehyde adhesives. *Wood research*, 56(1), 137-144.
- [5] Pradhan, P., Mahajani, S. M., & Arora, A. (2018). Production and utilization of fuel pellets from biomass: A review. *Fuel Processing Technology*, 181, 215-232.
- [6] Purba, C. Y. C., Pot, G., Viguiet, J., Ruelle, J., & Denaud, L. (2019). The influence of veneer thickness and knot proportion on the mechanical properties of laminated veneer lumber (LVL) made from secondary quality hardwood. *European Journal of Wood and Wood Products*, 77(3), 393-404.
- [7] Sedighzadeh, P., Moradpour, P., & Hosseinabadi, H. Z. (2023). Possibility of making flexible three-ply plywood using poplar (*Populus deltoides*) and Paulownia (*Paulownia fortunei*) veneers. *European Journal of Wood and Wood Products*, 81(1), 209-221.
- [8] Shu, Z., Liu, S., Zhou, L., Li, R., Qian, L., Wang, Y., ... & Huang, X. (2017). Physical and mechanical properties of modified poplar veneers. *BioResources*, 12(1), 2004-2014.
- [9] SRPS D. B4. 028 (1979) Proizvodi eksploatacije šuma – Trupci lišćara za rezanje, Institut za standardizaciju Srbije.

## LIGNOCELLULOSE COMPOSITION, PROXIMATE ANALYSIS AND HEAT VALUE OF CERTAIN FOREST AND ENERGY CROP BIOMASSES AND THEIR POTENTIAL AS RAW MATERIALS FOR THE PRODUCTION OF SOLID BIOFUELS

Božidar Matin<sup>1</sup>, Ana Matin<sup>2</sup>, Ivan Brandi<sup>2</sup>, Alen Adurovi<sup>1</sup>, Josip Ištvani<sup>1</sup>, Alan Antonovi<sup>1</sup>

<sup>1</sup>University of Zagreb, Faculty of Forestry and Wood Technology, Zagreb, Croatia,  
e-mail: bmatin@sumfak.hr; adurovic@sumfak.hr; jistvanic@sumfak.hr aantonovic@sumfak.hr;

<sup>2</sup>University of Zagreb, Faculty of Agriculture, Zagreb, Croatia,  
e-mail: amatin@agr.hr; ibrandic@agr.hr

### ABSTRACT

Biomass as a raw material is available in large quantities and inexpensive. Its renewable energy can reduce greenhouse gas emissions, and it depends primarily on the composition of lignocellulose, especially the lignin content. Forest biomass of oak and beech, as well as biomass of the energy crops switchgrass (*Panicum virgatum* L) and *Miscanthus x giganteus* were used for this study. The aim of the study was to determine the lignocellulosic composition (proportions of cellulose, lignin, hemicellulose), proximate analysis (proportions of moisture, ash, coke, fixed carbon, volatiles) and calorific value of the studied biomasses, as well as to examine the possibility of their use as raw materials for the production of solid biofuels. The research showed that both forest biomass and biomass of energy crops have favorable values of the studied parameters, which is best reflected in the excellent calorific value, ranging from 17.0 to 18.5 MJ kg<sup>-1</sup>. It was also found that the studied samples are ideal raw materials for the production of solid biofuel with lignin content between 20.0 and 30.0%.

**Keywords:** forest biomass, energy crops, lignocellulose, proximate analysis, calorific value, solid biofuel

### 1. INTRODUCTION

The burning of fossil fuels releases large amounts of CO<sub>2</sub> and other greenhouse gases (GHGs) into the atmosphere. These excessive GHG emissions lead to adverse climate changes that have recently manifested themselves in the form of droughts, rainfall accompanied by heavy storms, floods, etc., as well as the depletion of non-renewable energy sources (McKendry, 2002).

In the production of primary energy in 2020, fossil fuels had a share of 80% (oil 29.0%, coal 27.0%, natural gas 24.0%), while the share of renewable energy was 15.0% (WBA, 2022). All this drew the attention of mankind to the use of lignocellulosic biomass, which could replace fossil fuels thanks to its energy potential (Bilandžija et al., 2016).

Lignocellulosic biomass, as a source of organic material in which solar energy is stored through the process of photosynthesis, is becoming an increasingly important component of society and the economy itself. Biomass releases stored energy when the bonds between molecules are broken, whether through a decomposition, digestion or combustion process. Burning biomass also releases certain amounts of CO<sub>2</sub> into the atmosphere; however, replanting plants ensures that these amounts are absorbed through their new growth cycle (McKendry, 2002).

However, the potential of biomass as one of the renewable energy sources depends on the amounts of feedstock available globally from forestry, agriculture, wood processing, or industrial production (Li, Rezgui, Zhu, 2017).

In 2020, the global biomass supply was 57.5 Exajoule (10<sup>18</sup> Joules), with 86.0% of the total supply coming from solid biomass such as wood chips, wood pellets, and other traditional biomass sources, 7.0% from liquid biofuels, 3.0% from municipal waste, 2.0% from industrial waste, and 2.0% from biogas (WBA, 2022).

For agricultural biomass, which includes energy crops, there is almost no systematic data on available quantities. The amount of available agricultural biomass is mainly determined by empirical models through various deductions from total agricultural production, rarely taking into account variables that occur due to varietal differences, agrotechnical measures, or agroclimatic conditions, and the calculation is also affected by the lack of data on the method of collection and use of agricultural residues (Camia et al., 2018).

In recent decades, research has focused on fuel properties and the technology of processing, refining, and using biomass for energy production (Saleem, 2022). Biomass-derived renewable energy, i.e., biofuel, can be divided into primary and secondary energy. Primary fuels include firewood, wood chips, wood pellets, and post-harvest residues, which are mainly used in heating systems (Rodionova et al., 2017), while secondary biofuels include solid (coal), liquid (biodiesel, bioethanol), and gaseous (hydrogen, biogas) fuels as derivatives of the primary fuels. Liquid and gaseous biofuels can also be produced by processing biomass and used as an energy source in certain industrial processes or transportation (Doshi et al., 2016). Secondary biofuels are divided into four generations: the first and second generations are based on primary biomass sources (Azad et al., 2015), the third on microalgae (Chew et al., 2018), and the fourth on genetically modified microalgae (Zhu et al., 2017). It has become clear that the first two generations will not be sufficient to meet growing energy demand, and therefore more work will be needed to develop third and fourth generation biofuels (Osman et al., 2021).

Recently, lignocellulosic biomass of forest or agricultural origin has gained importance as a feedstock for energy production (Arteaga-Perez et al., 2015). Lignocellulosic biomass is a valuable renewable feedstock source that can be used directly or indirectly to produce bioproducts through chemical, physical, enzymatic, or microbial processes in the energy and industrial sectors (heat and/or electricity) and in the chemical industry (chemicals, adhesives) (Guo, Sun, Grebner, 2010; Rodriguez and Espinosa, 2021).

Forest biomass remains the most important feedstock source for solid biofuel production. However, new European Union legislation to prevent excessive deforestation and use of forest biomass requires a change in biomass sources, which is expected to increase the share of biomass use from agriculture and the agri-food industry (Grzybek, 2008, Budzy ski, Szczukowski, Tworkowski, 2009). The agricultural sector contributes about 10.0% of the global biomass supply, but there is significant potential for increasing its contribution. For this reason, agriculture could be a key sector for bioenergy use in the future, especially for energy crops (WBA, 2022).

Various studies show that energy crops are an environmental and economic option for sustainable energy production. Energy crops can be annual or perennial and grown on poorer quality soils, tolerate moisture deficiencies well, and can provide high biomass yields. These energy crops include switchgrass and *Miscanthus x giganteus*, which have already been researched (Koçar and Civas, 2013; Bilandžija et al., 2014). However, biomass as a fuel also has disadvantages such as irregular shape, large volume, low bulk density (up to 100 kg m<sup>3</sup> in agriculture, up to 200 kg m<sup>3</sup> in forestry), uneven combustion due to different moisture content, and lower calorific value compared to fossil fuels (Mitchell et al., 2007; Vassilev, Vassileva, Vassilev, 2015). The composition of the biomass itself can vary due to several variables, such as: the type or part of the plant, the ability to absorb nutrients from soil, water, and sunlight during growth and their accumulation in plant tissues, the amount of artificial fertilizers and preservatives used, agroecological growing conditions, the timing and method of harvesting, the collection method and conditions during transportation and storage, differences in ash content, and the combination of different types of biomass (Vassilev et al, 2010).

It is necessary to know the physicochemical properties as well as the methods for analytical characterization of these properties because they can significantly affect the conversion process as well as the supply chain network for raw materials and transportation (Cai et al., 2017). In addition, physicochemical properties serve as protection against infestation by pathogens and pests (Bhuiyan et al., 2009). The chemical composition of biomass is determined by several main components, namely polymers: cellulose, lignin, and hemicellulose (Williams, Emerson, Tumuluru, 2017), which provide structure and strength to plants (Sanderson, 2011), and their proportion and structure depend on the type of plant cell wall (Barakat, de Vries, Rouau, 2013). Cellulose and hemicellulose together with lignin account for more than 90.0% of the composition of lignocellulosic biomass, and biomass with higher lignin content is more suitable for conversion into solid biofuels because it increases the

calorific value (Li et al., 2003; Chen and Dixon, 2007). This is because lignin has an upper heating value (HHV) between 22.2 and 28.5 MJ kg<sup>-1</sup> (Demirbas, 2017), while the heating value of cellulose and hemicellulose is slightly lower at 18.6 MJ kg<sup>-1</sup> (Demirbas, 2001).

Proximate analysis includes non-combustible materials that do not ignite under normal conditions, even when exposed to elevated temperatures, and includes moisture, ash, coke, solid carbon, and volatiles.

Calorific value is a basic parameter for calculating the energy and potential of biomass, as well as a basic parameter for classifying the quality of the biofuel itself. The heating value is divided into the higher heating value (HHV) and the lower heating value (LHV). The HHV is the heat released during the combustion of the fuel, additionally utilizing the condensation heat of the water vapor from the flue gasses, i.e., it is the highest possible energy that can be obtained during the combustion of a fuel. The LHV is the heat released by the combustion process of the fuel without additional use of the condensation heat of the water vapor, and therefore the LHV is always lower than the HHV. For biomass, the difference between these values is about 7.0% on average (Lewandowski et al., 2003; Garcia et al., 2012).

The objective of this work was to determine the lignocellulosic composition, proximate analysis, and heating value of two forest species (oak and beech) and two agricultural energy crops (switchgrass and *Miscanthus x giganteus*). In addition, the possibility of their use for the production of solid biofuels such as pellets and briquettes was determined, depending to a large extent on the lignocellulosic composition itself and on the energy potential of each of the above biomasses.

## **2. MATERIALS AND METHODS**

### **2.1 Raw material collection and sampling**

Two agricultural energy crops (switchgrass and *Miscanthus*) were collected at the Šašinovec Experimental Station of the Faculty of Agriculture, University of Zagreb (N 45° 85' 01", E 16° 17' 67"). The sampled switchgrass and *Miscanthus* biomass was harvested in March 2022. Two forest species (oak and beech) were collected from company Bjelin Spa va d.o.o. in the town of Vinkovci, Croatia.

Chemical analyses were performed in the laboratory of the University of Zagreb, Faculty of Forestry and Wood Technology, and in the laboratory of the University of Zagreb, Faculty of Agriculture, according to standard methods. Prior to the chemical analyses, the biomass was dried for 48 hours using a laboratory dryer UF 160 Memmert (Mettler-Toledo GmbH, Germany) at a temperature of 60 °C in order to achieve equilibrium in the material so that the comparison of the samples could be performed under identical operating conditions.

#### **2.2. Methods**

After drying, the biomass was comminuted with a laboratory mill SM400 Retsch (Retsch GmbH, Germany) using a sieve with round openings 4.0 mm Retsch (HRN EN ISO 14780:2017) and then further comminuted with a rotating hammer mill SR300 Retsch (Retsch GmbH, Germany) using a sieve with trapezoidal openings 2.0 mm Retsch (HRN EN ISO 14780:2017). Each sample was analyzed at least three times to ensure reproducibility of the analyzes.

#### **2.2.1 Lignocellulosic composition**

In the analysis of lignocellulosic composition, the percentage of accessory substances (TAPPI 204 cm-2007) was determined using the Soxhlet R108S BEH Rotest extraction instrument (Behr, Labor-Technik GmbH, Germany), cellulose (a mixture of HNO<sub>3</sub> and CH<sub>2</sub>OH) by boiling in a Hydro H9V Lauda water bath (Lauda GmbH, Germany), lignin (TAPPI T 222 - 2002) by boiling on a magnetic stirrer with an IKA C- MAG HS 7 heater (IKA®-Werke GmbH & Co. KG Germany), while the percentage of hemicellulose was determined by calculation.



### 2.2.2 Proximate analysis

For proximate analysis, samples were characterized using standard methods: moisture content (HRN EN 18134-2:2017) was determined in a laboratory dryer UF 160 Memmert (Memmert GmbH, Germany), while ash content (HRN EN ISO 18122:2015), coke (HRN EN ISO 18123:2015), fixed carbon (HRN EN ISO 18123:2015), and volatile matter (HRN EN ISO 18123:2015) were determined using a Nabertherm L9/11/B170 muffle furnace (Nabertherm GmbH, Germany).

### 2.2.3 Heating value

HHV was determined according to the method (HRN EN ISO 18125:2017) using an IKA C 6000 adiabatic calorimeter (IKA® -Werke GmbH & Co. KG, Germany), while LHV was determined by calculation.

### 2.2.4 Statistical analysis

After analysis, results were evaluated using PROC MIXED from the SAS software package (SAS Institute Inc., SAS 9.1.2 Help and Documentation, Cary, NC: SAS Institute Inc., 2002–2004, Raleigh, NC, USA, North Carolina State College).

## 3. RESULTS AND DISCUSSION

### 3.1 Laboratory tests

The lignocellulose composition results are shown in Table 1, while proximate analysis results are shown in Table 2. Lignocellulosic composition and proximate analysis are considered as one of the most important parameters in evaluating biomass as more or less suitable feedstock for use in direct combustion systems. Moisture content (MC), ash content (AC), and volatile matter (VM) are undesirable components of biomass, while higher fixed carbon content (FC) and coke content (CK) and higher heating values are desirable and improve the quality of biomass in direct combustion systems.

### 3.2 Lignocellulosic composition

Lignocellulosic biomass has a cellulose content between 30.0 and 50.0%, 10.0 to 30.0% lignin, and 20.0 to 35.0% hemicellulose, while ash, oils, and proteins make up the rest (Saha, 2005). Forest biomass contains on average between 50.0 and 55.0% cellulose, 20.0 to 30.0% lignin, and between 15.0 and 30.0% hemicellulose (Antonovi, 2004). Agricultural biomass has an average cellulose content between 40.0 and 50.0%, 10.0 to 30.0% lignin, and between 20.0 and 30.0% hemicellulose (Malherbe and Cloete, 2002; Kumar et al., 2009; Iqbal et al., 2011). Comparing the average percentages of lignocellulosic composition of the studied forest species and agricultural energy crops listed in Table 1, it can be concluded that the obtained values are in agreement with the above studies of the mentioned authors.

*Table 1: Lignocellulosic composition*

Sample	Cellulose (%)	Lignin (%)	Hemicellulose (%)	Extractives (%)
Oak	50.39b±0.09	26.02b±0.29	21.98ab±0.29	1.59ab±0.36
Beech	45.78a±0.10	25.50b±0.22	23.61b±0.01	1.34a±0.29
Switchgrass	46.42a±0.52	21.34a±0.61	20.55a±0.05	3.81b±0.10
Miscanthus	47.85b±0.55	21.61a±0.42	22.89b±0.19	1.22a±0.06
Significance	***	***	***	***

Values in the column with the same letter are not statistically significantly different with  $p < 0.05$ . Statistical difference: \*\*\*  $p < 0.001$ , NS—not significant.

### 3.3 Proximate analysis

All examined proximate parameters showed a significant statistical difference. As shown in Table 2, MC of the studied samples ranged from 9.09% for oak to 14.02% for Miscanthus. AC was also lowest in oak at 0.35% while the highest AC of 3.74% was recorded in switchgrass samples. Switchgrass and oak had the highest contents of CK at 14.79% and 14.29%, respectively. The highest content of FC (13.01%) was recorded in oak, while beech and Miscanthus had the lowest FC content with 8.91% and 9.01%, respectively. The highest VM content was found in Miscanthus (85.44%) and Beech (83.19%), and the lowest in Oak (79.99%).

**Table 2:** Proximate analysis

Sample	MC (%)	AC (%)	CK (%)	FC (%)	VM (%)
Oak	9.09a±0.04	0.35a±0.02	14.29b±0.29	13.01ab±0.26	79.99a±0.26
Beech	11.89b±0.10	0.55a±0.01	10.19a±0.09	8.91a±0.70	83.19b±0.56
Switchgrass	10.98a±0.22	3.74b±0.08	14.79b±0.67	10.29b±0.63	80.89a±0.72
Miscanthus	14.02b±0.18	1.73ab±0.26	13.87b±0.84	9.01a± 0.79	85.44ab±0.85
Significance	***	***	***	***	***

Values in the column with the same letter are not statistically significantly different with  $p < 0.05$ . Statistical difference: \*\*\*  $p < 0.001$ , NS—not significant.

Noncombustible components of biomass include MC, AC, and FC. MC in biomass can vary widely and is an undesirable component of any fuel (Oberberger and Thek, 2004). For example, Carvalho et al. (2017) reported a MC of 9.7% for oak, which is almost identical to the result of this study. In general, biomass AC can contain between 1.0 and 40.0% (forest less than 0.5%, agriculture up to 25.0%). Feedstocks with a higher AC have a lower calorific value, so a lower percentage is desirable, and biomass with a higher AC significantly reduces the efficiency of the combustion system (Vo a et al., 2021).

Telmo, Lousada, Moreira (2010) and Ulusal et al. (2021) reported for hardwood AC up to 0.8%, VM up to 85.9% and FC up to 16.4%, so the AC, VM and FC of the studied oak and beech were below the literature limits. In the literature, MC (spring harvest) for switchgrass varies from 6.0 to 9.1% (Sadaka et al., 2014; Tumuluru, 2015), while for Miscanthus (spring harvest) it ranges from 7.5 to 11.5% (McKendry, 2002; Garcia et al., 2012), therefore MC for the studied switchgrass is below the literature limits, while it is much higher for Miscanthus. In the literature, Clarke and Preto (2011) reported AC of 5.7% for switchgrass, Sadaka et al. (2014) reported FC of 23.1% and Kumar and Ghosh (2018) reported VM of 83.2%, so it can be concluded that AC, VM and FC of the studied switchgrass are below the literature values. For Miscanthus, Bilandžija et al. (2018) reported AC of 1.78% in the literature, for FC Jackson et al. (2016) reported 14.49% and for VM Bilandžija et al. (2017) reported 86.52%. The results of the study show that for the studied Miscanthus, only the percentage of VM was above the limits of the literature reports, while the percentages of AC and FC were below.

### 3.4 Heat value

In this type of research, calorific value is one of the most important parameters because it represents the energy value that can be obtained by burning certain biomass or biofuels (Garcia et al., 2012). Of the heating values, the HHV and LHV have been studied, and the differences that occur are mainly the result of unequal cell structure and different MC and AC (Lewandowski et al., 2003). For example, forest biomass has a slightly higher calorific value than agricultural biomass, so that the calorific value of forest biomass ranges from 18.0 to 23.0 MJ kg<sup>-1</sup>, while most agricultural biomass has a calorific value between 15.5 and 19.5 MJ kg<sup>-1</sup> (Cai et al., 2017). As shown in Table 3. Switchgrass had the highest HHV and LHV, while beech had the lowest HHV and oak had the lowest

LHV of all samples studied. However, when all results are considered, it can be seen that the values of HHV and LHV were nearly identical for all samples.

**Table 3: Heat values**

Sample	HHV (MJ kg <sup>-1</sup> )	LHV (MJ kg <sup>-1</sup> )
Oak	18.34a±0.02	17.10a±0.03
Beech	18.09a±0.11	17.23a±0.15
Switchgrass	18.50a±0,29	17.39a±0,27
Miscanthus	18.41a±0,25	17.19a±0,31
Significance	NS	NS

Values in the column with the same letter are not statistically significantly different with  $p < 0.05$ . Statistical difference: \*\*\*  $p < 0.001$ , NS—not significant.

Comparing the average values of the determined HHV and LHV of the investigated forest and energy crops presented in Table 3, it can be concluded that the values determined in this study are within the ranges reported by the mentioned authors in the literature.

### 3.5 Biomass potential for the production of solid biofuels

The study shows that the lignocellulosic composition of forest species and agricultural energy crops is within the average limits for each biomass. Lignocellulosic biomass, which has higher lignin content, is more suitable for conversion of feedstocks into solid biofuels through the pressing process, which can later be used for heat or power generation through direct combustion. It is obvious that the studied forest species have higher lignin content than energy crops, but their slightly higher content of cellulose and hemicellulose affects the calorific value, so it is almost the same for all studied biomasses. Studies have shown that there is a significant relationship between the lignin content and the HHV and LHV of biomass (Demirbas, 2001; Demirbas, 2004).

Conversion to a solid fuel by pressing can significantly improve the above disadvantages of biomass (Barry et al., 2022). Biomass pressing depends mainly on the system used and the working conditions (mill, pressure, temperature), as well as on the physicochemical properties of the feedstock (MC, AC, lignocellulosic composition, heating value). When biomass is pressed by the thermoplastic process of pelleting and briquetting, the biomass particles are compressed into compact pellets and briquettes under the action of high pressure and temperature, which increases the low bulk density of biomass to almost 1300 kg m<sup>-3</sup> (Mani, Tabil, Sokhansanj, 2004; Tumuluru et al., 2011). In the pressing process, moisture plays a crucial role and is one of the most important parameters for the durability of pellets and briquettes, together with the lignin content. For efficient pressing, biomass moisture content should be between 5.0 and 20.0%, while ash content should be less than 4.0%, as higher content causes lower HHV (Maia et al., 2014; Mopoung and Udeye, 2017).

It is estimated that about 44.3 million tons of pellets were produced worldwide in 2021. Most of the pellets available on the market are produced exclusively from wood biomass, but there are also pellets produced from post-harvest residues of primary agricultural production. Pellets produced in this way are not widely used due to the higher AC (3.0 – 5.0%), which requires more frequent maintenance of combustion equipment at the user's site, so they are increasingly used by industry as a biofuel for heating or electricity generation. The calorific value of agropellets ranges from 12.0 to 18.0 MJ kg<sup>-1</sup>, while AC is above 1.0%. However, the solution to this problem can be seen in the combination of the right ratio of the different biomasses. Biomass that produces a smaller AC can be combined with one that produces a larger one, i.e., by mixing biomass, MC, and AC, the calorific value can be adjusted to obtain a suitable product that meets all quality parameters (Smaga et al., 2018).

Comparing all the research results with the cited literature, it can be concluded that the two studied forest species and two agricultural energy crops can indeed be used as feedstock for solid biofuel production through the compression process.

#### 4. CONCLUSION

Based on this study, it was found that all parameters studied were within the limits or showed a slight deviation from the listed literature data and from the standard for solid biofuels. Forest species had slightly higher lignin content, while energy crops had significantly higher ash content. The calorific value was higher for energy crops due to a slightly higher content of cellulose and hemicellulose in forest species, and as mentioned earlier, cellulose and hemicellulose have a lower calorific value than lignin. Certain deviations of the determined parameters from the literature data can be attributed to the influence of different cultivation sites, agroecological conditions, and other factors. When analyzing the possibility of using the biomass of the investigated forest species and agricultural energy crops as raw material for the production of solid biofuels such as pellets and briquettes, it was found that all parameters meet the physicochemical properties that the biomass must have during the pressing process.

#### REFERENCES

- [1] Antonovi, A. (2004): Spektrofotometrijska analiza lignina bukovine. Magistarski rad. Sveučilište u Zagrebu, Šumarski fakultet: 1-214.
- [2] Arteaga-Pérez, L.E., Segura, C., Espinoza, D., Radovic, L.R., Jiménez, R. (2015): Torrefaction of *Pinus radiata* and *Eucalyptus globulus*: A combined experimental and modeling approach to process synthesis. *Energy Sustain. Dev.*, 29: 13–23.
- [3] Azad, A.K., Rasul, M., Khan, M.M.K., Sharma, S.C., Hazrat, M. (2015): Prospect of biofuels as an alternative transport fuel in Australia. *Renew. Sust. Energy Rev.*, 43: 331-351.
- [4] Barakat, A., de Vries, H., Rouau, X. (2013). Dry fractionation process as an important step in current and future lignocellulose biorefineries: a review. *Bioresource technology*, 134: 362-373.
- [5] Barry, F., Sawadogo, M., Ouédraogo, I.W., Bologo, M., Dogot, T. (2022): Geographical and economic assessment of feedstock availability for biomass gasification in Burkina Faso. *Energy Conversion and Management*: X, 13, 100163.
- [6] Bhuiyan, N. H., Selvaraj, G., Wei, Y., King, J. (2009): Role of lignification in plant defense. *Plant signaling & behavior*, 4(2): 158–159.
- [7] Bilandžija, N., Jurišić, V., Vođa, N., Leto, J., Matin, A., Antonovi, A., Križka, T. (2016): Lignocelulozni sastav trave *Miscanthus x giganteus* u odnosu na različite tehnološke i agroekološke uvjete. In *51st Croatian and 11th International Symposium on Agriculture, Opatija*: 450-454.
- [8] Bilandžija, N., Križka, T., Matin, A., Leto, J., Grubor, M. (2018): Effect of harvest season on the fuel properties of *Sida hermaphrodita* (L.) Rusby biomass as solid biofuel. *Energies*, 11(12): 3398.
- [9] Bilandžija, N., Leto, J., Fabijanić, G., Sito, S., Smiljanović, I. (2017): Tehnike žetve poljoprivrednih energetskih kultura. *Glasnik zaštite bilja*, 40(4): 112-119.
- [10] Bilandžija, N., Leto, J., Kiš, D., Jurišić, V., Matin, A., Kuže, I. (2014): The impact of harvest timing on properties of *Miscanthus x giganteus* biomass as a CO<sub>2</sub> neutral energy source. *Collegium antropologicum*, 38(1): 85-90.
- [11] Budzyński, W., Szczukowski, S., Tworkowski, J. (2009): Wybrane problemy z zakresu produkcji rolniczej na cele energetyczne. *I Kongres Nauk Rolniczych Nauka–Praktyce. s.*, 77: 87.
- [12] Cai, J., He, Y., Yu, X., Banks, S.W., Yang, Y., Zhang, X., Yu, Y., Liu, R., Bridgwater, A.V. (2017): Review of physicochemical properties and analytical characterization of lignocellulosic biomass. *Renewable and sustainable energy reviews*, 76: 309-322.
- [13] Camia, A., Robert, N., Jonsson, K., Pilli, R., Garcia Condado, S., Lopez Lozano, R., Van Der Velde, M., Ronzon, T., Gurria Albusac, P., M'barek, R., Tamosiunas, S., Fiore, G., Dos Santos Fernandes De Araujo, R., Hoepffner, N., Marelli, L., Giuntoli, J. (2018): Biomass production, supply, uses and flows in the European Union: First results from an integrated assessment, EUR 28993 EN, Publications Office of the European Union, Luxembourg.

- [14] Carvalho, J., Cardoso, Ó., Costa, M., Rodrigues, A. (2017): Variation of the chemical composition of Pyrenean oak (*Quercus pyrenaica* Willd.) heartwood among different sites and its relationship with the soil chemical characteristics. *European journal of forest research*, 136: 185-192.
- [15] Chen, F., Dixon, R.A. (2007): Lignin modification improves fermentable sugar yields for biofuel production. *Nat Biotechnol* 25: 759–761.
- [16] Chew, K.W., Chia, S.R., Show, P.L., Ling, T.C., Arya, S.S., Chang, J.S. (2018): Food waste compost as an organic nutrient source for the cultivation of *Chlorella vulgaris*. *Bioresour Technol.*, 267: 356- 362.
- [17] Clarke, S., Preto, F. (2011): *Biomass burn characteristics* (pp. 11-033). Guelph, ON, Canada: Ministry of Agriculture, Food and Rural Affairs.
- [18] Demirba , A. (2001): Relationships between lignin contents and heating values of biomass. *Energy conversion and management*, 42(2): 183-188.
- [19] Demirbas, A. (2004): Combustion characteristics of different biomass fuels. *Progress in Energy and Combustion Science*, 30: 219 – 230.
- [20] Demirbas, A. (2017): Higher heating values of lignin types from wood and non-wood lignocellulosic biomasses, *Energy Sources, Part A: Recovery, Utilization, and Environmental Effects*, 39(6): 592-598.
- [21] Doshi, A., Pascoe, S., Cogle, L., Rainey, T.J. (2016): Economic and policy issues in the production of algae-based biofuels: A review. *Renew. Sustainable Energy Rev.*, 64: 329-337.
- [22] Garcia, R., Pizarro, C., Lavín, A.G., Bueno, J.L. (2012): Characterization of Spanish biomass wastes for energy use. *Bioresource Technology*, 103: 249 – 258.
- [23] Grzybek, A. (2008). Ziemia jako czynnik warunkuj cy produkcj biopaliw. *Problemy In ynierii Rolniczej*, 16: 63-70.
- [24] Guo, Z., Sun, C., Grebner, D. (2010): Utilization of forest derived biomass for energy production in the USA: status, challenges, and public policies. *International Forestry Review*, 9(3): 748-758.
- [25] HRN EN ISO 14780:2017 Solid biofuels – Sample preparation (ISO 14780:2017; EN ISO 14780:2017).
- [26] HRN EN ISO 18122:2015 Solid biofuels -- Determination of ash content (ISO 18122:2015; EN ISO 18122:2015).
- [27] HRN EN ISO 18123:2015 Solid biofuels -- Determination of the content of volatile matter (ISO 18123:2015; EN ISO 18123:2015).
- [28] HRN EN ISO 18125:2017 Solid biofuels -- Determination of calorific value (ISO 18125:2017; EN ISO 18125:2017).
- [29] HRN EN ISO 18134-2:2017 Solid biofuels -- Determination of moisture content -- Oven dry method -- Part 2: Total moisture -- Simplified method (ISO 18134-2:2017; EN ISO 18134-2:2017).
- [30] <https://www.worldbioenergy.org/uploads/221223%20WBA%20GBS%202022.pdf>(accessed 04.08.2023.)
- [31] Iqbal, H.M.N., Ahmed, I., Zia, M.A., Irfan, M. (2011): Purification and characterization of the kinetic parameters of cellulase produced from wheat straw by *Trichoderma viride* under SSF and its detergent compatibility. *Advances in Bioscience and Biotechnolog.* 2(3): 149-156.
- [32] Jackson, J., Turner, A., Mark, T.B., Montross, M. (2016): Densification of biomass using a pilot scale flat ring roller pellet mill, *Fuel Processing Technology* 148: 43-49.
- [33] Koçar, G., Civa , N. (2013): An overview of biofuels from energy crops: Current status and future prospects. *Renewable and Sustainable Energy Reviews*, 28: 900-916.
- [34] Kumar, P., Barrett, D.M., Delwiche, M.J., Stroeve, P. (2009). Methods for pretreatment of lignocellulosic biomass for efficient hydrolysis and biofuel production. *Industrial & Engineering Chemistry Research*, 48: 3713-3729.
- [35] Kumar, S., Ghosh, P. (2018): Sustainable bio-energy potential of perennial energy grass from reclaimed coalmine spoil (marginal sites) of India. *Renewable Energy*, 123: 475-485.
- [36] Lewandowski, I., Clifton-Brown, J.C., Andersson, B., Basch, G., Christian, D.G., Jergensen, U., Jones, M.B., Riche, A.B., Schwarz, K.U., Tayebi, K., Teixeira, F. (2003): Environment

- and harvest time affects the combustion qualities of Miscanthus genotypes. *Agronomy Journal*, vol 95: 1274-1280.
- [37] Li, L., Zhou, Y., Cheng, X., Sun, J., Marita, J., Ralph, J., Chiang, V. (2003): Combinatorial modification of multiple lignin traits in trees through multigene cotransformation. *Proc Natl Acad Sci USA*, 100: 4939–4944.
- [38] Li, Y. Rezgui, Y., Zhu, H. (2017): District heating and cooling optimization and enhancement—Towards integration of renewables, storage and smart grid. *Renew. Sustain. Energy Rev.* 72: 281–294
- [39] Maia, B.G.D., Souza, O., Marangoni, C., Hotza, D., Oliveira, A.P.N., Sellin, N. (2014): Production and characterization of fuel briquettes from banana leaves waste production and characterization of fuel briquettes from banana leaves waste. *Chemical Engineering Transactions* 37: 439–444.
- [40] Malherbe, S., Cloete, T.E. (2002). Lignocellulose biodegradation: fundamentals and applications. *Reviews in Environmental Science and Biotechnology*, 1: 105-114.
- [41] Mani, S., Tabil, L.G., Sokhansanj, S. (2004): Grinding performance and physical properties of wheat and barley straws, corn stover and switchgrass. *Biomass and bioenergy*. 27(4): 339-352.
- [42] McKendry, P. (2002): Energy production from biomass (part 1): overview of biomass. *Bioresource Technology*, 83: 37–46.
- [43] Mitchell P., Kiel J., Livingston B., Dupont-Roc G. (2007): Torrefied biomass. A foresighting study into the business case for pellets from torrefied biomass as a new solid fuel. *All Energy*. 24: 1-27.
- [44] Mopoung, S., Udeye, V. (2017): Characterization and evaluation of charcoal briquettes using banana peel and banana bunch waste for household heating. *American Journal of Engineering and Applied Sciences*.10(2): 353–365.
- [45] Obernberger, I., Thek, G. (2004): Physical characterisation and chemical composition of densified biomass fuels with regard to their combustion behaviour. *Biomass and Bioenergy*, 27: 653 – 669.
- [46] Osman, A.I., Qasim, U., Jamil, F., Al-Muhtaseb, A.H., Abu Jrai, A., Al-Riyami, M., Al-Maawali, S., Al-Haj, L., Al-Hinai, A., Al-Abri, M. (2021): Bioethanol and biodiesel: Bibliometric mapping, policies and future needs. *Renew. Sustain. Energy Rev.* 152: 111677.
- [47] Rodionova, M., Poudyal, R., Tiwari, I., Voloshin, R., Zharmuk-hamedov, S., Nam, H., Zayadan, B., Bruce, B., Hou, H., Al-lakhverdiev, S. (2017): Biofuel production: challenges and opportunities. *Int. J. Hydrog. Energy*, 42(12): 8450-8461
- [48] Rodríguez, A., Espinosa, E. (2021): Special Issue “Lignocellulosic Biomass”. *Molecules*, 26(5), 1483.
- [49] Sadaka, S., Sharara, A.M., Ashworth, A., Keyser, P., Allen, F., Wright, A. (2014): Characterization of biochar from switchgrass carbonization. *Energies*, 7(2): 548-567.
- [50] Saha, B.C. (2005): Enzymes as biocatalysts for conversion of lignocellulosic biomass to fermentable sugars. *Handbook of industrial biocatalysis*, 1-12.
- [51] Saleem, M. (2022): Possibility of utilizing agriculture biomass as a renewable and sustainable future energy source. *Heliyon*. 8(2): e08905.
- [52] Sanderson, K. (2011). Lignocellulose: a chewy problem. *Nature*, 474(7352): S12-S14.
- [53] Smaga, M., Wielgosinski, G., Kocha ski, A., Korczak, K. (2018): Biomass as a major component of pellets. *Acta Innovations*: 81-92.
- [54] TAPPI – T 204 Solvent Extractives of Wood and Pulp 2007, Technical Association of the Pulp and Paper Industry.
- [55] TAPPI - T 222 Acid-insoluble lignin in wood and pulp 2002, Technical Association of the Pulp and Paper Industry.
- [56] Telmo, C., Lousada, J., Moreira, N. (2010): Proximate analysis, backwards stepwise regression between gross calorific value, ultimate and chemical analysis of wood. *Bioresource Technology*, 101: 3808 – 3815.
- [57] Tumuluru, J.S. (2015): Comparison of chemical composition and energy property of torrefied switchgrass and corn stover. *Frontiers in Energy Research*, 3: 46.

- [58] Tumuluru, J.S., Wright, C.T., Hess, J.R., Kenney, K.L. (2011): A review of biomass densification systems to develop uniform feedstock commodities for bioenergy application. *Biofuels, Bioproducts and Biorefining* 5: 683-707.
- [59] Ulusal, A., Apaydin Varol, E., Bruckman, V.J., Uzun, B.B. (2021): Opportunity for sustainable biomass valorization to produce biochar for improving soil characteristics. *Biomass Conversion and Biorefinery*, 11: 1041-1051.
- [60] Vassilev S.V., Baxter D., Andersen L.K., Vassileva C.G. (2010): An overview of the chemical composition of biomass. *Fuel*. 89(5): 913-933.
- [61] Vassilev S.V., Vassileva C.G., Vassilev V.S. (2015): Advantages and disadvantages of composition and properties of biomass in comparison with coal: An overview. *Fuel*. 158: 330-350.
- [62] Vo a, N., Leto, J., Karažija, T., Bilandžija, N., Peter, A., Kutnjak, H., Šuri , J., Poljak, M. (2021): Energy properties and biomass yield of miscanthus x giganteus fertilized by municipal sewage sludge. *Molecules*, 26(14): 4371.
- [63] Williams, C.L. , Emerson, R.M. , Tumuluru, J.S. (2017): Biomass compositional analysis for conversion to renewable fuels and chemicals. Biomass volume estimation and valorization for energy, 251-270.
- [64] Zhu, B., Chen, G., Cao, X., Wei, D. (2017): Molecular characterization of CO<sub>2</sub> sequestration and assimilation in microalgae and its biotechnological applications. *Bioresour Technol.*, 244: 1207- 1215.

#### **The Authors' Address:**

Božidar Matin MSc, University of Zagreb Faculty of Forestry and Wood Technology, Svetošimunska cesta 23, Zagreb, Croatia,

Associate Professor PhD Ana Matin, University of Zagreb Faculty of Agriculture, Svetošimunska cesta 25, Zagreb, Croatia,

Ivan Brandi MSc, University of Zagreb Faculty of Agriculture, Svetošimunska cesta 25, Zagreb, Croatia,

Alen urovi MSc, University of Zagreb Faculty of Forestry and Wood Technology, Svetošimunska cesta 23, Zagreb, Croatia,

Associate Professor PhD Josip Ištvan , University of Zagreb Faculty of Forestry and Wood Technology, Svetošimunska cesta 23, Zagreb, Croatia.

Professor PhD Alan Antonovi , University of Zagreb Faculty of Forestry and Wood Technology, Svetošimunska cesta 23, Zagreb, Croatia.

## ANALYSIS OF HEAT AND STEAM CONSUMPTION DURING ARTIFICIAL CONVECTIVE DRYING OF OAK SAWN TIMBER OF DIFFERENT THICKNESS

Goran Zlateski<sup>1</sup>, Ana Marija Stamenkoska<sup>1</sup>, Zoran Trposki<sup>1</sup>,  
Vladimir Koljozov<sup>1</sup>, Branko Rabadjiski<sup>1</sup>

<sup>1</sup>Ss. Cyril and Methodius University in Skopje, North Macedonia,  
Faculty of design and technologies of furniture and interior-Skopje  
e-mail: zlateski@fdtme.ukim.edu.mk, stamenkoska@gmail.com,  
trposki@fdtme.ukim.edu.mk, koljozov@fdtme.ukim.edu.mk

### ABSTRACT

In the paper, the consumption of heat and steam of oak sawn timber with a thickness of 25,0 and 50,0 (mm) are analyzed under conditions of classic convective drying. The drying mode is compiled on the basis of data on the temperature of the drying agent (air), the relative humidity of the air and the speed of air movement in accordance with the current value of moisture in the wood.

The heat consumption is analyzed in all stages of the drying cycle such as heating the wood, active drying of the wood, equalization of the average moisture in the wood and conditioning, i.e. equalization of the moisture in the cross-section within  $\pm 2.0$  (%). The moisture content of sawn timber at the beginning of drying is about 55,0 (%) and at the end of drying is 10,0 (%). The sawn timber are intended for the production of solid wood panels.

**Keywords:** oak, sawn timber, artificial drying, heat consumption, steam consumption

### 1.INTRODUCTION

The research related to energy consumption in the wood industry in general, and especially the research on the calculation of heat consumption for the purposes of wood drying, has always attracted the attention of the scientific public for obtaining results that will open opportunities for increasing energy efficiency. In every company from the wood industry that is engaged in the production of solid wood products (chairs, tables ...), it is necessary to have installed a dryer for artificial drying of the wood. The convective drying method is the most widely accepted method in wood drying technology, which uses hot air of certain thermodynamic parameters in order to evaporate moisture from the wood. It's the method of modern operation (drying) and timely delivery of quality dry wood with a final percentage of moisture suitable for the production of solid wood product.

These wood drying facilities are made with the most modern materials to prevent corrosion and equipped with modern devices for tracking, controlling and realizing the drying cycle defined by an appropriate schedule for drying the sawmill assortments.

The drying regime is composed of the values of the temperature and relative humidity of the drying agent (atmospheric air) matched with the values of moisture in the wood at the beginning, during and at the end of the drying process.

Several authors like Vengert and Meyer (1993), Denig et al (1996), Seeger (1989), Kolin (2000), Bariši (1957), Mili (2020) and FAO organzitaion (1990) as well reported energy consumption for hardwood species from 2,15 to 3,5 (GJ/m<sup>3</sup>) depending on the construction of dry kiln, wood species, wood thickness and initial moisture content of wood.

Kolin (2000), investigated the necessary quantity of water vapour for artificial drying of sawn timber from hardwood. He has determined water vapour values between 1,7 and 3,5 (kg/kg).

Taking into account that the largest part of the total energy consumption in the wood industry belongs to the consumption of heat energy for the purposes of artificial drying of the wood, we decided to make a detailed analysis (calculation) of the costs of heat in all stages of the drying cycle (heating, active drying, equalizing and conditioning of oak sawn timber with thickness of 25,0 (mm) and 50,0 (mm) as well.



We believe that the obtained results will contribute to the improvement and rationalization of the processes of wood drying and thus the realization of an economic benefit to the overall operation of the companies from the wood industry.

## 2. MATERIALS AND METHODS

The drying of sawn timber of oak (*Quercus sessiliflora*) was carried out in a dryer for artificial convective drying equipped with a device for automatic drying management. Sawn timber with a thickness of 25,0 (mm) are dried separately from those with a thickness of 50,0 (mm). Characteristics of the material as well as the dryer are shown in table 1 and table 2 as well.

**Table 1: Material properties**

Wood species	oak
Specific density	0,64 (g/cm <sup>3</sup> )
Thickness of wood	25,0 (mm) and 50,0 (mm)
Initial wood moisture content	55,0 (%)
Final wood moisture content	10,0 (%)
Wood saturation point	22,0 (%)
Specific heat of dry wood	1,3563 (kJ/(kg°C))
Length of the stack	10,5 (m)
Width of the stack	6,5 (m)
Height of the stack	4,1 (m)
Volume of the stack	279,825 (m <sup>3</sup> )
Thickness of the stickers	18,0 (mm) and 25,0 (mm)

**Table 2: Dry kiln properties**

Drying method	convective
Construction	metal
Control of drying process	automatic
Length	$l_s=8,5$ (m)
Width	$S_s=10,6$ (m)
Height	$h_s=5,26$ (m)
Capacity	$V_s=468,52$ (m <sup>3</sup> )
Thickness of floor	$d_p=200,0$ (mm)
Thickness of wall	$d_z=100,0$ (mm)
Thickness of ceiling	$d_t=100,0$ (mm)
Thickness of door	$d_v=100,0$ (mm)
Duration of the drying cycle of wood- 25,0 in thickness	336,0 (h)
Duration of the drying cycle of wood- 50,0 in thickness	860,25 (h)
Working hours per year	6000 (h),
Air movement speed in the dryer	$V_{vozduh}=2,5$ (m/s)
Specific gravity of dry air	$\rho_{suv\ vozduh}=0,87$ (kg/m <sup>3</sup> )
Specific weight of the wall construction material	$\rho_{zid}=2900$ (kg/ m <sup>3</sup> )
Specific gravity of the ceiling construction material	$\rho_{tavan}=2900$ (kg/ m <sup>3</sup> )
Specific gravity of the floor construction material	$\rho_{pod}=2400$ (kg/ m <sup>3</sup> )
Specific gravity of the door construction material	$\rho_{vrata}=2900$ (kg/ m <sup>3</sup> )
Specific heat of the wall construction material	$c_{zid}=0,85$ (kJ/(kg°C))
Specific heat of ceiling construction material	$c_{tavan}=0,85$ (kJ/(kg°C))
Specific heat of the floor construction material	$c_{pod}=0,922$ (kJ/(kg°C))
Specific heat of the door construction material	$c_{vrata}=0,85$ (kJ/(kg°C))
Specific heat for other equipment (average)	$c_{ostanato}=0,551$ (kJ/(kg°C))
Specific heat for dry air	$c_{suv\ vozduh}=1,003$ (kJ/(kg°C))
Maximum temperature on the inside of the walls ie. temperature of the medium in the chamber	$t_{sredina}=70,0$ (°C)

Outside air temperature	$t_{nad.vozduh}=20,0$ (°C)
Average wall temperature	$t_{zid}=45,0$ (°C)
Average ceiling temperature	$t_{tavan}=45,0$ (°C)
Average floor temperature	$t_{pod}=45,0$ (°C)
Average door temperature	$t_{vrata}=45,0$ (°C)
Average temperature of the rest	$t_{ostanato}=45,0$ (°C)
Coefficient of heat transfer - floor	$k_{pod}=13,84$ (kJ/(m <sup>2</sup> h°C))

### **(I) The total amount of heat for one drying cycle**

- heating the dryer,
- heating the wood and stickers to a drying temperature,
- heat loss during drying,
- heating the air in the dryer,
- heating and evaporation of moisture from the wood and
- heating the air in the dryer.

$$\Sigma Q = (Q_{komora} + Q_{drvo+letvi} + Q_{zaguba} + Q_{vozduh} + Q_{isparivanje}) \text{ (kJ)}$$

a) The amount of heat for heating the dryer is calculated as the sum of the amount of heat for heating the walls, ceiling, floor, door and other equipment of the dryer.

$$Q_{komora} = Q_{zid} + Q_{tavan} + Q_{pod} + Q_{vrata} + Q_{ostanato}$$

- wall

$$Q_{zid} = V_{zid} \times \gamma_{zid} \times c_{zid} \times (t_{zid} - t_{nad.vozduh}) \text{ (kJ)}$$

where:

$V_{zid}$  - volume of the walls (m<sup>3</sup>)

$\gamma_{zid}$  - specific weight of the material from which the wall is made (kg/m<sup>3</sup>)

$c_{zid}$  - specific heat of the material of the wall (kJ/kg °C)

$t_{zid}$  - wall temperature (°C)

$t_{nad.vozduh}$  - outdoor air temperature (°C)

- ceiling

$$Q_{tavan} = V_{tavan} \times \gamma_{tavan} \times c_{tavan} \times (t_{tavan} - t_{nad.vozduh}) \text{ (kJ)}$$

where:

$V_{tavan}$  - volume of the ceiling (m<sup>3</sup>)

$\gamma_{tavan}$  - specific weight of the material from which the ceiling is made (kg/m<sup>3</sup>)

$c_{tavan}$  - specific heat of the material from which the ceiling is made (kJ/kg °C)

$t_{tavan}$  - temperature of the ceiling (°C)

$t_{nad.vozduh}$  - outdoor air temperature (°C)

- floor

$$Q_{pod} = V_{pod} \times \gamma_{pod} \times c_{pod} \times (t_{pod} - t_{nad.vozduh}) \text{ (kJ)}$$

where:

$V_{pod}$  - floor volume (m<sup>3</sup>)

$\gamma_{pod}$  - specific weight of the material from which the floor is made (kg/m<sup>3</sup>)

$c_{pod}$  - specific heat of the material from which the floor is made (kJ/kg °C)

$t_{pod}$  - floor temperature (°C)

$t_{nad.vozduh}$  - outdoor air temperature (°C)

- door

$$Q_{vrata} = V_{vrata} \times \gamma_{vrata} \times c_{vrata} \times (t_{vrata} - t_{nad.vozudh})(kJ)$$

where:

$V_{vrata}$  - door volume (m<sup>3</sup>)

$\gamma_{vrata}$  - specific weight of the material from which the door is made (kg/m<sup>3</sup>)

$c_{vrata}$  - specific heat of the material from which the door is made (kJ/kg °C)

$t_{vrata}$  - door temperature (°C)

$t_{nad.vozudh}$  - outdoor air temperature (°C)

- rest of the dryer's equipment

$$Q_{ostanato} = 2000 \times c_{ostanato} \times (t_{ostanato} - t_{nad.vozudh})(kJ)$$

where:

$c_{ostanato}$  - specific heat of the material from which the rest of the equipment is made (kJ/kg °C)

$t_{ostanato}$  - temperature of the rest of the equipment (°C)

$t_{nad.vozudh}$  - outdoor air temperature (°C)

b) the amount of heat to heat wood and stickers to drying temperature

$$Q_{drvo} = V_{drvo} \times \gamma_{drvo} \times c_{drvo} \times (t_{sredina} - t_{nad.vozudh})(kJ)$$

where:

$V_{drvo}$  - volume of wood in the chamber (m<sup>3</sup>)

$\gamma_{drvo}$  - specific weight of wood (kg/m<sup>3</sup>)

$c_{drvo}$  - specific heat of wood (kJ/kg °C)

$t_{zid}$  - ambient temperature (°C)

$t_{nad.vozudh}$  - outdoor air temperature (°C)

The amount of heat for heating the stickers is calculated according to the formula:

$$Q_{letvi} = V_{letvi} \times \gamma_{letvi} \times c_{letvi} \times (t_{sredina} - t_{nad.vozudh})(kJ)$$

where:

$V_{letvi}$  - volume of the stickers in the chamber (m<sup>3</sup>)

$\gamma_{letvi}$  - specific weight of the wood from which the stickers are made (kg/m<sup>3</sup>)

$c_{letvi}$  - specific heat of the wood from which the stickers are made (kJ/kg °C)

$t_{sredina}$  - middle temperature (°C)

$t_{nad.vozudh}$  - outdoor air temperature (°C)

$$Q_{drvo+letvi} = Q_{drvo} + Q_{letvi}$$

c) Heat loss through the walls, doors, ceiling and others during drying

The insulating materials from which the metal dryer is made - a combination of Al-sheet and mineral wool as an insulator give the right to not take heat energy losses through the walls, ceiling, door into account in the design task.

- heat loss through the dryer floor

$$Q_{zagubi} = F \times k \times Z_{25/50mm} \times (t_{sredina} - t_{pocva})(kJ)$$

where:

F- surface through which the heat passes (m<sup>2</sup>)

k- heat transfer coefficient

Z<sub>25/50 mm</sub> - duration of drying according to Sokolov (h)

t<sub>sredina</sub> - middle temperature (°C)

t<sub>pocva</sub> - soil temperature (°C)

d) The heat for heating the air in the dryer

$$Q_{\text{vozduh}} = L \times c_{\text{vozduh}} \times (t_{\text{sredina}} - t_{\text{nad.vozduh}}) \text{ (kJ)}$$

L- amount of air (kg vozduh)

$$L = \frac{W_{\text{polnenje}}}{0,039} \text{ (kg vozduh)}$$

where:

c<sub>vozduh</sub>- specific heat of dry air (kJ/kg °C)

t<sub>sredina</sub> - middle temperature (°C)

t<sub>nad.vozduh</sub> - outdoor air temperature (°C)

e) The total heat for evaporation of moisture from the wood for the entire drying cycle is a sum of the heat required for: breaking the hygroscopic bond, for heating and evaporating the moisture from the assortments and for heating and evaporating the moisture remaining in the wood after drying.

$$Q_{\text{vkupno isparuvanje}} = Q_{\text{hig.vlaga}} + Q_{\text{drvo vlaga}} + Q_{\text{ostanata vlaga}} \text{ (kJ)}$$

where:

Q<sub>hig.vlaga</sub>- heat to break the hygroscopic bond (kJ)

Q<sub>drvo vlaga</sub> - for heating and evaporation of moisture from the assortments (kJ)

Q<sub>ostanata vlaga</sub>- heating and evaporation of the moisture remaining in the wood after drying (kJ)

$$Q_{\text{hig.vlaga}} = \left[ \left( 18 - \frac{22 \times W_k}{B + W_k} \right) \times r_0 \times V_{\text{drvo}} \right] \times 4,18 \text{ (kJ)}$$

where:

r<sub>0</sub> - density of wood (kg/m<sup>3</sup>)

W<sub>k</sub> - final wood moisture

V<sub>drvo</sub>- useful capacity of the dryer (m<sup>3</sup>)

$$Q_{\text{drvo vlaga}} = r_0 \times V_{\text{drvo}} \times \frac{W_p - W_k}{100} \times (608 + 0,311 \times t_{\text{sredina}}) \times 4,18 \text{ (kJ)}$$

$$Q_{\text{ostanata vlaga}} = V_{\text{drvo}} \times r_0 \times W_k \times (t_{\text{sredina}} - t_{\text{nad.vozduh}}) \times 4,18 \text{ (kJ)}$$

f) The coefficient of useful heat

$$K_{\text{toplina}} = \frac{Q_{\text{drvo vlaga}}}{\Sigma Q} \times 100 \text{ (%)}$$

where:

Q<sub>drvo vlaga</sub> - for heating and evaporation of moisture from the assortments (kJ)

Q- total amount of heat in one drying cycle (kJ)

The following formula is used to calculate the amount of heat for evaporation of 1,0 (kg) of wood moisture for one filling of the chamber:

$$q_{1\text{kgvlaga}} = \frac{\sum Q}{W_{\text{polnenje}}} \left( \frac{\text{kJ}}{\text{kg}} \right)$$

where:

Q- total amount of heat for one drying cycle (kJ)

$W_{\text{polnenje}}$  - the amount of evaporated moisture from the entire amount of wood from one filling of the chamber (kg moisture)

For the calculation of the amount of heat for moisture evaporation of 1,0 (m<sup>3</sup>) for one filling of the chamber for one cycle, the following formula is applied:

$$q_{1\text{m}^3} = \frac{\sum Q}{V_{\text{drvo}}} \left( \frac{\text{kJ}}{\text{m}^3} \right)$$

where:

Q- total amount of heat for one drying cycle (kJ)

$V_{\text{drvo}}$  - useful volume of the dryer (m<sup>3</sup>)

To calculate the amount of heat for 1,0 (h) drying, the following formula is applied:

$$q_{1\text{h}} = \frac{Q_{\text{vkupno isparuvanje}}}{Z_{25/50\text{mm}}} \left( \frac{\text{kJ}}{\text{h}} \right)$$

where:

$Q_{\text{vkupno isparuvanje}}$  - total heat for evaporation of moisture from wood for the entire drying cycle (kJ)

$Z_{25/50\text{mm}}$  - duration of drying according to Sokolov (h)

## **(II) Amount of water vapour to realize the drying cycle**

a) amount of water vapour for evaporation of 1,0 (kg) of moisture from one charge of the chamber for one cycle

$$D_{\text{para 1kg vlaga}} = \frac{q_{1\text{kg vlaga}}}{2264} \left( \frac{\text{kg para}}{\text{kg vlaga}} \right)$$

b) amount of water vapour for drying 1,0 (m<sup>3</sup>) of wood from one charge of the chamber for one cycle

$$D_{\text{para 1m}^3} = r_0 \times (W_p - W_k) \times D_{\text{para 1kg vlaga}} \left( \frac{\text{kg para}}{\text{m}^3} \right)$$

c) amount of water vapour for drying the total amount of sawn assortments from one charge of the chamber for one cycle

$$\sum D_{\text{para}} = V_d \times r_0 \times (W_p - W_k) \times D_{\text{para 1kg vlaga}} \text{ (kg para)}$$

### 3. RESULTS AND DISCUSSION

As we mentioned before, the consumption of heat and water vapor for the purposes of artificial drying of oak sawn timber with two thicknesses of 25,0 and 50,0 (mm) was investigated. The results are shown in Tables 3,4,5,6,7,8 and 9 respectively.

*Table 3: Heat required for heating the dryer*

Wood thickness	25,0 (mm)	50,0 (mm)
	kJ (GJ)	kJ (GJ)
Heat for heating the longitudinal walls	544765,00	544765,00
Heat for heating the transverse wall	339677,00	339677,00
Heat for heating the longitudinal walls and the transverse wall	884442,00	884442,00
Heat to heat the ceiling	555241,25	555241,25
Heat for floor heating	996866,40	996866,40
Heat to warm the door	339677,00	339677,00
Heat - the rest	27550,00	27550,00
<b>Total heat for heating the dryer</b>	<b>2803776,65 (2,80)</b>	<b>2803776,65 (2,80)</b>

*Table 4: Heat required for heating of wood and stickers to the drying temperature*

Wood thickness	25,0 (mm)	50,0 (mm)
	kJ (GJ)	kJ (GJ)
<b>Total heat for heating wood and stickers</b>	<b>7397790,10 (7,40)</b>	<b>8438160,773 (8,44)</b>

*Table 5: Heat loss during drying*

Wood thickness	25,0 (mm)	50,0 (mm)
	kJ (GJ)	kJ (GJ)
Heat loss through longitudinal walls	13217568,00	29385486,00
Heat loss through the transverse wall	8241542,40	18322714,80
Heat loss through the ceiling	10175760,00	22622895,00
Heat loss through the floor	10474665,60	23287426,20
Heat loss through the door	7435908,48	16531617,96
Total heat loss	49545444,48	110150139,96
<b>Total heat loss with average heat transfer coefficient</b>	<b>70375591,44 (7,38)</b>	<b>156460020,26 (156,46)</b>

*Table 6: Heat required for heating the air in the dryer*

Wood thickness	25,0 (mm)	50,0 (mm)
	kJ (GJ)	kJ (GJ)
<b>Heat to heat the air in the dryer</b>	<b>60527084,65 (60,53)</b>	<b>69404390,40 (69,40)</b>

*Table 7: Heat required for heating and evaporating the moisture from the wood*

Wood thickness	25,0 (mm)	50,0 (mm)
	kJ (GJ)	kJ (GJ)
Heat to break up hygroscopic moisture	2211855,36	2536260,81
Heat to heat and evaporate the moisture from the wood	151443923,29	173655698,71
Heat to heat the moisture that remains in the wood after drying	2186136,11	2506769,41
<b>Total heat of evaporation of moisture from wood</b>	<b>155841914,76 (155,84)</b>	<b>178698728,93 (178,70)</b>

**Table 8: Total heat for drying**

<b>Wood thickness</b>	<b>25,0 (mm)</b>	<b>50,0 (mm)</b>
Total required drying heat for one drying cycle	kJ (GJ) (kWh)	kJ (GJ)
Total required heat for drying with coefficient of safety	276116010,65 (276,12)	369495196,71 (369,50)
<b>Heat to evaporate moisture from 1m<sup>3</sup> of wood for one cycle</b>	<b>331339212,78 (1,69)(469,3)</b>	<b>443394236,05 (1,97) (547,6)</b>
Heat to evaporate moisture from 1kg of wood moisture for one charge	1689431,75 (0,006)	1971608,45 (0,007)
Heat for 1h active drying	5866,08 (0,82)	6845,86 (0,49)

**Table 9: Required amount of water vapour for realization of drying process**

<b>Wood thickness</b>	<b>25,0 (mm)</b>	<b>50,0 (mm)</b>	<b>unit</b>
Coefficient of heat utilization	0,85	0,85	
Heat given by vapor at an average pressure of 3.5 atm according to Sokolov	2642,00	2642,00	kJ
Amount of heat used by 1kg of vapor - approx	2245,70	2245,70	kJ/kg
<b>Amount of vapor to evaporate 1kg of moisture for one charge</b>	<b>2,61</b>	<b>3,05</b>	<b>kg para/kg vlaga</b>
Amount of vapor for drying 1m <sup>3</sup> of wood for one charge	752,30	877,95	kg para/m <sup>3</sup>
Amount of vapor to dry the total amount of wood in the dryer for one cycle	122953,20	164534,53	kg para
Amount of vapor for heating the walls (surfaces) of the dryer	1248,51	1248,51	kg para
Amount of vapor for heating the wood	3294,20	3757,47	kg para
Amount of vapor to cover losses during drying	31337,93	69670,94	kg para
Amount of vapor to heat the air in the dryer	26952,44	30905,46	kg para
Amount of vapor for heating and evaporating moisture from the wood	69395,70	79573,73	kg para
Total amount of vapor during drying	132228,77	185156,11	kg para
Total amount of vapor during drying with safety factor	158674,53	222187,33	kg para
Amount of vapor for 1h drying	472,25	297,44	kg para/1h

The results presented in Tables above show that the drying process requires very high energy heat consumption compared to other energy needs for wood processing. As we can see from the Table 8 the total consumption of the total heat energy necessary to evaporate moisture from 1,0 (m<sup>3</sup>) of sawn timber 25,0 (mm) and 50,0 (mm) in thickness wood for one drying cycle is 1,69 (GJ/m<sup>3</sup>) or 469,3 (kWh/m<sup>3</sup>) and 1,97 (GJ/m<sup>3</sup>) or 547,6 (kWh/m<sup>3</sup>), respectively. The results in our research are similar to those achieved Vengert and Meyer (1993), Seeger (1989) Denig et al (1996), Mili (2020) and FAO (1990).

The data in Table 9 shows that for production of heat energy for realization of the drying process is necessary water vapour in amount of 2,61 (kg/kg) for wood with 25,0 (mm) in thickness and 3,05 (kg/kg) for wood with 50,0 (mm) in thickness. The results of our research are similar to those by Kolin (2000) and Barišić (1957).

#### 4. CONCLUSIONS

The analysis of heat and steam consumption for convective drying of oak sawn timber with different thickness of 25,0 and 50,0 (mm) with initial moisture content of 55,0 (%) and final moisture content of 10,0 (%) showed:

- Total heat for heating the dryer is 2,80 (GJ).
- Heat required to heat wood and stickers to drying temperature varies from 7,40 (GJ) for sawn timber 25,0 (mm) in thickness to 8,44 (GJ) for sawn timber 50,0 (mm) in thickness.
- Total heat loss is between 7,38 to 156,46 (GJ) depending on duration of drying process.
- Heat required to heat the air in the dryer varies from 60,53 to 69,40 (GJ).
- Heat required to heat and evaporate the moisture from the wood varies between 155,84 and 178,70 (GJ).
- Heat to evaporate moisture from 1m<sup>3</sup> of wood for one cycle is between 1,69 and 1,97 GJ or between 469,3 and 547,6 (kWh).
- Total heat for 1h active drying of wood is from 0,82 and 0,49 (GJ).
- Amount of vapor to evaporate 1kg of moisture for one charge is from 2,61 and 3,05 (kg/kg).
- Amount of vapor for 1h drying varies from 472,25 to 297,44 (kg/h).

#### REFERENCES

- [1] Bariši , T. (1957): Umjetno sušenje drveta, Beograd (in Serbian).
- [2] Danon., G. (2003): Energy efficiency of artificial wood drying, Prerada drveta, p. 23-31(in Serbian).
- [3] Dening., Wengert, E., Simpson, W. (1996): Drying Hardwood Lumber, United States Department of Agriculture, Forest Service, Forest Products Laboratory General Technical Report FPL - GTR-118, p 186.
- [4] Dul u, M., Madaras, I., (2019): The 12th International Conference Interdisciplinarity in Engineering,, Development of a monitoring and Control System for Timer’s Drying Process, Procedia manufacturing 32, p. 545- 552.
- [5] FAO Energy Conservation in Mechanical Forest Industries (1990), Forestry paper No. 93, Rome, Italy, p.72-73.
- [6] Gorišek Z., Pervan, S., Stra e, A. (2008): Kakovostno izvajanje sušenja lesa – prvi korak za optimalno izkoriš anje lesne surovine. Ljubljana 25 Septemvri, p.26 (in Slovenian).
- [7] Jorgensen, N. (2000): How to Improve Drying Quality while Lowering Energy Consumption European COST Action E15 Workshop, Sopron, p.4.
- [8] Kolin, B. (2000): Hidrotermi ka obrada drveta, Jugoslavijapublik, Beograd p.214 (in Serbian).
- [9] Krpan, J. (1965): Sušenje i parenje drva. Drugo izdanje, Sveu ilište u Zagrebu (in Croatian).
- [10] Mili , G. (2020): Hidrotermi ka obrada drveta, Šumarski fakultet, Beograd (in Serbian).
- [11] Pervan, S. (2000): Priru nik za tehni ko sušenje drva. Sand d.o.o., Zagreb, 1, 1-272 (in Croatian).
- [12] Rabadjiski, B., Zlateski, G.: (2007): Hudrotermi ka obrabotka na drvoto I del- Sušenje na masivno drvo, UKIM - Šumarski fakultet, Skopje (in Macedonian).
- [13] Seeger, K. (1989): Energietechnik in der Holzverarbeitung, DRW - Verlag Wienbrener GmbH, p.120 (in German).
- [14] Simpson,W.T. (1989): Drying wood: a review. Drying technology. An International journal.
- [15] Vengert, G (2003): Kiln insulation, Wood dryig Forum, WoodWEB, Inc.
- [16] Vengert, G., Mayer, D. (1993): Energy in the Sawmills - Conservation and Cost Reduction. Forestry Facts, School of Natural Resources, Department of Forestry, No. 61, p.8.
- [17] Zlateski, G. (1999): Prou uvanje na režimite na konvektivno sušenje na bi ena gragja od ela i buka so razli ni dimenzii, Magisterski trud, Skopje (in Macedonian).



CIP -

" . "

674-045.431(062)

684.4(062)

INTERNATIONAL scientific conference (6 ; 2023 ; Ohrid)

Wood technology & product design : proceedings / 4th International scientific conference, 13-15 September, 2023, University congress centre - Ohrid. - Skopje : Faculty of design and technologies of furniture and interior, 2023. - 218 . : . ; 30

.

ISBN 978-608-4723-05-9

) - - ) - -

COBISS.MK-ID 104170762